AN INVESTIGATION OF THE REACTIONS OF PYRIDOXAL-PHOSPHATE WITH AMINO-ACIDS AND METAL IONS

by

Joanna Mastrantoni

A thesis submitted for the degree of

Doctor of Philosophy

in the University of London

Bedford College
Regent's Park

December 1981

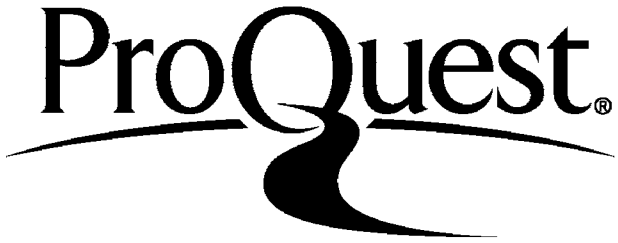

To my parents

thanking them for their constant help,

encouragement and support.

ACKNOWLEDGEMENTS

I would like to express my gratitude to my supervisor Dr. M.E. Farago for the guidance, helpful criticism and encouragement throughout the period of this work. I would like also to thank Dr. K.E. Howlett, Dr. D. Murphy and Dr. J.P.B. Sandall for helpful discussions, and Professor G.H. Williams for the provision of research facilities. My thanks are also due to Dr. M.W. McDonough for the use of the amino acid analyser and to D.R. Parkinson for instruction in the use of the JEOL 90 MHz n.m.r. spectrometer, and to the entire technical staff of the Chemistry Department for various help and technical assistance. My thanks also to Miss K. Anderson for the typing of this thesis.

ABSTRACT

The reactions of pyridoxal phosphate with amino acids and metal ions have been investigated. The kinetics have been studied by spectrophotometric and by polarimetric techniques. The reaction products were analysed by chromatography (paper and liquid column). ^{71}Ga, ^{27}Al, ^{115}In, ^{1}H, ^{31}P and ^{13}C n.m.r. techniques have been used to identify the structures of the complexes in solution.

The rates of formation of Cu^{2+}-SB and Zn^{2+}-SB complexes were dependent on the concentration of pyridoxal phosphate and the amino acid, the metal concentration had no effect on the rate, showing that the metal traps the Schiff base.

Cu^{2+} was the only metal to cause racemization of the aldimine complex formed from L-glutamate and pyridoxal phosphate. No Schiff base of any other amino acid was racemized by Cu^{2+} or by any other metal.

The rates of formation of M^{3+}-SB complexes are dependent, however, on the concentrations of the M^{3+} ions when these are low.

Multinuclear n.m.r. studies show that the M^{3+}-PLP complexes are symmetrical in acid media and coordination is through the phosphate group. ^{13}C n.m.r. shows that M^{3+}-SB complexes are asymmetrical species. M^{3+} are never coordinated through the phosphate in SB complexes.

The possibilities of establishing the stoichiometry mode of bonding and symmetry of M^{3+} complexes from the spectral widths of ^{71}Ga and ^{115}In m.m.r. spectroscopy are discussed. ^{31}P and ^{27}Al n.m.r. has also been studied and types of coordination have been suggested from numbers and chemical shifts and widths of the observed signals.

CONTENTS

CHAPTER 1

INTRODUCTION

(i) Transamination Reactions and Formation of Schiff-bases

In 1939, Braunstein[1] and Cohen[2] demonstrated the transamination reaction, by using an amino acid and a keto-acid.

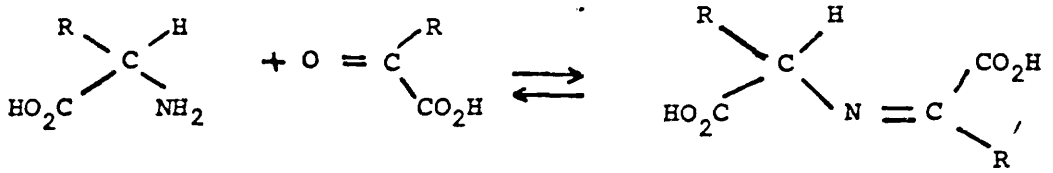

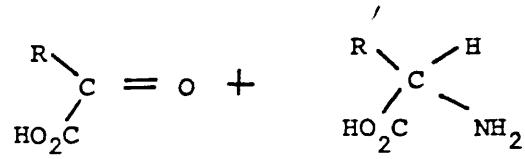

In 1945 Snell[3] defined the transamination reaction as 'the intermolecular transfer of an amino group from an α-amino-acid to an α-keto-acid'. This is also an oxidative deamination[4] reaction.

The intermediate in the transamination reaction which is called a Schiff-base or azomethine, can exist in tautomeric forms: ketimine and aldimine.

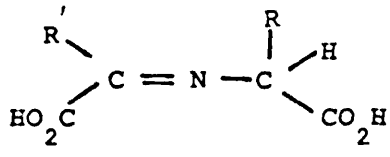

(ketimine)

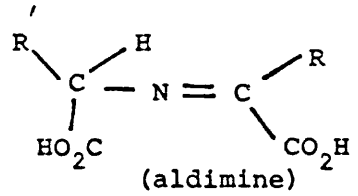

(aldimine)

The transamination reaction involves Schiff-base formation, prototropic shift from aldimine to ketimine Schiff-base, and then hydrolysis of the Schiff-base to give the amine.

(ii) The Discovery and the Biochemical Functions of Vitamin B_6 and its Coenzyme Forms

In 1934 Stanton and K. Folkers[5] isolated vitamin B_6 from liver,

rice bran and yeast and then tried to synthesise it. Kuln et al[6], in 1936, determined the structure and called it "pyridoxine" (I). In 1945, Snell showed that vitamin B_6 could also exist in two other forms, i.e. an amine (II) and an aldehyde (III), which are interconvertable one into the other, during the transamination reaction.

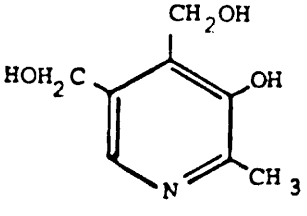

(I) pyridoxine

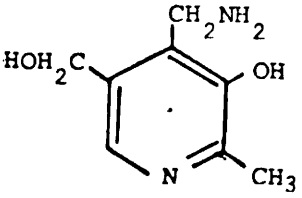

(II) pyridoxamine

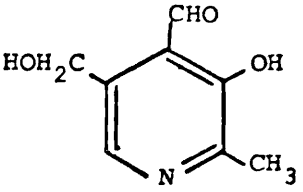

(III) pyridoxal

Vitamin B_6 has been found to prevent dermatitis, epilepsy and disturbance of the central nervous system. It also facilitates the growth of some bacteria[7] .

Pyridoxal and Pyridoxamine occur in nature and their phosphate derivatives (IV,V) are the coenzyme* forms of the vitamin

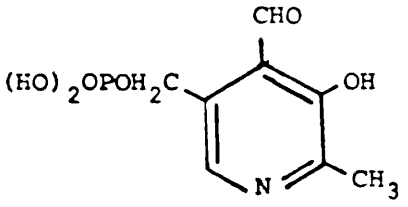

(IV) pyridoxal phosphate

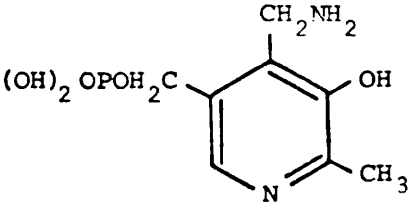

(V) pyridoxamine phosphate

The coenzyme of vitamin B_6, pyridoxal phosphate, catalyses several important reactions in the metabolism of amino acids such as transamination[3], decarboxylation[8], racemization[9], beta and gamma elimination and carbon-carbon bond cleavage[10]. There are about twenty specific reactions of amino-acids involving PLP. Although each of

*Coenzymes are substances activating the enzymes. Enzymes are globular proteins which catalyze specific biochemical reactions (being able to bind very selectively to a (substrate) reactant molecule) and control their rates. Hence enzymes direct the chemical reactions that take place in a living cell.

those reactions is catalyzed by a different, specific enzyme, pyridoxal-phosphate coenzyme, is necessary in all of them. The coenzyme is weakly bound to the enzyme forming a Schiff base which has such orientation to facilitate the displacement of the amino group of the enzyme by an amino-acid.[11]

(iii) Metal Ion Catalysis of Transamination Reactions

In the non-enzymatic transamination reactions catalyzed by metals, the essential groups for the formation of the Schiff-base-metal intermediates are the aldehyde group, the hydroxy group and the heterocyclic nitrogen.

The aldehyde group is bound to the amino-acid forming the Schiff-base which is stabilized by chelation with the metal ion via the phenolic oxygen, the carboxyl group of the amino acid and the nitrogen of the azomethine linkage. The chelation of the metal ion with the ring gives a planar conjugated intermediate (Scheme 1). This intermediate assists in the displacement of the electron pair from the α-carbon atom of the amino acid to the metal which acts as an electro-attracting species. This is similar to the effect of the heterocyclic nitrogen, as Metzler[12] suggested. The metal ion catalysis involves two inter-convertable chelates: an aldimine and a ketimine.

Morman and Porter[13] suggested that the hydroxyl and the aldehyde groups are the ones mainly involved in the biological functions of pyridoxal, since they react with amino acids to form Schiff-bases, which can then undergo a variety of reactions (see page 9). Hence for the enzymatic reactions two other groups are also important, the methyl and the phosphate groups. The methyl group is necessary for the formation of the co-enzyme i.e. phosphorylated pyridoxal; and the phosphate is important because it prevents the formation of internal hemiacetal forms so that a high concentration of the free

aldehyde, which is the active form in catalysis, is maintained.

Braunstein[14] also suggested that the enzyme would attach to the phosphate group and the nitrogen in the ring (i.e. heterocyclic) (see VI).

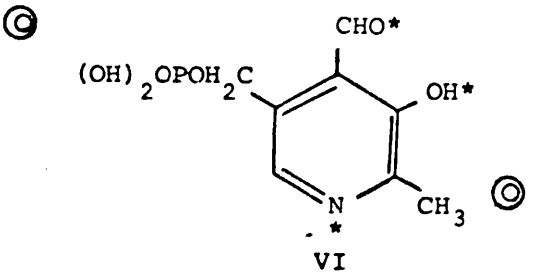

VI

* groups necessary for reactions in the presence of metal ions or enzymes

groups necessary for enzymatic reactions only

The present work however, suggests that the phosphate group is also necessary for the reactions in the presence of metal ions of group III in a certain pH range.

In 1952 Metzler and Snell[15] studied the effect of some di- and trivalent metal ions on the reversible rate of transamination of pyridoxal with various amino acids. The reactions were non-enzymatic in which the metal ion was acting as a catalyst. In 1954[16] they suggested the following mechanism, Scheme 1, which is similar to Braunstein's mechanism .

Metzler and Snell were able to prove the transamination reaction by observing the electronic spectrum at 24,000 cm^{-1} using an excess of ethanolamine in the reaction mixture. Ethanolamine reacts with PL and the produced ethanolamine - SB absorbs at 24,000 cm^{-1} while PL does not.

It was proved by Eichhorn and Dawes[17] that a mixture of tautomers exists in solution by recording the spectra of PL-metal-alanine and PM-metal-pyruvate, which were indistinguishable. Banks et al[18] also showed tautomerism by recording spectra in the absence of metal ions.

Scheme 1

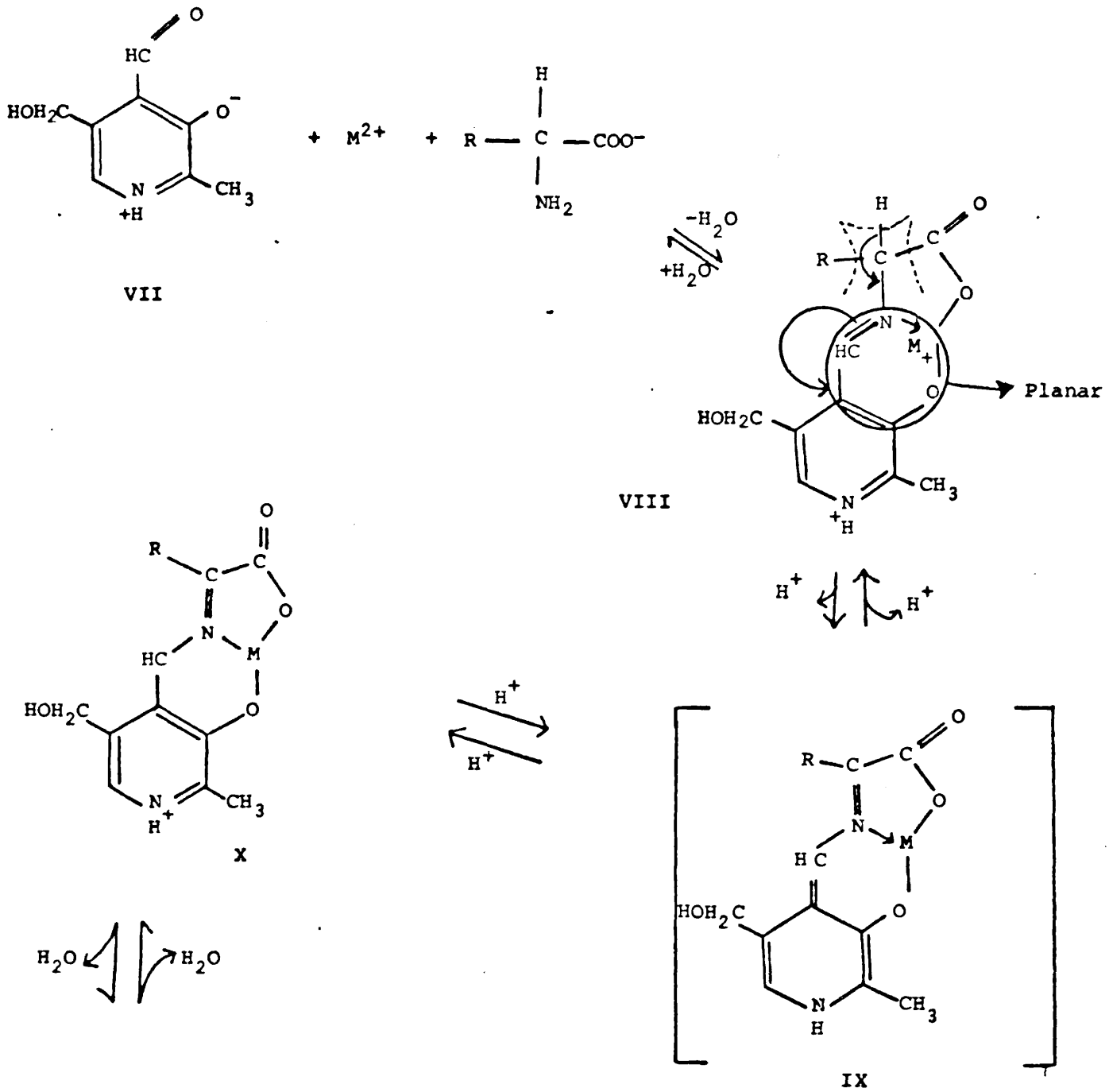

The process of tautomerism was slow.

Metzler and Snell[15] suggested that the metal was acting as a catalyst by:

a) maintaining the planarity of Schiff-base complex in such a way that electron displacement is aided,

b) directing the displacement of electrons towards the heterocyclic nitrogen,

c) forming a thermodynamically stable intermediate which can assist the formation or the hydrolysis of either Schiff-base (Scheme 1),

d) acting as a Lewis acid can make coordinated bonds which bring groups near enough, enabling stereospecific reactions between them. The metal can increase the inductive withdrawal of electrons from the α-carbon and hence can labilize the groups attached to it.

The imines (VIII) and (X) in scheme I have been detected spectrophotometrically but not the imine (IX).

Longenecker and Snell[19] investigated the effect of metal ions on the rate of transamination of pyridoxamine with α-ketoglutarate (scheme 2). They found PL and Glutamic acid to be the products of the reaction.

$$\text{Pyridoxal + amino-acid} \overset{M^{n+}}{\rightleftharpoons} \text{pyridoxamine + α-Keto-acid.}$$

They also indicated the catalytic activity towards pyridoxal transamination in the order

$$Cu^{2+} > Al^{3+} > Fe^{2+} > Fe^{3+} > Zu^{2+} > Ni^{2+} > Co^{2+}$$

Using aluminium they showed that the rate of appearance of PL was proportional to the concentration of aluminium, in a range of low concentrations. In high aluminium concentration however, the rate was independent of increase in concentration.

Farago and Matthews[20] found that the metal ions do not kinetically

Scheme 2

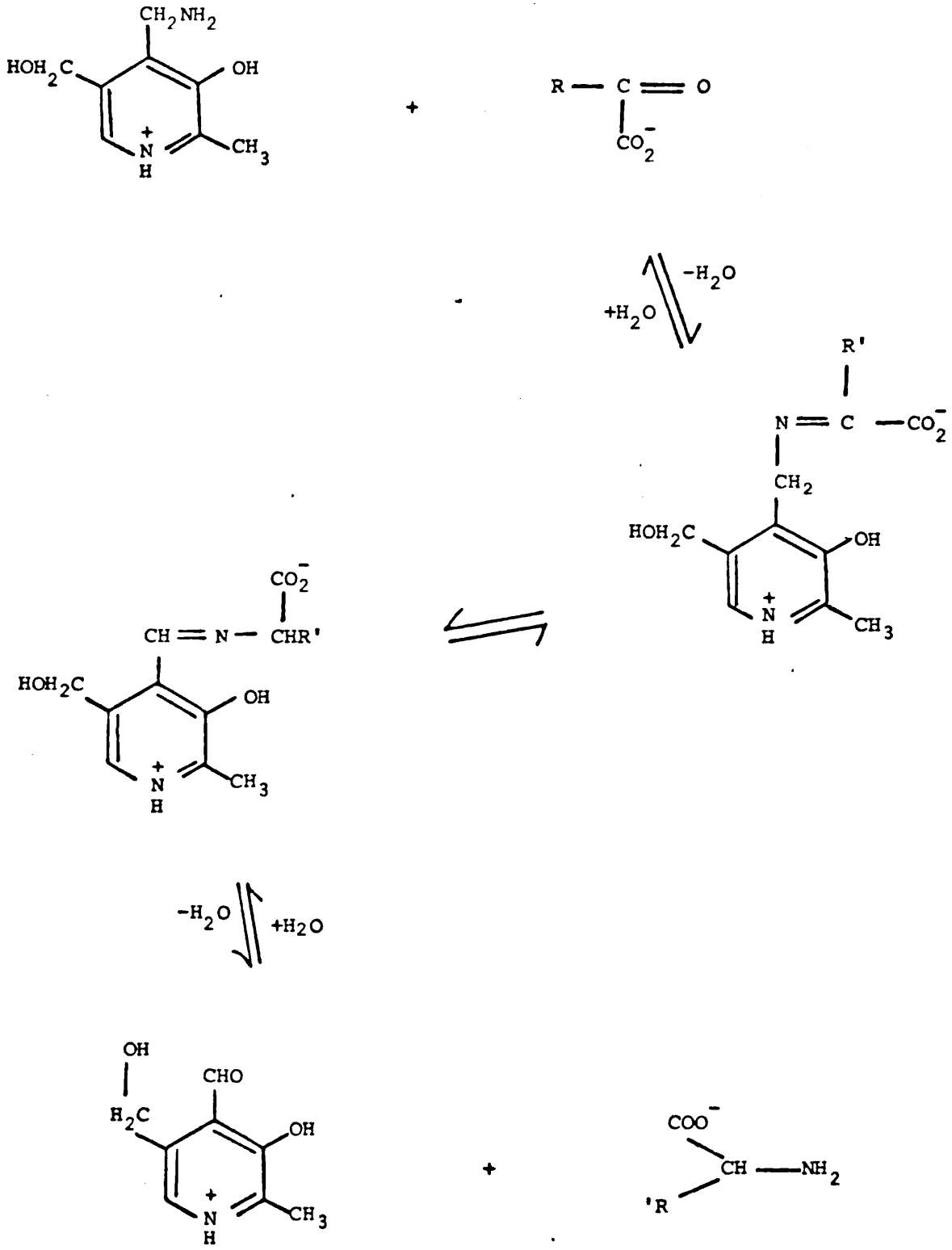

affect the rate of formation of the Schiff-base, so, metals must act as Snell et al[16] suggested.

The stability of the Schiff-base species increases with the ring formation.[16] The more planar the ring is, the more stable the M-SB complex.

Metzler[21] showed that the two tautomeric Schiff-bases (VIII) and (IX) in Scheme 1 can decompose in three different ways to give racemisation of the amino acid, transamination, or decarboxylation by release of the R -group, and all are followed by hydrolysis of the C=N bond. Metzler[15] also suggested that phenolic and formyl groups are used in the chelation of metal ions, but only the formyl group is important in the transamination of the pyridoxal to pyridoxamine.

Metzler[22] found that the relative strength of coordinate bonds[23] of metals with PLP and amino acids was in the order:

$$Ga^{III} > Cu^{II} > Fe^{III} > Al^{III} > Ni^{II} > Co^{II} > Mn^{II} > Mg^{II}$$

Fasella[20] found that the phosphorylated M-Schiff-base-complexes had metal to Schiff-base ratio 1:1, but the non-phosphorylated Schiff-bases could possibly give 1:1, 1:2 or even 1:3 metal to Schiff-base ratio. Matsuo[24] suggested that the phosphate group can be bound to the enzyme, because of the steric effect.

Fasella et al[25] using paper chromatography and electrophoresis, analysed samples from reaction mixtures of Al^{3+}-PLP-alanine, and Al^{3+}-PAMP-pyruvate. They showed the existence of two intermediate chelates (XII) and (XIII) and they found that for their formation there was just enough Al^{3+}, PLP + alanine or Al^{3+}, PAMP and pyruvate. The two intermediates had no free NH_2 and carboxylic groups. They also found that (XII) and (XIII) were interconvertable as their only difference was the position of the labile proton.

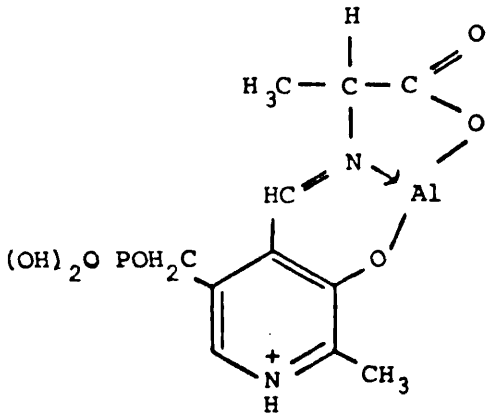

XII

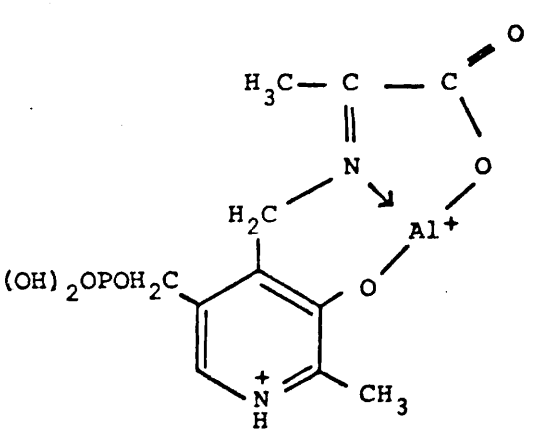

XIII

Cattaneo et al[26] also used paper chromatography to prove that the transamination reaction takes place with pyridoxal-phosphate and glutamate, giving pyridoxamine phosphate and α-ketoglutarate at 37°C in the presence of Cu^{II}. This was confirmed in the present study (see page 116).

The mechanism of the reaction of PLP and amino acids in the presence of metal ions was studied by Nakamoto and Martell[27]. By using spectroscopic techniques, they found that the concentration of the aluminium does not affect the rate of the reaction. Subsequently this behaviour was found in the case of copper.[20]

Abbott and Martell[28] studied the structures of Bis [pyridoxylidene (amino acidato)] aluminium (III) complexes using ^1H n.m.r. and suggested that the Schiff-bases were coordinated to the Al^{3+} ion as planar, terdendate ligands. They[28] also proved that these diamagnetic complexes exist as three diastereoisomers, using the 2-CH_3 resonances of PL. That was possible since the 2-CH_3 of one ligand (Fig.1) was in the shielding region of the azomethine π system of the other ligand and therefore the chemical shifts are very much affected by the small steric interactions with the asymmetric center of the amino-acid of the other ligand.

Fig. 1

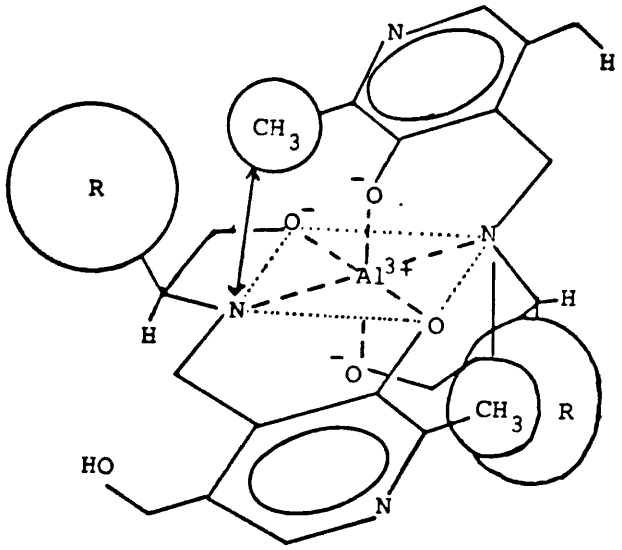

II MAXIMUM STERIC REPULSION: MINIMUM SHIELDING

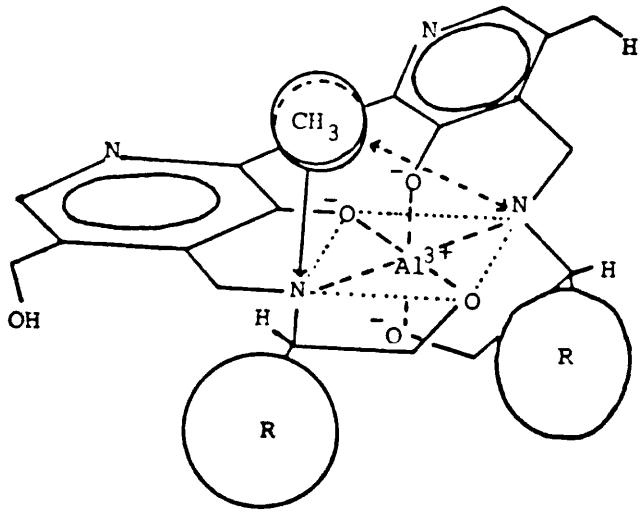

III MINIMUM STERIC REPULSION: MAXIMUM SHIELDING

Marcello, Abbott and Martell[10] found that C-C bond fission was taking place in a reaction of an α-amino acid having an α-proton in the presence of PL and metal ions. This was demonstrated using ^1H n.m.r. and observing the appearance of acetaldehyde, while the resonances due to threonine disappeared. They[10] also used β—hydroxyvaline, PL and Al^{3+} and showed acetone to be one of the products (Scheme 3). The mechanism they suggested was a development of Snell's[16] earlier mechanism.

Abbott and Martell[29] further used serine, homoserine and threonine to demonstrate the formation of Schiff-bases which had azomethines with internal hydrogen binding (XIV).

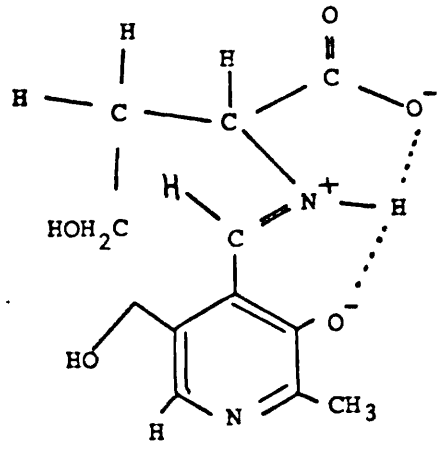

XIV

Martell[30] studied the rates of the formation of the intermediate complex in the transamination reaction using ^1H n.m.r. techniques (Scheme 4).

Previously Martell[31] already had demonstrated the reverse process using PM and α-keto-acids in the presence of metal ions (Scheme 5). He found[31] that the relative overall rates were in the order

Scheme 3

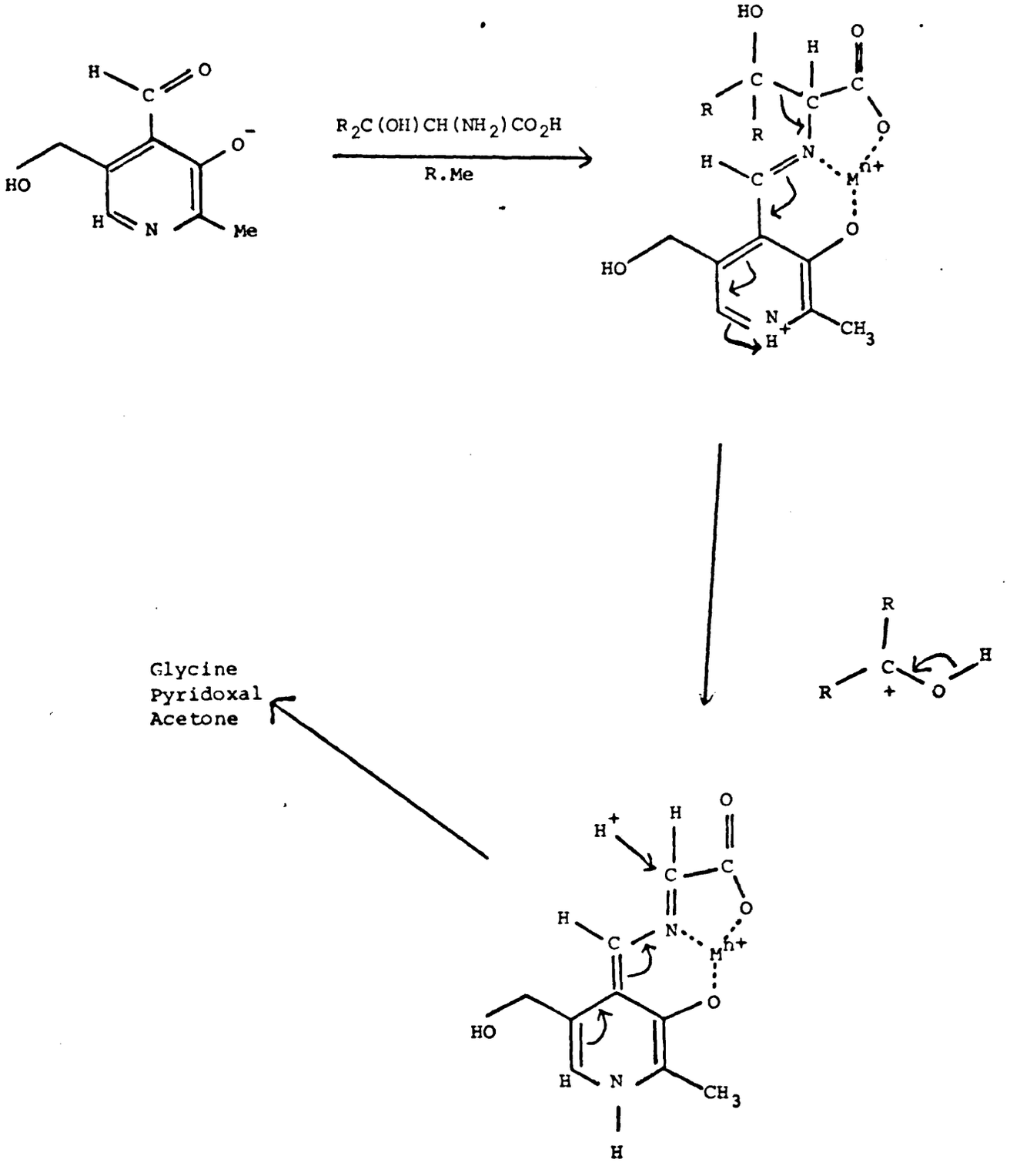

Scheme 4

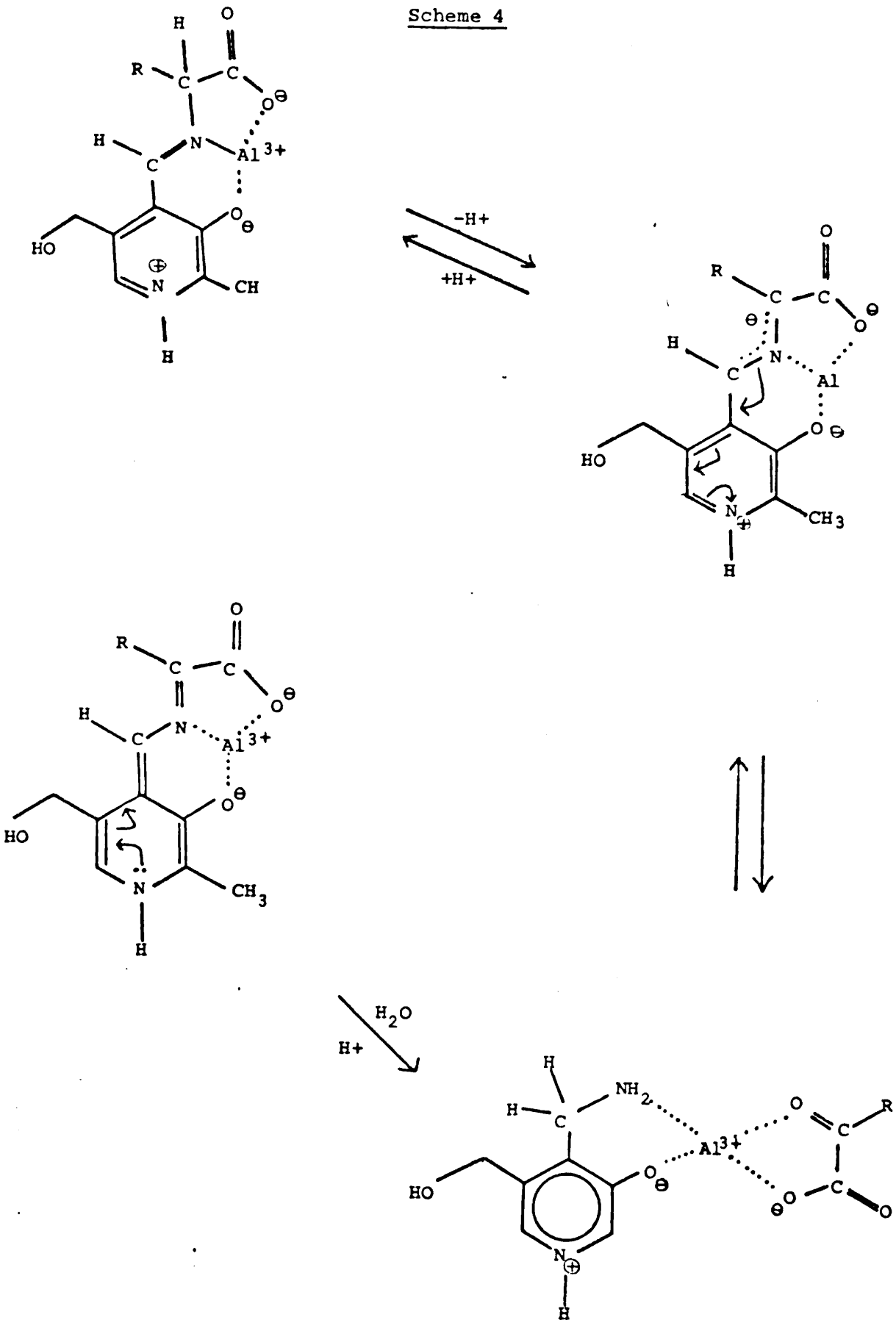

Scheme 5

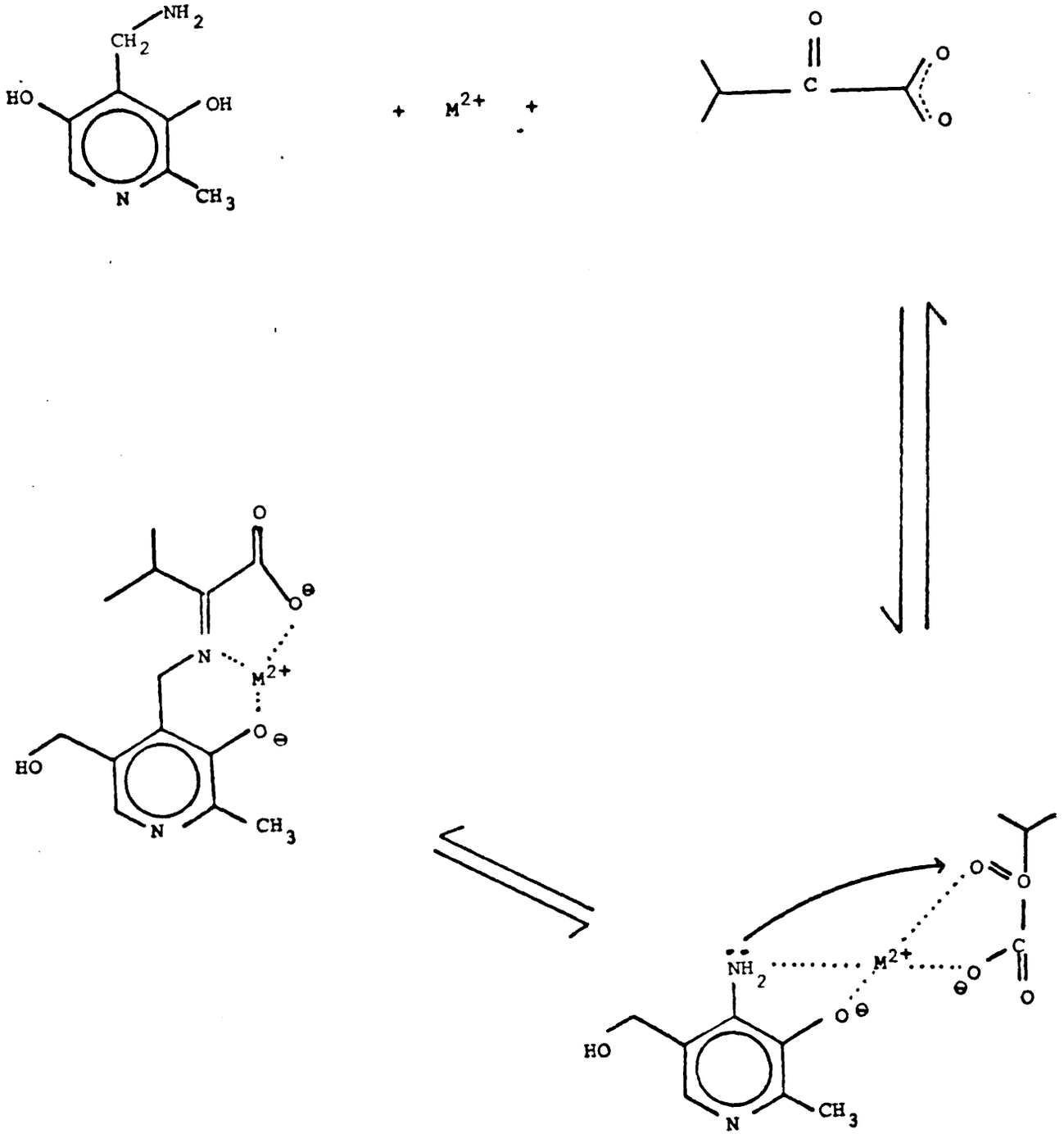

$$Zn^{2+} > H^{+} >> Ni^{2+} > Cu^{2+}$$

and that, he thought, was the result of the promnastic effect[32] (προμνάσθαι - to be a matchmaker). The metal ions were acting as catalysts by increasing the weakness of the amino group bond to the metal and hence increasing the probability of nucleophilic attack on the carbonyl group of the Schiff-base ligand.

(iv) Racemization Reactions

Much work has been done on racemization of optically active amino acids in the presence of PLP using enzymes to catalyze the reaction[11,33-35]. As Dunathan[36] in 1971 suggested, the enzymes control the reaction specificity by controlling the conformation about the N-Cα bond at the Schiff's base intermediate. The bond perpendicular to the π-system can break easier than others because of the maximum σ-π overlap. Hence the enzymes catalyze the reaction in their active sites by helping the bond to be cleaved, to overlap with the π-systems in a suitable way.

Metals have also been used in the place of enzymes to produce similar results[35-37,42].

In 1965 Williams[43] and Reiley[44] suggested that the α-CHR-proton undergoes base-catalyzed exchange in aqueous solution and this exchange involves the formation of a coordinated carbanion which can take up a

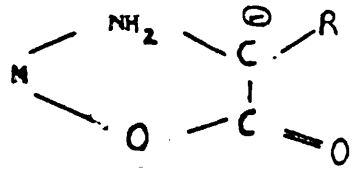

proton with retention of configuration or invert the asymmetric

grouping about the carbon atom. Hence, coordinated amino acids can mutarotate more easily than uncoordinated ones. In 1967 further studies by Buckingham and Sargeson[45] using diamagnetic complexes of cobalt (III) establish the rates of racemization and isotope exchange and also suggested that the reactions occur via a simple carbanion intermediate (Scheme 6).

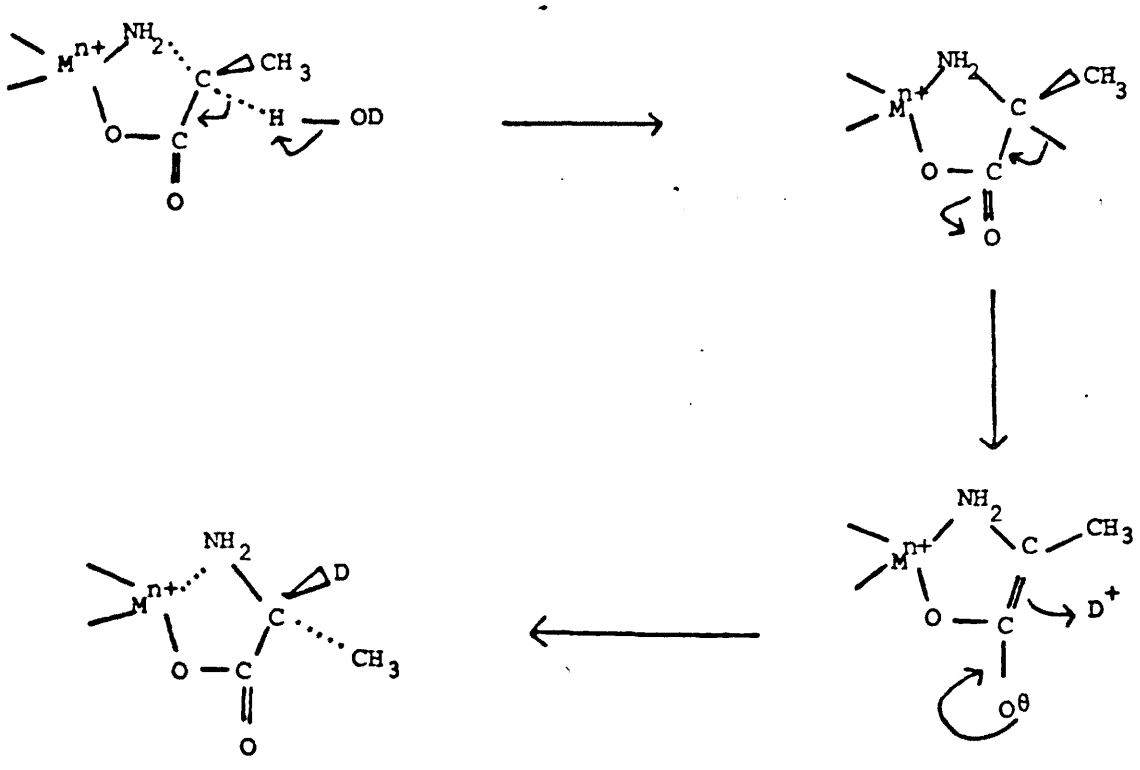

Scheme 6

In 1977 Gillard et al[27] studied the Racemization of L-alanine in the presence of Cu^{2+} ions at alkaline pH and although the simple carbanion intermediate can be formed, it was proved that Cu^{2+} was necessary for the racemization to take place. Also Cu^{2+} catalyzed the oxidation of L-alanine to yield pyruvate, the condensation of pyruvate and L-alanine yields the copper complex of the Schiff-base which is followed by the base catalyzed racemization occurring via

carbanion formation in the Schiff-base. In 1979 Dempsey[37] tried to repeat the work of Gillard but with Zn^{2+}. It was found that Zn^{2+} had almost no effect. It could not catalyze the oxidation of L-alanine, neither form the Schiff-base complex as Cu^{2+} did.

In 1978 Tsai et al[39] tested the racemization of some optically active amino acids in the PL-Schiff-base system in the absence of enzymes and of metals. The Schiff-bases were prepared under a nitrogen atmosphere in methanol and the racemization was base-catalyzed. Tsai et al[39] used polarimetric ^{1}H and ^{13}C n.m.r. analysis and found that the order of the rates of racemization and Hα exchange of a series of PL-amino acid Schiff-bases were not related to electronic and steric effects, but were affected by the bond angle of the Cα-Hα bond with the π-system, in the reactive conformers (XV).

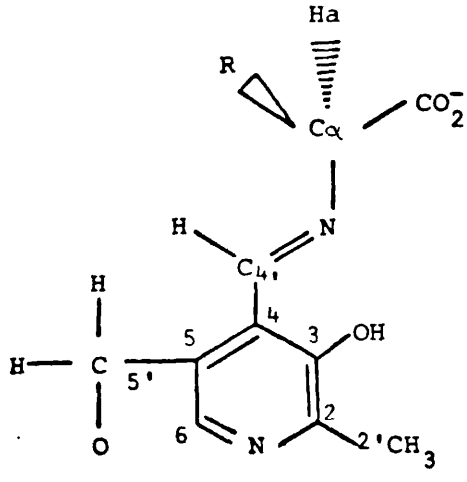

XV

Tsai et al[46] also proved that the racemization of optically active amino acids was base-catalyzed. Using[39] ^{13}C, ^{1}H n.m.r. and NOE measurements, it was shown that the π system of the pyridine ring and the π-electron pair of the imine double bond were coplanar, and that the C_4-C_4' bond has a cis conformation.

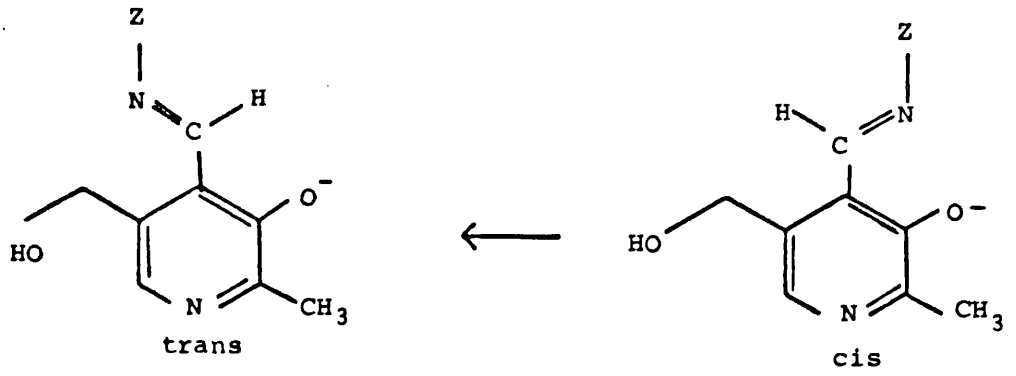

It was also shown[39] that H_4' and Hα had a close spatial relationship and their simultaneous upfield shifts were one more evidence for the cis conformation of C_4-C_4' bond.

Fischer[40] using ^1H n.m.r., studied the deuterium exchange reactions of glycine α-protons in bis (pyridoxylideneglycinato)-cobalt (III) which were also base catalysed and suggested the following mechanism (Scheme 7).

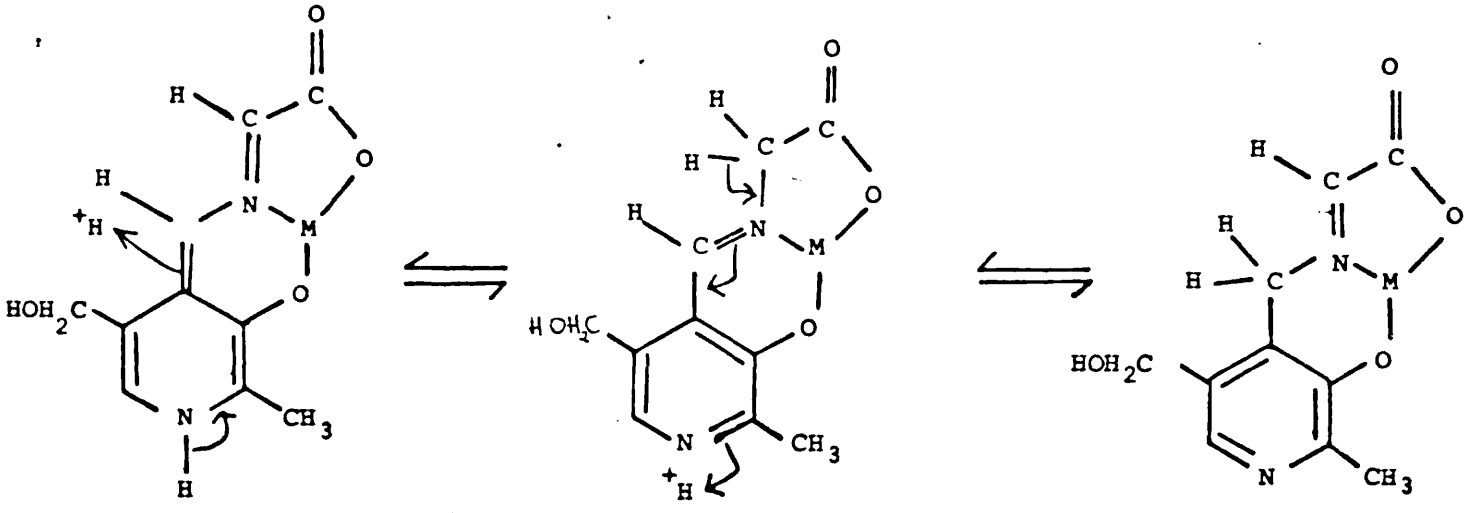

The reaction could either proceed by the mechanism XVI → XVII → XVIII or by XVI → XVII → XVIII → XVII → XVI as Tenenbaum suggested[8]. Fischer[40] found a second order rate constant at pH = 8.9 and suggested a base catalyzed H^+ exchange of one complex

by the pyridine nitrogen of another complex. Belokon[41] and Blake et al[47] believe that proton transfers in coordinated Schiff-bases take place only in basic solutions. Present work shows, however, that this is not the case.

REFERENCES

1. A.E. Braunstein, Enzymologia, 7, 25 (1939).

2. P.P. Cohen, Biochemistry J., 33, 1478 (1939).

3. E.E. Snell, J.A.C.S. 67, 194 (1945).

E.E. Snell, P. Fasella, A.E. Braunstein and R. Fanelli, "Chemical Biological aspects of Pyridoxal catalysis" Interscience Publishers John Wiley U.S.R. (1968).

4. R.M. Herbst, "Advances in Enzymology", Interscience Publishers New York 4, 75 (1944).

5. S.A. Harris and K. Folkers, J.A.C.S. 61, 1245 (1953).

6. B. Kuhn and R. Wendt, Ber, 305, 311 (1972).

7. Eric E. Conn and P.K. Stumpf, Outlines of Biochemistry, third edition, J. Wiley and Sons Inc. (1972).

8. A. Tenenbaum, Biochem., Biophys. Acta 362, 308 (1974).

9. R.D. Gillard and P. O'Brien, J.C.S. Dalton, 1988 (1977).

10. J.A. Marcello, A.E. Martell and E.H. Abbott, J.C.S. Chem. Comm. 16 (1975).

11. Harmon C. Dunathan, Haverford, Pennsylvania 'Sterochemical apsects of Pyridoxal-phosphate catalysis' (1971).

12. D.E. Metzler and J. Fischer, J.A.C.S. 91, 138 (1969).

13. K. Morman and A.Porter, S.S. Sabir's thesis, Bedford College, Chemistry Department (1971).

14. A.E. Braunstein 'The enzymes' Ed. P.D. Boyer, H. Lardy, and K. Myrback, vol.2, p.140.

15. D.E. Metzler and E.E. Snell, J.A.C.S. 74, 979 (1952).

16. D.E. Metzler, M. Ikawa and E.E. Snell, J.A.C.S. 76, 648 (1954).

17. G.L. Eichorn and J.W. Bawes, J.A.C.S. 79, 5663, (1954).

18. E.C.B. Blanks, A.A. Diamants and C.A. Vernon, J.C.S. 4235 (1961).

19. J.B. Longenecker and E.E. Snell, J.A.C.S. 79, 142 (1957).

20. M.E. Farago and T. Mattheus, J.A.C.S. 609 (1969).

21. J.J. Delpuech, M.R. Khaddar, A. Peguy and P. Rubini, J.A.C.S. 97, 3373 (1975).

22. L. Davies, F. Roddy and D.E. Metzler, J.A.C.S. 83, 127 (1961).

23. F.A. Cotton and G. Wilkinson, 'Advanced Inorganic Chemistry' Third edition. Interscience Publishers, J. Wiley (1972).

24. Y. Matsuo, J.A.C.S. 79, 2011 (1957).

25. P. Fasella, H. Lis, C. Balioni and N. Siliprandi, J.I.N.C. 8, 620 (1958).

26. J. Cattaneo, J.C. Senez and P. Beaumont, Bioch. Biophys. Acta 44, 543 (1960).

27. K. Nakamoto and A.E. Martell, J.A.C.S. 85, 188 (1963).

28. E.H. Abbott and A.E. Martell, J.A.C.S., 92:20, 5845 (1970).

29. E.H. Abbott and A.E. Martell, J.A.C.S. 92:6, 1754 (1970).

30. E.H. Abbott and A.E. Martell, J.A.C.S. 95, 5014 (1973).

31. Y. Matsushima and A.E. Martell, J.A.C.S. 89, 1322 (1967).

32. A. Hopgood and K. Leussing, J.A.C.S. 91, 3740 (1969).

33. Rosso G. Takashima and Adams, Biochem. Biphys. Res. Commun. 34, 134 (1969).

34. A. Morino and E.E. Snell, J. Biol. Chem., 242, 2800 (1967).

35. D.E. Gout, D.C.G. Bequin, D.M. Zador (C.E.R.M.O. (Grenoble, France, ERA CHRS 573, Universite de Montreal, Canada). (1980).

36. H.C. Dunathan, Adv. Enzymol. 35, 79 (1971).

37. A. Dempsey and D.A. Phipps, Inorganica Chemica Acta, 36, 425 (1979).

38. Ming-Daw Tsai, Herschel J.R. Weintraub, Stephen R. Byrn, Ching-Jer Chang, and Heinz G. Floss, Biochemistry 17, 3183 (1978).

39. M.D. Tsai, S.R. Byrn, C-J. Chang, H.G. Floss and J.R. Weintraub, Biochemistry 17, 3177 (1978).

40. J.R. Fischer, E.H. Abbott, J.A.C.S. 2781 (1979).

41. K. Belokon, Tetrahedron 33, 2551 (1977).

42. M.I. Blake, F.P. Siegel, J.J. Katz and M. Kilpatrick, J.A.C.S. 85, 294 (1963).

43. D. Williams and D.H. Busch, J.A.C.S., 87, 4644 (1965).

44. C.N. Reiley, Inorganic Chemistry 5, 1988 (1966).

45. D.A. Buckingham, L.G. Marzilli and A.M. Sargeson, J.A.C.S. 1082, 825 (1967).

CHAPTER 2

RATES OF RACEMIZATION

The series of metal ions used in buffered solutions of PLP and optically active amino acids were: Cu^{2+}, Ni^{2+}, Co^{2+}, Fe^{3+}, Zn^{2+}, Cd^{2+}, Al^{3+}, Ga^{3+}, In^{3+} and Tl^{3+}. They were chosen to investigate whether they can control the conformation about the N-C_α bond of the Schiff-base intermediate, in the same way enzymes do , and therefcre whether they can cause labilization of the C_α-H_α bond of the L-amino-acids and inversion of their configuration at C_α.

The L-amino-acids used were: Aspartic acid, Glutamic acid, Leucine, Isoleucine, Cysteine, Methionine, Histidine, Valine, Phenylalanine and Threonine. It was known previously[2,3] that some of these amino acids are racemized in very basic media in the presence of PLP only, and that the rates of racemization and H_α exchange are dependent on the steric interaction between β substituents and the pyridoxal ring. In the present work an attempt was made to show that racemization takes place in the acidic pH range as well, but in the presence of metal ions, and it is shown that the rates are related to the number of β substituents and their steric effects.

1. Experimental Procedure

All materials used were Analar grade. Solutions of amino acids, PLP and metal salts were prepared using distilled water. The reactions were carried out in a series of sodium acetate buffers, (prepared as in Appendix I), but some of them were also tried at alkaline pH values adjusted by adding NaOH and a calculated amount of KCl so that a constant ionic strength was maintained. Reactions were carried out at 20°C, but some of the reactions were repeated at higher temperatures (i.e.

Fig. 2

Structures of amino-acids used

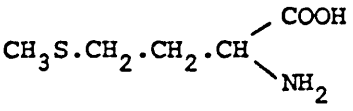

Methionine

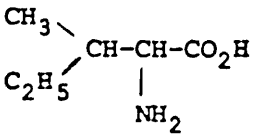

iso-Leucine

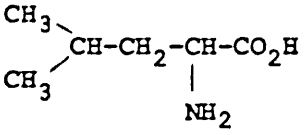

Leucine

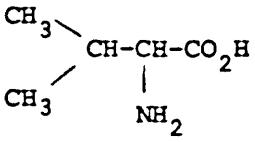

Valine

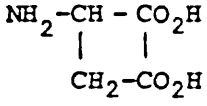

Aspartic acid

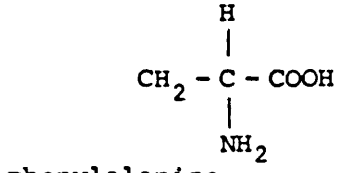

phenylalanine

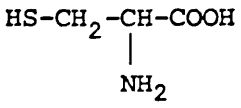

cysteine

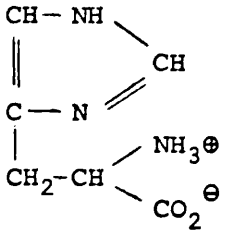

Histidine

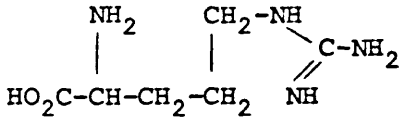

Arginine

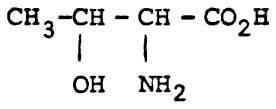

Threonine

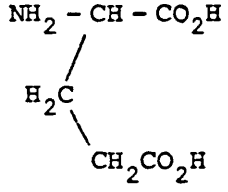

Glutamic acid

35°C and 40°C). All reactions were followed in a 1-dm thermostatted cell using a Perkin-Elmer 241 polarimeter. Ultra-violet solution spectra were determined in silica cells using a SP8-100 spectrophotometer.

2. Results

(i) Racemization of L-Na-glutamate in the presence of Cu^{2+} ions and PLP

A series of solutions was made up using 0.25 mol.dm^{-3} L-glutamate, 0.04 mol.dm^{-3} Cu^{2+} and 0.0038 mol.dm^{-3} PLP solutions in an acetate buffer. Table 1 contains the concentration of each compound in the cell.

The rotation of L-Na-Glu in just buffer; PLP and buffer; and Cu^{2+} and buffer was tested for each concentration and pH. Although there are small differences between them, the rotation of each of these mixtures does not change as a function of time. Table 2 gives the values of the rotation at 436nm for each case.

The effect of the concentration of the various materials on the shape of the rotation-time curves and on the rates, at each pH, was studied by maintaining the concentrations of all but one component at set values and just increasing the concentration of one of the materials each time. Fig.3 shows how the rotation changes as the concentration of PLP increases at pH = 3.86. Similar types of curves were obtained, at all pH values studied, but the rotation, as a function of time, was different (Fig.4).

The change in rotation during each reaction, indicates that two different reactions are involved. The first part of the reaction during which mutarotation occurs, is probably due to the Metal-Schiff-Base complex formation, while the second part indicates a racemization reaction. That was proved by U.V. spectroscopy. As Fig.5 shows, the absorbance increases as the time increases, indicating formation of a complex. Then at a certain time the absorbance remains constant showing

Table 1

Concentrations of the materials in the cell.

Solution	pH	$10^4 \times$[PLP]/mol.dm^{-3}	$10^3 \times$[L-glutamate]/mol.dm^{-3}	$10^3 \times$[Cu^{2+}]/mol.dm^{-3}
1	1.62	3.6	70.75	2.26
2	2.63	3.6	70.75	2.26
3	3.89	3.6	70.75	2.26
4	5.13	3.6	70.75	2.26
5	6.96	3.6	70.75	2.26
6	3.86	0.755	70.75	2.26
7	3.86	1.89	70.75	2.26
8	3.86	3.77	70.75	2.26
9	3.86	5.66	70.75	2.26
10	3.86	1.89	23.58	2.26
11	3.86	1.89	47.17	2.26
12	3.86	1.89	70.75	2.26
13	3.86	1.89	94.34	2.26
14	3.86	1.89	70.75	0.755
15	3.86	1.89	70.75	1.509
16	3.86	1.89	70.75	2.264
17	3.86	1.89	70.75	3.774
18	1.61	0.755	70.75	2.26
19	1.61	1.89	70.75	2.26
20	1.61	37.73	70.75	2.26
21	1.61	5.660	70.75	2.26
22	1.61	7.547	70.75	2.26
23	1.61	1.89	23.6	2.26
24	1.61	1.89	47.2	2.26
25	1.61	1.89	70.7	2.26
26	1.61	1.89	94.3	2.26
27	1.61	1.89	70.75	1.509
28	1.62	1.89	70.75	2.26
29	1.62	1.89	70.75	3.77
30	1.62	1.89	70.75	7.55
31	6.98	0.755	70.75	2.26
32	6.98	1.887	70.75	2.26
33	6.98	3.774	70.75	2.26
34	6.98	5.66	70.75	2.26
35	6.98	3.774	23.58	2.26
36	6.98	3.774	47.17	2.26
37	6.98	3.774	70.75	2.26
38	6.98	3.774	93.34	2.26
39	6.98	3.774	70.75	0.98
40	6.98	3.774	70.75	2.26
41	6.98	3.774	70.75	3.77
42	6.98	3.774	70.75	7.547
43	5.16	0.755	70.75	2.26
44	5.16	1.887	70.75	2.26
45	5.16	3.774	70.75	2.26
46	5.16	5.66	70.75	2.26
47	5.16	3.774	23.58	2.26
48	5.16	3.774	47.17	2.26
49	5.16	3.774	70.75	2.26
50	5.16	3.774	94.34	2.26
51	5.16	3.774	70.75	0.75
52	5.16	3.774	70.75	1.51
53	5.16	3.774	70.75	2.26
54	5.16	3.774	70.75	3.77

Table 2

Measured rotations at 436nm for various mixtures

pH	L-Glu	L-Glu-PLP	L-Glu-Cu^{2+}
1.62	+0.147	+0.145	+0.127
2.63	+0.097	+0.099	+0.080
3.89	+0.036	+0.030	+0.024
5.13	-0.048	-0.049	-0.053
6.96	-0.082	-0.083	-0.112
H_2O	-0.86	-0.92	-0.120

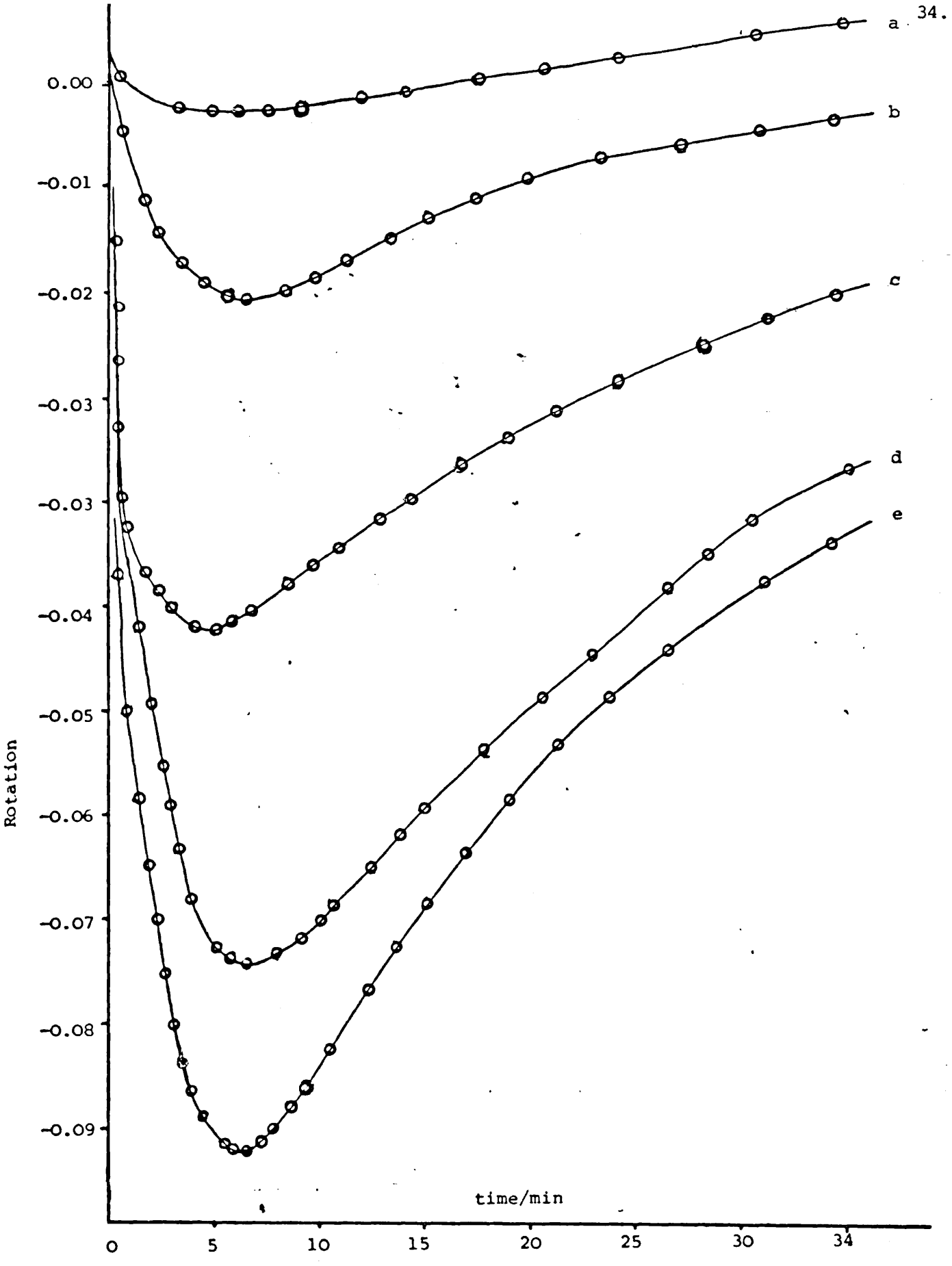

Fig. 3: Plot of the Rotation against time/min at 20°C and at 436 nm.

a=run 6, b=run 7, c=run 8, d=run 9, e=run 10
(For conditions see Table 1)

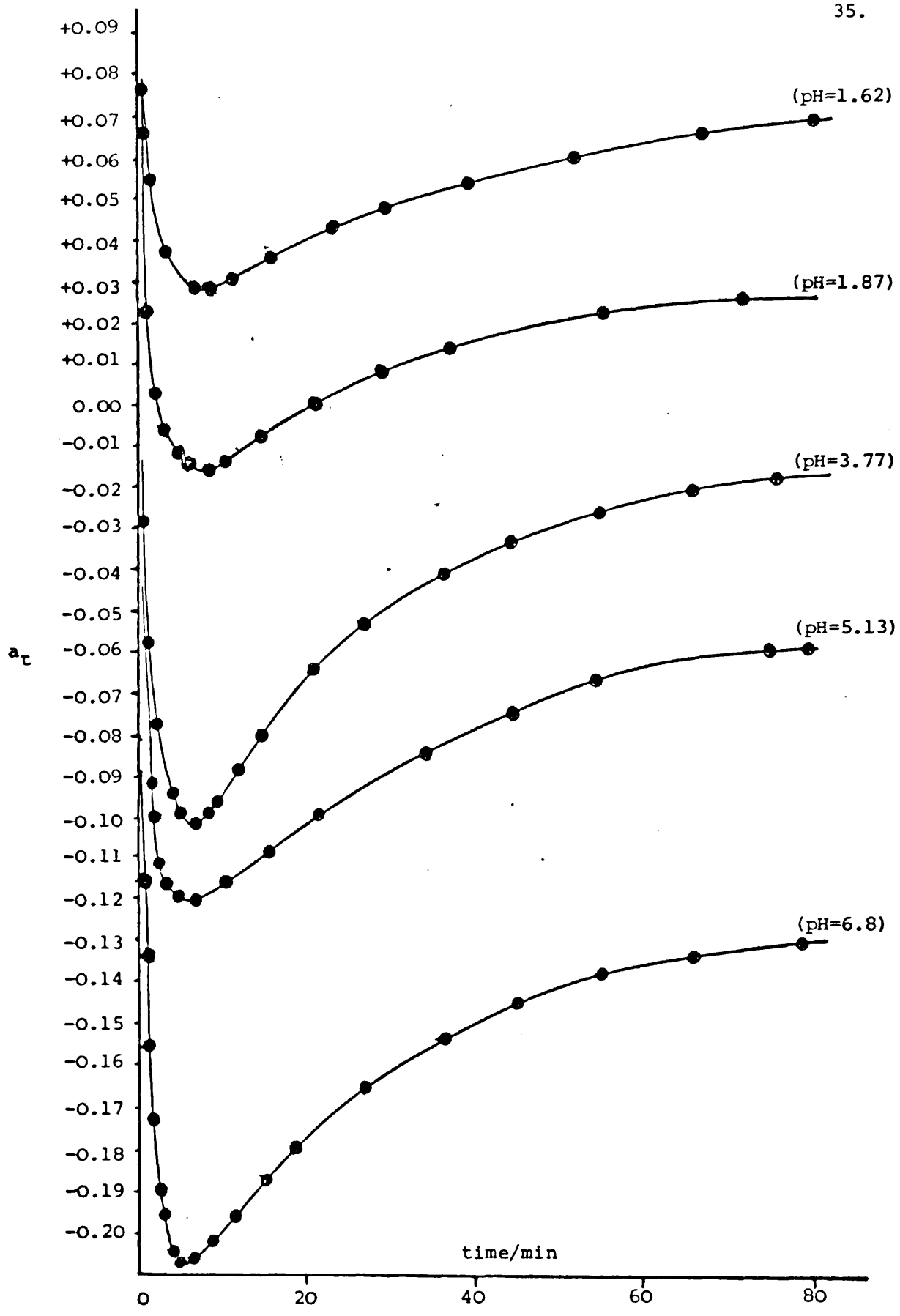

Fig. 4: Plot of Rotation (a_t) against time/min for the reaction of 2.26×10^{-3} mol.dm^{-3} Cu^{2+} with 3.6×10^{-4} mol.dm^{-3} PLP and 70.75×10^{-3} mol.dm^{-3} Glu at 20^{o}C and at 436 nm.

Fig.5

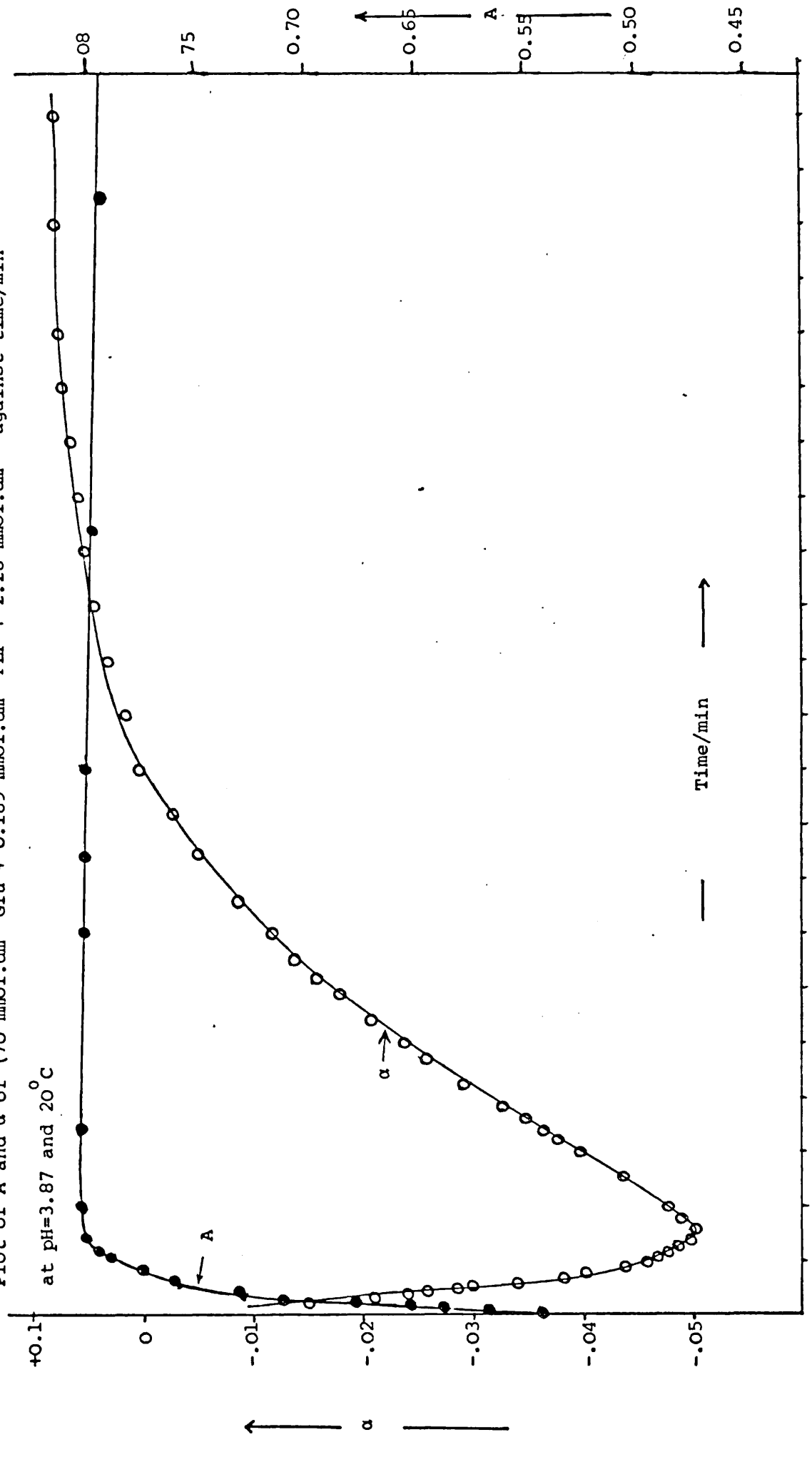
Plot of A and α of (70 mmol.dm^{-3}Glu + 0.189 mmol.dm^{-3}PLP + 2.26 mmol.dm^{-3} against time/min
at pH=3.87 and 20°C
A
α
Time/min
+0.1
0
-.01
-.02
-.03
-.04
-.05
0.80
0.75
0.70
0.65
0.55
0.50
0.45
0 5 10 15 20 25 30 35 40 45 50 55 60 65 70 75 80 85 90 95 100 105 110

that the complex is completely formed and it is quite stable for about two hours. Then, the absorbance decreases as reactions such as transamination, dephosphorylation or decomposition proceed, proved by paper chromatography and n.m.r. studies (see relevant chapters). During the time the Absorbance increases, the rotation decreases, and during the time the absorbance remains constant, the rotation increases indicating that the racemization reaction takes place in the complex.

The reaction of L-Na-Glu with Cu^{2+} and PLP can be represented as

$$A \xrightarrow{k} B \xrightarrow{k'} C$$

where A represents the initial reactants, B the intermediate, and C the final products.

The reaction from A → B represents the formation of Cu^{2+}-SB complex which has been shown[4,5] to obey a second order kinetics. The concentration of one of the reactants in the reaction studied in this work was in an excess, and therefore the rate constants were calculated, both by the pseudo-first order method[6] and by the initial slope method[4] (table 3).

The rotations are very small, the first part of the reaction is very fast, there are difficulties of obtaining α_∞, because the second part overlaps and difficulty of obtaining initial slope because of the time required to prepare the solutions. Thus observed rate constants are not very accurate but nevertheless appear to be of the same order as those obtained by spectrophotometric methods. This shows that the change of rotation during the first part of the reaction is due to the formation of Cu^{2+}-SB.

The reaction from B → C represents the racemization of the L-amino acid part of the M^{n+}-Schiff-Base complex, and it is a first order reaction.

First order rate constants k were obtained from the equation

$$k = \frac{2.303 \log_{10}}{t} (a_t - a_\infty)$$

while k' was given by

$$k' = \frac{2.303 \log_{10}}{t} (a_\infty - a_t)$$

where a_t is the rotation at time t, and a_∞ is the rotation taken when each reaction was completed. (i.e. a_∞, in k, was the final reading for the first part of the reaction, and a_∞ in k' was the final reading for the second part of the reation.)

Since both $A \xrightarrow{k} B$ and $B \xrightarrow{k'} C$ reactions behave as first order reactions, and the first part is much faster than the second, the following is true.

$$-\frac{dA}{dt} = kA$$

or $$[A]_t = [A]_0 \, e^{-kt}$$

$$\frac{dc}{dt} = k'.B$$

where $K = \frac{k'}{k}$

$$\frac{dB}{dt} = kA - k'B$$

$$= KA_0 e^{-kt} - k'B$$

which on integration gives $[B] = A_0 \frac{k}{k'-k} (e^{-kt} - e^{-k't})$.

When B reaches its maximum value

$$\frac{dB}{dt} = 0$$

and $$t'_{max} = \frac{1}{k'-k} \ln \frac{k'}{k}$$

or $$= \frac{1}{k(K-1)} \ln K$$

t'_{max}, the time at which the first stage was completed, is shown in table 3 and the results agree with the time at the minimum of the curve.

Table 3 shows how the first order rate constant for the first part of the reaction increases as the pH increases, while the rate constant of the second part is less dependent of pH changes. Fig.6 shows the

Table 3

Reactions of L-glutamate and PLP in the presence of Cu^{2+}. First part of reaction calculated rate constants and t_{max}

Run	pH	10^3k /s^{-1}	$10^4k'$ /s^{-1}	K	ln K	max /min	k_2 * /$s^{-1}l^{-1}mol^{-1}$	k_2' ** /$s^{-1}l^{-1}mol^{-1}$
1	1.62	7.47	3.581	0.0479	-3.0378	7.1		0.106
2	2.63	7.66	4.525	0.0591	-2.8289	6.5		0.108
3	3.89	13.38	6.550	0.0489	-3.0169	3.9	0.127	0.189
4	5.13	18.16	7.044	0.0388	-3.2496	3.1		0.256
5	6.96	17.47	5.480	0.0314	-3.4620	3.4		0.2469
6	3.86	7.16	5.788	0.0808	-2.5153	6.4	0.157	0.1012
7	3.86	8.16	6.56	0.0804	-2.5208	5.6	0.141	0.115
8	3.86	12.68	5.78	0.0456	-3.0882	4.3	0.139	0.179
9	3.86	7.25	5.913	0.0816	-2.5064	6.3	0.138	0.1025
10	3.86	4.976	8.359	0.1680	-1.7838	7.2	0.127	0.211
11	3.86	9.309	8.817	0.0947	-2.3571	4.7	0.129	0.1974
12	3.86	7.837	7.965	0.1016	-2.2867	5.4	0.137	0.1108
13	3.86	7.945	8.264	0.1040	-2.2634	5.3	0.099	0.0842
14	3.86	10.44	5.331	0.0511	-2.9747	5.0	0.143	0.1476
15	3.86	10.88	4.46	0.041	-3.1944	5.1	0.141	0.1538
16	3.86	8.16	6.56	0.0804	-2.5208	5.6	0.138	0.1153
17	3.86	10.37	6.89	0.0665	-2.7114	2.8		0.1466
18	1.61	12.00	1.152	0.0096	-4.6460	6.5	0.111	0.1696
19	1.61	6.4	2.4	0.0332	-3.4051	9.2	0.124	0.0905
20	1.61	10.56	4.28	0.0405	-3.2057	5.3	0.107	0.1493
21	1.61	15.8	3.359	0.0213	-3.8510	4.2	0.074	0.2233
22	1.61	10.27	4.7	0.0458	-3.0842	5.3	0.095	0.1452
23	1.61	1.47	16.75	1.1395	0.1306	10.6		0.0623
24	1.61	5.11	7.437	0.1455	-1.9273	7.4	0.163	0.1083
25	1.61	7.0	2.5	0.0543	-2.9135	7.3		0.0989
26	1.61	9.12	12.9	0.1415	-1.9558	4.2	0.0643	0.0967
27	1.61	6.24	3.2	0.0513	-2.9704	8.4		0.088
28	1.61	7.0	2.4	0.0543	-2.9135	7.3		0.0989
29	1.61	7.36	3.3	0.0448	-3.1047	7.4	0.089	0.1040
30	1.62	7.29	3.4	0.0466	-3.0653	7.4	0.086	0.1030
31	6.98							
32	6.98	7.5	1.21	0.0161	-4.1269	9.3		0.106
33	6.98	15.59	6.45	0.0414	-3.1851	3.6		0.2204
34	6.98	21.88	6.94	0.0317	-3.4509	2.7		0.3093
35	6.98	5.63	7.49	0.1331	-2.0171	11.8		0.2388
36	6.98	15.83	5.12	0.0323	-3.4314	3.7		0.3356
37	6.98	15.59	10.23	0.0656	-2.7239	3.9		0.2204
38	6.98	31.18	4.5	0.0144	-4.2383	2.3		0.3305
39	6.98	17.66	7.72	0.0437	-3.1307	3.1		0.2496
40	6.98	15.59	6.45	0.0414	-3.1851	3.6		0.2204
41	6.98	14.32	7.26	0.0507	-2.9819	3.7		0.2024
42	6.98	15.66	7.56	0.0483	-3.0308	3.4		0.2213
43	5.16	11.43	8.226	0.0719	-2.6315	3.2		0.1616
44	5.16	14.88	10.347	0.0695	-2.6664	3.2		0.2103
45	5.16	10.967	8.797	0.0802	-2.5231	4.2		0.1550
46	5.16	11.31	7.266	0.0642	-2.7451	4.3		0.1599
47	5.16	4.412	7.588	0.1720	-1.7603	8.0		0.1871
48	5.16	6.973	6.437	0.0923	-2.3826	6.3		0.1478
49	5.16	9.329	8.245	0.0884	-2.4262	4.8		0.1319
50	5.16	11.518	6.625	0.0575	-2.8556	4.4		0.1221
51	5.16	11.564	9.715	0.0840	-2.4768	3.9		0.1635
52	5.16	11.13	8.371	0.0752	-2.5875	4.2		0.1573
53	5.16	9.331	8.318	0.0891	-2.4175	4.7		0.1319
54	5.16	13.40	10.235	0.0765	-2.5720	3.5		0.1894

Continued...

Table 3 continued

* The second order rate constant was calculated from:

$$k_2 = \frac{\text{initial slope}}{\Delta\alpha.[\text{Glu}]}$$

where initial slope is the slope of the rotation against time plot and it was calculated for the first few seconds of the initial part of the reaction; $\Delta\alpha$ is the difference in rotation in the beginning and the end of the first part of the reaction.

** k_2' was obtained from $\frac{k}{[\text{Glu}]}$.

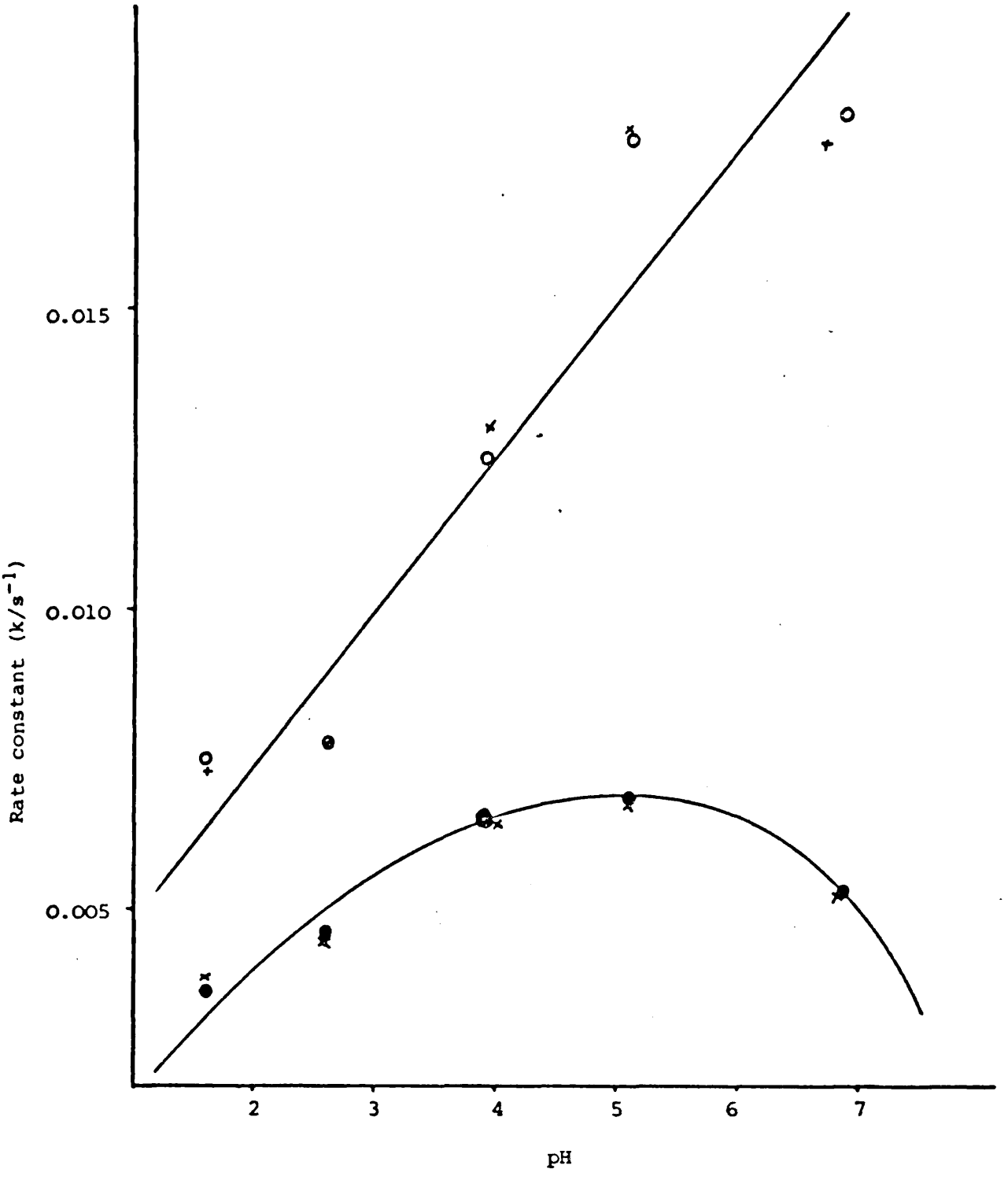

Fig. 6: The effect of pH on the rate constants.

- O variation of k with the acid concentration
- ● variation of k' with the acid concentration
- × calculated rate constant with SR-51-II Texas calculator

k values as a function of the pH graphically.

Table 4 contains the results of adding the materials in the order: Buffer, L-Na-Glu, Cu^{2+} and PLP.

Changing the order to:

Buffer, PLP, Cu^{2+}, L-Na-Glu,

there were small changes in the rates too, as table 5 describes.

(ii) Results from the reaction of various amino acids in the presence of Cu^{2+}, Al^{3+}, Ga^{3+}, In^{3+}, Tl^{3+}, Co^{2+}, Fe^{3+}, Cd^{2+}, Zn^{2+} ions and PLP

The following combinations (tables 6-14 and Fig. 8-12) were investigated under varying conditions of pH in order to see if other amino acids behaved similarly to Glutamic acid. The solutions used contained 70.75×10^{-3} mol.dm^{-3} amino acid, 1.89×10^{-3} mol.dm^{-3} PLP and 2.26×10^{-3} mol.dm^{-3} metal ion. The measurements were carried out at 35^{o}C and at wavelength 436 nm.

(iii) The effect of Zn^{2+} on the racemization of L-glutamate in the presence of PLP. Zn^{2+}-Cu^{2+} exchange in the Schiff-Base complex

The reactions have been studied at pH = 3.8 and at wavelengths 436 nm. The temperature remained constant at 20^{o}C. (Table 15)

L-glutamate in the presence of PLP and Zn^{2+} forms only the Zn^{2+}-SB complex. (Fig. 13)

The rate constants have been again calculated using both pseudo-first order rate constant and the initial slope method. (Table 16)

The rotation of L-Glu in just buffer was a_t = -0.033; in PLP a_t = -0.049; and in Zn^{2+} a_t = -0.034.

Table 4

First order rate constants for the reaction of L-Glutamate with PLP and Cu^{2+}.

Run no.	pH	First part of reaction			Second part of reaction			k/s^{-1}	k'/s^{-1}	pH after 21h
		slope	intercept	correl.	slope	intercept	correl.			
1	1.62	-0.19456	-1.2723	-0.9927	-0.00933	-1.2075	-0.99923	0.00747	0.0003581	1.60
2	2.63	-0.19955	-1.2615	-0.99115	-0.01179	-1.1819	-0.9981	0.0076594	0.0004525	2.60
3	3.89	-0.3486	-0.9935	-0.98618	-0.01707	-0.92697	-0.9995	0.01338	0.000655	3.86
4	5.15	-0.4731	-1.08479	-0.9966	-0.01835	-1.3461	-0.9992	0.01816	0.0007044	5.09
5	6.96	-0.4551	-1.01697	-0.45511	-0.01428	-0.99317	-0.9995	0.01747	0.000548	6.88

Table 5

First order rate constants for the reaction of L-glutamate with PLP and Cu^{2+}

Run No.	pH	First part (Complex formation)		Second part (Racemization)		K	t_{max} /min
		slope	k	slope	k'		
1	1.62	0.19456	$0.00747s^{-1}$	0.0095	$3.6\times10^{-4}s^{-1}$	0.02467	8.09
2	2.63	0.172	$0.0066019s^{-1}$	0.0115	$4.4\times10^{-4}s^{-1}$	0.06665	7.33
3	3.89	0.310	$0.012667s^{-1}$	0.017	$6.5\times10^{-4}s^{-1}$	0.051314	4.12
4	5.13	0.460	$0.01791s^{-1}$	0.01769	$6.8\times10^{-4}s^{-1}$	0.03797	3.16
5	6.96	0.4775	$0.01833s^{-1}$	0.01393	$5.346\times10^{-4}s^{-1}$	0.02913	3.31

Table 6(a)

Rotations of L-leucine in the presence of Ni^{2+}

time /min	pH=1.7	pH=1.8	pH=3.8	pH=5	pH=6.8
1	-0.010	-0.008	-0.009	-0.017	-0.043
2	-0.009	-0.008	-0.009	-0.016	-0.043
3	-0.008	-0.009	-0.011	-0.017	-0.044
5	-0.008	-0.009	-0.012	-0.018	-0.044
15	-0.009		-0.012	-0.018	-0.044
20	-0.009		-0.012	-0.018	-0.044
30	-0.009		-0.012	-0.018	-0.044

Table 6(b)

Rotations of L-leucine in the presence of Ni^{2+} and PLP

time /min	pH=1.7	pH=1.8	pH+3.8	pH=5	pH=6.8
1	-0.016	-0.009	-0.013	-0.025	-0.035
2	-0.013	-0.014	-0.014	-0.025	-0.036
3	-0.013	-0.014	-0.014	-0.026	-0.037
4	-0.013	-0.015	-0.015	p0.027	-0.038
5	-0.014	-0.016	-0.016	-0.028	-0.040
10	-0.016	-0.019	-0.019	-0.031	-0.042
15	-0.018	-0.021	-0.020	-0.033	-0.044
20	-0.019	-0.022	-0.022	-0.033	-0.044
25	-0.019	-0.023	-0.023	-0.033	-0.044
30	-0.019	-0.023	-0.025		-0.044
50	-0.019	-0.023	-0.024		
∞			-0.025		

In this thesis rotations are given in degrees

Table 7(a)

Rotations of L-leucine in the presence of Cu^{2+}

time /min	pH=1.7	pH=1.8	pH=3.8	pH=5	pH=6.8
1	-0.053	-0.062	-0.065	-0.017	-0.013
2	-0.054	-0.057	-0.065	-0.017	-0.013
3	-0.055	-0.060	-0.067	-0.018	-0.014
5	-0.054	-0.059	-0.068	-0.018	-0.014
10	-0.055	-0.060	-0.068	-0.018	-0.014
20	-0.054	-0.060	-0.067	-0.018	

Table 7(b)

Rotations of L-Leucine in the presence of Cu^{2+} and PLP

time /min	pH=1.7	pH=1.8	pH=3.8	pH=5	pH=6.8
1	-0.062	-0.063	-0.068	-0.019	-0.018
2	-0.062	-0.062	-0.068	-0.022	-0.023
3	-0.063	-0.064	-0.070	-0.025	-0.026
4	-0.064	-0.065	-0.071	-0.026	-0.028
5	-0.064	-0.066	-0.072	-0.028	-0.030
7	-0.067	-0.068	-0.076	-0.033	
10	-0.069	-0.069	-0.080	-0.036	-0.033
15	-0.069	-0.072	-0.082	-0.038	-0.033
20	-0.069	-0.074	-0.087	-0.038	-0.033
30			-0.086	-0.036	-0.031
50			-0.087		
∞	-0.076	-0.080	-0.084		

Table 8(a)

Rotations of L-Leucine in the presence of Al^{3+}

time /min	Rotation	
	pH=5	pH=6
1	-0.009	-0.007
2	-0.010	-0.008
3	-0.009	-0.009
5	-0.011	-0.009
10	-0.012	-0.009
15	-0.011	-0.009
	-0.012	-0.009

Table 8(b)

Rotations of L-Leucine in the presence of PLP and Al^{3+}

time /min	Rotation	
	pH=5	pH=6
1	-0.012	-0.011
2	-0.014	-0.013
3	-0.016	-0.014
4	-0.016	-0.015
5		-0.016
7	-0.017	-0.017
13	-0.018	-0.020
15	-0.019	-0.021
16	-0.019	-0.019
17	-0.020	-0.020
45	-0.020	-0.022
75		-0.022

Table 9(a)

Rotations of L-isoleucine in the presence of Ga^{3+}

time /min	pH=1.7	pH=1.8	pH=3.8	pH=5	pH=6.8
1	+0.030	+0.029	+0.028	+0.028	+0.030
2	+0.030	+0.029	+0.028	+0.028	+0.029
3	+0.030	+0.029	+0.028	+0.028	+0.029
5	+0.030	+0.029	+0.028	+0.028	+0.029
10	+0.030	+0.029	+0.028	+0.028	+0.030
15	+0.030	+0.029	+0.028	+0.028	+0.030
20	+0.030	+0.029	+0.028	+0.028	+0.030

Table 9(b)

Rotations of L-isoleucine in the presence of Ga^{3+} and PLP

time /min	pH=1.7	pH=1.8	pH=3.8	pH=5	pH=6.8
1	+0.026	+0.025	+0.025	+0.020	+0.029
2	+0.025	+0.025	+0.025	+0.020	+0.030
3	+0.024	+0.025	+0.023	+0.019	+0.028
5	+0.023	+0.023	+0.021	+0.013	+0.030
10	+0.019	+0.019	+0.017	+0.011	+0.028
15	+0.017	+0.018	+0.016	+0.010	+0.027
20	+0.016	+0.016	+0.015	+0.009	+0.026
25	+0.015	+0.016	+0.015	+0.009	+0.024
28	+0.015	+0.015	+0.015	+0.009	+0.025
∞	+0.015	+0.014	+0.013	+0.009	

Table 10(a)

Rotations of L-isoleucine in the presence of Al^{3+}

time /min	Rotation				
	pH=1.7	pH=1.8	pH=3.8	pH=5	pH=6.8
1	+0.027	+0.026	+0.026	+0.026	+0.025
2	+0.027	+0.025	+0.028	+0.025	+0.026
5	+0.027	+0.026	+0.028	+0.025	+0.026
10	+0.027	+0.026	+0.028		+0.026

Table 10(b)

Rotations of L-isoleucine in the presence of Al^{3+} and PLP

(only the first state of the reaction is obtained)

time /min	Rotation				
	pH=1.7	pH=1.8	pH=3.8	pH=5	pH=6.8
1	+0.025	+0.025	+0.027	+0.024	+0.028
2	+0.023	+0.024	+0.027	+0.024	+0.027
3	+0.024	+0.023	+0.026	+0.023	+0.028
4	+0.023	+0.021	+0.025	+0.023	+0.026
5	+0.024	+0.020	+0.024	+0.022	+0.025
6	+0.023	+0.020	+0.021	+0.022	+0.027
10	+0.024	+0.019	+0.020	+0.021	+0.028
15	+0.023	+0.017	+0.019	+0.020	+0.025
20	+0.020	+0.016	+0.018		+0.023
30	+0.016	+0.015	+0.017		+0.020
50	+0.010	+0.009	+0.014		
70	+0.006	+0.007			

Table 11(a)

Rotations of L-isoleucine in the presence of Ni^{2+}

time /min	Rotation				
	pH=1.7	pH=1.8	pH=3.8	pH=5	pH=6
1	+0.031	+0.028	+0.029	+0.024	-0.014
2	+0.031	+0.028	+0.028	+0.024	-0.014
5	+0.033	+0.029	+0.028	+0.023	-0.014
10	+0.033	+0.028	+0.028	+0.023	-0.014
20	+0.033	+0.029	+0.028	+0.023	-0.014

Table 11(b)

Rotation of L-isoleucine in the presence of Ni^{2+} and PLP

time /min	Rotation				
	pH=1.7	pH=1.8	pH=3.8	pH=5	pH=6
1	+0.028	+0.027	+0.026	+0.016	-0.012
2	+0.028	+0.026	+0.024	+0.016	-0.013
5	+0.026	+0.025	+0.021	+0.013	-0.018
10	+0.026	+0.024	+0.018	+0.012	-0.020
18	+0.025	+0.023	+0.016	+0.010	-0.021
30	+0.024	+0.021	+0.014	+0.009	-0.020
70	+0.022	+0.018	+0.012	+0.009	-0.021

Table 12

Rotation of various mixtures of PLP, AA and M^{n+}. (These did not change with time†)

pH	Cu^{2+} PLP L-histidine	Cu^{2+} PLP L-aspartic	Co^{2+} PLP L-isoleucine	In^{3+} PLP L-isoleucine	Al^{3+} PLP L-aspartic	Ni^{2+} PLP L-leucine
1.78	-0.808	-0.185	+0.026	+0.029	-0.235	-0.018
1.87	-0.754	-0.190	+0.028	+0.029		-0.
3.85	-0.854	-0.210	+0.024	+0.027		
5.00	-0.919	-0.227	+0.018	+0.028		
6.0	-0.708	-0.219	+0.004	+0.030	-0.279	

pH	Cu^{2+} L-histidine	Cu^{2+} L-aspartic	Co^{2+} L-isoleucine	In^{3+} L-isoleucine	Al^{3+} L-aspartic
1.78	-0.675	-0.160	+0.029	+0.031	-0.204
1.87	-0.785	-0.159	+0.030	+0.021	
3.85	-0.877	-0.191	+0.028	+0.029	
5.00	-0.937	-0.209	+0.027	+0.026	
6.80	-0.725	-0.173	+0.019	+0.029	-0.258

† The rotation was constant for the hour that the solution was tested indicating that complex formation or/and Racemization either are very fast or do not occur.

Table 13(a)

Rotations of L-aspartic acid in the presence of metal ions

time /min	Rotation					
	Cu^{2+}	Al^{3+}	Ni^{2+}	Ga^{3+}	Co^{2+}	In^{3+}
1	-0.126	-0.213	-0.106	-0.201	-0.204	-0.223
2	-0.125	-0.213	-0.105	-0.205	-0.195	-0.221
3	-0.125	-0.213	-0.105	-0.206	-0.189	-0.218
5	-0.122	-0.208	-0.105	-0.205	-0.188	-0.207
6	-0.122				-0.192	-0.204
7				-0.205	-0.190	
10	-0.122	-0.209	-0.105		-0.190	-0.205
25	-0.123	-0.209	-0.105	-0.205	-0.190	-0.205
40	-0.122	-0.209	-0.105	-0.206	-0.190	-0.205

Table 13(b)

Rotations of L-aspartic acid in the presence of metal ions and PLP

time /min	Rotation					
	Cu^{2+}	Al^{3+}	Ni^{2+}	Ga^{3+}	Co^{2+}	In
1	-0.143	-0.219	-0.163	-0.216	-0.200	-0.221
2	-0.144	-0.221	-0.163	-0.216	-0.204	-0.220
3	-0.145	-0.220	-0.164	-0.215	-0.200	-0.219
4	-0.144	-0.219	-0.165	-0.216	-0.199	-0.220
5	-0.144	-0.220	-0.166	-0.217		-0.220
6		-0.220	-0.167	-0.217		-0.220
9	-0.143		-0.172	-0.217	-0.200	-0.220
17	-0.144		-0.178			-0.220
25	-0.145		-0.178	-0.218	-0.200	-0.218
30	-0.144					-0.218
50	-0.144	-0.222	-0.178		-0.201	
60		-0.220		-0.217		
66		-0.221			-0.200	
75		-0.220				
85		-0.219	-0.178			

Table 14(a)

Rotations of L-cysteine in the presence of metal ions

time /min	Cu^{2+} Roth	Al^{3+} (1:10) Roth	Co^{2+} Roth	Ni^{2+} * Roth	Cd^{2+} * (1:10) diluted	In * (0.03a)	Ga^{3+} *
1	-0.360	-0.125	-0.119	-0.305	-0.137	-0.130	-0.080
2	-0.364	-0.125		-0.308	-0.128	-0.131	-0.081
3	-0.370	-0.125	-0.116		-0.126	-0.133	-0.083
4	-0.378	-0.126	-0.115	-0.320	-0.123	-0.137	
5	-0.380			-0.323	-0.128	-0.140	-0.092
7	-0.388			-0.335	-0.131	-0.147	
8	-0.391				-0.132		-0.098
9	-0.395	-0.127	-0.115			-0.153	
10	-0.398				-0.147	-0.157	-0.101
11	-0.400	-0.128					
12	-0.403		-0.115		-0.150		-0.104
13	-0.405	-0.127					
15	-0.409	-0.129			-0.158		
17	-0.413	-0.130					-0.117
20	-0.416	-0.131		-0.335	-0.154		-0.122
25							-0.128
30	-0.424	-0.132	-0.115			-0.193	-0.
35	-0.426	-0.133		-0.328	-0.159		-0.139
53				-0.329		-0.211	
60	-0.431						-0.153
90	-0.435				-0.168		-0.167
120					-0.169	-0.222	
177							-0.178
12 hours	-1.092	-0.320	+0.003	-0.407			

*The concentration of L-cysteine in the reaction mixture is 0.0226M

Table 14(b)

Rotations of L-cysteine in the presence of PLP and metal ions

time /min	Cu^{2+}	Al^{3+}	Co^{2+}	Ni^{2+} *	Cd^{2+}	In^{3+}*	Ga^{3+}
1	-0.360	-0.127	-0.124	-0.350		-0.219	-0.091
2	-0.365	-0.127	-0.122	-0.339	-0.214	-0.220	
3	-0.370	-0.128	-0.118	-0.342	-0.235	-0.221	-0.094
5	-0.379	-0.129	-0.115	-0.329	-0.239	-0.225	
6	-0.383	-0.129	-0.116		-0.239		-0.099
8	-0.392	-0.130	-0.114				-0.103
9	-0.395	-0.131	-0.114		-0.253	-0.231	
10	-0.398	-0.132	-0.113				
11						-0.233	
13	-0.405	-0.132	-0.114			-0.237	-0.111
15	-0.409	-0.135	-0.115		-0.250		
17	-0.413	-0.135	-0.117		-0.246		-0.119
18						-0.244	
20	-0.416	-0.135	-0.116				
23						-0.250	
25	-0.422		-0.114	-0.366			
28				-0.372	-0.249		
30	-0.425		-0.111	-0.379	-0.247		
32					-0.252		
36						-0.260	
38	-0.427	-0.135	-0.105				
39				-0.387		-0.262	
46	-0.429		-0.100			-0.267	
47	-0.430		-0.100			-0.269	
51					-0.252	-0.271	
58							-0.158
60	-0.431		-0.074			-0.275	
70			-0.064				-0.164
75			-0.061		-0.378		
80			-0.056				
90	-0.435		-0.039			-0.281	-0.168
95						-0.284	-0.170
100	-0.435		-0.033		-0.376		
105			-0.029				
110			-0.021				
120			-0.006				
124			0.000				
127						-0.289	
135			+0.008				
140						-0.290	
150			+0.032				
160			+0.055			-0.289	
180			+0.088				
	-0.990	-0.301	0.000	-0.423			-0.294

*the concentration of L-cysteine in the reaction mixture is 0.0226M

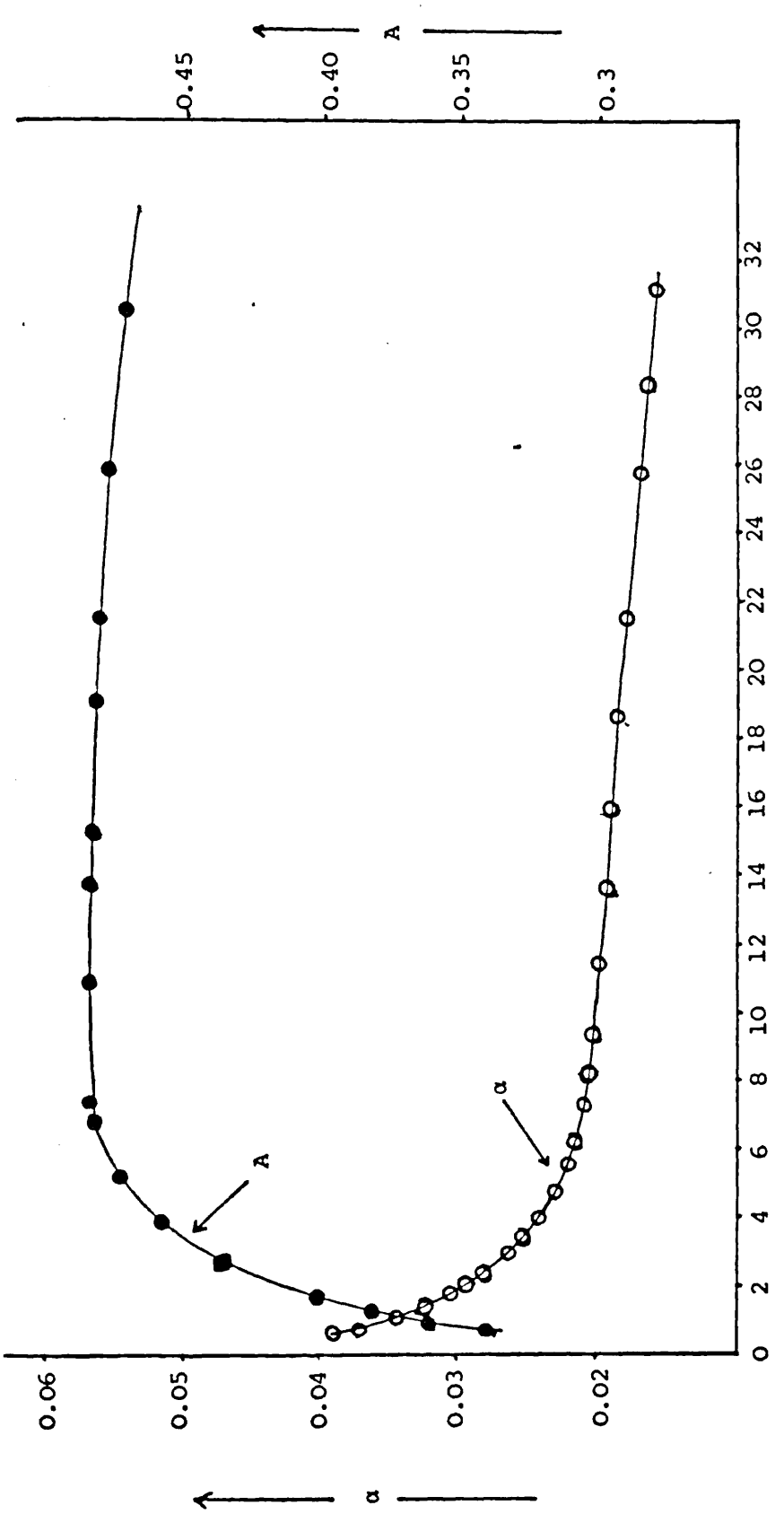

Fig. 8 : Plot of A and α of 70 mmol.dm^{-3} Glu + 0.189 mmol.dm^{-3}PLP + 2.26 mmol.dm^{-3} Co^{2+} against time/min at pH = 3.87.

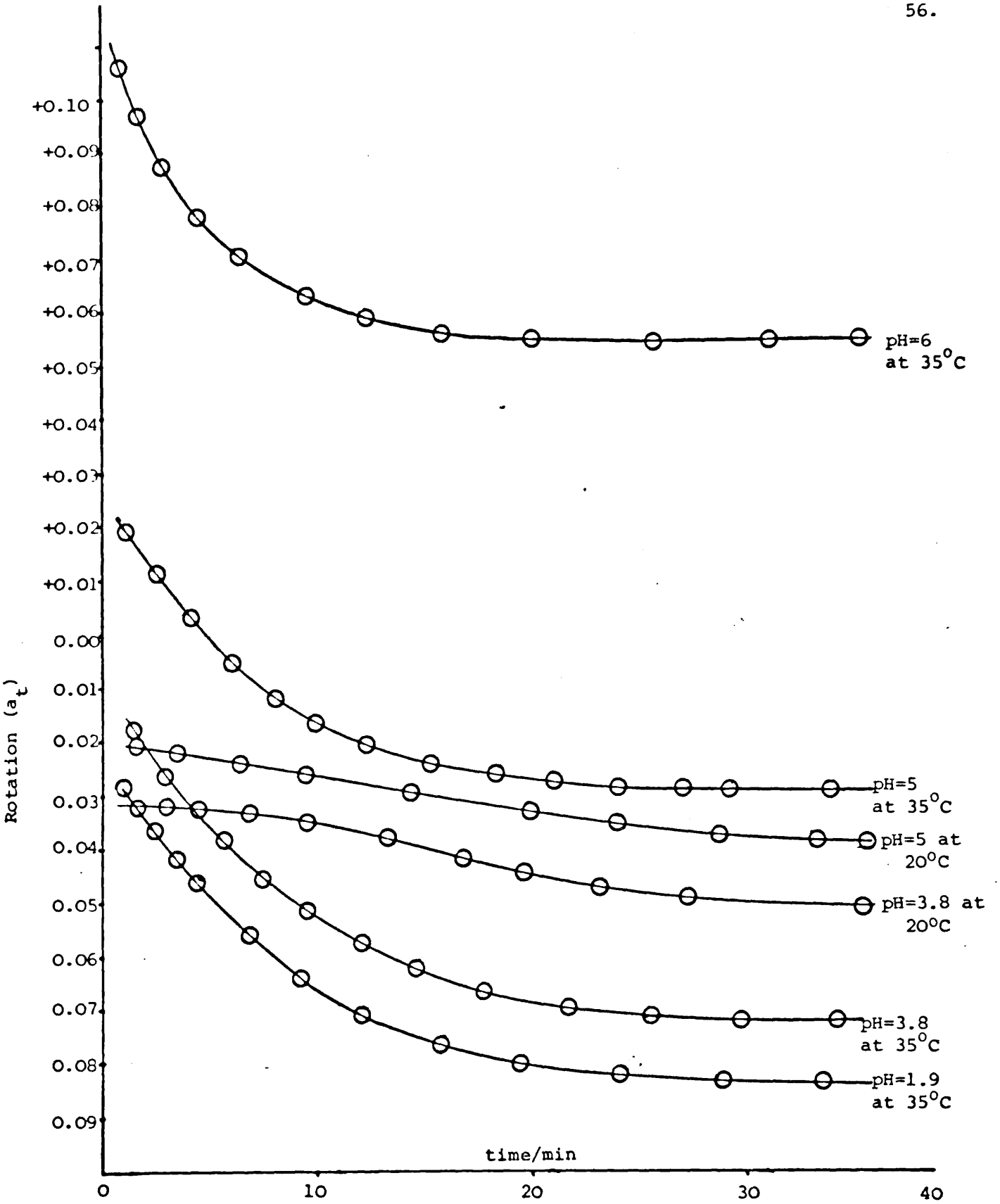

Fig. 9 : Rotations of L-isoleucine, as a function of pH, in the presence of Cu^{1+} and PLP.

Fig. 10: Plot of Rotation against time/min at pH=6.92 20°C and 436 nm

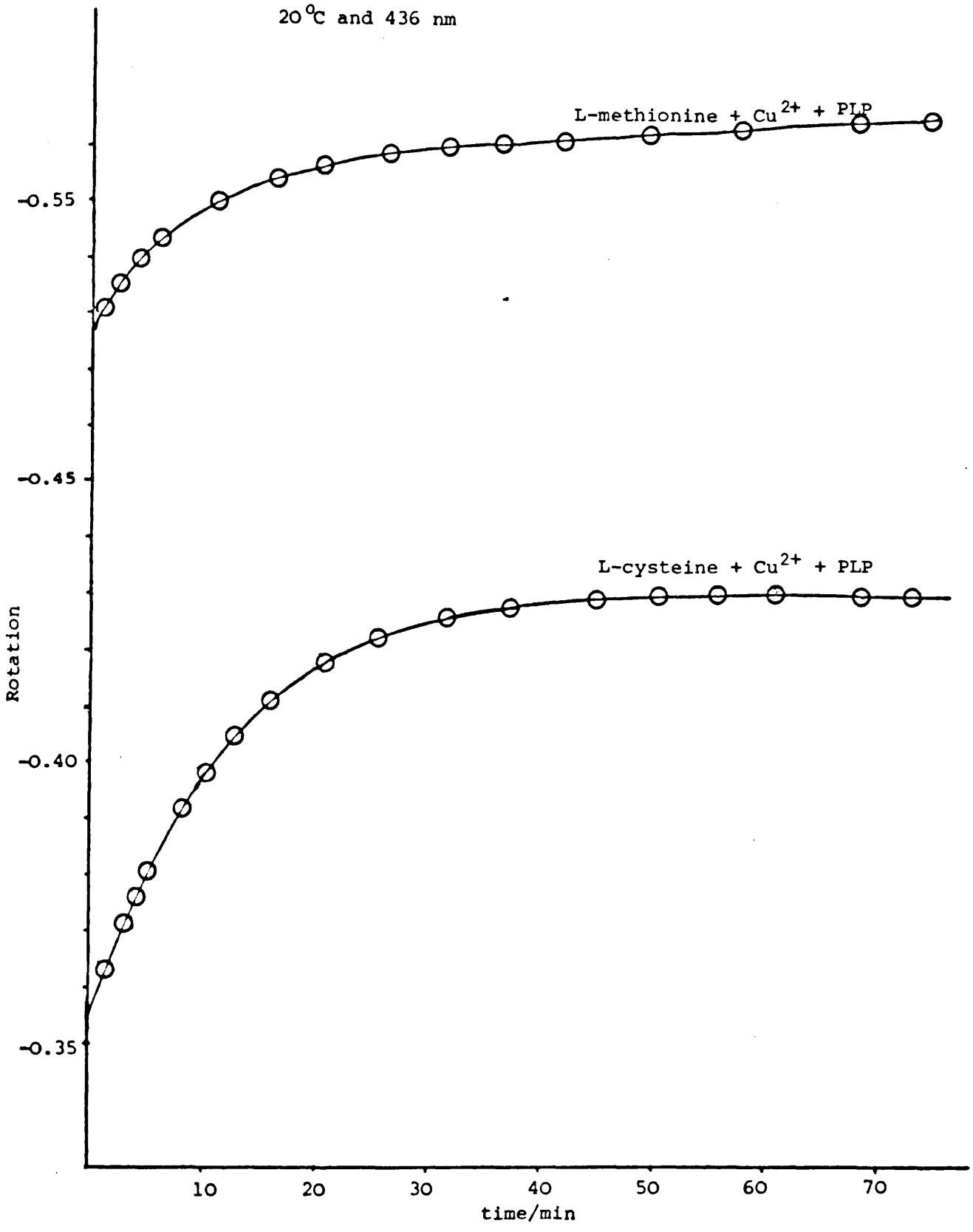

Similar plots were obtained in the absence of PLP, indicating that Cu^{2+} was racemizing both amino acids.

Fig. 11: Plot of Rotation vs time/min for the reaction of Co^{2+} with L-cysteine and PLP at pH = 6.92

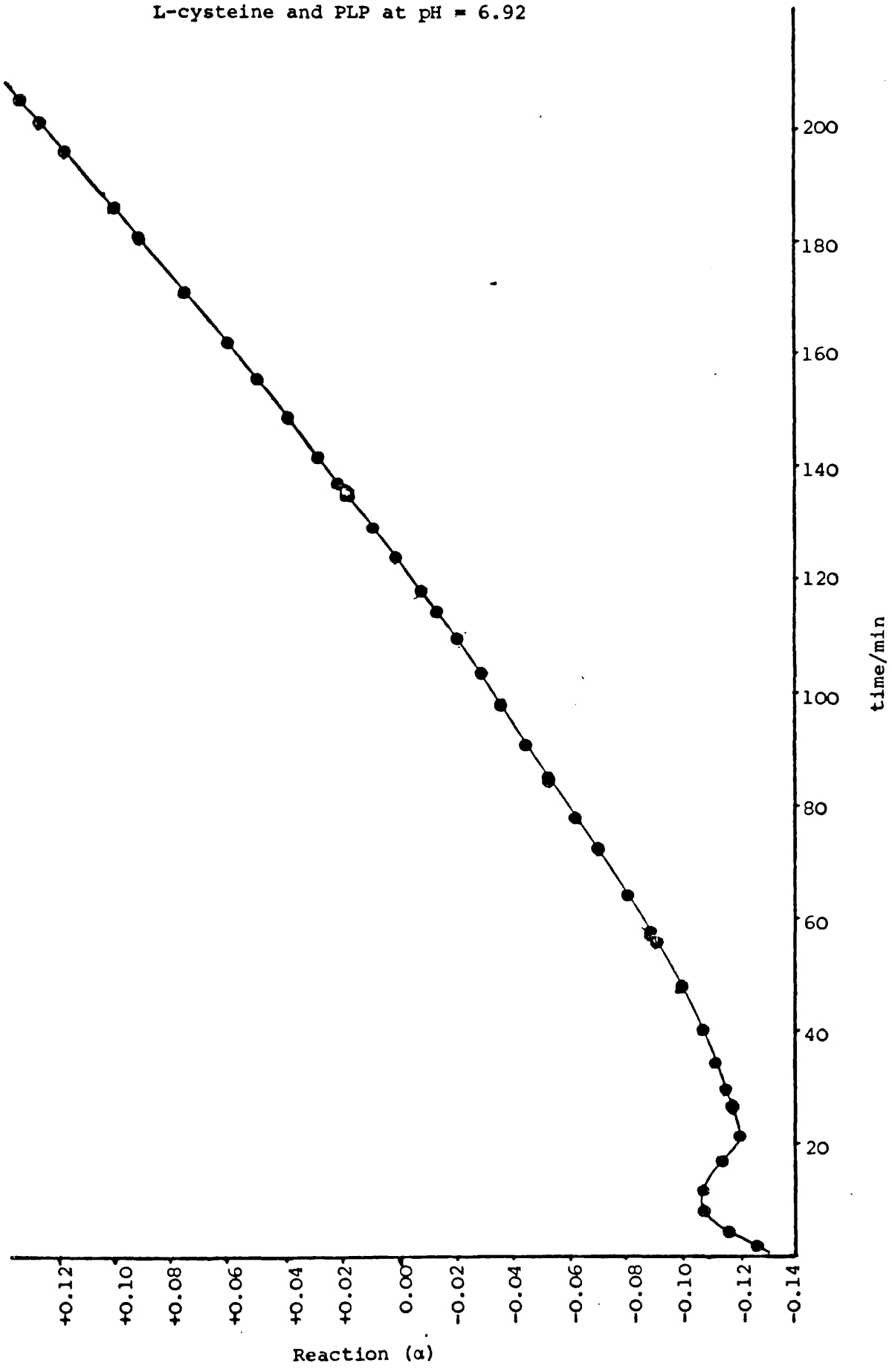

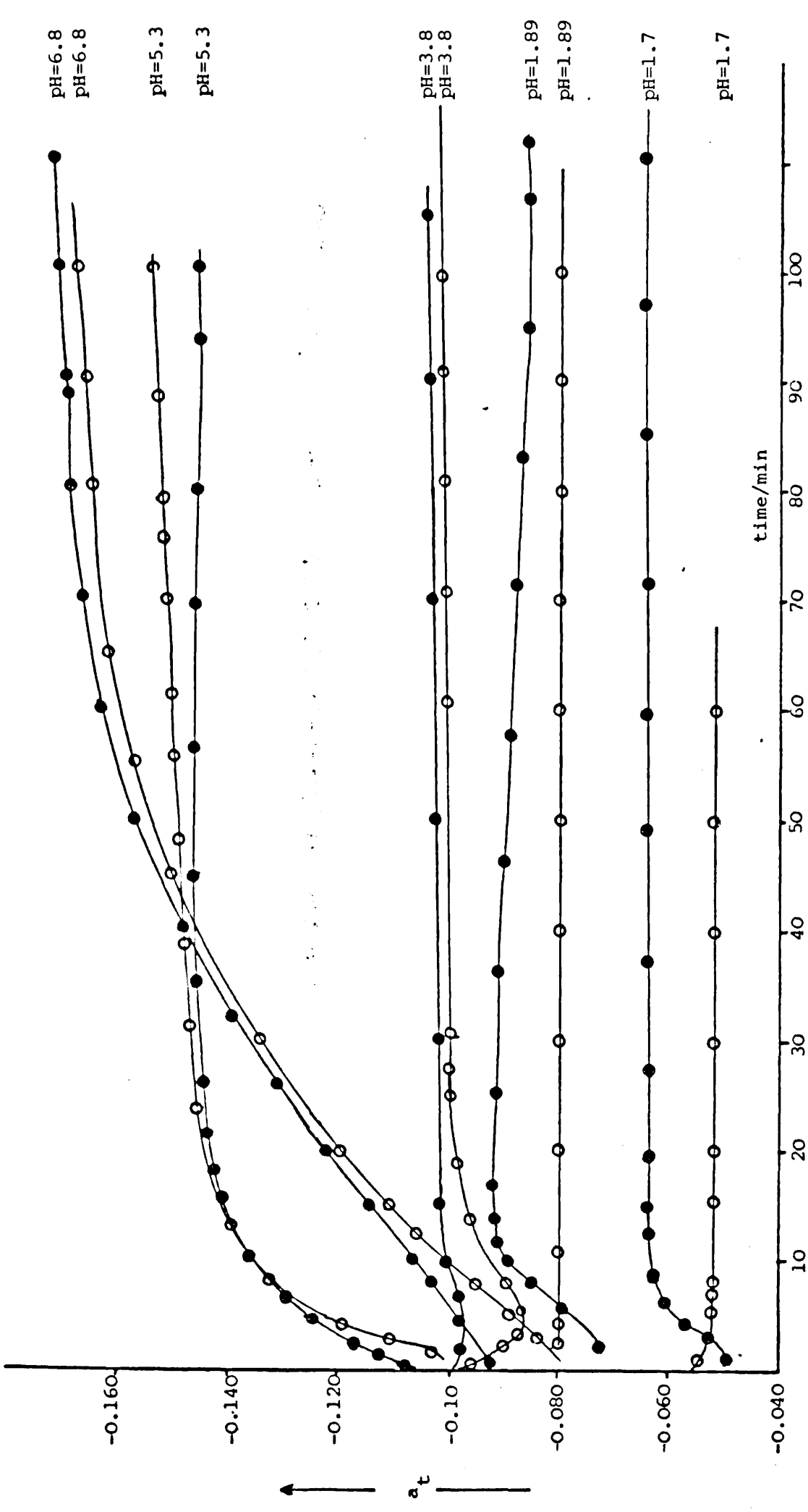

Fig.12: Plot of Rotation against time/min for the reaction of L-cysteine and Ga^{3+} and L-cysteine with PLO and Ga^{3+}

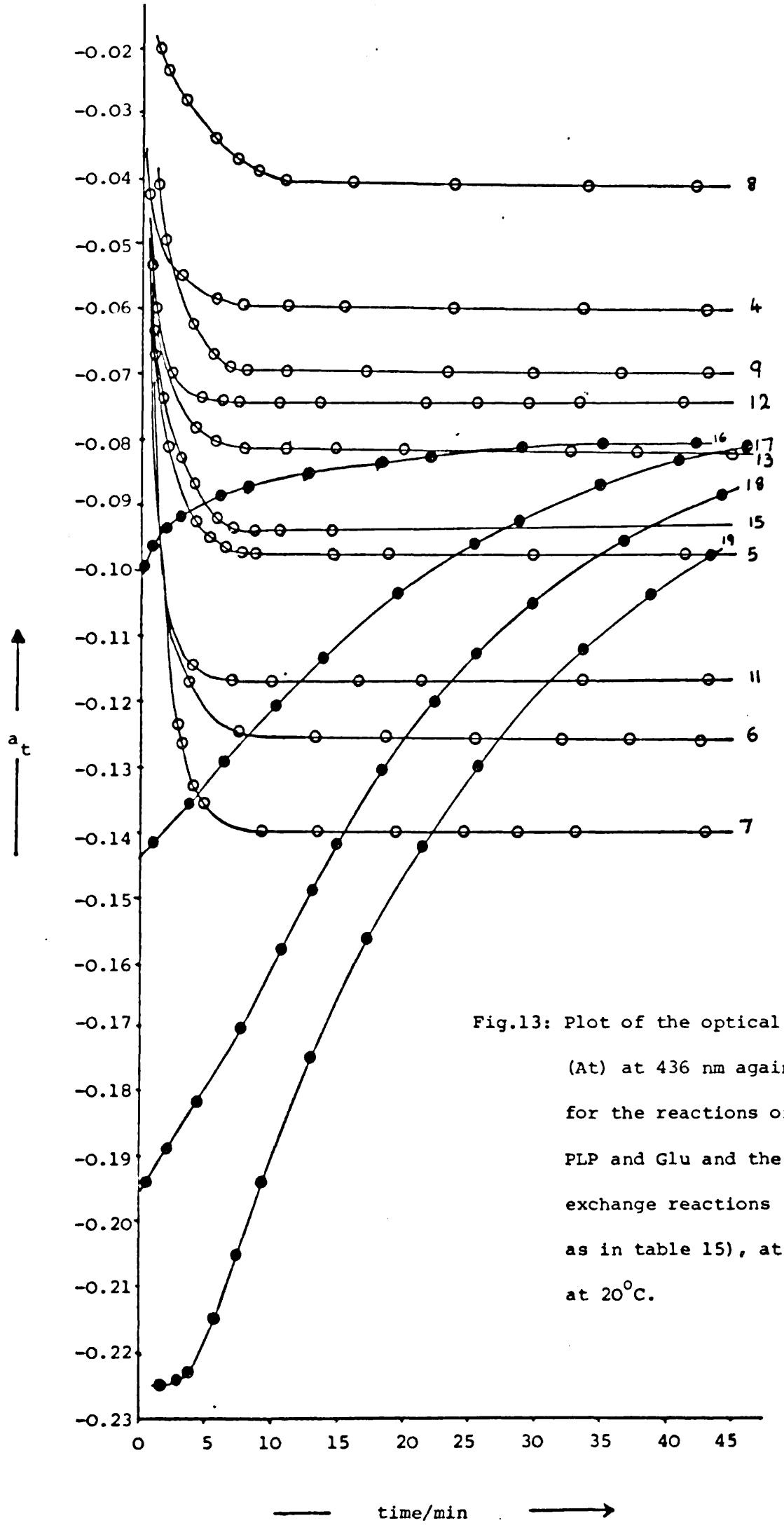

Fig.13: Plot of the optical rotation (At) at 436 nm against time/min for the reactions of Zn^{2+} with PLP and Glu and the Cu^{2+}-Zn^{2+} exchange reactions (numbered as in table 15), at pH=3.8 and at 20°C.

Table 15

Concentration of the solutions in the cell

Reaction No.	$10^2 \times$[L-Na-Glu] /mol.dm^{-3}	$10^3 \times$[Zn^{2+}] /mol.dm^{-3}	$10^4 \times$PLP /mol.dm^{-3}	Cu^{2+} /mol.dm^{-3}
1	7.0755			
2	7.076		-	-
3	7.076	-	2.8	-
4	7.076	2.26	1.13	-
5	7.076	2.26	2.8	-
6	7.076	2.26	4.5	-
7	7.076	2.26	5.66	-
8	2.358	2.26	2.8	-
9	4.717	2.26	2.8	-
10	7.076	2.26	2.8	-
11	9.434	2.26	2.8	-
12	7.076	0.755	2.8	-
13	7.076	1.509	2.8	-
14	7.076	2.26	2.8	-
15	7.076	3.77	2.8	-
16	7.076	2.26	1.13	2.26
17	7.076	2.26	2.8	2.26
18	7.076	2.26	4.5	2.26
19	7.076	2.26	5.66	2.26
20	2.358	2.26	2.8	2.26
21	4.717	2.26	2.8	2.26
22	7.076	2.26	2.8	2.26
23	9.434	2.26	2.8	2.26
24	7.076	0.755	2.8	0.755
25	7.076	1.509	2.8	1.509
26	7.076	2.26	2.8	2.260
27	7.076	3.77	2.8	3.770

Table 16

Reaction of L-glutamate with PLP in the presence of Zn^{2+}. Second order rate constants calculated by initial slope method.

Run	slope	$10^2 \times k/s^{-1}$	initial slope	$\Delta\alpha$	$k_2/s^{-1}.dm^3.mol^{-1}$
4	0.2675	1.026	0.010	0.022	0.10792
5	0.2725	1.046	0.028	0.058	0.1137
6	0.285	1.09	0.036	0.083	0.1022
7	0.2925	1.12	0.042	0.093	0.1064
8	0.115	0.44	0.004	0.028	0.1009
9	0.2525	0.969	0.009	0.035	0.0908
10	0.2725	1.046	0.008	0.39	0.1137
11	0.370	1.42	0.028	0.050	0.0989
12	0.350	1.343	0.010	0.024	0.0982
13	0.280	1.075	0.012	0.037	0.0884
14	0.2725	1.046	0.008	0.047	0.1137
15	0.235	0.902	0.010	0.038	0.0905
16	0.0232	0.0891			
17	0.0161	0.0618			
18	0.0163	0.0626			
19	0.0260	0.0998			
20	0.0120	0.0461			
21	0.0195	0.0749			
22	0.0161	0.0618			
23	0.0180	0.0691			
24	0.0150	0.0576			
25	0.0168	0.0645			
26	0.0161	0.0618			
27	0.02	0.0768			

3. Discussion

Several minor difficulties were encountered in the measurement of the rate constants.

Although the buffer was quite concentrated and it was expected to produce a constant, known pH in the mixture, very small differences in the pH were recorded during the reaction.

The concentrations of the solutions used were low, as in higher concentrations precipitates formed and disturbed the readings. This caused an increase in the error in the observed readings.

As glutamate is in an excess and itself is optically active, it gives a background rotation which must be taken into account.

For each pH value, a graph of rotation versus time has the same general shape and the time at which the maximum concentration of the intermediate is reached is the same (Fig. 4) for all the reactions. But at a specific time the value of rotation becomes more positive as the pH decreases. At lower pH values, the rotation is higher, but the shape of the curves remain the same (Fig.4).

To test the kinetics of these reactions, the plot of $\log a_t$ against time/min was obtained. The first part of the graph is not linear; it seems to be a continuous curve. This indicates that the treatment as a pseudo first-order reaction is not completely valid. However the second part seems to be linear from 7 min onwards so this part does seem to be first order.

Since Cu^{2+} and PLP are in much smaller concentration than L-glutamate, it is possible to think that the Kinetic order, initially depends upon Cu^{2+} and/or PLP. Table 3 proves this point. No order can be found in Glutamate or its reaction product because they are present in an excess.

Glutamate does not seem capable of mutarotation unless PLP and Cu^{2+} are present (Table 2). The first part of reaction is more likely to be

due to the formation of the Cu^{2+}-SB. This was also proved from the ultraviolet spectra, where the absorbance as a function of time (table 5) increases up to a certain point (about 7-10 min) at which it remains constant and then again (after 30-50 min) drops from that constant value. In the second part of the reaction, not all the glutamate, which is present in an excess, is racemized. The final rotation is due to the presence of the unreacted optically active glutamate. Only that glutamate which forms the Schiff-Base-Cu^{2+} complex undergoes steric change at the α-carbon atom.

Table 17 contains some spectrophotometric results[4,5] for the reaction of PLP in the presence of L-glutamate and Cu^{2+}. These results[4,5] show that the formation of Cu^{2+}-Schiff-Base complex should obey a second order kinetics and they agree with the results obtained by the polarimetric technique (table 3).

If we consider the series of reactions to be:

$$\underset{A}{Cu^{2+} + PLP + Glu} \xrightarrow{k} \underset{B}{SB\text{-}Cu^{2+}\ complex} \xrightarrow{k'} \underset{C}{rac.\ SB\text{-}Cu^{2+}\ complex}$$

then, using numerical integration for the two rate constants k and k', the change in rotation with time and hence t_{max} was calculated. See table 3. The results however were not completely satisfactory because of the experimental errors involved.

The line for the first process of the plot $\log(a_t - a_\infty)$ vs time, was extrapolated back to t = 0, using the value of k, the value of a_0 was derived using $\log_{10}(a_0 - a_\infty)$. These values were in good agreement with the rotation of L-glutamate observed in the presence of just Cu^{2+}.

Changing the concentrations of Cu^{2+}, PLP and L-glutamate and observing the effect on the rates, it was found that the reactions were dependent upon the PLP concentration. The rates increase as the

Table 17

Spectrophotometric rate data for the reaction of pyridoxal phosphate, sodium glutamate, and Cu^{2+} at 25°C in acetate buffer.

pH	10^3[PLP] /mol.dm^{-3}	10^3[Glu] /mol.dm^{-3}	10^3[Cu^{2+}] /mol.dm^{-3}	k_2 /mol^{-1}.dm^3.s^{-1}
3.99	0.1	8.0	0.2	0.146
3.99	0.1	8.0	1.0	0.138
3.99	0.2	8.0	0.2	0.146
3.99	0.3	8.0	1.0	0.138
3.99	0.5	8.0	1.0	0.140
3.99	0.5	8.0	0.2	0.148
3.99	0.2	6.8	0.4	0.148
3.99	0.2	1.86	0.4	0.146
3.99	0.2	8.0	0.4	0.146
3.99	0.2	11.0	0.4	0.146
3.99	0.2	3.16	0.4	0.139
3.55	0.2	3.16	0.4	0.147
3.55	0.2	8.0	0.4	0.126
3.55	0.2	11.0	0.4	0.122
3.55	0.2	18.6	0.4	0.119
5.7	0.1	8.0	0.2	0.410
5.7	0.2	8.0	0.2	0.407
5.7	0.3	8.0	0.2	0.405
5.7	0.1	8.0	4.0	0.402

concentration of PLP increases. Cu^{2+} has almost no effect in the rate, it only traps the SB formed hence promoting the reactions towards the SB formation.

The rate of formation of Zn^{2+}-Schiff-Base complex was found to be equal to the rate of formation of Cu^{2+}-Schiff-Base complex again proving that the metal traps the SB. The stable value of rotation after the first part of the reaction was completed indicated that there was no racemization taking place, as it appears in Cu^{2+} case. When an equivalent amount of Cu^{2+} was added to the solution at the end of the reaction with Zn^{2+}, the rotation increased at the same rate, as in the second part of the reaction with Cu^{2+} alone with PLP and L-Glu. This indicated that a fast replacement of Zn^{2+} by Cu^{2+} took place in the SB complex. This was then followed by Cu^{2+} racemization of L-glutamate part of the copper Schiff-Base complex as before.

From the rotation measurements it appeared that all in the reactions of L-glutamate and PLP with Al^{2+}, Co^{2+}, Ga^{3+} and Zn^{2+} (Fig.8); of leucine and PLP with Ni^{2+}, Cu^{2+} and Al^{3+} (tables 6 - 8); of isoleucine and PLP with Cu^{2+}, Ga^{3+}, Al^{3+} and Ni^{2+} (Fig.9, Tables 9-11) and of valine with PLP and Cu^{2+} only of the first stage of the reaction occurred. The reaction mixtures of histidine and PLP with Cu^{2+}, Al^{3+} and Zn^{2+}; isoleucine with Co^{2+} and In^{3+}; and aspartic acid with Cu^{2+} and Al^{3+} had a constant rotation (tables 12,13) throughout the estimated time required for the reaction to take place, indicating that there was no first or second part of the reaction.

Co^{2+}, Cu^{2+} and Ga^{3+} appear to give immediately the second part of the reaction, only with Cysteine and Methionine (Table 14, Fig.11,12). Further work is required using Stopped flow measurements to show if there is initially a very fast complex formation which immediately leads to racemization, or the changes in rotation are only related to the complex formed, or the dissociation of the amino acids under the

conditions employed. It appears also (Fig. 10) that Cu^{2+} racemizes methionine even when PLP is absent. (Similar kind of curves appear with and without PLP under the same experimental conditions.

Cu^{2+} ion however was the only one to give the first and the second stage of the reaction and L-glutamate was the only amino acid to racemize under the experimental conditions used, only in the presence of PLP and Cu^{2+}.

The explanation for the behaviour of Cu^{2+} in this system could arise from its electronic configuration. The d electron configuration of this ion is d^9 and it is capable of forming square planar, tetrahedral and octahedral complexes. An octahedral or tetragonally distorted octahedral structure is the most probable for the Cu^{2+}-SB complexes. For this configuration the Jahn-Teller effect is operative, with an elongation along one four-fold axis, producing a planar array of four short and two trans long Cu^{2+}-ligand bonds. The complete removal of the two ligands along the z axis leads to a square planar complex.

In the case of racemization, the planarity of the ligand system in the xy plane in the transition state means that the electrons are directed toward the heterocyclic nitrogen; therefore the inductive withdrawal of electrons from the C_α of the amino acid is increased, labilising the groups attached to it. In the transition state, C_α is sp^2 hybridized, and it is trigonally planar bonded with the other atoms.

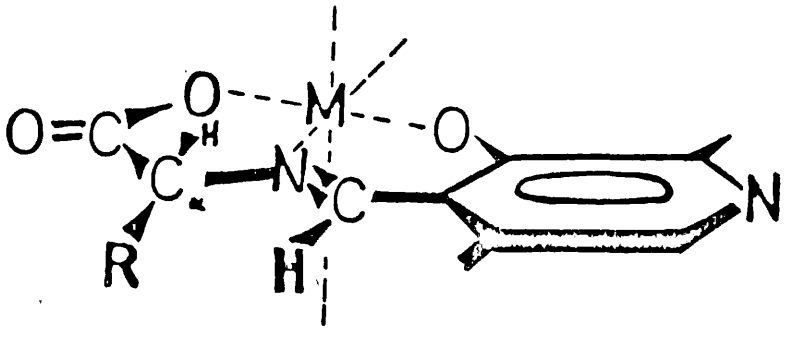

$SB-Cu^{2+}$ complex

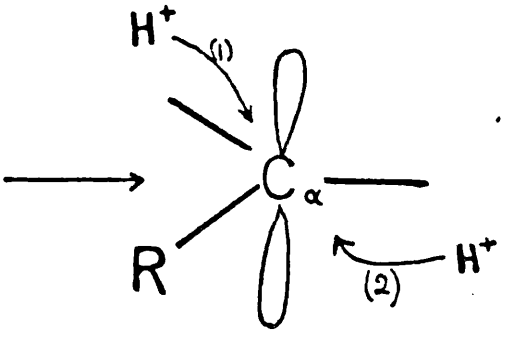

Transition state,
Sp^2 hybridization
planar trigonal bonding

A new proton can attack this intermediate in two ways: (1) and (2) In the first case the product will be an optical isomer, racemization takes place while in the second case, steric retention of configuration will give the initial amino acid.

The Cr^{2+} ion (configuration $t_g^3 e_g'$) is also subject to Jahn-Teller effect, and would therefore be expected to give similar results to Cu^{2+}. However, the Cr^{2+} system can not be investigated under the present conditions, as it is oxidised to Cr^{3+}, unless the reactions can be repeated under nitrogen atmosphere.

If the racemization by Cu^{2+} is due to the planar system formed, then other metals which can form such square planar structures might be active. Further work on this point is required.

It was previously[2,9] found using CPK models, that in SB, in the absence of metals, but planar because of H-bonding, that the reactivity of the C_α-H_α bond is very sensitive to the number of C substituents[3,5] on the amino acid side chains. It was also suggested that bonds parallel to π-orbitals are more labile than others for example the C_α-H bond, in certain compounds. If R (Fig.14) is bulky, reduction in the coordination number of C_α relieves steric strain, so the bulky R group would be expected to produce a faster rate of racemization for a dissociative mechanism. The fact that Schiff-bases with bulky (R) groups racemise slowly or not at all, leads to the conclusion that the main effect is steric, in that in the transition state, the bulky R group and the C_4' proton would be close together and give steric strain, thus increasing the activation energy of the reaction.

Tsai et al[1] have discussed the steric effects of the substituents in the following way:

The C substituents of the amino acids should also affect the angle between σ-π orbitals in a way, and this can cause a major effect on the rate constant

$$k \text{ actual} = kN_A.\cos^2\theta_A + kN_B.\cos^2\theta_B$$

where k is the rate constant at 100% σ-π orbital overlap; θ_A and θ_B are the angles between the σ orbital of the conformers A and B respectively, and the π orbital; and N_A and N_B are the percentage of conformers A and B respectively. A small steric interaction between the R group and the C_4'-H_4' group, will cause a small θ_A and therefore the result will be a higher rate constant for the reaction. Coplanarity of the σ-π orbitals will give 100% overlap as $\cos^2\theta = 1$.

REFERENCES

1. Dunathan, H.C., Adv. Enzymol. 35, 79 (1971).

2. Ming-Daw Tsai, Herschel, J.R. Weintraub, Stephen R. Byrn, Ching-Jer Chang, and Heinz G. Floss, Biochemistry, 17, 16, 3177 (1978).

4. M.E. Farago, Personal communication.

5. M.E. Farago, M.M. McMillan and S.S. Sabir, Inorg. Chem. Acta 14, 207 (1975).

6. E.A. Moelwyn-Hughes, "Kinetics of Reactions in Solution" Oxford University Press (1933).

7. M.L. Tobe "Inorganic reaction mechanisms", Nelson Publication (1972).

8. R. Potenzone, Jr. Cavicchi, E. Weintraub, H.J.R. and A.J. Hopfinger, Comput. Chem. 1, 187 (1977).

9. M.D. Tsai, S.R. Byrn, C.-J. Chang, H.G. Floss and J.R. Weintraub, Biochemistry, 17, 3183 (1978).

CHAPTER 3

RATES OF FORMATION OF METAL-SCHIFF-BASE COMPLEXES

1. Experimental

Ultraviolet and visible spectra in solution were recorded on a Unicam SP8-100 recording spectrophotometer fitted with a scale expansion unit and a thermostat, using 1 cm silica cells. The rates of the reactions were determined by recording the change in the absorbance as a function of time at a certain wavelength. The reactions were carried out at 25°C but higher and lower temperature range has been used in some cases. The concentration of the complexes was between $1\text{-}2\times10^{-4}$ mol.dm^{-3}. The molecular weights were assumed from the analysis. The reactions were taking place in buffer solutions. The buffers used were containing sodium acetate and hydrochloric acid and each of them was calibrating in a different pH value (see Appendix I). The cells and solutions were thermostatted for 20 minutes and the pH was measured with a Pye Dynacap pH meter. The ionic strength of the solutions was maintained constant using KCl. Initial slopes were measured over the first 40 s from the absorbance vs time plots. The paper flow was arranged so that approximately linear lines about 45° to the axes were obtained over this time period.

2. Results from the ultraviolet spectra measurements

Initially the ultraviolet spectra of the ligands were recorded under the same experimental conditions used for the study of Metal(III)-Schiff-base complexes. Shifts from the bands of the free ligands were used as a proof for the Metal-Schiff-base formation and the products

of the reactions.

The molecular extinction coefficient (ε_m), calculated from the u.v. spectra of PLP in a series of pH values for each wavelength and the absorption maxima (table 18, Fig. 14), are in good agreement with previous work[1].

The spectrophotometric changes occurring during the reaction of metal ions, PLP and amino acids in a series of pH values are shown in Figs. 20, 22 - 26 . These u.v. spectra are characterised by an initial shift of the u.v. bands and by a large increase in absorption between 310 and 340 nm.

When the kinetics of the reactions were studied at 374 nm, there was an initial induction period (Fig.15a) for the first few seconds, the first stage of the reaction with the higher concentrations of PLP or metal ion, where the reactions are much faster, the induction period cannot be detected (Fig.15b).

After the induction period the absorbance increases until the second stage becomes significant, causing the absorbance to decrease.

The first stage of the reaction is due to the formation of the Metal(III)-Schiff-base complexes, while the second stage of the reaction is probably a complicated process, involving not only transamination, but other processes including dephosphorylation as the n.m.r. and chromatography results have shown.

(i) Formation of M^{3+}-PLP complex

Unlike Cu^{2+}, Ga^{3+} and Al^{3+} form a strong complex with PLP, as the u.v. spectra show. (Fig. 16, 17).

From the spectrophotmetric results a simple value of K can be obtained from

$$K = \frac{[PLP\text{-}Ga]}{[PLP][Ga^{3+}]}$$

Table 18

pH	maxima/cm^{-1}	Absorbance	ε_m
1.68	33,900	1.268	6340
	29,860	0.362	1810
1.86	33,850	1.195	5975
	29,800	0.340	1700
3.88	33,800	0.510	2550
	30,000	0.460	2300
	25,860	0.740	3700
4.90	30,500	0.490	2450
	25,800	0.950	4750
6.65	30,500	0.510	2550
	27,780	1.05	5000

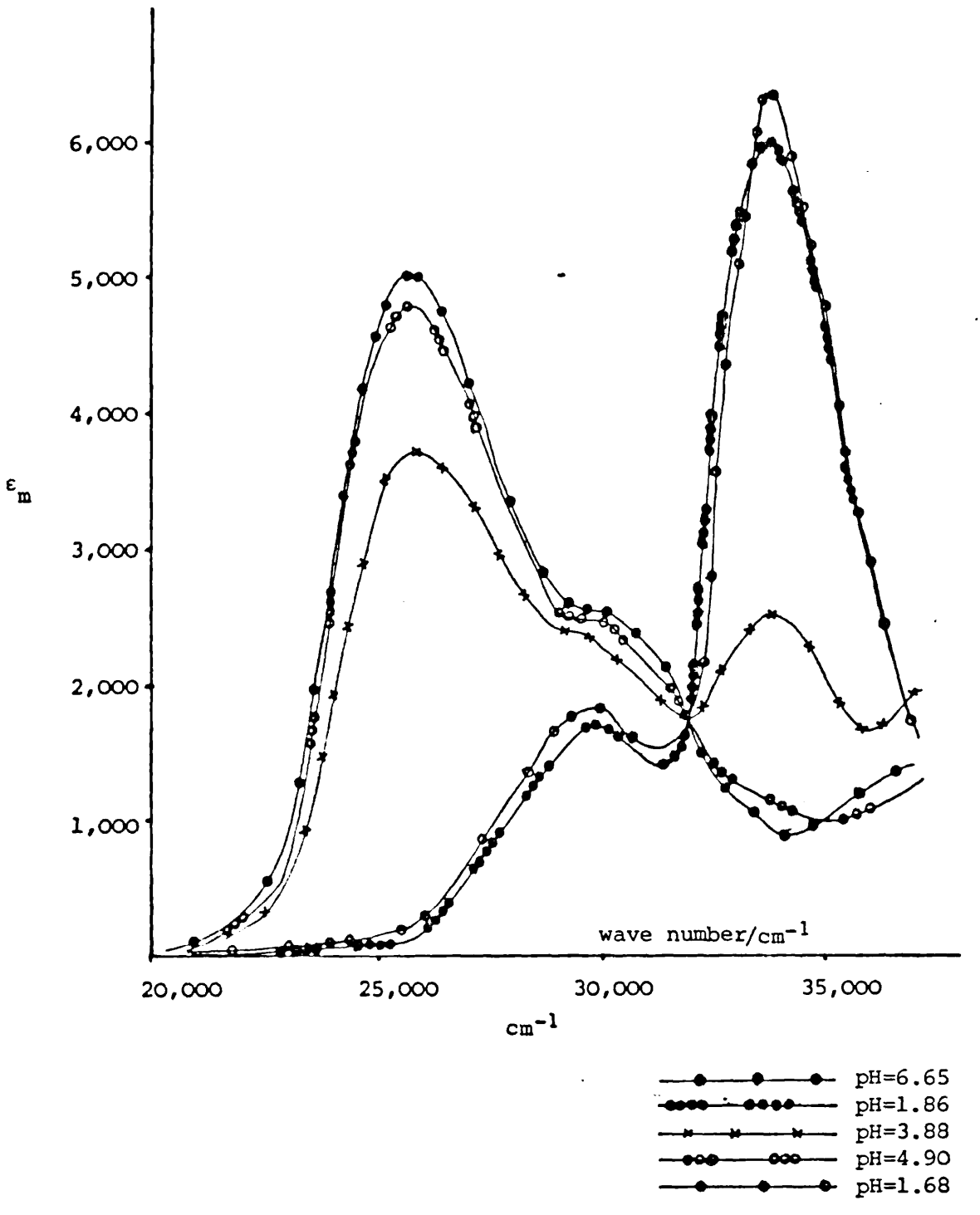

Fig. 14: Plot of ε_m against wavenumber for PLP in acetate buffer

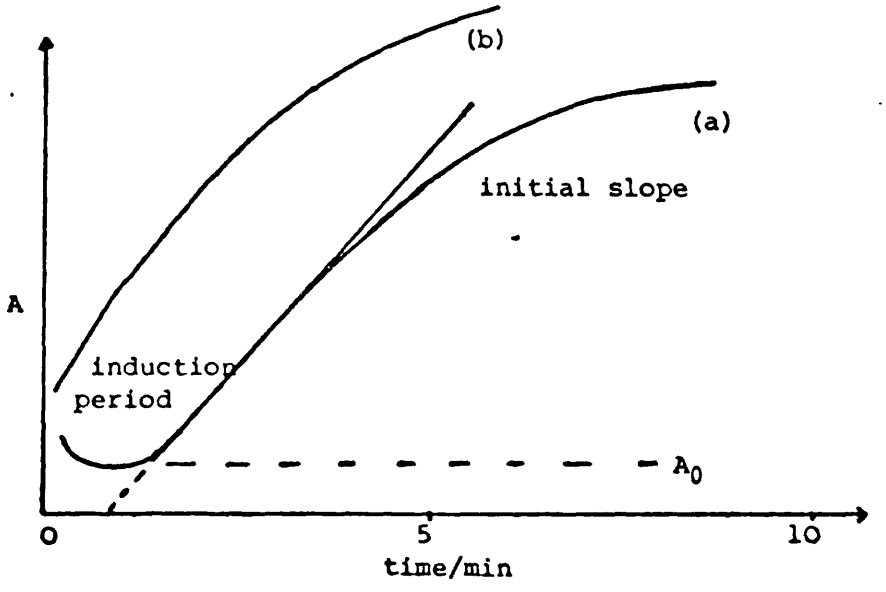

Fig.15: Plot of A vs time

(a) for solution (1)

(b) for solution (2)

(in table 20)

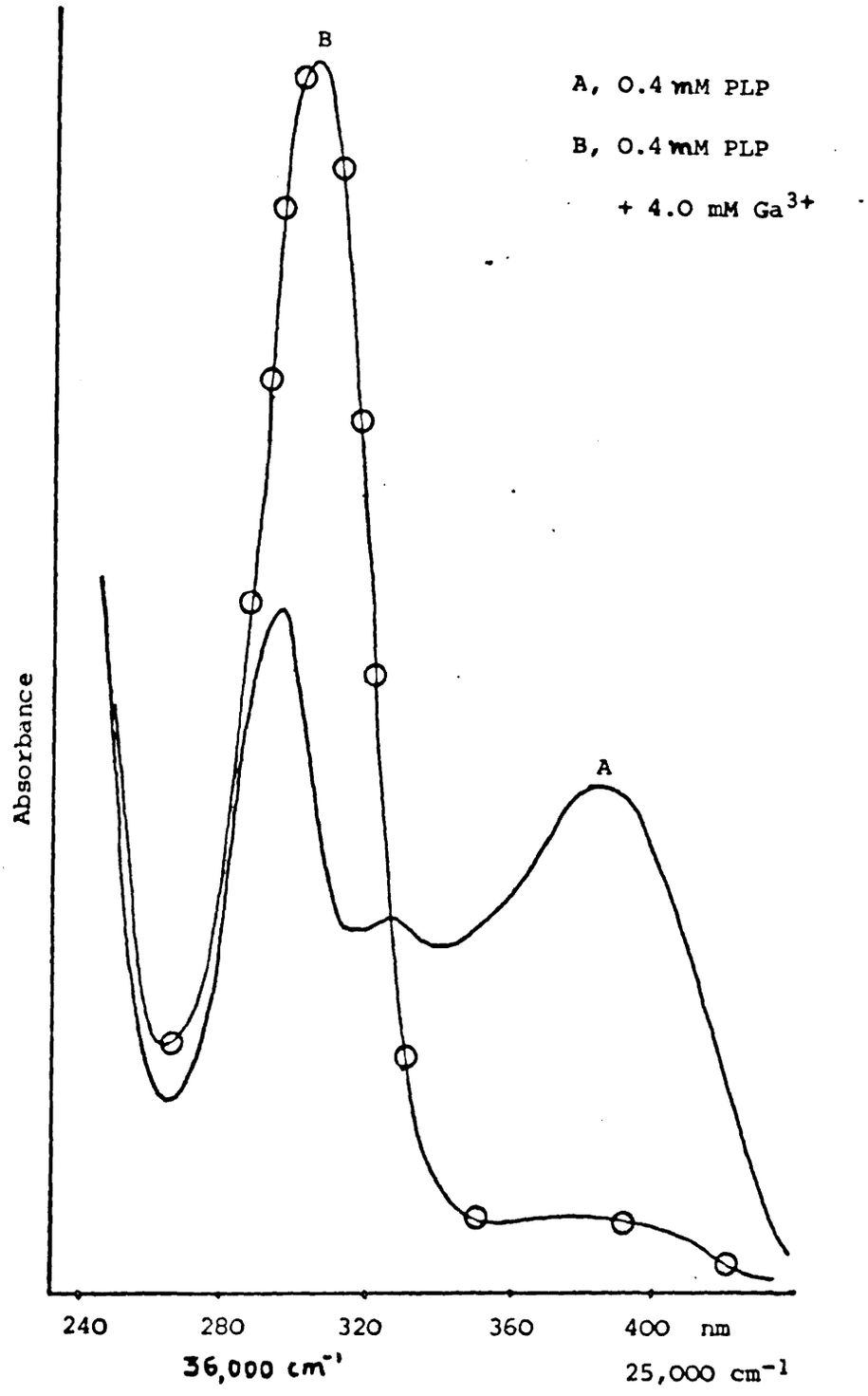

Fig.16: u.v. spectra at 25°C and at pH=3.88.

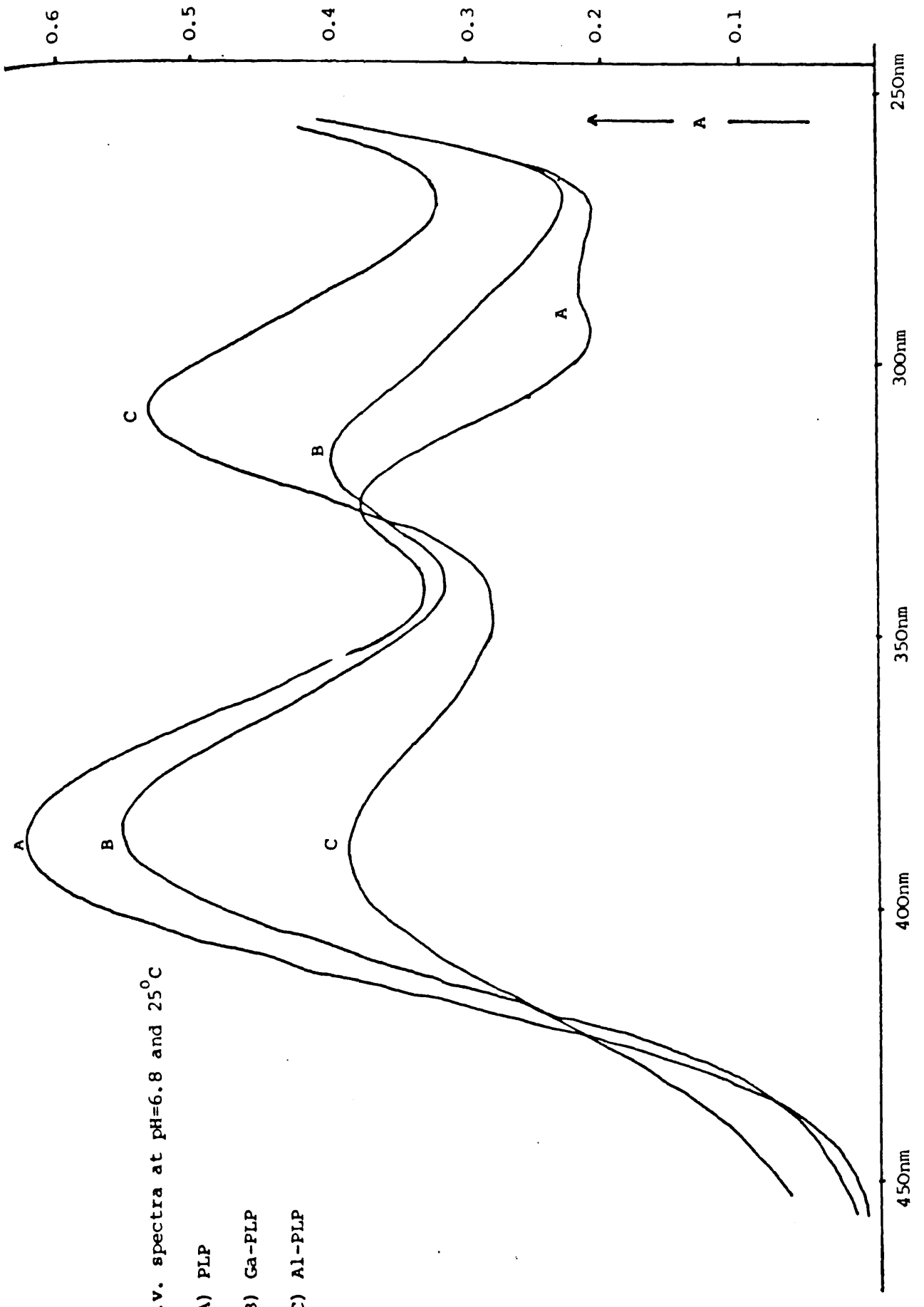

Fig. 17: u.v. spectra at pH=6.8 and 25°C

(A) PLP

(B) Ga-PLP

(C) Al-PLP

where [PLP-Ga] is the concentration of the complex formed estimated from the absorbance at 374 nm. The absorbance A was taken as zero for a 100% reaction. A series of mixtures of varying concentrations of Ga^{3+} and PLP were made up and the absorbances were measured at 374 nm. From these values the equilibrium constant was determined (Table 19).

(ii) First Stage of the Reactions

(a) Determination of the Rate of the Reaction of Ga^{3+} with PLP and L-aspartic acid at pH=3.8

The following series of solutions was made up by using 0.0038 $mol.dm^{-3}$ of PLP, 0.08 $mol.dm^{-3}$ L-aspartic acid, 0.01 $mol.dm^{-3}$ $Ga(NO_3)_3.9H_2O$ and buffer acetate (pH=3.8).

solution	Buffer	L-Aspartic acid	PLP	Ga^{3+}
1	2.65 cc	0.2 cc	0.1 cc	0.05 cc
2	2.60 cc	0.2 cc	0.1 cc	0.10 cc
3	2.55 cc	0.2 cc	0.1 cc	0.15 cc
4	2.45 cc	0.2 cc	0.1 cc	0.25 cc

The change in the absorbance as a function of time was recorded at 374 nm. The absorbance initially increased and then gradually decreased (Fig.15).

The graphs obtained from the plots of $\log(A_\infty - A_t)$ against time/min (Fig. 18), were linear for the first 7 minutes, indicating a possible first order or pseudo first order reaction, but after 7 minutes a curve was obtained. The absorbance gradually increased up to about 40 min and then slightly decreased. Table 20 shows the first order rate constants determined from the plots of log $(A_\infty - A_t)$ against time. Table 20 contains also the values of the second order reaction constants

Fig.18

Plot of $\log_{10}(A_\infty - A_t)$ against t/min for absorbances at solutions (1),(2),(3),(4) at pH=3.8

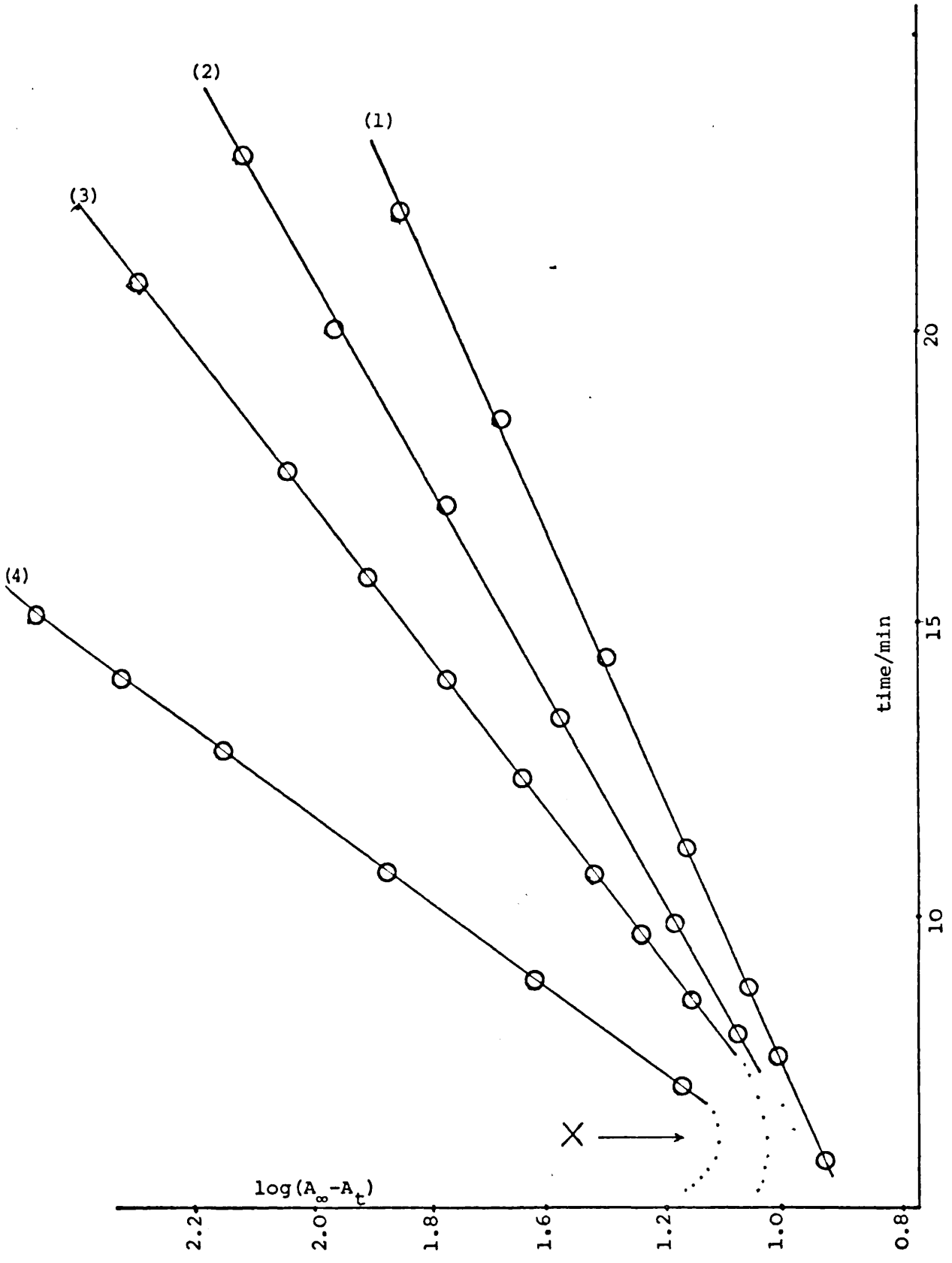

× shows the induction period. At high $[M^{3+}]$ the reaction is fast and the induction period cannot be detected.

Table 19

. Estimation of the conditional equilibrium constant for the reaction of Ga^{3+} with PLP at pH=3.88

$10^4\times$ Ga^{3+} /mol.dm^{-3}	PLP $\times10^4$ /mol.dm^{-3}	A	% reaction	$10^4\times$ Ga-PLP /mol.dm^{-3}	$10^4\times$ PLP /mol.dm^{-3}	$10^4\times$ Ga^{3+} /mol.dm^{-3}	K
26.0	2.0	0.100	82	1.64	0.36	24.36	0.187×10^4
13.3	2.0	0.175	67	1.34	0.66	11.96	0.167×10^4
4.0	2.0	0.333	40	0.80	1.2	3.2	0.208×10^4
2.6	2.0	0.390	27	0.54	1.46	2.06	0.1795×10^4
1.33	2.0	0.452	16	0.32	1.01	1.68	0.1189×10^4

K average = 0.184×10^4

log K = 3.27

Table 20

Calculation of the rate constants for the reaction of Ga^{3+} with PLP and L-aspartic acid at 374 nm in buffer pH=3.8

soln.	[L-Aspartic a] /mol.dm^{-3}	[PLP] /mol.dm^{-3}	[$Ga(NO_3)_3.9H_2O$] /mol.dm^{-3}	A_0	A_∞	ΔA*	ΔE**	10^3 initial slope/s^{-1} ***	10^6 initial Rate	K_2 ***** (a)	10^3K_1 /s ††	K_2 **** (b)
(1)	5.3333×10^{-3}	1.267×10^{-4}	1.667×10^{-4}	0.420	0.540	0.12	947.12	0.1167	0.1	0.1824	1.64	0.1731
(2)	5.333×10^{-3}	1.267×10^{-4}	3.333×10^{-4}	0.420	0.540	0.12	947.12	0.1333	0.1	0.208	2.431	0.218
(3)	5.333×10^{-3}	1.267×10^{-4}	5.000×10^{-4}	0.42	0.540	0.12	947	0.2614	0.3	0.4085	2.92	0.401
(4)	5.333×10^{-3}	1.267×10^{-4}	8.333×10^{-4}	0.420	0.540	0.12	947	0.2609	0.3	0.417	5.15	0.432

* $\Delta A = A_\infty - A_0$

** $\Delta E = \Delta A/[PLP]$

**** Initial Rate $= \frac{\text{initial slope}}{\Delta E}$

†† $k = \frac{\text{slope}\times 2.303}{60}$ (for each $\log(A - A_t)$ vs t/min plot)

***** $K_2 = \frac{\text{initial rate}}{[PLP][L\text{-Asp}]}$ $(mol^{-1}.dm^3.s^{-1})$

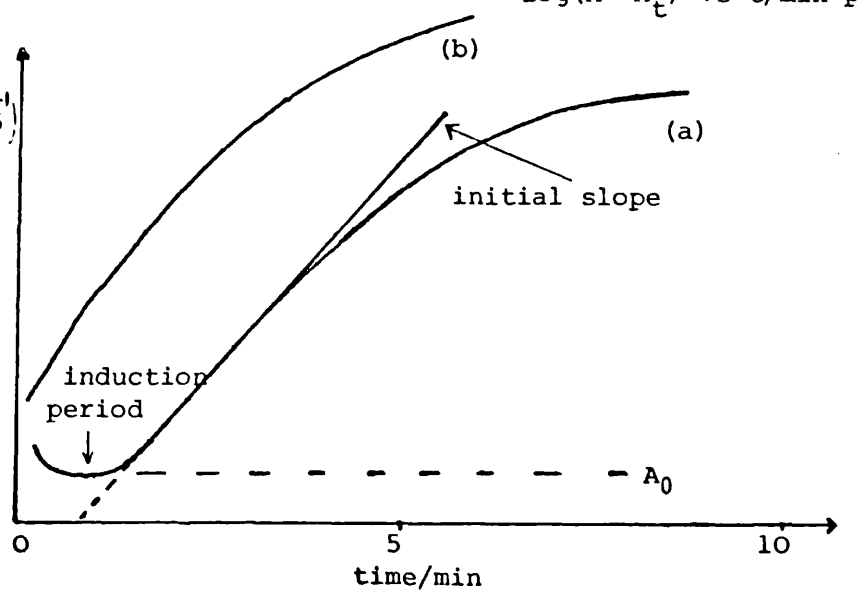

Fig.15: Plot of A vs time

(a) for solution (1)

(b) for solution (2)

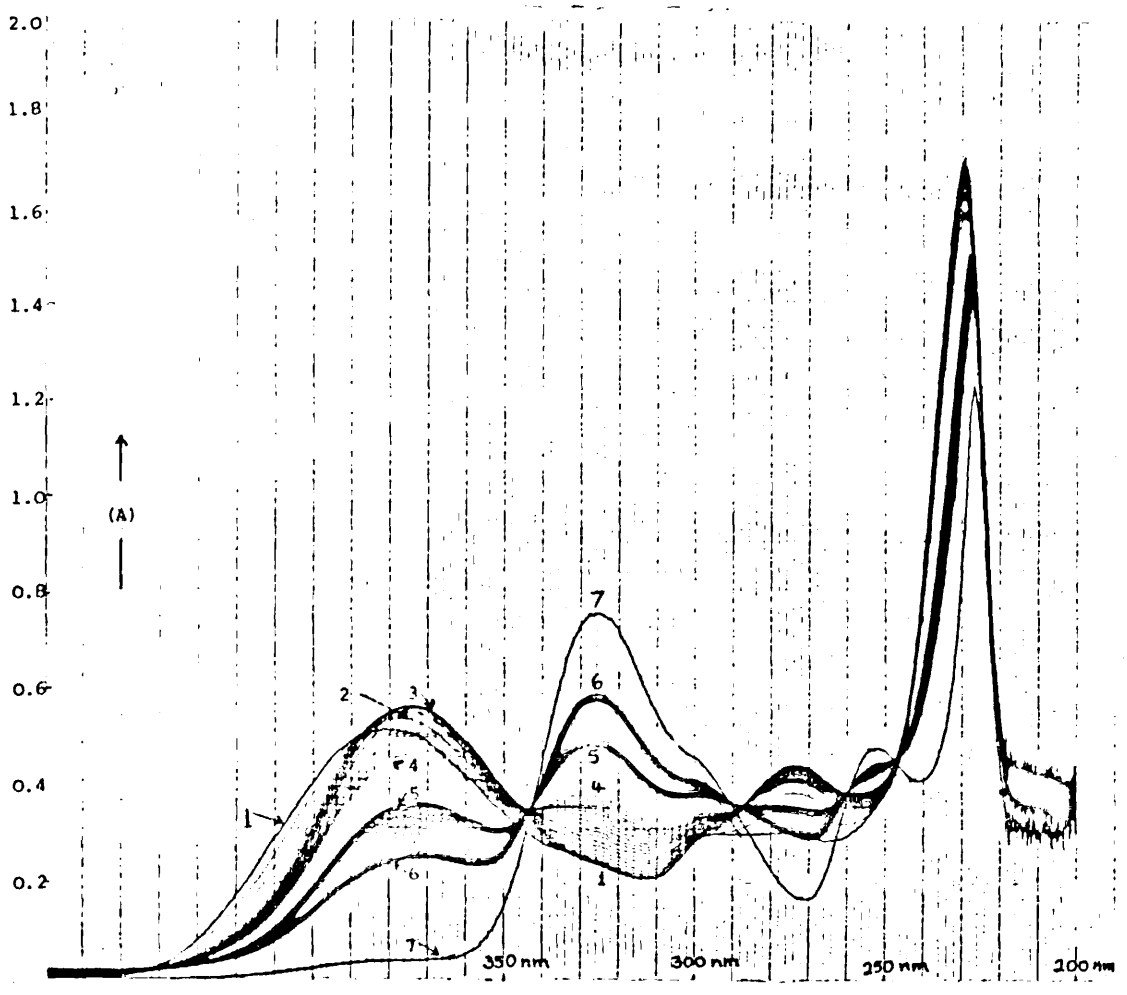

Fig. 19: Spectrophotometric changes occurring during the reaction of PLP with L-aspartic acid and Ga^{3+} at 25°C and pH=3.8

$[Ga^{3+}] = 1.667 \times 10^{-4}$ mol.dm^{-3}

$[PLP] = 1.267 \times 10^{-4}$ mol.dm^{-3}

$[L\text{-}Asp] = 5.333 \times 10^{-3}$ mol.dm^{-3}

1, spectrum at beginning of reaction

2,3,4,5,6,7 spectra at increasing lengths of time.

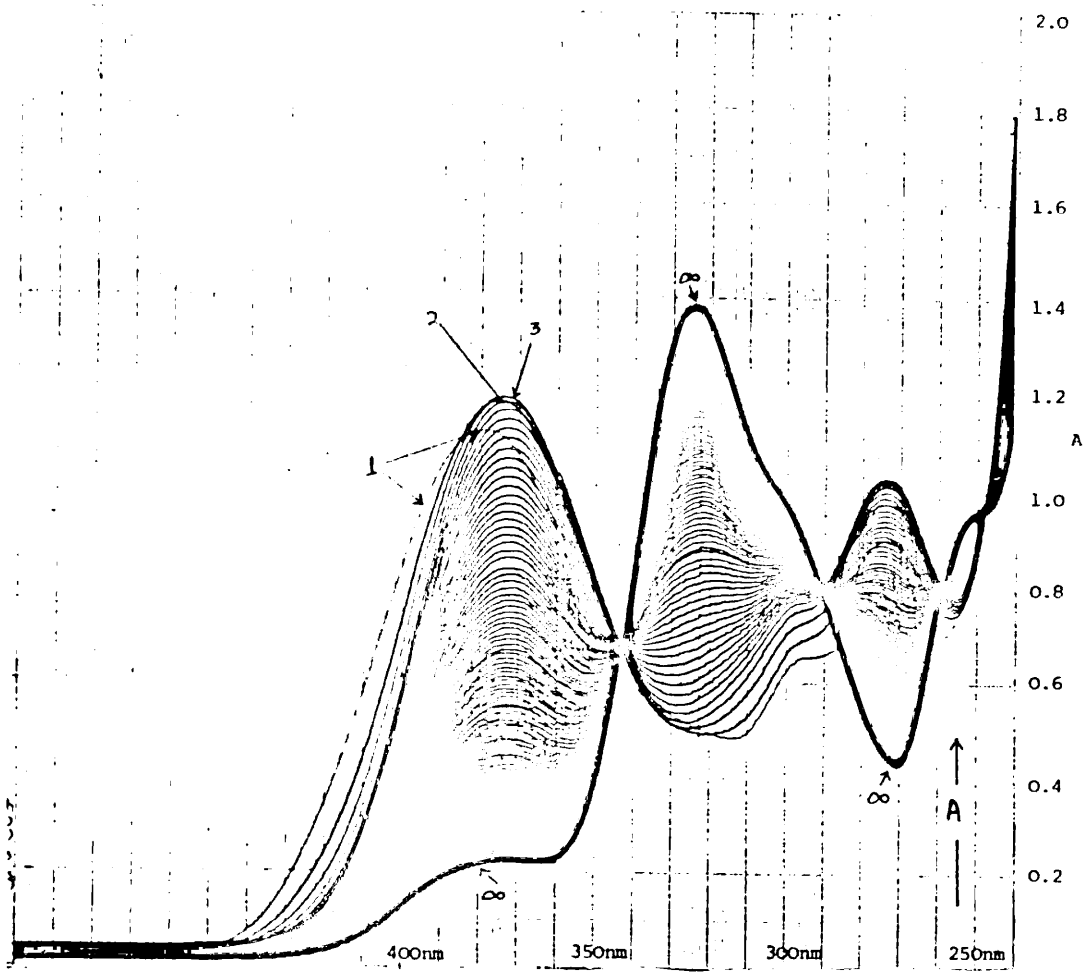

Fig. 20: Spectrophotometric changes occurring during the reaction of Ga^{3+} + PLP + L-Asp at pH=3.8 and 25°C

$[Ga^{3+}] = 5.000 \times 10^{-4}$ mol.dm^{-3}

$[PLP] = 1.267 \times 10^{-4}$ mol.dm^{-3}

$[L\text{-}Asp] = 5.333 \times 10^{-3}$ mol.dm^{-3}

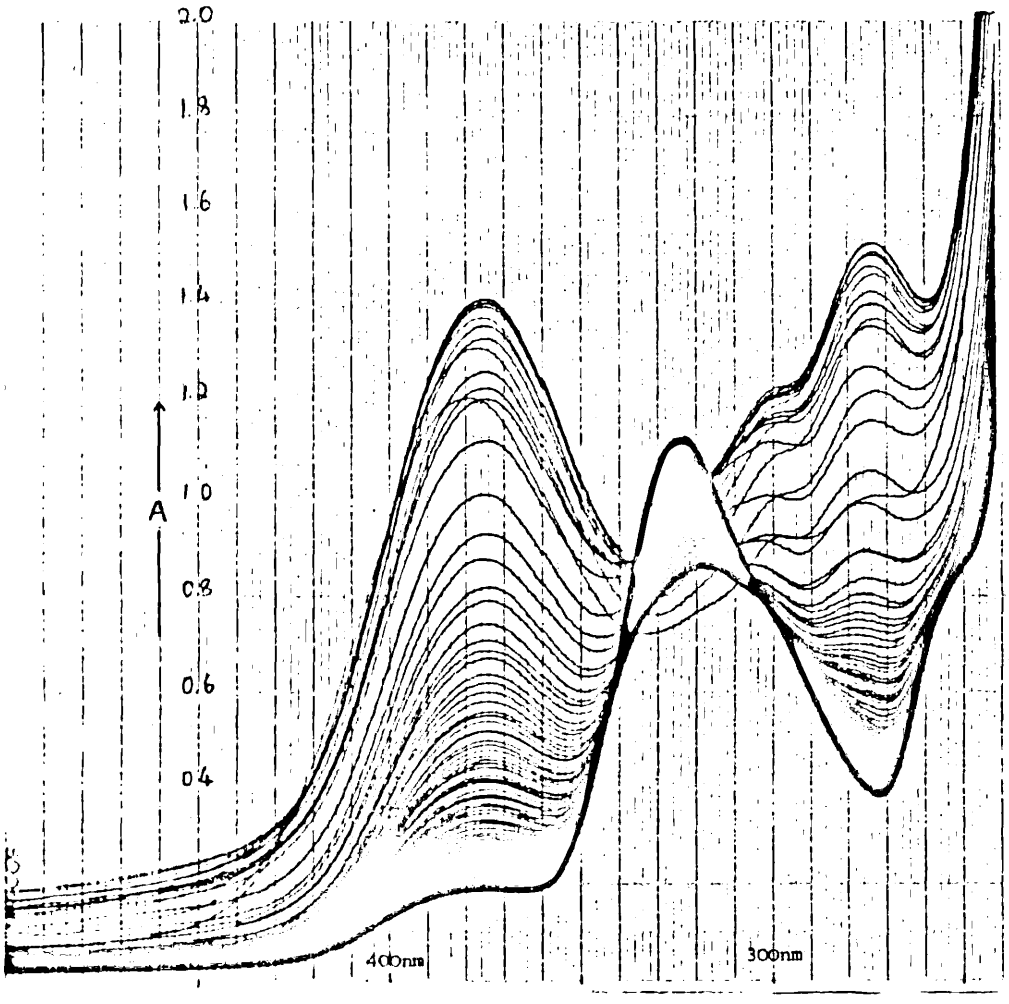

Fig. 21: Spectrophotometric changes occurring during the reaction Ga^{3+} + PLP + L-Asp at pH=3.8 and at 25°C

$[Ga^{3+}] = 8.333 \times 10^{-4}$ mol.dm^{-3}

$[PLP] = 1.267 \times 10^{-4}$ mol.dm^{-3}

$[L\text{-}Asp] = 5.333 \times 10^{-3}$ mol.dm^{-3}

(b) Determination of the Rate of the Reaction of Ga^{3+} with PLP and L-aspartic acid at pH=1.6

Table 21

Linear Regression Results for the reaction of Ga^{3+} + PLP + L-Aspartic acid at pH=1.6, 25°C and fixed wavelength at 374 nm

No. of run	1st slope	1st intercept	1st correlation factor	10^3K_1 /s^{-1}
1	-0.0652	-0.4851	-0.9998	2.5
2	-0.0729	-0.2851	-0.9995	2.8
3	-0.0735	-0.1858	-0.9994	2.82
4	-0.0871	-0.0336	-0.9970	3.34
5	-0.0159	-0.0792	-0.9986	0.61
6	-0.0733	-0.0737	-0.9995	2.81
7	-0.0735	-0.1858	-0.9994	2.82
8	-0.0954	-0.1868	-0.9942	3.66
9	-0.0433	-0.2459	-0.9972	1.66
10	-0.0611	-0.1997	-0.9981	2.35
11	-0.0735	-0.1858	-0.9994	2.82
12	-0.1051	-0.1341	-0.9879	4.034
13	-0.0245	-0.2945	-0.9556	0.94

Table 22

Calculation of second order rate constants from initial slopes

solution	concn. of Ga^{3+} in the cell /mol.dm^{-3}	concn. of PLP in the cell /mol.dm^{-3}	conc. of L-Aspartic acid /mol.dm^{-3}	A_0	A_∞	ΔA	ΔE	10^3 initial slope/s^{-1}	10^6 initial Rate	K_2 /mol^{-1} dm^3 s^{-1}
1	0.001	0.667×10^{-4}	8.0×10^{-3}	0.147	0.457	0.310	4648	0.750	0.2	0.3024
2	0.001	1.333×10^{-4}	8.0×10^{-3}	0.300	0.817	0.517	3878	1.817	0.5	0.4393
3	0.001	2.000×10^{-4}	8.0×10^{-3}	0.400	1.025	0.625	3125	2.667	0.9	0.5333
4	0.001	2.670×10^{-4}	8.0×10^{-3}	0.490	1.388	0.898	3363	4.900	1.5	0.6820
5	0.001	2.000×10^{-4}	2.67×10^{-3}	0.104	0.947	0.843	4215	0.7833	0.2	0.3480
6	0.001	2.000×10^{-4}	5.33×10^{-3}	0.215	1.004	0.789	3945	2.270	0.6	0.540
7	0.001	2.000×10^{-4}	8.0×10^{-3}	0.400	1.025	0.625	3126	2.667	0.9	0.530
8	0.001	2.000×10^{-4}	10.67×10^{-3}	0.505	0.925	0.420	2100	2.233	1.1	0.498
9	3.33×10^{-4}	2.000×10^{-4}	8.0×10^{-3}	0.280	0.826	0.546	2730	1.2667	0.5	0.290
10	6.67×10^{-4}	2.000×10^{-4}	8.0×10^{-3}	0.377	0.899	0.522	2610	1.880	0.7	0.451
11	10.00×10^{-4}	2.000×10^{-4}	8.0×10^{-3}	0.400	1.025	0.625	3125	2.667	0.9	0.5333
12	13.33×10^{-4}	2.000×10^{-4}	8.0×10^{-3}	0.530	1.002	0.472	2360	2.333	1.0	0.618

(c) The Reaction of Ga + PLP + L-Asp at pH=5.6

Table 23

Linear Regression Results for the reaction of Ga^{3+} + PLP + L-Aspartic acid at pH=5.6, 25°C and fixed wavelength at 374 nm.

Calculation of the first order rate constants from semi-log plots

No.of run	1st slope	1st intercept	1st correlation factor	10^3K_1 /s^{-1}
1	-0.0329	-1.2579	0.8675	1.263
2	-0.0343	-1.2199	0.6725	1.317
3	-0.0687	-1.0728	0.9929	2.637
4				
5	-0.0393	-1.2484	0.9829	1.509
6	-0.0552	-1.1175	0.9933	2.119
7	-0.0687	-1.0728	0.9929	2.637
8	-0.0586	-1.1558	0.9531	2.249
9	-0.0687	-1.0728	0.9929	2.637
10	-0.036159	-0.5509	0.9857	1.388
11	-0.02498	-0.2372	0.9916	0.959
12				

Table 24

Calculation of the second order rate constant from initial slopes for the reaction of Ga^{3+} + PLP + L-Aspartic acid at pH=5.6

Solution pH=5.6	concn. of Ga^{3+} in the cell /mol.dm^{-3}	concn. of PLP in the cell /mol.dm^{-3}	concn. of L-Asp in the cell /mol.dm^{-3}	A_0	A_∞	ΔA	ΔE	10^3 initial slope/s^{-1}	10^6 initial Rate	K_2 /mol^{-1}dm^{3}s^{-1}
1	3.33×10^{-4}	0.67×10^{-4}	0.008	0.263	0.326	0.062	940	0.1033	0.1	0.20496
2	3.33×10^{-4}	1.33×10^{-4}	0.008	0.484	0.562	0.078	587	0.1367	0.2	0.2188
3	3.33×10^{-4}	2.00×10^{-4}	0.008	0.743	0.832	0.089	445	0.2017	0.5	0.2832
4	3.33×10^{-4}	2.67×10^{-4}	0.008	0.						
5	3.33×10^{-4}	2.00×10^{-4}	0.00267	0.630	0.690	0.060	300	0.683	0.2	0.4266
6	3.33×10^{-4}	2.00×10^{-4}	0.0053	0.630	0.710	0.080	400	0.1183	0.3	0.2775
7	3.33×10^{-4}	2.00×10^{-4}	0.008	0.743	0.832	0.089	445	0.2017	0.5	0.2832
8	3.33×10^{-4}	2.00×10^{-4}	0.01067	0.649	0.730	0.081	405	0.1683	0.4	0.1948
9	3.33×10^{-4}	2.00×10^{-4}	0.008							
10	10.00×10^{-4}	2.00×10^{-4}	0.008	0.678	0.995	0.317	1585	0.485	0.3	0.1912
11	16.67×10^{-4}	2.00×10^{-4}	0.008	0.618	1.425	0.757	3785	1.0017	0.3	0.1654
12		2.00×10^{-4}	0.008							

(d) Determination of the Rate of the Reaction of Ga^{3+} + PLP + L-Asp at pH=6.8

Table 25

Linear Regression Results for the reaction of Ga^{3+} + PLP + L-aspartic acid at pH=6.8, 25°C and fixed wavelength at 374 nm.

Calculation of first order rate constants from semi-log plots.

No. of run	1st slope*	1st intercept	1st correlation factor	10^3K_1 /s
1	-0.0301	-1.2133	0.9707	1.155
2	-0.04152	-1.4631	0.9824	1.594
3	-0.0582	-1.3490	0.9931	2.234
4	-0.07292	-1.3732	0.9447	2.799
5	-0.0231	-1.6996	0.8562	0.887
6	-0.0573	-1.7051	0.8101	2.199
7	-0.0582	-1.3490	0.9931	2.234
8	-0.07232	-1.7920	0.9584	2.776
9	-0.0582	-1.3490	0.9931	2.234
10	-0.0610	-1.2917	0.7610	2.3490
11	-0.0701	-1.0830	0.9160	2.691
12	-0.0891	-1.0027	0.9816	3.420

*for $\log(A_\infty - A_t)$ vs time

Table 26

Calculation of the second order rate constants from initial slopes for the reaction of Ga^{3+} + PLP + L-Aspartic acid at pH=6.8

Solution	Concn. of Ga^{3+} in the cell /mol.dm^{-3}	Concn. of L-Aspartic /mol.dm^{-3}	Concn. of PLP /mol.dm^{-3}	initial slope /min^{-1}	initial Rate$\times 10^6$	A_0	A_∞	ΔE	K_2 /mol^{-1}dm^{3}s^{-1}	10^3 initial slope/s^{-1}
1	3.33×10^{-4}	0.008	0.67×10^{-4}	0.0026	0.0528	0.241	0.296	821	0.099	0.0430
2	3.33×10^{-4}	0.008	1.33×10^{-4}	0.0028	0.200	0.485	0.521	271	0.162	0.0467
3	3.33×10^{-4}	0.008	2.00×10^{-4}	0.0032	0.300	0.751	0.800	245	0.188	0.0533
4	3.33×10^{-4}	0.008	2.67×10^{-4}	0.0038	0.400	1.000	1.041	154	0.193	0.0633
5	3.33×10^{-4}	2.67×10^{-3}	2.00×10^{-4}	0.0023	0.3	0.719	0.744	125	0.498	0.0333
6	3.33×10^{-4}	5.33×10^{-3}	2.00×10^{-4}	0.0023	0.3	0.750	0.779	145	0.248	0.0383
7	3.33×10^{-4}	8.00×10^{-3}	2.00×10^{-4}	0.0032	0.3	0.751	0.800	245	0.188	0.0533
8	3.33×10^{-4}	10.67×10^{-3}	2.00×10^{-4}	0.0034	0.4	0.773	0.799	130	0.204	0.0567
9	3.33×10^{-4}	8.00×10^{-3}	2.00×10^{-4}	0.0032	0.3	0.751	0.800	245	0.188	0.0533
10	6.67×10^{-4}	8.00×10^{-3}	2.00×10^{-4}	0.004	0.2	0.726	0.800	370	0.113	0.0667
11	10.00×10^{-4}	8.00×10^{-3}	2.00×10^{-4}	0.005	0.2	0.699	0.795	480	0.108	0.0833
12	13.33×10^{-4}	8.00×10^{-3}	2.00×10^{-4}	0.0054	0.1	0.671	0.800	645	0.087	0.0900

(e) Determination of the Rate of the Reaction of Ga^{3+} with PLP and L-Threonine at pH=1.6

Table 27

Linear Regression Results for the reaction of Ga^{3+} = PLP + L-Threonine, 25°C at pH=1.6 and at fixed wavelength 377 nm.

Calculation of the first order rate constants from semi-log plots

No. of run	1st slope	1st intercept	1st correlation factor	10^3K_1 /s
1	-0.01237	-0.6411	0.9987	0.475
2	-0.00655	-0.5887	0.9965	0.252
3	-0.01397	-0.1614	0.9992	0.536
	-0.01262	-0.1340	0.9998	0.485
4	-0.01155	-0.07912	0.9556	0.443
5	-0.0123	-0.8999	0.9969	0.472
6	-0.00996	-0.3869	0.9991	0.383
7	-0.01397	-0.1614	0.9992	0.536
8	-0.01499	-0.1088	0.9996	0.575
9	-0.01951	-0.73169	0.9997	0.749
10	-0.01397	-0.1614	0.9992	0.536
11	-0.0110	-0.09009	0.9997	0.422
12	-0.01621	-0.09212	0.9995	0.622

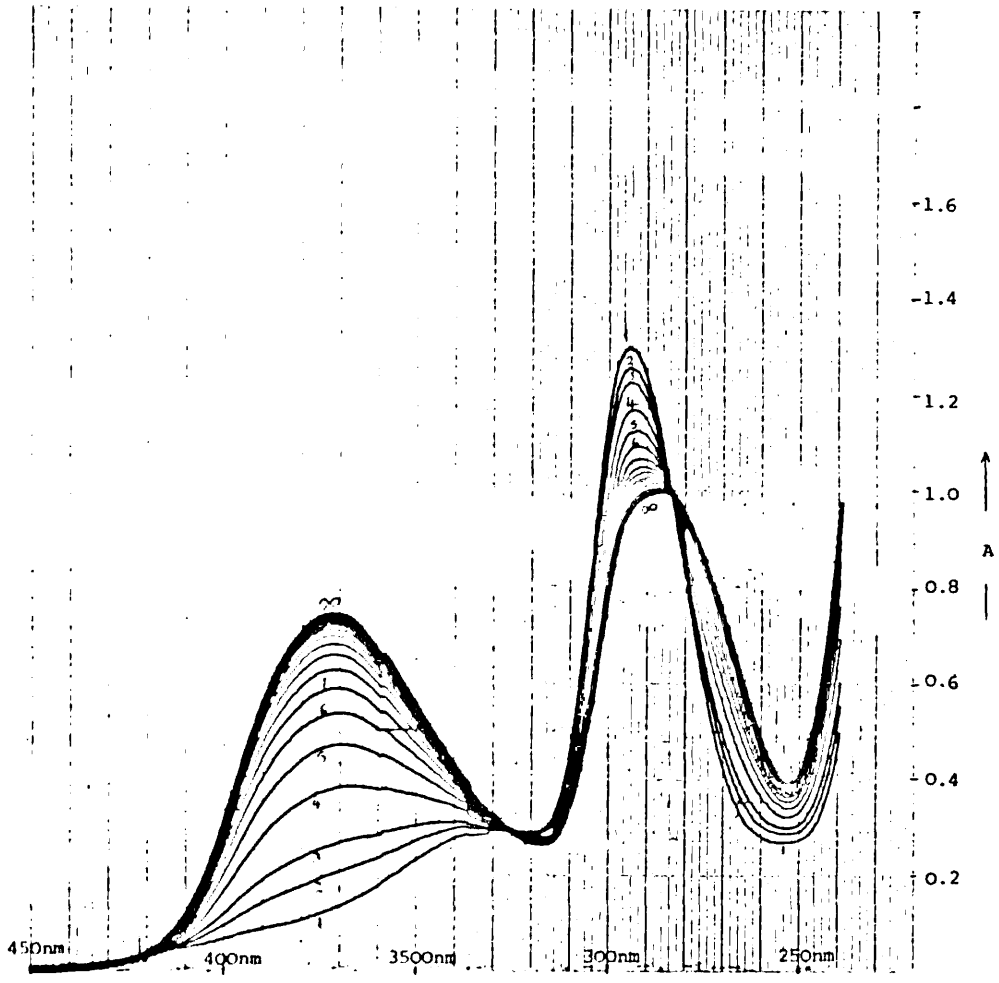

Fig. 22: Spectrophotometric changes occurring during the reaction No.3 of Ga^{3+} + PLP + L-Threonine at pH=1.6 and 25°C.

Table 28

Calculation of the second order rate constants from initial slope method for the reaction of Ga^{3+} + PLP + L-Threonine at pH=1.6

soln.	$[Ga^{3+}]$ /mol.dm^{-3}	[PLP] /mol.dm^{-3}	[L-Threonine] /mol.dm^{-3}	-slope /min^{-1}	$10^3 \times K_1$ /s	A_0	A_∞	ΔA	ΔE	10^3 initial slope/s^{-1}	10^6 initial Rate	K_2 /mol^{-1}.dm^3.s^{-1}
1	3.33×10^{-4}	0.67×10^{-4}	0.008	0.014	0.475	0.038	0.264	0.226	3373	0.233	0.069	0.1289
2	3.33×10^{-4}	1.33×10^{-4}	0.008	0.0145	0.252	0.066	0.319	0.253	1902	0.242	0.100	0.1194
3	3.33×10^{-4}	2.00×10^{-4}	0.008	0.025	0.485	0.108	0.833	0.725	3625	0.417	0.100	0.0625
4	3.33×10^{-4}	2.67×10^{-4}	0.008	0.026	0.443	0.170	0.991	0.821	3075	0.433	0.100	0.0660
5	3.33×10^{-4}	2.00×10^{-4}	0.00267	0.004	0.472	0.086	0.212	0.126	630	0.067	0.100	0.0661
6	3.33×10^{-4}	2.00×10^{-4}	0.00533	0.009	0.383	0.098	0.507	0.409	2045	0.150	0.073	0.0456
7	3.33×10^{-4}	2.00×10^{-4}	0.008	0.025	0.485	0.108	0.833	0.725	3625	0.417	0.100	0.0718
8	3.33×10^{-4}	2.00×10^{-4}	0.01067	0.027	0.575	0.134	0.905	0.771	3855	0.450	0.100	0.07296
9	0.67×10^{-4}	2.00×10^{-4}	0.008	0.009	0.749	0.108	0.293	0.185	925	0.150	0.200	0.1014
10	3.33×10^{-4}	2.00×10^{-4}	0.008	0.025	0.485	0.108	0.833	0.725	3625	0.417	0.100	0.07184
11	6.67×10^{-4}	2.00×10^{-4}	0.008	0.026	0.422	0.128	0.920	0.792	3960	0.433	0.100	0.0684
12	$10.00\ 10^{-4}$	2.00×10^{-4}	0.008	0.028	0.622	0.127	0.920	0.793	3965	0.467	0.100	0.0736

(f) The Reaction of Ga^{3+} + PLP + L-threonine at pH=3.8

Table 29

Concentrations used in the cell.

Solution	concn. of Ga^{3+} in the cell /mol.dm^{-3}	concn. of PLP in the cell /mol.dm^{-3}	concn. of L-Threonine /mol.dm^{-3}
1	3.333×10^{-4}	0.67×10^{-4}	0.008
2	3.333×10^{-4}	1.33×10^{-4}	0.008
3	3.333×10^{-4}	2.00×10^{-4}	0.008
4	3.333×10^{-4}	2.67×10^{-4}	0.008
5	3.333×10^{-4}	2.00×10^{-4}	0.00133
6	3.333×10^{-4}	2.00×10^{-4}	0.00267
7	3.333×10^{-4}	2.00×10^{-4}	0.0080
8	3.333×10^{-4}	2.00×10^{-4}	0.01067
9	1.67×10^{-4}	2.00×10^{-4}	0.008
10	3.33×10^{-4}	2.00×10^{-4}	0.008
11	10.00×10^{-4}	2.00×10^{-4}	0.008

Table 30

Linear Regression Results for the reaction of Ga^{3+} + PLP + L-Threonine at pH=3.8, 25°C and fixed wavelength at 377 nm.

Calculation of the first rate constants from semi-log plots.

No. of run	1st slope	1st intercept	1st correlation factor	10^3K_1 /s
1	-0.0765	-0.6870	0.9999	2.936
2	-0.0652	-0.48062	0.9816	2.503
3	-0.0627	-0.2603	0.9997	2.407
4	-0.05899	-0.2192	0.8985	2.2642
5	-0.0130	-0.2905	0.9991	0.499
6	-0.0205	-0.2197	0.9998	0.787
7	-0.0627	-0.2603	0.9997	2.407
8	-0.08477	-0.2365	0.9980	3.254
9	-0.0626	-0.2593	0.9995	2.403
10	-0.0627	-0.2603	0.9997	2.407
11	-0.0943	-0.1632	0.9993	3.620

Table 31

Reaction of Ga^{3+} + PLP + L-Threonine at pH=3.8

A_0	A_∞	ΔA	ΔE	10^3 initial slope/s^-	10^6 initial Rate	K_2
0.215	0.408	0.193	2881	0.517	0.2	0.370
0.370	0.745	0.375	2820	0.9850	0.3	0.328
0.560	1.090	0.530	2650	1.4170	0.5	0.334
0.710	1.394	0.684	2562	1883	0.7	0.344
0.475	0.987	0.512	2560	0.220	0.086	0.323
0.450	1.040	0.590	2950	0.433	0.1	0.275
0.560	1.090	0.530	2650	1.417	0.5	0.334
0.580	1.145	0.565	2825	2.367	0.8	0.393
0.502	1.040	0.538	2690	1.533	0.6	0.356
0.560	1.090	0.530	2650	1.417	0.5	0.334
0.440	1.030	0.590	2950	1.617	0.5	0.343

(g) The Reaction of Ga^{3+} + PLP + L-threonine at pH=5.6

Table 32

Linear Regression Results for the reaction of Ga^{3+} + PLP + L-Threonine at pH=5.6, 25°C and at fixed wavelength 377 nm.

Calculation of first order rate constants from semi-log plots.

No. of run	1st slope	1st intercept	1st correlation factor	10^3K_1 /s
1	-0.0385	-0.8829	0.9984	1.478
2	-0.0538	-0.7282	0.9895	2.065
3	-0.0518	-0.5846	0.9815	1.988
4	-0.0477	-0.4933	0.9887	1.831
5	-0.03265	-0.8805	0.9966	1.253
6	-0.0334	-0.7596	0.9823	1.282
7				
8	-0.0511	-0.6227	0.9880	1.961
9	-0.0538	-0.7282	0.9895	2.065
10				1.988
11	-0.0484	-0.4602	0.9965	1.858
12	-0.0257	-0.4327	0.9993	0.9865

Fig. 23

Ultra-Violet Spectra

of PLP + L-Threonine + Ga^{3+}

at 25°C and pH-5.6

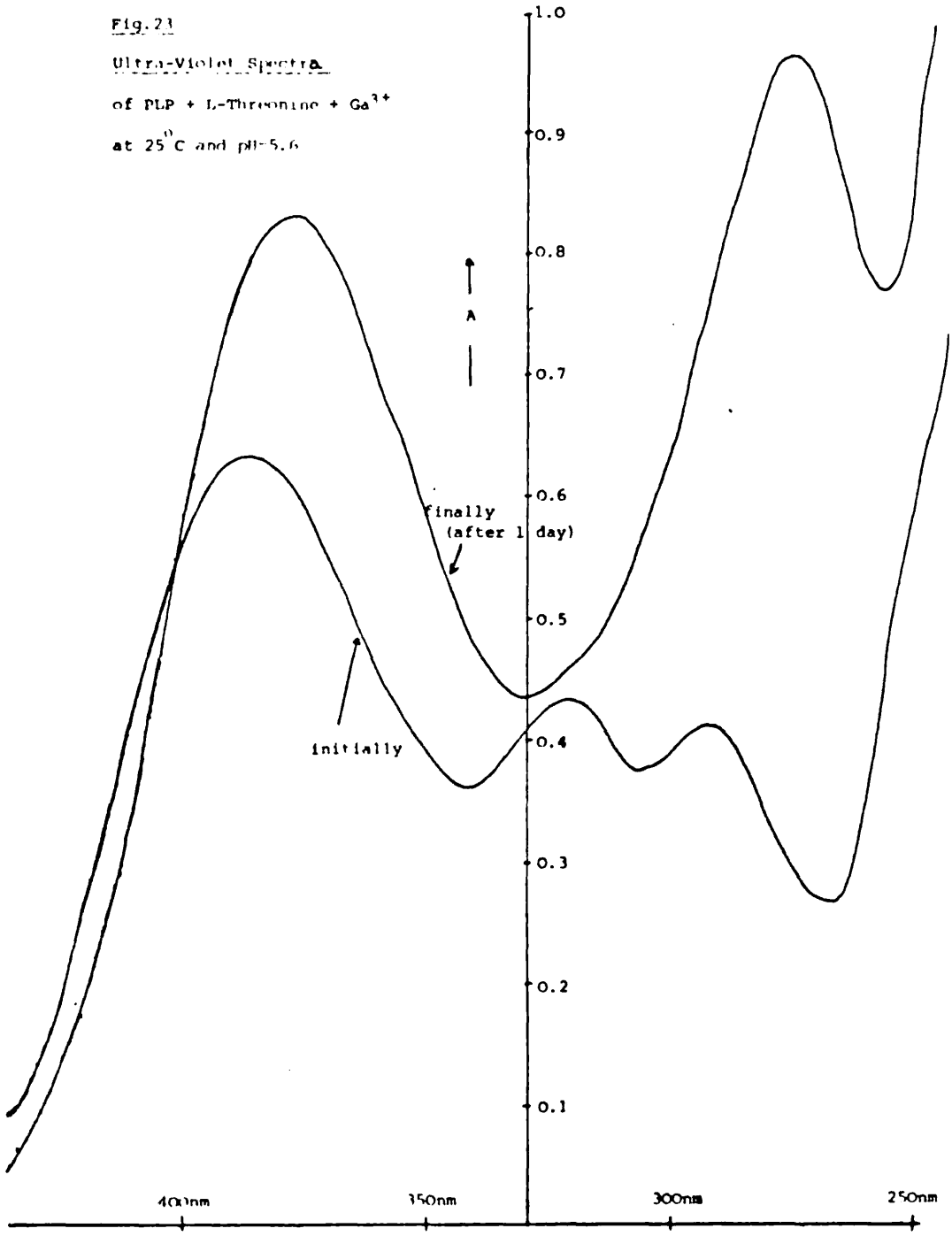

Table 33

Calculation of second order rate constants by initial slope method. The reaction of Ga^{3+} + PLP + L-Threonine at pH=5.6.

Solution (pH=5.6)	concn. of Ga^{3+} in the cell /mol.dm^{-3}	concn. of PLP in the cell /mol.dm^{-3}	concn. of L-Threonine in the cell /mol.dm^{-3}	-slope /min^{-1}	A_0	A_∞	ΔA	ΔE	10^3 initial slope/s^{-1}	10^6 initial Rate	K_2 /mol^{-1} dm^3 s^{-1}
1	3.33×10^{-4}	0.67×10^{-3}	0.008	0.011	0.151	0.286	0.135	2015	0.1833	0.091	0.1697
2	3.33×10^{-4}	0.133×10^{-3}	0.008	0.029	0.324	0.520	0.196	1474	0.4833	0.3	0.3082
3	3.33×10^{-4}	0.2×10^{-3}	0.008	0.032	0.560	0.834	0.274	1370	0.5333	0.4	0.2433
4	3.33×10^{-4}	0.267×10^{-3}	0.008	0.043	0.720	1.062	0.342	1281	0.7167	0.6	0.2619
5	5.55×10^{-4}	0.2×10^{-3}	0.00133	0.011	0.480	0.625	0.145	725	0.1833	0.3	0.9507
6	3.33×10^{-4}	0.2×10^{-3}	0.00267	0.015	0.491	0.686	0.195	975	0.2500	0.3	0.4802
7	3.33×10^{-4}	0.2×10^{-3}	0.01067	0.033	0.513	0.770	0.257	1285	0.5500	0.4	0.2006
8	0.67×10^{-4}	0.2×10^{-3}	0.008	0.022	0.500	0.690	0.190	950	0.3667	0.4	0.2412
9	6.67×10^{-4}	0.2×10^{-3}	0.008	0.037	0.401	0.755	0.354	1770	0.6167	0.3	0.2177
10	10.00×10^{-4}	0.2×10^{-3}	0.008	0.022	0.338	0.700	0.362	1810	0.3667	0.2	0.1266

(h) Determination of the Rate of the Reaction of Al^{3+} with PLP and L-NaGlu at pH=3.8

Table 34

Concentrations used in the cell

Solution (pH=3.8)	concn. of Al^{3+} in the cell /mol.dm^{-3}	concn. of PLP in the cell /mol.dm^{-3}	concn. of L-NaGlu in the cell /mol.dm^{-3}
1	3.33×10^{-4}	0.67×10^{-4}	8.0×10^{-3}
2	3.33×10^{-4}	0.133×10^{-3}	8.0×10^{-3}
3	3.33×10^{-4}	0.200×10^{-3}	8.0×10^{-3}
4	3.33×10^{-4}	0.267×10^{-3}	8.0×10^{-3}
5	3.33×10^{-4}	0.200×10^{-3}	1.33×10^{-3}
6	3.33×10^{-4}	0.200×10^{-3}	2.67×10^{-3}
7	3.33×10^{-4}	0.200×10^{-3}	8.00×10^{-3}
8	3.33×10^{-4}	0.200×10^{-3}	10.67×10^{-3}
9	3.33×10^{-4}	0.200×10^{-3}	8.00×10^{-3}
10	6.67×10^{-4}	0.200×10^{-3}	8.00×10^{-3}
11	10.00×10^{-4}	0.200×10^{-3}	8.00×10^{-3}
12	13.33×10^{-4}	0.200×10^{-3}	8.00×10^{-3}

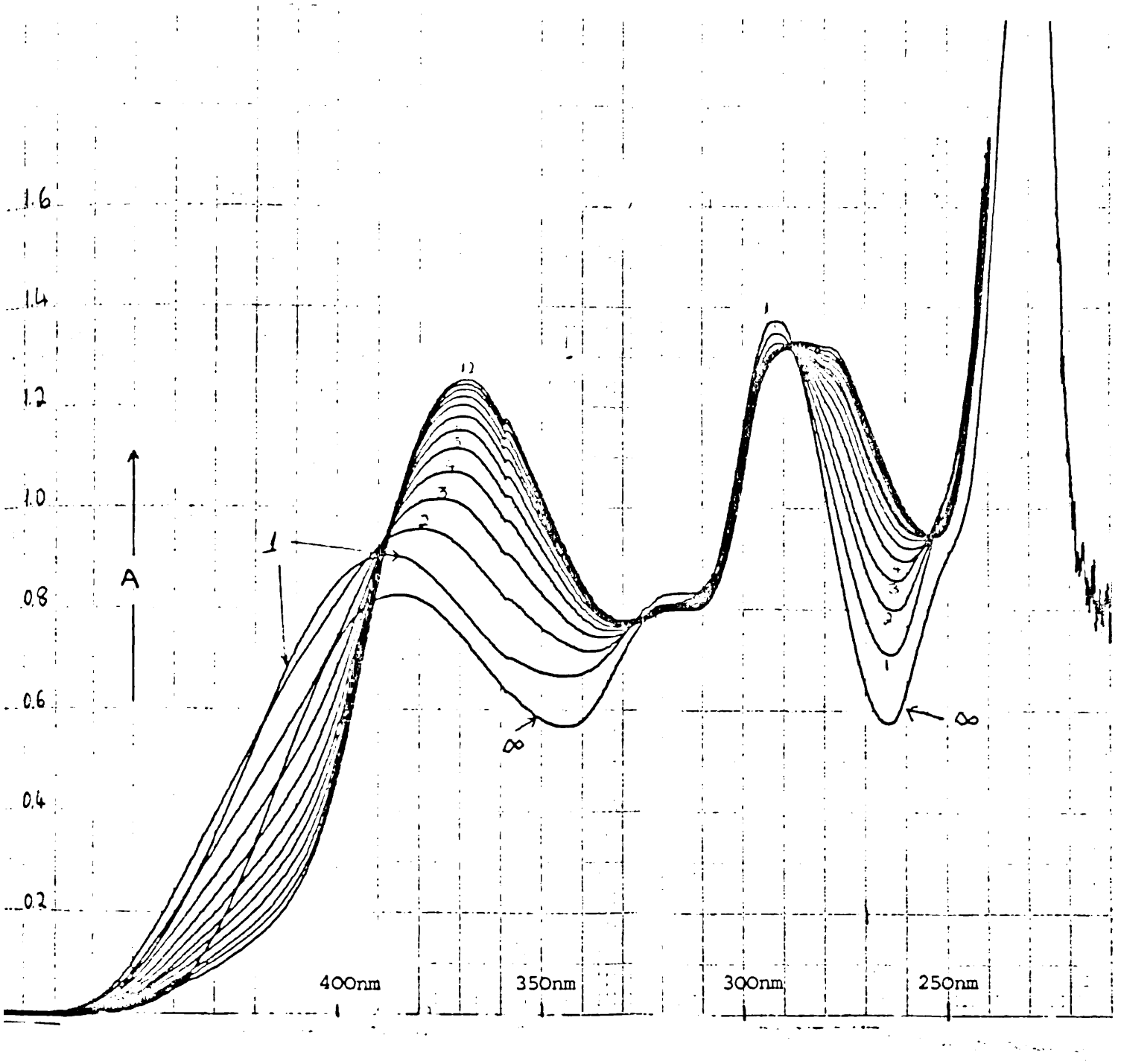

Fig. 24 : Spectrophotometric changes occurring during the reaction No.3 of Al + L-NaGlu + PLP at pH=3.8 and at 20°C.

Table 35

Linear Regression Results for the reaction of Al^{3+} + PLP + L-NaGlu at pH=3.8, 25°C and at 370 nm.

Calculation of the first order rate constants from semi-log plots

No. of run	1st slope	1st intercept	1st correlation factor	10^3K_1 /s
1	-0.01913	-0.9103	-0.9993	0.7343
2	-0.0199	-0.6717	-0.9969	0.764
3	-0.0237	-0.5557	-0.9994	0.9097
4	-0.0261	-0.4832	-0.9973	10.022
5	-0.0162	-0.6957	-0.9998	0.622
6	-0.0199	-0.5957	-0.9973	0.764
7				0.9097
8	-0.0290	-0.5080	-0.9996	1.1113
9				
10	-0.0235	-0.5184	-0.9989	0.902
11	-0.0251	-0.5098	-0.9975	0.9634
12	-0.0260	-0.4795	-0.9987	0.998

Table 36

Calculation of second order rate constants using the initial slope method for the reaction of Al^{3+} + PLP + L-Na Glutamate at pH=3.8, 25°C and 370 nm.

A_0	A_∞	ΔA	ΔE	10^3 initial slope/s^{-1}	10^6 initial Rate	K_2 $/mol^{-1} \cdot s^{-1} \cdot dm^3$
0.109	0.227	0.118	1761	0.05	0.0284	0.0597
0.211	0.415	0.204	1534	0.12	0.0782	0.0735
0.321	0.587	0.266	1330	0.22	0.2000	0.1034
0.351	0.681	0.330	1236	0.27	0.2000	0.10227
0.354	0.553	0.199	995	0.10	0.1000	0.3759
0.368	0.612	0.244	1220	0.15	0.1000	0.1873
0.321	0.587	0.266	1330	0.22	0.2000	0.1034
0.381	0.680	0.299	1495	0.27	0.2000	0.0846
0.321	0.587	0.266	1330	0.22	0.2000	0.1034
0.347	0.639	0.292	1460	0.22	0.2	0.0942
0.359	0.652	0.293	1465	0.23	0.2	0.0981
0.359	0.676	0.317	1585	0.22	0.1	0.0868

Determination of the Rates of the Reaction of Al^{3+} with PLP and L-Na-Glu at pH=5.6

Table 37

Linear Regression Results for the reaction of Al^{3+} + PLP + L-NaGlu at pH=5.6, 25°C and at 370 nm.

Calculation of the first order rate constants from semi-log plots

Solution	1st slope	1st intercept	1st correlation factor	$10^3 k_1$ /s
1	-0.04849	-1.0542	0.9961	1.86
2	-0.0259	-0.5891	0.9961	0.994
3	-0.0314	-0.6502	0.9985	1.205
4	-0.0317	-0.5524	0.9989	1.217
5	-0.0188	-0.7296	0.9520	0.722
6	-0.0261	-0.6997	0.9973	1.0018
7	-0.0314	-0.6502	0.9985	1.205
8	-0.0360	-0.6526	0.9973	1.382
9	-0.0314	-0.6502	0.9985	1.205
10	-0.0409	-0.5648	0.9974	1.570
11	-0.044	-0.5432	0.9981	1.6889
12	-0.049	-0.5104	0.9972	1.8808

*The concentrations of each material in solution is given in Table 34.

Table 38

Calculation of the second order rate constants from initial slopes for the reaction of Al^{3+} + L-Na Glu + PLP at pH=5.6.

A^0	A^∞	ΔA	ΔE	10^3 initial slope/s^{-1}	10^6 initial Rate	K_2 /mol^{-1}·dm^3·s^{-1}
0.105	0.186	0.081	1209	0.10	0.0827	0.1543
0.225	0.478	0.253	1898	0.18	0.0948	0.0891
0.252	0.467	0.215	1075	0.30	0.3000	0.1875
0.312	0.582	0.270	1011	0.37	0.3660	0.17135
0.230	0.406	0.176	880	0.10	0.1000	0.3759
0.239	0.431	0.192	960	0.21	0.2000	0.3745
0.252	0.467	0.215	1075	0.30	0.3000	0.1875
0.269	0.478	0.209	1045	0.28	0.3000	0.5618
0.252	0.467	0.215	1075	0.30	0.3000	0.1875
0.239	0.499	0.260	1300	0.45	0.3462	0.2164
0.213	0.416	0.203	1015	0.45	0.4433	0.2771
0.199	0.440	0.241	1205	0.46	0.4000	0.2386

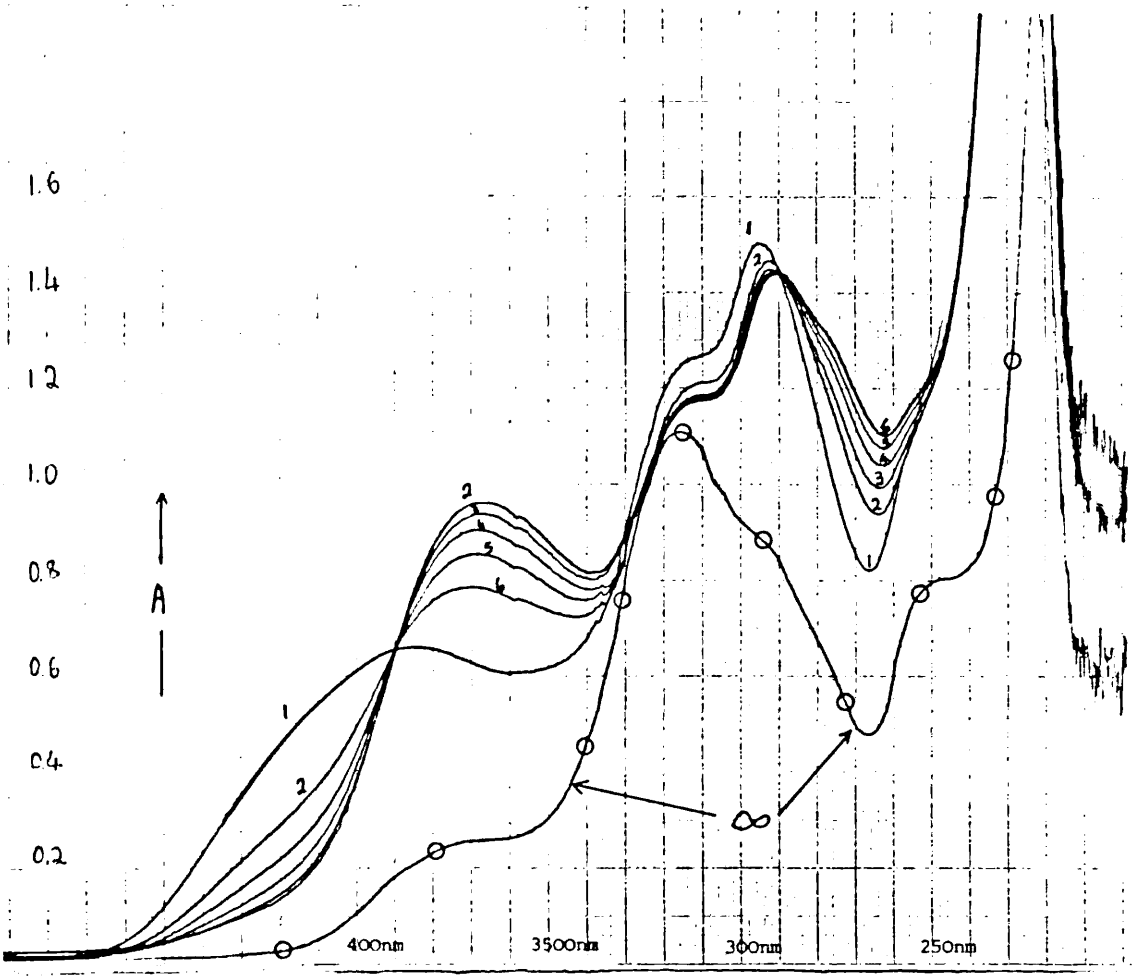

Fig. 25 : Spectrophotometric changes occurring during the reaction No.3 of Al^{3+} + PLP + L-Glu at pH=5.6 and at 25°C.

(k) The Reaction of Al^{3+} in the presence of PLP and L-threonine at pH=3.8

Table 39

Determination of the rate constant for the reaction of Al^{3+} with PLP and L-Threonine at pH=3.8, 25°C×372nm

soln	[Al $^{+}$] /mol.dm^{-3}	[PLP] /mol.dm^{-3}	[L-Threonine] /mol.dm^{-3}	-slope /min^{-1}	$10^3 \times k_1$ /s	A_0	A_∞	ΔA	ΔE	10^3 initial slope/s^{-1}	10^6 initial Rate	K_2 / mol^{-1} dm^3 s^{-1}
1	3.33×10^{-4}	0.67×10^{-4}	0.008	-0.00425	0.163	0.169	0.338	0.169	2522	0.042	0.02	0.03
2	3.33×10^{-4}	1.33×10^{-4}	0.008	-0.00597	0.229	0.336	0.609	0.273	2053	0.167	0.08	0.076
3	3.33×10^{-4}	2.00×10^{-4}	0.008	-0.00706	0.271	0.509	0.882	0.373	1865	0.217	0.10	0.073
4	3.33×10^{-4}	2.67×10^{-4}	0.009	-0.00769	0.295	0.684	1.100	0.416	1558	0.233	0.10	0.070
5	3.33×10^{-4}	3.33×10^{-4}	0.008	-0.01219	0.468	0.939	1.489	0.55	1652	0.333	0.20	0.07568
6	3.33×10^{-4}	2.00×10^{-4}	0.00267	-0.00566	0.217	0.498	0.749	0.251	1255	0.039	0.0311	0.0586
7	3.33×10^{-4}	2.00×10^{-4}	0.0053	-0.00667	0.256	0.499	1.032	0.533	2665	0.211	0.0792	0.07469
8	3.33×10^{-4}	2.00×10^{-4}	0.010667	-0.00952	0.368	0.498	0.904	0.406	2030	0.219	0.100	0.0506
9	0.33×10^{-4}	2.00×10^{-4}	0.009	-0.00625	0.239	0.510	0.618	0.108	540	0.028	0.052	0.032
10	1.67×10^{-4}	2.00×10^{-4}	0.008	-0.00686	0.263	0.509	0.879	0.37	1850	0.211	0.10	0.075
11	10.00×10^{-4}	2.00×10^{-4}	0.008	-0.01148	0.441	0.509	1.009	0.50	2500	0.298	0.10	0.0745
12	13.33×10^{-4}	2.00×10^{-4}	0.009	-0.01484	0.569	0.510	1.014	0.504	2520	0.300	0.10	0.0744

Fig. 27: Ultra-violet spectrum of Ga^{3+} + L-Threonine + PLP No.3 at pH=3.8 and 25°C

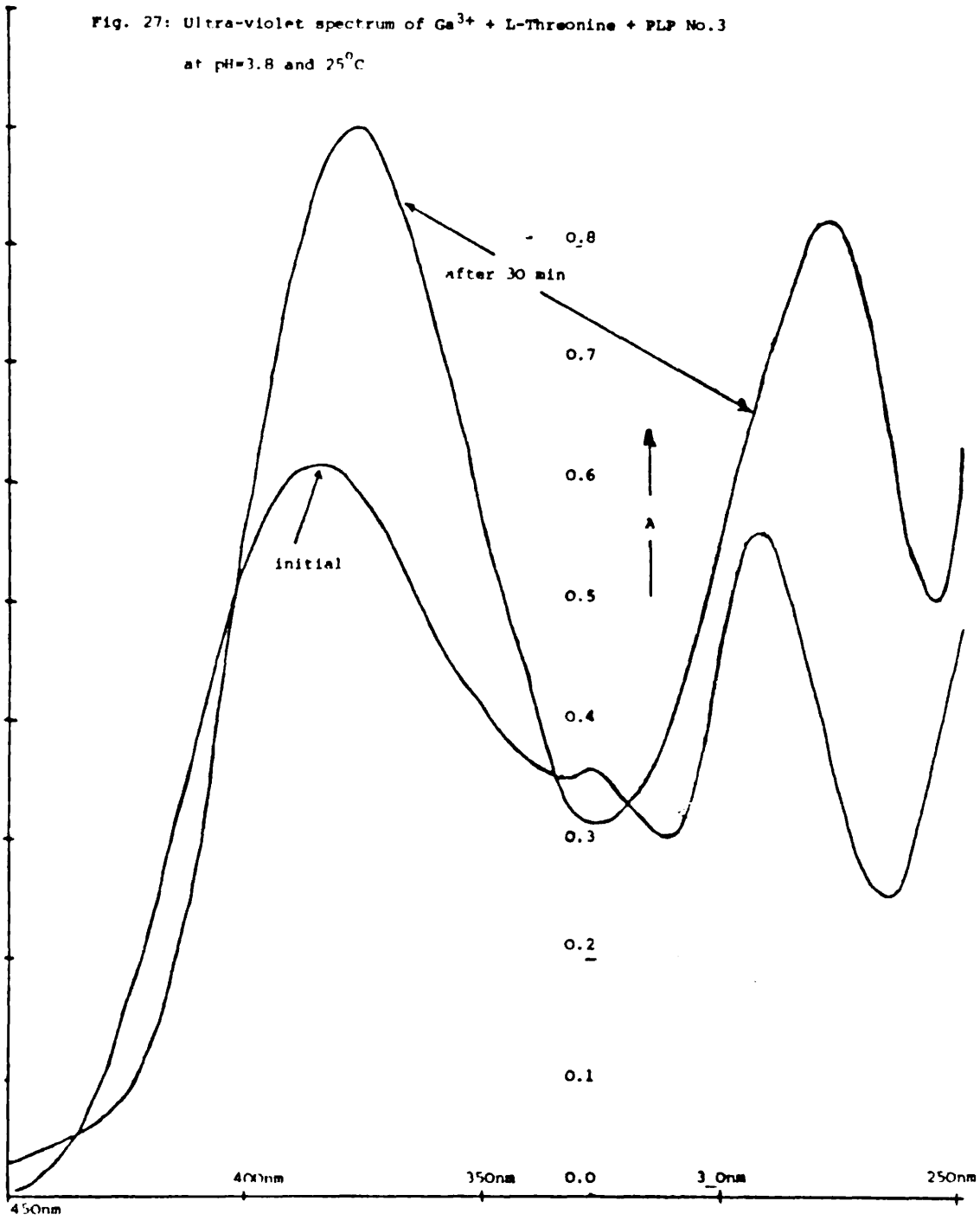

(1) The Reaction of Al^{3+} in the presence of PLP and L-threonine at pH=5.6

Table 40

Determination of the first and second rate constants for the reaction of Al^{3+} + PLP + L-Threonine at pH=5.6, T = 25°C and λ = 372 nm

Rⁿ	Al^{3+} /mol.dm^{-3}	PLP /mol.dm^{-3}	L-Thr /mol.dm^{-3}	-slope	$k_1 \times 10^3$	A_0	A_∞	ΔA	ΔE	initial slope	$10^6 \times$initial Rate	k_2 /mol^{-1}dm^{3}s^{-1}
1	3.33×10^{-4}	0.667×10^{-4}	0.008	0.016538	0.635	0.090	0.216	0.126	1889	0.003267	1.7	3.2
2	3.33×10^{-4}	1.33×10^{-4}	0.008	0.0175	0.6717	0.365	0.594	0.229	1722	0.009286	5.4	5.0682
3	3.33×10^{-4}	2.00×10^{-4}	0.009	0.0184	0.7078	0.398	0.810	0.412	2060	0.01655	8.0	5.02123
4	3.33×10^{-4}	2.667×10^{-4}	0.008	0.02062	0.7915	0.776	1.268	0.492	1845	0.0199	10.8	5.0553
5	3.33×10^{-4}	2.00×10^{-4}	0.00133	0.00054	0.0207	0.410	0.707	0.297	1485	0.002	1.3	5.063
6	3.33×10^{-4}	2.00×10^{-4}	0.00533	0.00875	0.3359	0.40	0.716	0.380	1901	0.005	2.6	2.467
7	3.33×10^{-4}	2.00×10^{-4}	0.010667	0.01186	0.4554	0.442	0.796	0.354	1770	0.019	10.7	5.0316
8	1.667×10^{-4}	2.00×10^{-4}	0.008	0.006	0.2303	0.595	0.917	0.322	1610	0.013	8.1	5.04658
9	10.00×10^{-4}	2.00×10^{-4}	0.008	0.0108	0.4145	0.395	0.866	0.471	2355	0.0189	8.0	5.0159
3	at 55°C			0.1154	4.4294	0.395	0.622	0.227	1135	0.0350	30.8	19.27312
3	at 45°C			0.0636	2.4412	0.395	0.609	0.214	1070	0.0246	23.0	14.369
3	at 35°C			0.02174	0.8345	0.395	0.624	0.229	1145	0.0168	14.7	9.1700

(m) Determination of the Rate of the reaction of Al^{3+} with PLP and L-NaGlu at pH=9.0

Table 41

Determination of the first and second rate constant for the reaction of Al^{3+} with PLP and Glutamate at pH=9.0, 25°C and 212nm.

soln	$[Al^{3+}]$ /mol.dm^{-3}	[PLP] /mol.dm^{-3}	[Glu] /mol.dm^{-3}	-slope /min^{-1}	10^3k_1 /s	A_0	A_∞	ΔA	ΔE	10^3 initial slope/s$^-$	10^6 initial Rate	k_2 /mol.dm^3.s
1	0.33×10^{-3}	0.67×10^{-4}	0.8×10^{-2}	0.03515	1.2095	0.219	0.441	0.222	3313	18.2	5.5	10.25
2	0.33×10^{-3}	1.33×10^{-4}	0.8×10^{-2}	0.04133	1.5864	0.347	0.715	0.368	2767	29.6	10.7	10.1
3	0.33×10^{-3}	2.00×10^{-4}	0.8×10^{-2}	0.0439	1.685	0.451	0.999	0.548	2740	44.02	16.1	10.04
4	0.33×10^{-3}	2.67×10^{-4}	0.8×10^{-2}	0.0457	1.7541	0.559	1.324	0.765	2865	61.41	21.4	10.03
5	0.33×10^{-3}	2.00×10^{-4}	0.0027	0.0092	0.3531	0.450	0.994	0.544	2720	1469	5.4	10.00
6	0.33×10^{-3}	2.00×10^{-4}	0.0053	0.0352	1.3511	0.449	0.989	0.540	2700	29.11	10.8	10.17
7	0.33×10^{-3}	2.00×10^{-4}	0.01067	0.0529	2.0305	0.459	0.992	0.533	2665	57.14	21.4	10.05
8	0.03×10^{-3}	2.00×10^{-4}	0.8×10^{-2}	0.0311	1.1937	0.450	0.967	0.517	2585	20.31	7.9	4.9
9	0.167×10^{-3}	2.00×10^{-4}	0.8×10^{-2}	0.0389	1.4931	0.451	0.998	0.547	2735	44.01	16.1	10.05
10	0.667×10^{-3}	2.00×10^{-4}	0.8×10^{-2}	0.0498	1.9115	0.458	0.992	0.534	2670	42.95	16.1	10.05
11	1.00×10^{-3}	2.00×10^{-4}	0.8×10^{-2}	0.067	2.5717	0.486	0.963	0.477	2385	32.04	13.4	8.396

(n) Determination of the Rate of the Reaction of Ga^{3+} with PLP and L-NaGlu at pH=9.0

Table 42

Determination of the first and second rate constants for the reaction of Ga^{3+} with PLP and Glutamate at pH=9.0, T=25°C and λ = 272nm.

soln	$[Ga^{3+}]$ /mol.dm^{-3}	[PLP] /mol.dm^{-3}	[Glu] /mol.dm^{-3}	-slope /min^{-1}	$10^3 k_1$ /s	A_0	A_∞	ΔA	$\Delta\varepsilon$	10^3 initial slope/s^{-1}	10^6 initial Rate	K_2 /mol^{-1} dm^3 s^{-1}
1	0.33×10^{-3}	0.67×10^{-4}	0.8×10^{-2}	0.03898	1.496	0.214	0.437	0.223	3328	20.00	6.0	11.211
2	0.33×10^{-3}	1.33×10^{-4}	0.8×10^{-2}	0.0492	1.888	0.340	0.690	0.35	2632	30.90	11.7	11.034
3	0.33×10^{-3}	2.00×10^{-4}	0.8×10^{-2}	0.0475	1.8232	0.440	1.013	0.573	2865	52.00	18.2	11.344
4	0.33×10^{-3}	2.67×10^{-4}	0.8×10^{-2}	0.0486	1.8643	0.545	1.339	0.794	2974	71.00	23.9	11.1768
5	0.33×10^{-3}	2.00×10^{-4}	0.0027	0.00857	0.329	0.385	1.015	0.63	3150	14.39	0.5	0.84597
6	0.33×10^{-3}	2.00×10^{-4}	0.0053	0.0346	1.3287	0.44	0.745	0.305	1525	22.60	14.8	13.98
7	0.33×10^{-3}	2.00×10^{-4}	0.01067	0.06094	2.339	0.435	0.783	0.348	1740	41.58	23.9	11.198
8	0.033×10^{-3}	2.00×10^{-4}	0.008	0.00533	0.20471	0.420	0.888	0.468	2340	21.43	9.2	5.724
9	0.167×10^{-3}	2.00×10^{-4}	0.008	0.04273	1.64	0.409	0.940	0.531	2655	48.00	18.1	11.299
10	0.667×10^{-3}	2.00×10^{-4}	0.008			0.430	0.94	0.51	2550	47.02	18.4	11.525
11	1.00×10^{-3}	2.00×10^{-4}	0.008	0.0846	3.2478	0.57	0.892	0.332	1610	29.09	18.1	11.293

for the same system. The values of k_1 were calculated from

$$k_1 = \frac{2.303 \log_{10}(A_\infty - A_t)}{t}$$

where A_∞ and A_t are the measured optical densities at time ∞ and t.

The second order rate constants k_2 were calculated by the initial rate method.

3. Discussion

(a) Spectra of PL-type compounds

As Martell[2] and Peterson[1] showed, the band at 34,000 cm^{-1} due to the neutral non-polar Schiff-base, which exists in acidic pH values. When the pH increases the intensity of the peak decreases (Figs. 20,22,24 25, 26). This band was also suggested[2] to due partly to the free PLP and PAMP which exists after transamination.

The band between 30,000 and 31,000 cm^{-1} due to $\pi \rightarrow \pi_1^*$ transition of ketimine in the M^{3+}-SB and it is absent in the very acidic pH values.

The band around 25,000-26,000 cm^{-1} has been assigned to the imine π-π_1^* transition for the PLP. This band is almost absent in the low pH values i.e. pH 1.8 and 1.6.

Bands at 26,600 and 23,900 cm^{-1} due to the intermediate species of aldimine-ketimine tautomers[3]. The bands at 35,000-36,000 cm^{-1} may be due to the hydrolysis products.

The band at 28,000 cm^{-1} which occurs in the free PLP and was assigned by Martell[2] to the ionized phenolic group, is absent from the u.v. spectra of M^{3+}-S B complexes in any pH value, indicating coordination through the phenolic oxygen as well.

Metal-Schiff-base complexes produced from PAMP and α-keto-glutaric acid have similar absorption maxima to the ones of M-PLP-Glu complexes. They also contain the bands at 26,600 cm^{-1} and 34,000 cm^{-1} at the acidic

pH range, indicating shift from Ketimine to aldimine Schiff-base, which is promoted by acidic conditions.

The molar extinction coefficient increases with increasing pH in the range of 3.85-4.83, but at pH=6.55 and 6.65 decreases (Fig. 14) as the ionic species change around pH≈5.6.

Protonation of the heterocyclic nitrogen of the Ketimine Schiff-base (Fig. 22), causes shifting of the bands to the longer wavelengths, while the protonation of the aldimine's hererocyclic nitrogen makes the bands go to the shorter wavelengths. Shifts to the shorter wavelengths could also be the result of the chelation of the Schiff-base to the metal ion which stabilizes the complex and makes therefore the aldimine Ketimine forms interconvertable.

Generally, the spectra were very complicated because of the dissociation of the M^{3+}-Schiff-base complexes which occurs in aqueous solutions or the hydrolysis which forms the PLP and aminoacids, or because of the transamination reaction which brings into the solution a number of different species which cause the appearance of extra $\pi\rightarrow\pi_1^*$ and $\pi\rightarrow\pi_2^*$ absorption bands and hence, the identification of the bands was very difficult.

(b) Kinetics

The graphs obtained from the plot of $\log(A_\infty - A_t)$ against time/min were linear for the first 7 min, but after 7 min a curve was obtained. The absorbance gradually increased up to about 40 min and then slightly decreased.

There was a small difference in k_1 when the solutions were added to the cell in the reverse order.

Since the plot of $\log(A_\infty - A_t)$ against time showed that the reaction was not of first order, the results were tested for a second order reaction. Tables 20,22,24,26,28,31,33,36,38-41 show the value of

K_2 (i.e. second order reaction constant), for each solution. K_2 values are almost the same within an experimental error limit. This suggests that the reactions must be of second order and applies only for the reactions in which the metal ions are in excess to the other species.

When the concentration of metal was lower than that of PLP, the reaction of formation of the M-SB complex was dependent on the concentration of the metal ion while when the concentration of the metal ion was higher than the concentration of PLP, the rate constant was independent of the metal ion concentration, and the reaction was second order.

In the alkaline pH range (pH=9.0), the reactions proceed much faster than in the acidic range (tables 40,41). Again only for the first 7 min the semi log plot is linear. The rate of the reaction increases as the concentration of the metal increases but then again after a certain value the metal concentration seems to have no effect on the rate.

REFERENCES

1. E.A. Peterson and N.A. Sober, J.A.C.S., 169, 76 (1954).

2. D. Heinert and A.E. Martell, J.A.C.S., 183, 85 (1963).

3. H.N. Christensen, J.A.C.S. 2305, 80 (1958).

CHAPTER 4

CHROMATOGRAPHY

Paper chromatography is a separation technique, based on the different rates of flow of the different solvent mixtures, on a paper. The partition coefficient of a substance between solvent and the mobile phase is related[1] to Rf value which initially was considered as a physical constant, but experience has shown that temperature, solvent, size of the tank, paper and nature of the mixture can affect its value. Paper chromatography has been used to identify the products of the reactions studied.

1. Experimental

The paper chromatographs were prepared using Whatman No.1 paper. The solvent used was a mixture of n-butanol, acetic acid and water in a volume ratio[2] of 12:3:5. The dried papers were viewed under ultra-violet light, then were exposed to ammonia vapour and viewed again under u.v. light. Finally the papers were sprayed[3] successively with ninhydrin and dithizone (0.05% in chloroform). The colour spots were marked and the Rf values were obtained.

Other chromatographs were sprayed with dimethylglyoxime, rubeanic acid and ammonium sulphide. Each detecting reagent was sprayed in a different paper and pure solutions of metals and amino acids were used as reference.

2. Results and Discussion

(i) Reaction of L-glutamate in the presence of PLP and Cu^{2+}

The reaction of L-glutamate in the presence of PLP and Cu^{2+} in the

series of buffer solutions (Appendix 1) and by changing the concentration of the initial compounds used, was studied by paper chromatography, 30 minutes after mixing the reactants, just at the end of the second stage of the reaction studied using the polarimeter (see Chapter 2). The Rf values and the colour produced with certain conditions are shown in table 43. From these results it is clear that for the first 30 minutes either there is no transamination reaction or that the amount of PAMP formed is so small that no orange spot develops with ninhydrin. All the papers showed that glutamate was still present but it is possible that a very small amount of α-keto-glutaric acid coexists with glutamate and it is difficult to be detected because of its very low concentration. α-keto-glutaric is a quite labile compound and therefore it has to be converted to a more stable derivative (i.e. hydrazone)[4] before it appears on the chromatogram, otherwise it can very easily decompose. Although paper chromatography did not reveal the presence the the transamination reaction in the first 30 minutes, an unusual spot appeared, which was blue under u.v. and yellow with ninhydrin and possibly this could be due to the dephosphorylated PLP as PL gives a similar spot but with a slightly higher Rf value[5].

(ii) Reaction of L-glutamate with PLP in the presence of Al^{3+}, Ga^{3+}, In^{3+}

These chromatographs were made six hours after mixing the reactants. Although the Rf values did not agree very well with the theoretical ones, due to the low temperature and quality of the paper, it was very clear that transamination reaction had been taking place. Evidence was the appearance of brown spot (Rf $\sim$ 62-60) with u.v. light which was green with dithizone, and the dissappearance of the glutamate's purple spot (Rf $\sim$ 20-25). Some chromatographs contained both spots due to α-Kg and Glu (Table 44). The presence of the orange spot, due to PAMP, revealed

also the transamination process. Some chromatographs still had PLP present (Rf = 12, blue under u.v. and no colour with ninhydrin). The blue spot (under u.v. light which turns yellow with ninhydrin) was again present suggesting that dephosphorylation was also taking place.

Table 44 proves that transamination and dissociation reactions take place and that both are faster in acidic conditions.

An attempt was made to determine the amount of the products of the transamination reaction by using an LC3 high pressure liquid chromatograph, fitted with a Partisil OPS column. But the results were not successful because α-keto-glutaric acid, L-glutamate and PLP had similar retention times and could not be resolved. Further work is required using different types of columns for a better resolution.

However, using[6] an LKB 4101 single column analyser containing a sulphonated polystyrene cation exchange resin, was able to separate the products of the reaction of PLP with L-glutamate and Al^{3+}. Preliminary work shows that by recording the absorbance in the presence of ninhydrin, the amount of transamination taking place could be deduced from the area of the peak due to L-glutamic acid, which was reduced, because of its conversion to α-keto-glutaric acid, while a new peak identified as that due to PAMP was also present. Detailed work using this technique is not yet complete, results of further analyses are awaited. The technique, however, was shown to be very successful and it is anticipated that it will be possible to calculate the amounts of the products at various times during the reaction and therefore work out the details of the kinetics and mechanism.

Table 43

Results from paper chromatography for the reaction of Cu^{2+} with PLP and Glu

Run	100 Rf	conditions	colour	compound
1	18	u.v.	blue	PLP
	25	ninhydrin	purple	Glu
	26	dithizone	yellow	Cu^{2+}
2	17	u.v.	blue	PLP
	57	u.v.	blue	?
	57	ninhydrin	yellow	?
	26	ninhydrin	purple	Glu
3	16	u.v.	blue	PLP
	20	ninhydrin	purple	Glu
	24	dithizone	yellow	Cu^{2+}
4	20	u.v.	blue	PLP
	27	ninhydrin	purple	Glu
	25	dithizone	yellow	Cu^{2+}
5	22	u.v.	blue	PLP
	46	u.v.	blue	?
	46	ninhydrin	yellow	
	29.5	ninhydrin	purple	Glu
6	17	u.v.	blue	PLP
	20	ninhydrin	purple	Glu
7	17	u.v.	blue	PLP
	21	ninhydrin	purple	Glu
	25	dithizone	yellow	Cu^{2+}
8	16	u.v.	blue	PLP
	20	ninhydrin	purple	Glu
	24	dithizone	yellow	Cu^{2+}
9	15	u.v.	blue	PLP
	19	ninhydrin	purple	Glu
	25	dithizone	yellow	Cu^{2+}
10	17	u.v.	blue	PLP
	21	ninhydrin	purple	Glu
	50	ninhydrin	yellow	?
	24	dithizone	yellow	Cu^{2+}
11	17	u.v.	blue	PLP
	21	ninhydrin	purple	Glu
	24	dithizone	yellow	Cu^{2+}
12	16	u.v.	blue	PLP
	19	ninhydrin	purple	Glu
13	17	u.v.	blue	PLP
	21	ninhydrin	purple	Glu
14	17	u.v.	blue	PLP
	20	ninhydrin	purple	Glu
15	16	u.v.	blue	PLP
	19	ninhydrin	purple	Glu
	24	dithizone	yellow	Cu^{2+}
16	17	u.v.	blue	PLP
	17	ninhydrin	purple	Glu
	23	dithizone	yellow	Cu^{2+}

continued...

Run	100×Rf	conditions	colour	compound
17	17	u.v.	blue	PLP
	19	ninhydrin	purple	Glu
	41	ninhydrin	yellow	?
	41	u.v.	yellow	
18	18	u.v.	blue	PLP
	26	ninhydrin	purple	Glu
	27	dithizone	yellow	Cu^{2+}
19	19	u.v.	blue	PLP
	25	ninhydrin	purple	Glu
	26	dithizone	yellow	Cu^{2+}
20	19	u.v.	blue	PLP
	27	ninhydrin	purple	Glu
	27	dithizone	yellow	Cu^{2+}
21	22	u.v.	blue	PLP
	28	ninhydrin	purple	Glu
22	22	u.v.	blue	PLP
	59	u.v.	blue	?
	28	ninhydrin	purple	Glu
23	20	u.v.	blue	PLP
	28	ninhydrin	purple	Glu
	27	dithizone	yellow	Cu^{2+}
24	19	u.v.	blue	PLP
	26	ninhydrin	purple	Glu
25	22	u.v.	blue	PLP
	26	ninhydrin	purple	Glu
26	22	u.v.	blue	PLP
	29	ninhydrin	purple	Glu
27	21	u.v.	blue	PLP
	57	u.v.	blue	?
	29	ninhydrin	purple	Glu
28	21	u.v.	blue	PLP
	27	ninhydrin	purple	Glu
29	20	u.v.	blue	PLP
	28	ninhydrin	purple	Glu
30	18	u.v.	blue	PLP
	60	u.v.	blue	?
	29	ninhydrin	purple	Glu
	27	dithizone	yellow	Cu^{2+}
31	23	u.v.	blue	PLP
	24	NH ,ninhydrin	purple	Glu
	26	dithizone	yellow	Cu^{2+}
32	23	u.v.	bright blue	PLP
	29	ninhydrin	purple	Glu
	26	dithizone	yellow	Cu^{2+}
33	22	u.v.	blue	PLP
	30	ninhydrin	purple	Glu
	46	u.v.	yellow	?
			blue	
34	23	u.v.	blue	PLP
	19		brown	?
	28	ninhydrin	purple	Glu
35	30.5	ninhydrin	purple	Glu

continued...

Run	100×Rf	conditions	colour	compound
35	26	dithizone	yellow	Cu^{2+}
36	30	ninhydrin	purple	Glu
	26	dithiizone	yellow	Cu^{2+}
37	24	u.v.	violet-blue	PLP
	18	u.v.	brown	
	27	ninhydrin	purple	Glu
38	23	u.v.	blue	
	30	ninhydrin	purple	
39	23	u.v.	blue	PLP
	29	ninhydrin	purple	Glu
	27	dithizone	yellow	Cu^{2+}
40	23	u.v.	blue	PLP
	29	ninhydrin	purple	Glu
41	23	u.v.	blue	PLP
	52	u.v.	blue	?
	30	ninhydrin	purple	Glu
42	23	u.v.	blue-violet	PLP
	38		brown	
	29	ninhydrin	purple	Glu
43	19	u.v.	blue	PLP
	44	u.v.	blue	?
	28	ninhydrin	purple	Glu
44	19	u.v.	blue	PLP
	28	ninhydrin	purple	Glu
45	20	u.v.	blue	PLP
	27	ninhydrin	purple	Glu
46	20	u.v.	blue	PLP
	28	ninhydrin	purple	Glu
47	19	u.v.	blue	PLP
	28	ninhydrin	purple	Glu
48	19	u.v.	blue	PLP
	29	ninhydrin	purple	Glu
49	19	u.v.	blue	PLP
	44	u.v.	blue	?
	28	ninhydrin	purple	Glu
50	19	u.v.	blue	PLP
	26	ninhydrin	purple	Glu

Table 44

Results obtained from paper chromatography for the reaction of M^{3+}+PLP+L-Glu

reaction	pH	100xRf	conditions	colour	compound
Al^{3+}+PLP+L-Glu	6.8	62	u.v. dithizone	brown green	α-oxo-glutaric acid
		20	u.v. ninhydrin	violet purple	Glu
		16	u.v. ninhydrin	blue no colour	PLP
		7	ninhydrin u.v.	orange purple	PAMP
Ga^{3+}+PLP+L-Glu	6.8	60	u.v. dithizone	brown green	α-oxo-glutaric acid
		5	ninhydrin	orange	PAMP
		44	u.v.	blue	
		18	ninhydrin	purple	Glu
Al^{3+}+PLP+L-Glu	3.8	17	u.v.	blue	PLP
		22	ninhydrin	purple	Glu
		4	ninhydrin	orange	PAMP
		56	U.V.	blue	

continued...

reaction	pH	100×Rf	conditions	colour	compound
Ga^{3+}-PLP+L-Glu	1.86	18	u.v.	blue	PLP
		24	ninhydrin	purple	Glu
		59	u.v.	blue	PL
Al^{3+}+PLP+L-Glu	9.0	14	u.v.	blue	PLP
		18	ninhydrin	purple	Glu
		2	ninhydrin	orange	PAMP
Ga^{3+}+PLP+L-Glu	9.0	63	u.v. dithizone	brown green	α-oxo-glutaric acid
		3	ninhydrin	orange	PAMP
Ga^{3+}+PLP+L-Glu	11.0	15	u.v.	blue	PLP
		18	ninhydrin	purple	Glu
		2	ninhydrin	orange	PAMP
		56	u.v.	blue	
Al^{3+}+PLP+L-Glu	11.0	14	u.v.	blue	PLP
		19	u.v. ninhydrin	brown purple	Glu
		1	ninhydrin u.v.	orange purple	PAMP
		60	u.v.	brown	

REFERENCES

1. Hopgood and Leussing, J.A.C.S. 81, 3740 (1969).

2. Zweig Sherma "Handbook of Chromatography", Volume II.

3. R. Stock and C.B.E. Rice, "Crhomatographic Methods", 3rd edition, Chapman and Hall and Science Paperbacks (1974).

4. A.I. Vogel "Quantative Inorganic Analysis", third edition, Longmans, Green and Co.k (1951).

5. M.E. Farago, M.M. McMillan and S.S. Sabir, Inorg. Chim. Acta, 14, 207 (1975).

6. Dr. McDonough, Personal communication, Bedford College, University of London.

CHAPTER 5

MULTINUCLEAR n.m.r. STUDY OF Al^{3+}, Ga^{3+} AND In^{3+} COMPLEXES IN SOLUTION

1. Application of nuclear magnetic resonance (n.m.r.) techniques in order to obtain structural information

Nuclei having an odd number of nucleons of the same kind, possess an angular momentum, $\hbar[I(I+1)]^{\frac{1}{2}}$, and therefore they have nuclear-magnetic-resonance properties. They will have a magnetic moment, μ_I, due to the spinning nuclear charge, which is given by:

$$\mu_I = \gamma_I \hbar [I(I+1)]^{\frac{1}{2}}$$

and $$\gamma = \frac{2\pi}{h} \cdot \frac{\mu}{I} = \frac{\mu}{I\hbar}$$

where I is the nuclear spin quantum number, $\hbar$ is the reduced Planks' constant $h/2\pi$ and γ_I is the magnetogyric ratio which has a characteristic value for each magnetically active nucleus and is positive or negative depending on whether the magnetic moment vector is parallel or anti-parallel to the angular momentum vector. If $I > \frac{1}{2}$, the nucleus possesses an electric quadrupole moment Q, because the distribution of the charge in the nucleus is not spherical and can interact with the electric field gradients arising from the electric charge distribution in the molecule, exchanging energy.

Since I is quantised, a number of discrete values of angular momentum can be observed of a magnitude hm (where m, the magnetic quantum number is I, I-1, I-2...-I) and therefore 2I+1 equally spaced spin states of a nucleus with angular momentum quantum number I. μ has also 2I+1 components. In the absence of an external magnetic

field, all spin states possess the same potential energy. Isotopes of a non-zero nuclear-spin quantum number (I), placed in a strong magnetic field, B_0, have quantised orientations of their spin axis, each orientation having a different energy. The energy separation between the levels is constant and equal to $\mu B_0/I$.

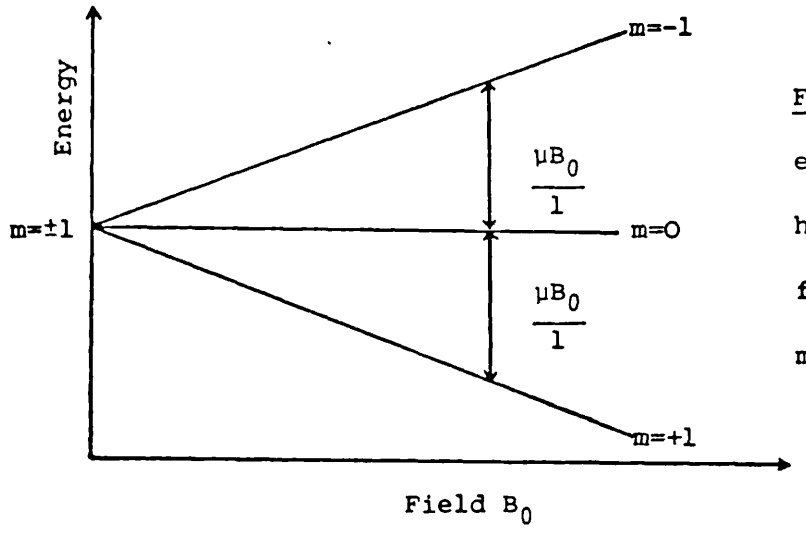

Fig.2: Nuclear spin-energy for a nucleus having I = 1, as a function of the magnetic field B_0

Since all the energy separations are equal and transitions are only allowed between levels at which the selection rule $\Delta m = \pm 1$ operates, transitions only occur at a certain frequency.

$$\nu = \gamma . \frac{B}{2\pi} \qquad \text{(Larmor equation)}$$

Thus the nucleus can interact with radiation whose frequency depends only upon the applied magnetic field and the nature of the nucleus.

The magnetic field causes motion of the electron cloud of the atoms or molecules, such that a secondary magnetic field is produced, which opposes the main field at the nucleus and therefore reduces the nuclear frequency. The magnitude of the electronic current is proportional to B_0 and determines the shielding of the nucleus from the applied field as it changes the nuclear frequency

$$\nu = \frac{\gamma B_0}{2\pi} \quad (1 - \sigma)$$

where σ is the screening constant which is a dimensionless quantity recorded in p.p.m. The magnetic field at the nucleus (B) is equal to

$$B = (1 - \sigma)B_0$$

Nuclei in different structural environments have different resonance frequencies. The difference in frequency from an arbitrarily chosen one is called chemical shift.

Complexation of metal ions with organic ligands affects the n.m.r. properties of the ligands such as chemical shifts, coupling constants and relaxation times. The resonance signals of the isotopes depend on the type of bonding and the spectral widths indicate the symmetry of the molecule. The apperance of new resonance signals indicates the different bonding interactions and the sites of coordination. ^{71}Ga, ^{27}Al, ^{13}C, ^{1}H, ^{31}P and ^{14}N n.m.r. techniques have been used to study the structural effects of complexation.

2. Experimental

All measurements were made using a JEOL FX 90 Q Fourier Transform n.m.r. Spectrometer.

The ^{27}Al n.m.r. spectra were obtained at 23.3 MHz OBFRQ; 47.05 Khz OBSET; 400 MS PD and 72 µS PW_1. $^{27}Al(H_2O)_6^{3+}$ was used as reference.

The ^{71}Ga spectra were obtained at 27.32 MHz OBFRQ; 6KHz OBSET; 75 µS PD; and 60 µS PW_1. $GaCl_4^-$ was used as an external reference which was prepared by dissolving Gallium metal in 7M HCl. For studies involving spectral widths of signals of a certain resonance frequency, the external reference was not used as the chemical shifts were determined.

^{115}In n.m.r. spectra were recorded at 19.5 MHz OBFRQ; 72.0 KHz OBSET; 0.5 S PD; and 70 μS PW. The external reference was $In(NO_3)_3$ in 30% HNO_3. ^{31}P n.m.r. spectra were recorded at 36.2 MHz OBFRQ; 72.5 KHz OBSET; 12 μS PW and 0.86 S PD; a solution of 8M H_3PO_4 was used as an external reference. ^{13}C n.m.r. spectra were obtained at 22.5 MHz OBFRQ; 33.11 KHz OBSET, 31 μS PW_1 and 1S PD. ^{1}H n.m.r. spectra were observed at 89.6 MHz OBFRQ and 44.55 KHz OBSET. For both ^{13}C and ^{1}H n.m.r. spectra, dioxan was used as reference and the chemical shifts were then corrected by adding 67.4 p.p.m. for TMS[1]. Sample tubes of 10 mm diameter were used and measurements made at room temperature. In this thesis positive chemical shifts are always downfield from the reference used.

Samples were prepared by mixing solutions of metal ion and ligands in D_2O:H_2O (1:9, v:v) solutions, for ^{27}Al, ^{71}Ga, ^{115}In and ^{31}P n.m.r. measurements. For ^{1}H n.m.r. measurements the solutions of ligands and metal ion were studied in D_2O only. For ^{13}C spectra the medium was D_2O:CD_3OD (1:1, v:v). Marlett had shown previously[2,3] (and it was checked in this work by uv measurements) that the ^{13}C spectra are easier to measure since reactions are faster in this solvent. Using this solvent mixture comparisons could be made with the ^{13}C n.m.r. data already in the literature.

The pH (determined by a Pye Dynacap pH meter) was adjusted with NaOD and/or D_2SO_4 for ^{1}H and ^{13}C n.m.r. measurements or with NaOH and/or HCl for ^{27}Al, ^{71}Ga, ^{115}In and ^{31}P n.m.r. measurements, and it was corrected to give pD by adding 0.41 to the observed reading on the meter[4].

NaOD was prepared by dissolving solid NaOH in D_2O. D_2SO_4, L-Na-glu and L-Threon. were purchased from BDH Chemicals Ltd. Gallium nitrate was obtained from Koch-Light Laboratories Ltd. (and some was given by Johnson and Matthey) and L-aspartic acid from Hopkin and Williams Ltd. D_2O and CD_3OH were produced by nuclear-magnetic resonance ltd

Table 45

Nuclear Properties of the Elements Associated with this N.M.R. Study

element	Spin	Natural Abundance N%	Magnetic moment μ/μ_N	Magnetogyric ratio $\gamma/10^7$ rad $T^{-1}S^{-1}$	Quadrupole Moment $Q/10^{-28}m^2$	NMR frequency /MHz	Receptivity relative to that of ^{13}C	Receptivity relative to that of ^{1}H
^{27}Al	5/2	100	4.3051	6.9706	0.149	26.057	1.17×10^{3}	0.206
^{71}Ga	3/2	39.6	3.2984	8.1578	0.112	30.495	3.19×10^{2}	5.62×10^{-2}
^{115}In	9/2	95.72	6.0892	5.8622	1.16	21.914	1.89×10^{3}	0.332
^{31}P	1/2	100	1.9581	10.829		40.4807	3.77×10^{2}	0.0663
^{13}C	1/2	1.108	1.2162	6.7263		25.1450	1.00	1.76×10^{-4}
^{1}H	1/2	99.985	4.8371	26.751		100.000	5.68×10^{3}	1.00

Data from Harris and Mann[18]

3. n.m.r. Results and Discussion

The structural information concerning the nature of the complexes in solution obtained using uv spectroscopy is limited. The breadth of the absorption bands limited the number of components which could be monitored and therefore restricted the amount of structural detail obtainable. By contrast n.m.r., through a multinuclear study, provided much structural detail.

A. ^{27}Al n.m.r.

Although ^{27}Al ($I = \frac{5}{2}$) possesses a quadrupole moment (table 45), it gives relatively narrow n.m.r. signals, the linewidths of which depend upon the geometry of the substituents[5,6]. Symmetrical molecules have small field gradients at the nucleus and therefore produce relatively narrow lines; however, less symmetrical molecules give rise to larger linewidths as there is a larger field gradient about the ^{27}Al nucleus.[7] The line widths vary from 3 to 6000 Hz and the chemical shift range of ^{27}Al resonances is approximately 450 ppm.[5] The chemical shifts are affected by the structure of the molecule[5] (e.g. octahedral species occur in the lower frequency range[8,9], tetrahedral species occur in an intermediate region[8,9] and at higher frequencies one can find species such as alkyl alanes)[5]. Akitt[5] suggested that in aqueous-organic solutions, the shifts are related to the number of ligands replacing a water molecule, and this is almost an additive effect[9,10,11]. Al^{3+} has a relatively large ratio of charge to ionic radius[12], hence it can interact quite strongly with the basic solvent molecules. The ^{27}Al chemical shifts in the coordination species with the same coordination number was found to be related to the basicity of the ligand molecule while the number of coordinated ligands[9,13] was causing large chemical shifts. The linewidths (and hence T_2*)[14,15] and the

---

* see p. 139

chemical shifts of ^{27}Al resonances provide information about the arrangement of ligands around Al^{3+} and indicate the type of bonding.

(i) The effect of concentration and pH on the resonance frequency of ^{27}Al $NH_4(SO_4)_2$

Before studying the Al^{3+}-Schiff-base complexes, an initial study of the ^{27}Al n.m.r. of Al $NH_4(SO)_2$ was carried out. By recording the spectrum of this compound at a series of concentrations and pH values, any differences observed under the same conditions when the complexes were studied could be attributed with certainty to complexation of the metal ion with the ligands.

Table 46, shows that the resonance frequency remains almost constant as the concentration changes. The peak shifts however, to lower field as the solution becomes more basic. In acidic solutions the signal is attributed to the symmetrical ion $Al(H_2O)_6^{3+}$ [16]; while that occurring in basic solution is due to aluminates[5], which are either dimers: $Al_2(OH)_2^{4+}$ or $Al(OH)_2(H_2O)_n^{4+}$ or polymers such as $Al_8(OH)_{20}^{4+}$. $Al(H_2O)_6^{3+}$ gives a very narrow line width in the presence of an excess of acid which broadens as the pH increases (table 46), but at pH ≥ 11 gives a narrow ^{27}Al resonance at lower field which due to the polymeric cation

$$Al_{13}O_4(OH)_{24}(H_2O)_{12}^{7+}$$

which contains a highly regular AlO_4 tetrahedron at its centre[17].

The aluminium complexes studied were: Al-PLP, Al-Glu, Al-Asp, Al-threonine, Al-PLP-glutamate, Al-PLP-aspartic, Al-PLP-threonine. Measurements were carried out at a series of concentrations and pH values as indicated in tables 47-50.

The complexes of the Lewis acid, Al^{3+}, with the donor molecules PLP, AA and SB gave ^{27}Al n.m.r. spectra very different in nature to

Table 46

The effect of concentration and pH on the resonance frequency of $^{27}AlNH_4(SO_4)_2$

pH	conc. of Al^{3+} /mol.dm^{-3}	Resonance frequency /Hz	Spectral width* /Hz	Chemical Shift from $Al(H_2O)_6^{3+}$ /Hz	/p.p.m.
1.0	0.5	23348044	7.45	0.00	0.00
2.0	0.5	"	9.71		
2.8	0.5	"	10.83		
3.7	0.5	"	13.25		
4.5	0.5	23348110	15.67	65	2.78
7.0	0.5	23348450	19.95	405	17.34
9.0	0.5	23349910	18.9	1879.88	80.49
11.0	0.5	"	12.0	"	"
12.0	0.5	"	10.7	"	"
3.0	0.064	23348044	13.68	0.00	0.00
3.0	0.128	"	12.57		
3.0	0.250	"	12.10		
3.0	0.500	"	12.06		

* The width of the peak was measured at half-height.

those of the aquated metal ion produced under the same conditions (Tables 47,49,50 and Fig.28-30). The spectral widths are larger and the resonances shifted from the initial resonance frequency of Al $NH_4(SO_4)_2$.

(ii) ^{27}Al n.m.r. study of Al^{3+}-PLP complex

Tables 47 and 48 show the chemical shifts of Al-PLP complex as a function of pH and concentration respectively. Spectra are given in fig. 17.

An attempt was made to obtain information about the symmetry of Al-PLP complex, from the spin-lattice relaxation time (T_1) (see appendix III). The results were not satisfactory, hence the spin-spin relaxation time (T_1) was tried, to test the possible symmetry of the complex form the spectra widths as they are directly related to the symmetry of the molecule.

The addition of PLP to Al^{3+} had very little effect on the line width, after the complex was formed (Fig. 18). The spectral width increases until the point at which the 1:3 complex is formed, at which the spectral width remains the same with further increase of the PLP-Al^{3+} mole ratio.

(iii) ^{27}Al n.m.r. of Al^{3+} in the presence of Amino-acids

Table 49 contains the results for Al^{3+} with various amino acids in order to identify the resonances due to aluminium coordinated to amino acid species. Later, when PLP was added, the resonance of any Al^{3+}-Schiff-base complexes could then be assigned by the elimination of those due to Al-PLP and Al-AA complexes.

(iv) ^{27}Al n.m.r. of Al^{3+}-Schiff-Base complexes

Table 50 contains the chemical shifts and the spectral widths of Al^{3+}-SB complexes in a series of pH values. Each of those species has a distinct chemical shift at a certain pH (compare this result for

Table 47

The effect of pH on the ^{27}Al n.m.r. spectra of Al^{3+}-PLP complex.

pH	$[Al^{3+}]$ /mol.dm^{-3}	[PLP] /mol.dm^{-3}	Chemical Shift from $Al(H_2O)_6^{3+}$ /Hz	/p.p.m.	Spectral width /Hz	$10^3 \times T_2^*$ /s	$\frac{[PLP]}{[Al^{3+}]}$
2.0	0.05	0.15	4.89	0.24	9	20.4	3
3.5	0.05	0.15	19.05	0.8157	14.7	12.5	3
7.0	0.05	0.15	901.45	38.597	1410	0.13	3
9.0	0.05	0.15	1874.09	80.3	99	1.86	3
11.0	0.05	0.15	1879.878	80.49	95	1.94	3

Table 48

The ^{27}Al n.m.r. spectra of Al^{3+}-PLP complex as a function of [PLP] at PH=9.0

$[Al^{3+}]$ /mol.dm^{-3}	[PLP] /mol.dm^{-3}	Chemical Shift from $Al(H_2O)_6^{3+}$ /Hz	/p.p.m.	Spectral width/Hz	$10^3 \times T_2^*$ /s	$\frac{[PLP]}{[Al^{3+}]}$
0.03	0.000	1879.88	80.49	14.5	12.68	-
0.03	0.009	1874.995	80.282	22.0	8.36	0.3
0.03	0.030	1875.00	80.283	35.0	5.25	1.0
0.03	0.045	1860.35	79.66	54.0	3.41	1.5
0.03	0.060	1860.35	79.66	90	2.04	2.0
0.03	0.090	1860.35	79.66	155	1.19	3.0
0.03	0.150	1860.35	79.66	162	1.135	5.0
0.03	0.250	1860.35	79.66	162	1.135	8.33

* T_2 was calculated from[15] $\Delta\nu = \frac{1}{\pi\sqrt{3}} \cdot T_2^{-1}$ (see p. 139)

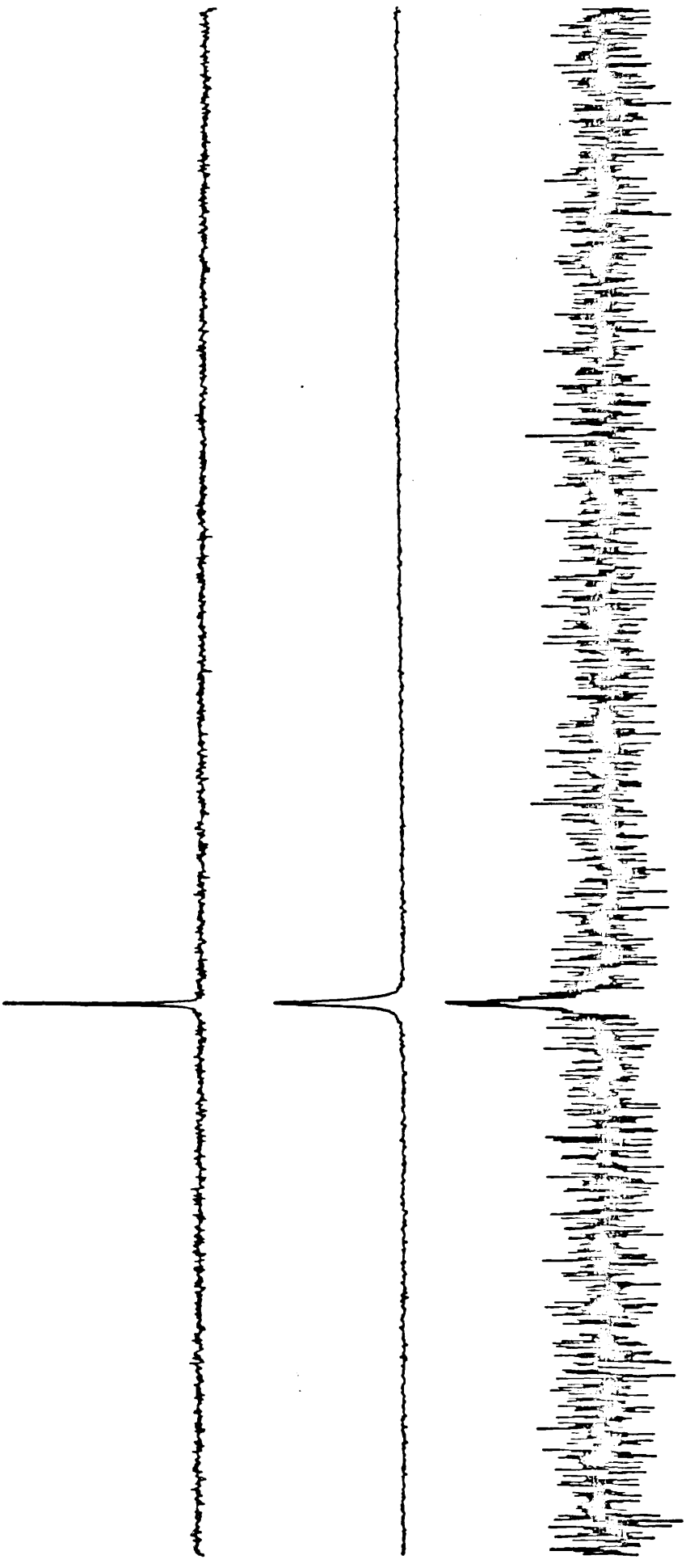

Fig.27: ^{27}Al n.m.r. spectra of 0.03M Al $NH_4(SO_4)_2$ in D_2O:H_2O (1:9,v:v) (pH = 9.0) after addition of 0.009, 0.045 and 0.090 equivalents of PLP.

Fig.28: the line width of Al^{3+}-PLP comples as a function of [PLP]:[Al^{3+}] mole ratio

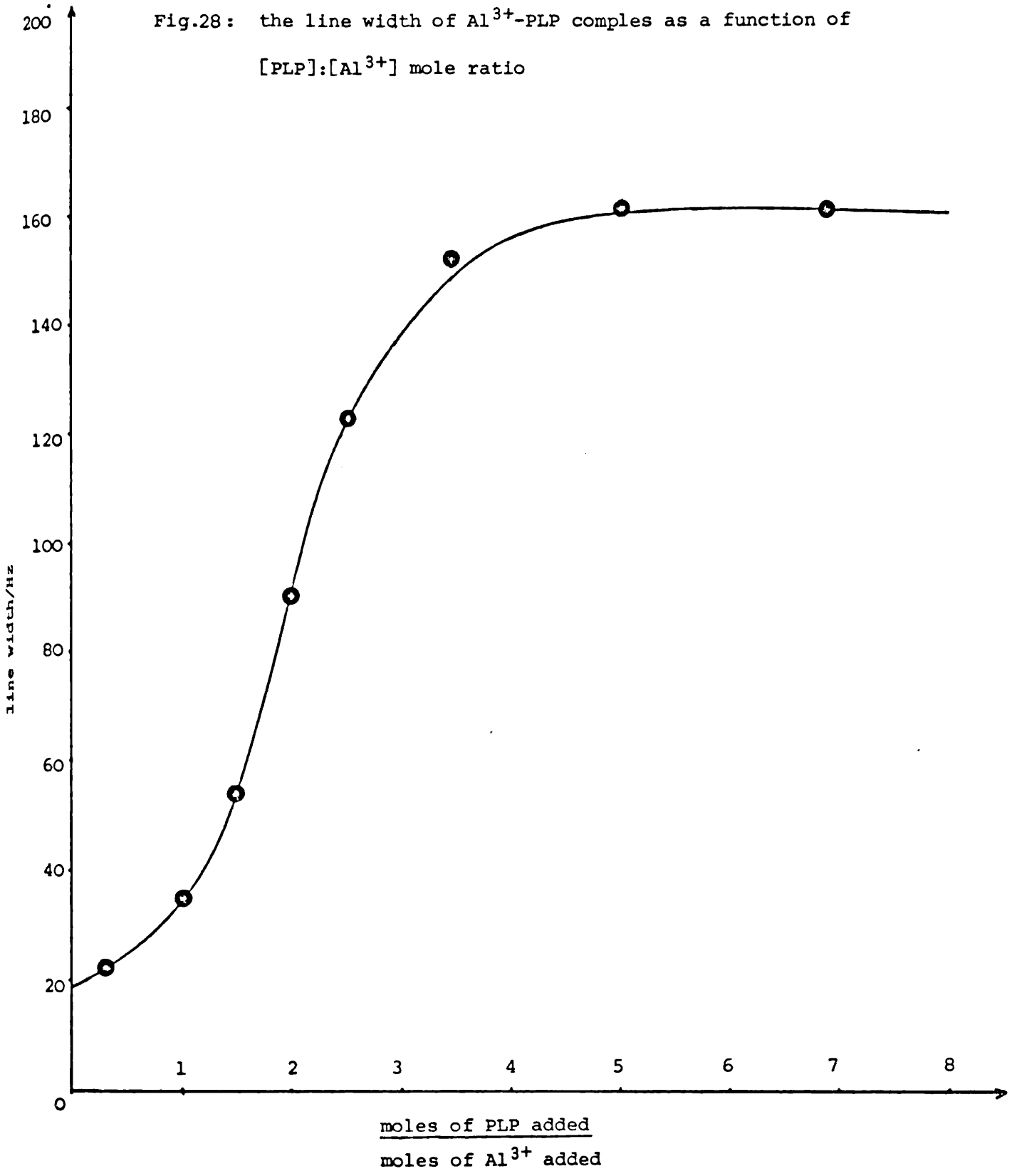

Table 49

^{27}Al n.m.r. spectra of Al^{3+}-amino acids complexes in a series of pH values.

complex	pH	$[Al^{3+}]$ and [AA] /mol.dm^{-3}	Chemical Shift from $Al(H_2O)_6^{3+}$ /Hz	/p.p.m.	Spectral width /Hz	$10^3 \times T_2$ /s
Al-Asp	7.0	0.1	442.72	18.964	46	3.997
	9.0	0.1	1874.995	80.282	80	2.298
	11.0	0.1	1879.100	80.4577	40	4.597
Al-Thr	7.0	0.1	457.92	19.62	50.0	3.68
	9.0	0.1	1874.995	80.282	47.5	3.87
	11.0	0.1	1874.995	80.282	47.5	3.87
Al-Glu	5.0	0.1	4.88	0.179	740	0.249
	7.0	0.1	462.11	19.795	110.00	1.67
	9.0	0.1	1873.2	80.205	34.0	5.41
	11.0	0.1	1879.88	80.49	33.75	5.45

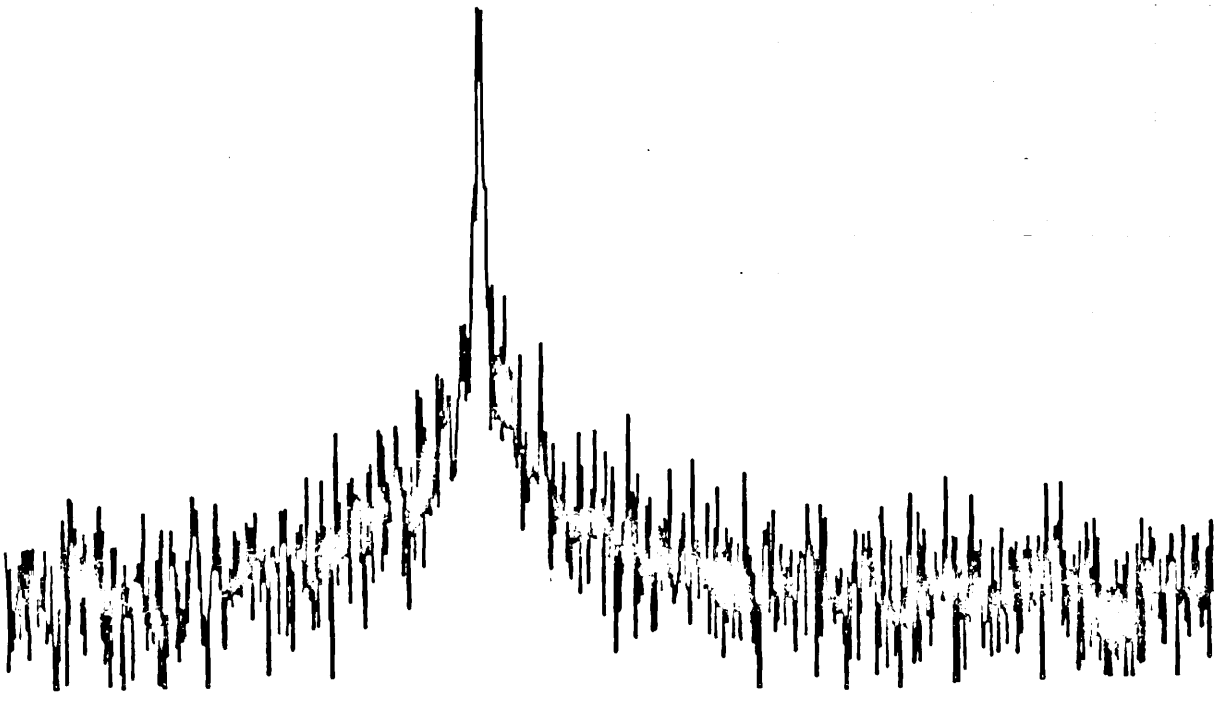

Fig. 99$_a$: ^{27}Al n.m.r. spectrum of 0.1 mol.dm^{-3} Al^{3+}-Glu (1:2 complex) at pH = 7.0

Table 50

^{27}Al n.m.r. spectra of Al^{3+}-Schiff-base complexes as a function of pH

Complex	pH	$[Al^{3+}]$ /mol.dm^{-3}	[PLP] and [AA] /mol.dm^{-3}	Chemical Shift from $^{27}Al(H_2O)_6^{3+}$ /Hz	/p.p.m.	Spectral width /Hz	$10^{-3}\times T_2$ /s
Al-PLP-GLu*	2.0	0.030	0.06	0.000	0.000	9.71	18.9
"	3.0	0.030	0.06	161.60	6.919	160	1.15
"	3.5	0.05	0.05	209.95	8.989	1200	0.15
"	5.6	0.05	0.10	418.66	17.921	1200	0.15
"	7.0	0.035	0.08	473.63	19.72	820	0.22
"	7.0	0.035	0.05	473.63	19.72	670	0.27
"	7.0	0.035	0.04	473.63	19.72	580	0.32
"	7.0	0.035	0.020	473.63	19.72	250	0.74
"	9.0	0.050	0.050	1879.87	80.491	27	6.81
				508.00	21.75	860	0.23
"	9.0	0.050	0.100	508.00	21.75	860	0.23
" **	9.0	0.050	0.100	524.00	22.436	860	0.23
				1882.0	80.58	30.3	10.61
Al-PAMP-α-Kg**	7.0	0.050	0.100	429.88	18.4	330	0.56
	"	"	"	473.7	19.7	842	0.22
" *	9.0	0.050	0.100	492.9	21.105	940	0.196
" **	"	"	"	1880.4	80.514	28	6.57
				598.9	25.64	340	0.54

* the spectra were obtained 30 min. after mixing

** the spectra were recorded 7 days later.

Table 50 continued

^{27}Al n.m.r. spectra of Al^{3+}-Schiff-base complexes as a function of pH

Complex	pH	$[Al^{3+}]$ /mol.dm^{-3}	[PLP] and [AA] /mol.dm^{-3}	Chemical Shift from $^{27}Al(H_2O)_6^{3+}$ /Hz	/p.p.m.	Spectral width /Hz	$10^{-3}\times T_2$ /s
Al-PLP-Asp**	7.0	0.05	0.10	429.7	18.37	842	0.22
	7.0	0.05	0.10	356.67	14.85	250	0.736
				429.68	18.41	950	0.194
	7.0	0.10	0.10	478.51	20.466	270	0.68
	9.0	0.10	0.20	431.1	18.458	260	0.71
	11.0	0.10	0.20	433.6	18.566	1.60	1.149
Al-PLP-Thr* after 20 min.	9.0	0.1	0.1	1874.995	80.28	26	7.072
				445.034	19.055	363.75	0.506
Al-PLP-Thr**	9.0	0.1	0.1	1874.99	80.28	28	6.567
				444.33	19.00	280	0.657
Al-PLP-Thr*	9.0	0.1	0.2	458.98	19.63	380	0.484
Al-PLP-Thr**	11.0	0.1	0.2	1874.49	80312	12	15.32

* the spectra were obtained 30 min. after mixing

** the spectra were recorded 7 days later.

Ga^{3+} complexes given in a later section (pages 149,152-154). The ^{27}Al spectral widths are different for each complex and this must come about as a result of the different arrangement of the ligands .

As fig.29 indicates, using ^{27}Al n.m.r. it was possible to show the stoichiometry of the Al-SB complexes. The Al-PLP-threonine complex at pD=9 has a metal to ligand ratio 1:2, because when 1:1 metal:ligand concentrations were used, a peak was observed due to free Al^{3+}. However, when concentrations to give a 1:2 complex were applied, the only signal observed was due to Al-SB: there was no free metal ion. Al-PLP-Glu and Al-PLP-Asp show similar behaviour, apart from spectral widths beeing slightly different (table 50).

An attempt was made to use T_2 (spin-spin relaxation time) to assess the geometry of the species in solution (tables 47-50).

The determination of the spin-lattice relaxation time (T_1), by varying the pulse interval was impossible because T_2 was very short. T_1 is equal to the spin-spin relaxation time (T_2) in the extreme narrowing limit when $(w_0\tau_c)^2 << 1$ where w_0 is the nuclear Larmor frequency and τ_c is the correlation time for molecular brownian motion[15,18]. Hence T_1 can be calculated using the equation[15]

$$\Delta\nu = \frac{1}{\pi\sqrt{3}} \cdot T_2^{-1}$$

where $\Delta\nu$ is the line width.

An increase of T_2 indicates the appearance of more symmetrical species[13] in the solution, when the viscosity remains the same, as the symmetry of a molecule affects the field gradient at the metal nucleus[19] (i.e. field gradient is very small or zero for a symmetrical environment, therefore the relaxation time should be long and the resonance lines narrow; while if the ligands are not symmetrically arranged the electron densities in the bonds are not equal and the field gradient and line widths may be increased[19]).

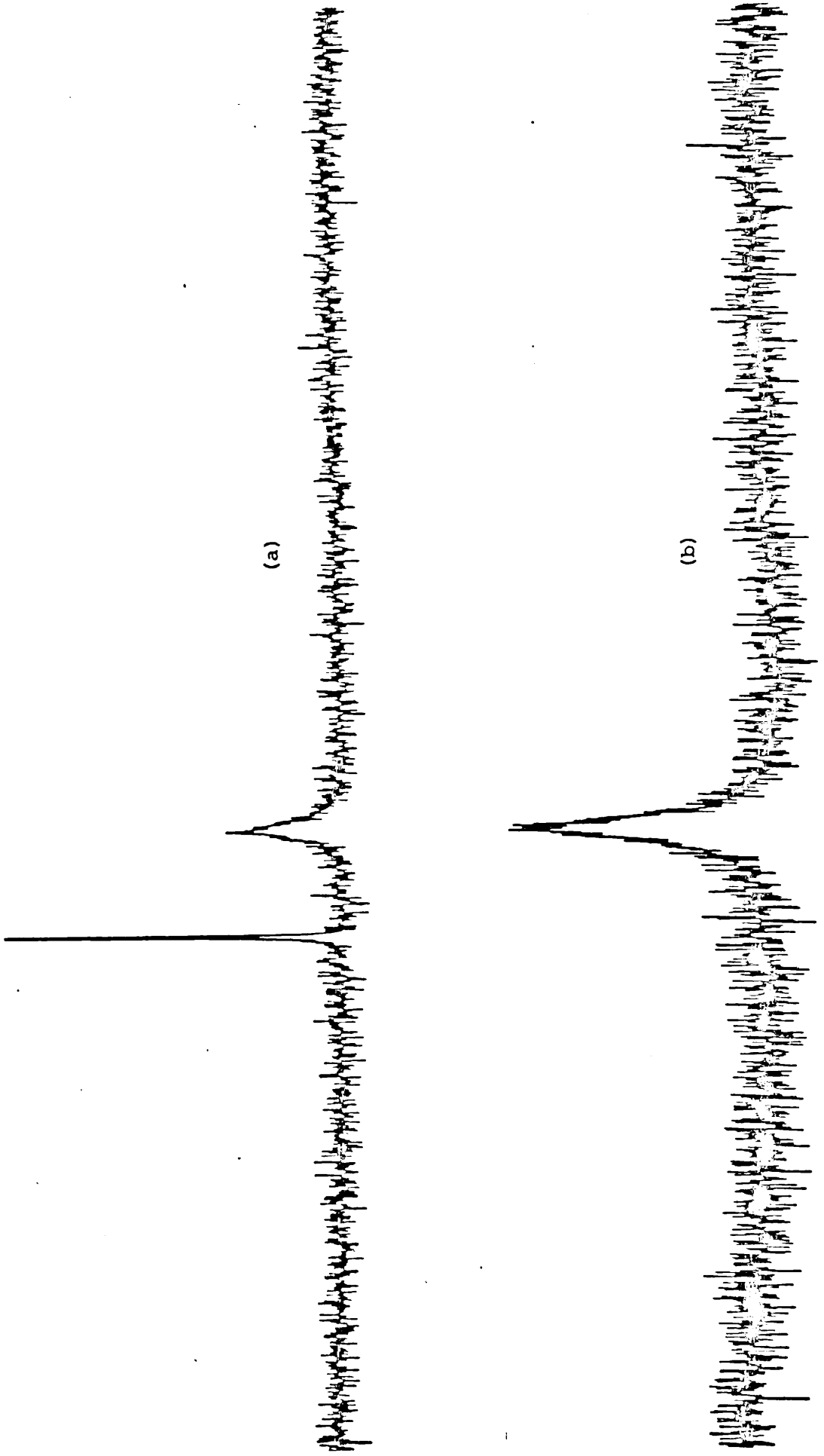

Fig. 29: ^{27}Al n.m.r. spectra of the Al-PLP-Threon complex.

(a) Al^{3+} : PLP : AA is 1 : 1 : 1 and (b) Al^{3+} : PLP : AA is 1 : 2 : 2

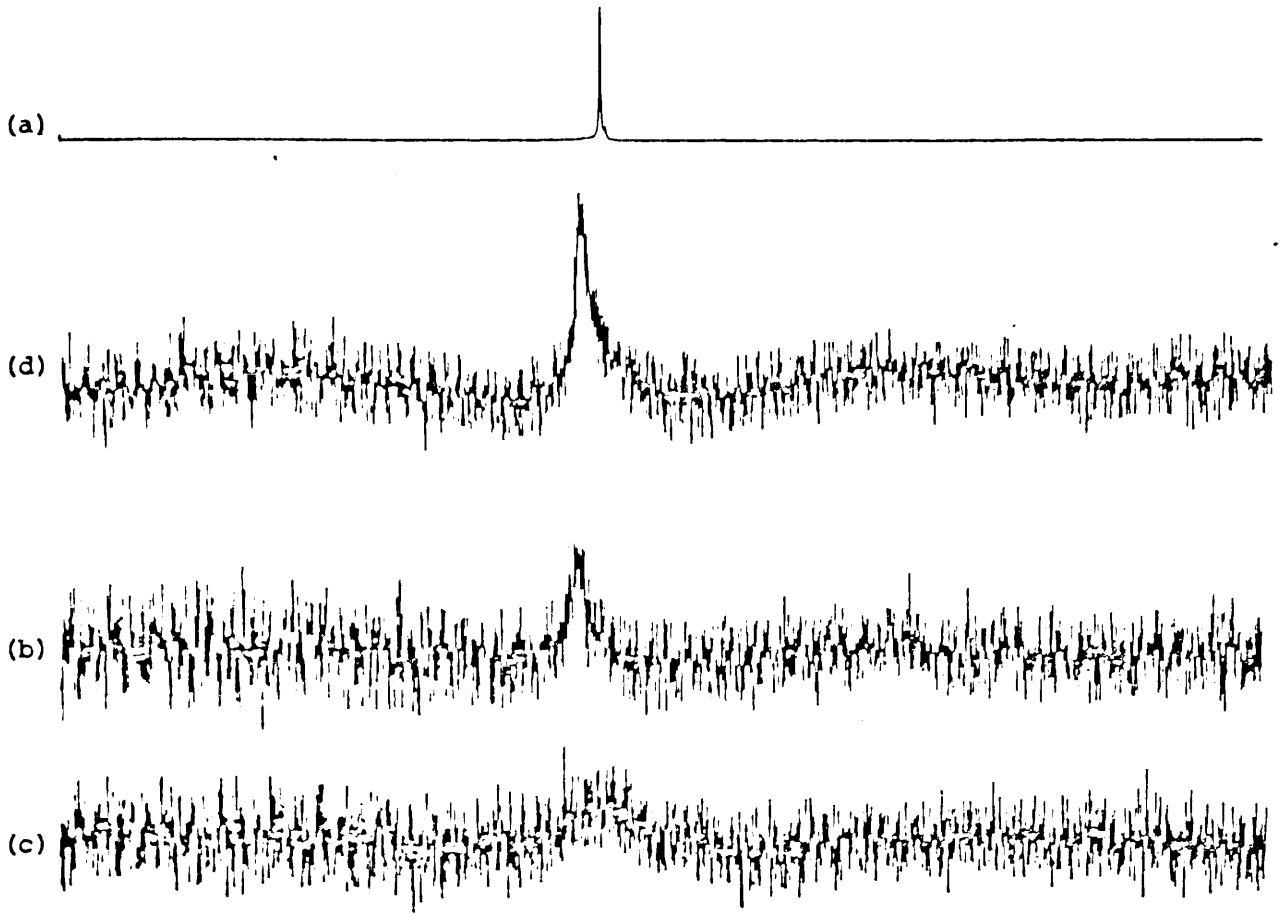

Fig. 30: ^{27}Al n.m.r. spectra of Al^{3+}-PLP-Glu 1:2:2 complex at pH = 7.0 at times a = 5 min, b = 2 hours, c = 18 hours, d = 54 hours after mixing.

The short relaxation times do not allow the spin-spin coupling to be observed in the ^{27}Al spectra and therefore was not possible to say[11] from this technique if there is a tetrahydral or an octahedral configuration.

(v) ^{27}Al n.m.r. spectra of a series of Al^{3+}-H_3PO_4 mixtures

Since ^{31}P n.m.r. spectra (see page 173) indicated that coordination was via the phosphate group, the ^{27}Al n.m.r. spectra of Al^{3+} and H_3PO_4 mixtures were studied in order to obtain further information concerning the n.m.r. spectra of Al^{3+} bound to phosphate group of PLP.

As table 51 and Fig.31 show, the narrow signal due to ^{27}Al $NH_4(SO_4)_4$ decreases in intensity as the concentration of Phosphoric acid increases, while a second much broader signal appears (due to Al^{3+}-H_3PO_4 complexation), which increases in intensity proportionally to the concentration of H_3PO_4. When there is enough H_3PO_4 to react with all Al^{3+}, the ^{27}Al n.m.r. spectrum shows only one broad asymmetric resonance (Fig. 31d) which is due to complexed aluminium-H_3PO_4 species. Increasing the concentration of H_3PO_4, the second resonance becomes broader; this broadening could result from the high viscosity of the solution.

B. ^{71}Ga n.m.r.

The isotope $^{71}Ga(I = \frac{3}{2})$ was used, although it occurs in lower abundance than ^{69}Ga, (60.2 and 39.8% respectively), because it has a smaller quadrupole moment and a greater nuclear magnetic moment than the latter, producing narrower, more intense signals.

$Ga(NO_3)_3.9H_2O$ was used to prepare the following complexes which were studied: Ga-PLP, Ga-Glu, Ga-Asp, Ga-threonine, Ga-PLP-Glu, Ga-PLP-Asp, Ga-PLP-threonine.

Table 51

^{27}Al n.m.r. spectra of Al^{3+}-H_3PO_4 mixtures of different molarities

$[Al^{3+}]$ /mol.dm^{-3}	$[H_3PO_4]$ /mol.dm^{-3}	Resonance frequency /Hz	Chemical Shift from $Al(H_2O)_6^{3+}$ /Hz	/p.p.m.	Spectral width /Hz	$10^3 \times T_2$ /s
0.5	2.0	23347845	214.85	9.2	166	1.108
0.5	1.8	23348035	14.65	0.63	3	61.3
		23347865	214.85	9.20	160	1.149
0.5	1.2	23348050	14.66	0.63	3	61.3
		23347870	214.85	9.2	143	1.289
0.5	0.5	23348030	14.65	0.63	5	36.8
		23347850	214.95	9.20	122	1.51
0.5	0.05	23348050	14.66	0.63	3	61.29

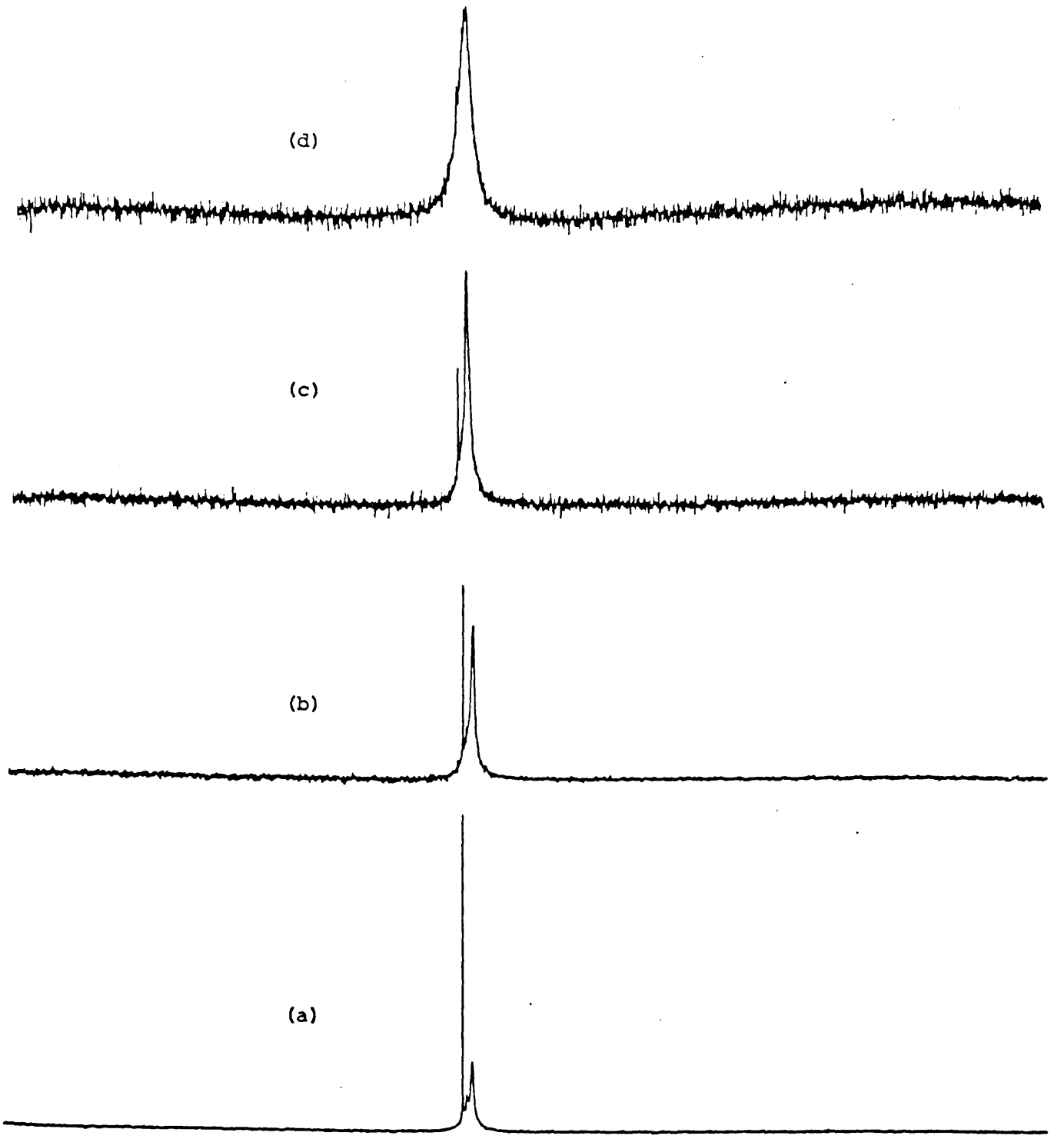

Fig. 31: ^{27}Al n.m.r. spectra of 0.1 mol.dm^{-3} Al^{3+} in D_2O/H_2O (1:9 v:v) (a) in the presence of 0.08 mol.dm^{-3} H_3PO_4, (b) 0.16 mol.dm^{-3} H_3PO_4 (c) 0.4 mol.dm^{-3} H_3PO_4 and (d) 1.2 mol.dm^{-3} H_3PO_4.

(i) The effect of concentration in the chemical shift of $^{71}Ga(NO_3)_3$ resonance signal

The spectra of $Ga(NO_3)_3$, (table 52) showed no shift from the $Ga(H_2O)_6^{3+}$ resonance frequency[5] as the concentration was varied, but the spectral width was concentration dependent.

(ii) ^{71}Ga n.m.r. spectra of Ga^{3+}-PLP complex

^{71}Ga n.m.r. spectra of Ga^{3+}-PLP in a series of concentrations showed no change in the resonance frequency as before. The chemical shift was indistinguishable from that due to $Ga(OH_2)_6^{3+}$ but the spectral width was noticeably smaller (table 53 and Fig. 32) indicating that the Ga^{3+}-PLP complex may be symmetrical[19]. Considered with previous analytical results, and the ^{31}P n.m.r. study of Ga-H_3PO_4 (table 66), the suggested structures are:

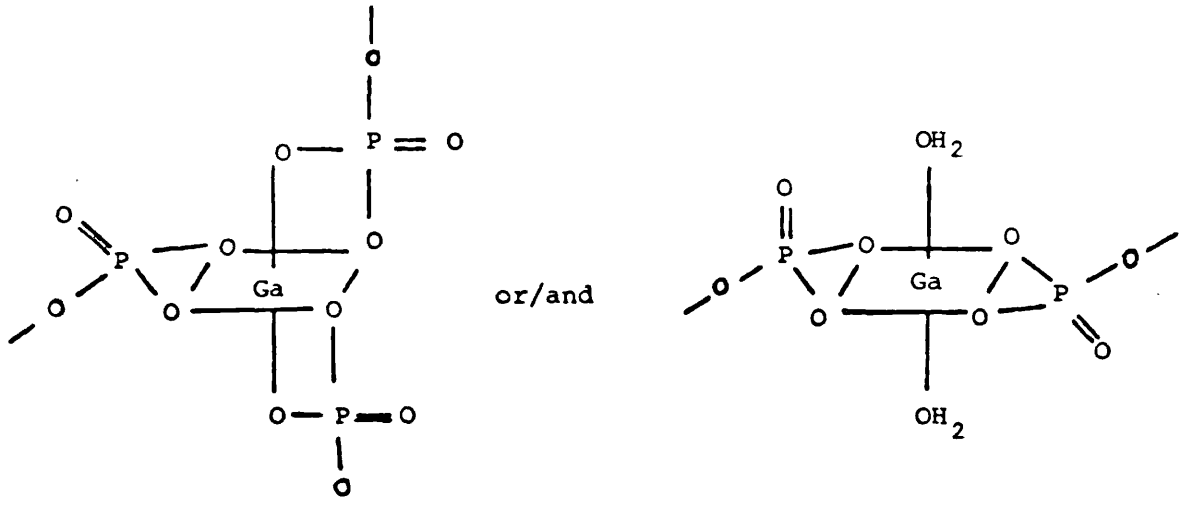

(iii) ^{71}Ga n.m.r. of Ga^{3+}-amino-acids complexes

Once again, the resonance frequencies of gallium-AA complexes were coincident with that of $Ga(H_2O)_6^{3+}$. Because of the magnitude of the spectral width, it was difficult to detect any chemical shift

Table 52

The effect of concentration in the chemical shift of $Ga(NO_3)_3.9H_2O$ resonance signal.

Concentration of $Ga(NO_3)_3.9H_2O$ /mol.dm^{-3}	Resonance frequency /Hz	line width /Hz	$10^4 \times T_2$ /s
Saturated Ga^{3+} solution	27326400	480	3.831
1	27326380	380	4.839
0.695	27326340	360	5.107
0.500	27326360	350	5.253
0.250	27326350	340	5.400
0.225	27326390	860	2.138
0.112	27326410	880	2.089
0.090	27326380	960	1.915
0.034	27326380	1040	1.768
0.026	27326360	1100	1.672
0.010	27326380	2090	0.880
0.006	27326400	2560	0.718
0.0016	27326400	very broad	0.000

Table 53

^{71}Ga n.m.r. spectra of $Ga(NO_3)_3.9H_2O$ in the presence of PLP at pH = 4.0

[PLP] /mol.dm^{-3}	[Ga^{3+}] /mol.dm^{-3}	Spectral width /Hz	Resonance frequency /Hz	Chemical shift from external $GaCl_4^-$ ion/Hz	$10^4 \times T_2$ /s
0.05	1.00	200	27326310	6760	9.193
0.05	0.50	160	27326310	6760	11.492
0.05	0.05	120	27326310	6760	15.322
0.05	0.035	120	27326310	6760	15.322
0.05	0.010	120	27326310	6760	15.322
0.05	0.009	500	27326310	6760	3.677

Fig. 32: ^{71}Ga n.m.r. spectra of Ga^{3+} in the presence of glutamate at various concentrations (see table 54).

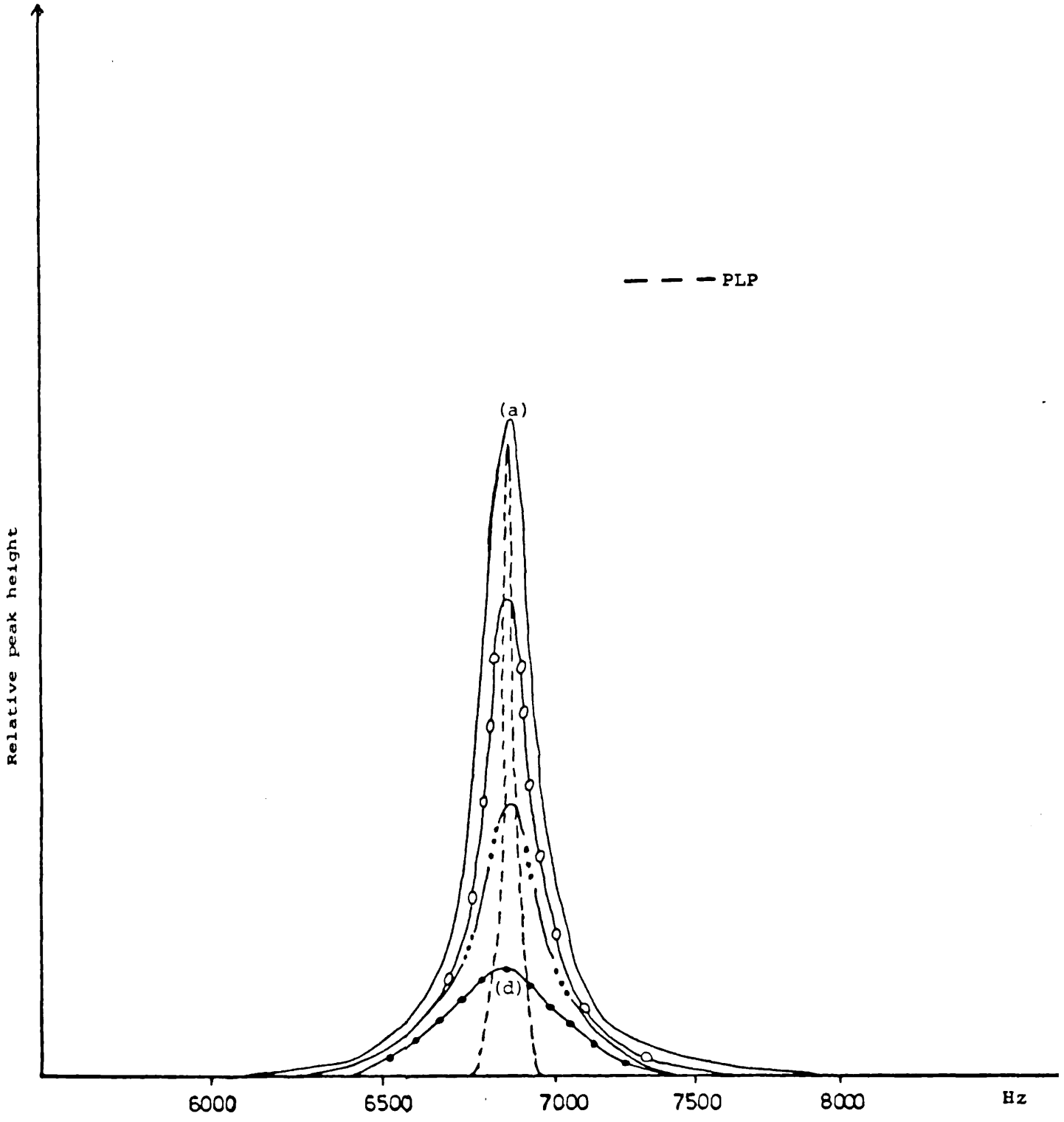

(e) is indistinguishable from the base line.

which might be occurring from the $Ga(OH_2)_6^{3+}$ resonance. All three amino acids investigated (L-glutamic, L-aspartic and L-threonine) behaved similarly, apart from small differences in their line widths arising from slightly different relaxation times, as table 54 shows. The single resonance which appears in ^{71}Ga n.m.r. spectrum of $Ga(NO_3)_3$ and which is due to $Ga(OH_2)_6^{3+}$ [20-24], decreases in intensity as the Ga^{3+}-AA complex is formed, and eventually the signal is broadened beyond detection, as a result of the quadrupolar relaxation[18]. Table 54 shows how the spectral width varies as the amount of the amino-acids added to Ga^{3+} is increased. When the gallium-AA concentration was 1:2 M:L, there was no resonance signal and it was assumed that all the Ga^{3+} was in the form of the amino acid complex (curve e Fig.32)

(iv) ^{71}Ga n.m.r. of Ga^{3+}-SB complexes

^{71}Ga n.m.r. spectra, produced in the presence of amino acids and PLP together were identical in character to those of the corresponding AA complexes as table 55 and fig.33 show. But again there were small differences in their spectral widths. Ga^{3+}-SB complexes are formed in solution, as uv (page 77) ^{13}C (p.62) and ^{1}H n.m.r. results (p.65) show. Slow addition of HCl to the solution caused an increase in the intensity of ^{71}Ga signal, indicating dissociation of the Ga^{3+} complexes (Fig.34). Increasing the concentrations of HCl, the broad resonance signal starts to shift to higher frequencies while its spectral width becomes narrower. The change is linear until a molarity of about 4.5 in HCl (Fig.34). Further increase in the molarity of HCl does not affect the resonance frequency of the signal, neither its spectral width and indicates the formation of the tetrahedral $GaCl_4^-$ ion.[20] On addition of NaOH to the SB-Ga^{3+} complex, $Ga(OH)_4^-$ is formed and gives rise to a signal[20] at a field strength 700 Hz higher than that due to $GaCl_4^-$, the spectral width increased to between 400-600 Hz, but the intensity was

Table 54

^{71}Ga n.m.r. spectra of Ga^{3+} in the presence of AA at pH = 7.0

$[Ga^{3+}]$ /mol.dm^{-3}	[L-NaGlu] /mol.dm^{-3}	[L-Asp] /mol.dm^{-3}	[L-Threonine] /mol.dm^{-3}	Spectral width/Hz			$10^4 \times T_2$ /s			plot*
				[Ga.Glu]	[Ga-Asp]	[Ga-Threon]	[GaGlu]	[GaAsp]	[GaThr]	
0.5	-	-	-	400	400	400	4.597	4.597	4.597	a
0.5	0.1	0.1	0.1	460	445	490	3.997	4.132	3.752	
0.5	0.25	0.25	0.25	680	670	765	2.704	2.744	2.404	b
0.5	0.35	0.39	0.35	840	890	920	2.189	2.066	1.999	c
0.5	0.60	0.60	0.60	1300	1240	1380	1.332	1.483	1.332	d
0.5	1.00	1.00	1.00	-	-	-				e
0.056	0.008			540			3.405			
0.030	0.008			580			3.170			
0.100	0.008			590			3.752			

Resonance frequency = 27326360 Hz

Chemical shift from external $GaCl_4^-$ = 6710 Hz

* see Fig. 32

Fig. 33: ^{71}Ga n.m.r. spectra of 0.5 mol.dm^{-3} Ga^{3+} in the presence of (a) 0.02 mol.dm^{-3} PLP-Threon (1:1 concentration ratio)

(b) 0.13 mol.dm^{-3}SB;

(c) 0.40 mol.dm^{-3}SB;

(d) 0.85 mol.dm^{-3}SB;

(e) 1.40 mol.dm^{-3}SB.

(a') 0.05 mol.dm^{-3} SB

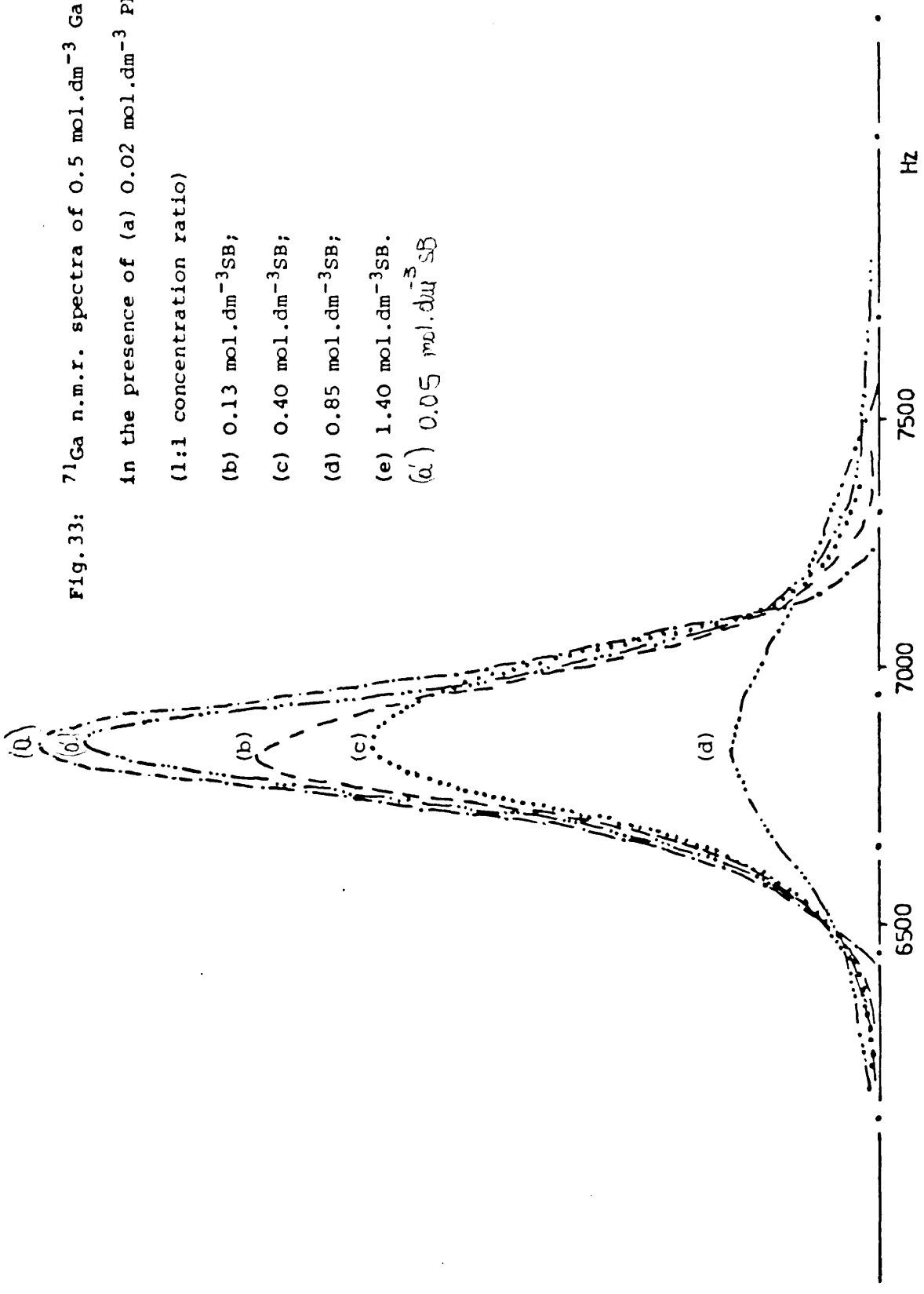

(a) is indistinguishable from the base line

Table 55

^{71}Ga n.m.r. spectra of Ga^{3+}-SB complexes at pH = 7.0

Complex	$[Ga^{3+}]$ /mol.dm^{-3}	[PLP] and [AA] /mol.dm^{-3}	Spectral width /Hz	$10^4 \times T_2$ /S	Resonance frequency /Hz	Chemical shift from the external $GaCl_4^-$ /Hz
Ga-PLP-Glu	0.5	0.1	560	0.3283	27326360	6700
	0.5	0.5	1210	0.152	27326360	6700
	0.5	1.0	1450	0.1268	27326360	6700
Ga-PLP-Asp	0.5	0.1	520	0.3536	27326360	6700
	0.5	0.5	1030	0.1785	27326360	6700
	0.5	1.0	1350	0.1362	27326360	6700
Ga-PLP-Threon	0.5	0.1	490	0.3752	27326360	6700
	0.5	0.5	1110	0.1656	27326360	6700
	0.5	1.0	1490	0.1234	27326360	6700

Fig. 34: ^{71}Ga resonances of Ga^{3+}-complexes as a function of the concentration of HCl.

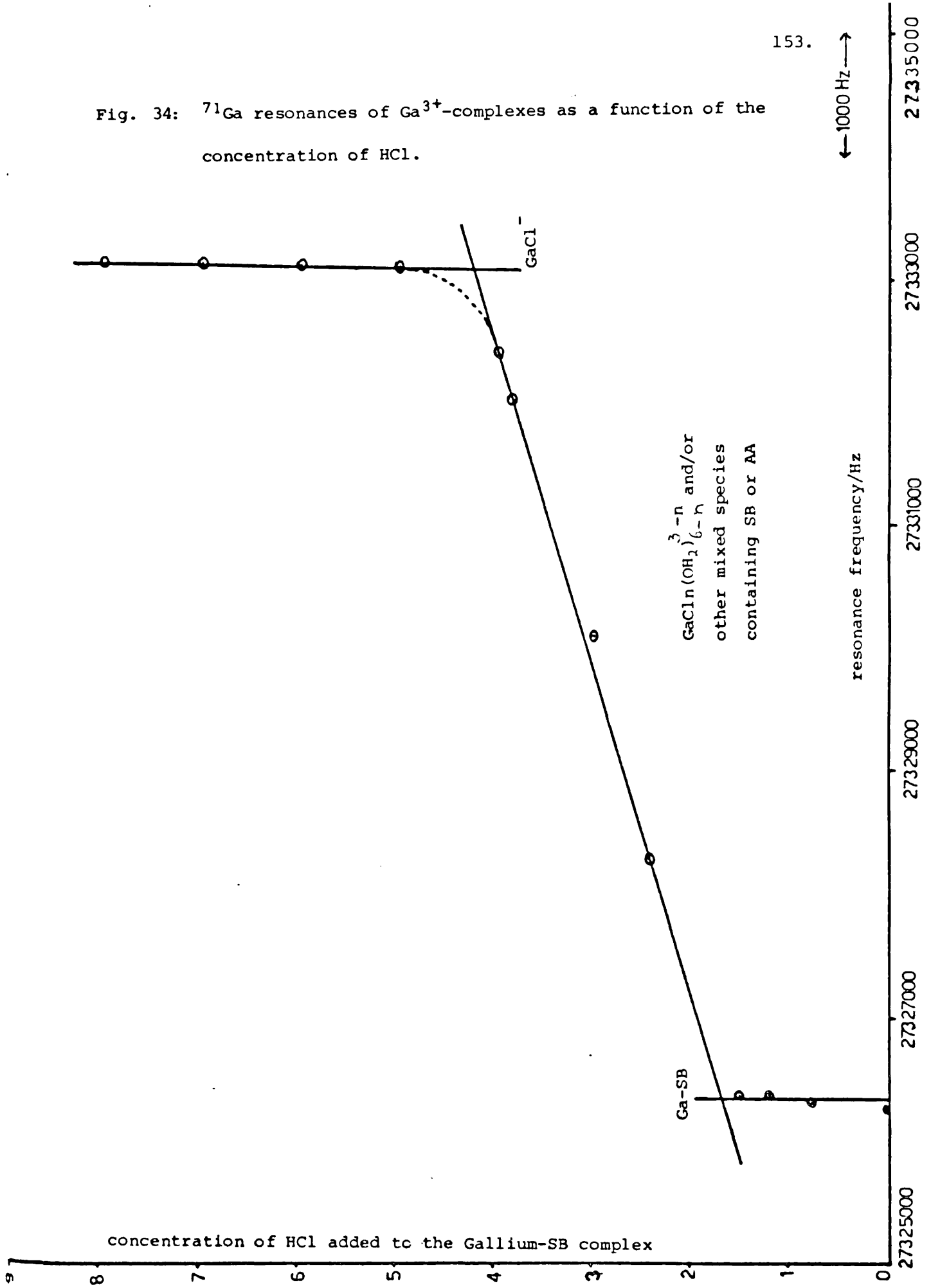

unaffected, within experimental error; this indicates either that only a very small amount of the complex was formed, or that no Ga-SB or Ga-AA complex formation had occurred and that the broadening was caused by an increase in viscosity or by rapid chemical exchange between $Ga(OD)_4^-$ and other less symmetrical species.

At pH = 7.0 the relative intensity (I/I_0) of the ^{71}Ga resonance was plotted against the concentration ratio of ligand to metal, as tables 56,57,58 and Fig.35 indicate, suggesting an 1:2 metal to ligand ratio for Ga-Asp, Ga-Glu, Ga-PLP-Asp, Ga-PLP-Glu and Ga-Threonine complexes and 1:1 metal to ligand ratio for the Ga-PLP-Threonine complex.

(v) ^{71}Ga n.m.r. of Ga^{3+} and H_3PO_4 mixtures

In order to study the behaviour of Ga^{3+} in the presence of H_3PO_4 and therefore to understand the mode of coordination with PLP, a series of ^{71}Ga n.m.r. spectra were recorded as table 59 and Fig. 36 show.

In low acid concentrations, there is one ^{71}Ga sharp resonance at high field due to complexation. At high acid concentrations (~4M) there are two overlapping broad resonances. The large spectral width could be due to the high viscosity as the bulk viscosity (η), for a spherical molecule from the Debye relation, is related to the correlation time (τ_c) for molecular brownian motion

$$\tau_c \propto \eta\, a^3$$

where a is the radius of the molecule. Hence, an increase in viscosity, increases the correlation time τ_c which has considerable influence on the relaxation times[15,25]

$$\frac{1}{T_2} = \frac{1}{T_1} = \frac{3}{40} \cdot \frac{3I+3}{I^2(2I-1)} \left(\frac{eQ}{h}\right)^2 \left(\frac{d^2v}{dz^2}\right)^2 \tau_c$$

where I is the nuclear spin quantum number, Q is the nuclear quadrupole

Table 56(a)

^{71}Ga n.m.r. spectra of Ga^{3+}-L-Glutamate

$[Ga^{3+}]$ /mol.dm^{-3}	[L-Glu] /mol.dm^{-3}	Relative intensities (I/I_0) of ^{71}Ga resonance	$\frac{[L\text{-Glut}]}{[Ga^{3+}]}$
0.5	-	1.000	0.0
0.5	0.25	0.802	0.5
0.5	0.35	0.735	0.7
0.5	0.60	0.525	1.2
0.5	0.80	0.400	1.6
0.5	1.00	0.120	2.0
0.5	2.00	-	4.0
0.5	2.50	-	5.0

Table 56(b)

^{71}Ga n.m.r. spectra of Ga^{3+}-PLP-Glutamate

$[Ga^{3+}]$ /mol.dm^{-3}	[PLP] and [Glu] /mol.dm^{-3}	Relative intensities (I/I_0) of ^{71}Ga resonance	$\frac{[SB]}{[Ga^{3+}]}$
0.5	-	1.000	0.0
0.5	0.25	0.7550	0.5
0.5	0.40	0.5600	0.8
0.5	0.50	0.4750	1.0
0.5	0.75	0.325	1.5
0.5	0.90	0.180	1.8
0.5	1.25	-	2.5

Table 57

^{71}Ga n.m.r. spectra of Ga^{3+}-L-Aspartate

$[Ga^{3+}]$ /mol.dm^{-3}	[L-Asp] /mol.dm^{-3}	I/I_0	$\frac{[L\text{-}Asp]}{[Ga^{3+}]}$
0.5	—	1.00	0.0
0.5	0.25	0.8	0.5
0.5	0.50	0.585	1.0
0.5	0.80	0.400	1.6
0.5	1.00	0.210	2.0
0.5	1.50	—	3.0

Table 57

^{71}Ga n.m.r. spectra of Ga-PLP-Asp complex

$[Ga^{3+}]$ /mol.dm^{-3}	[PLP] and [ASP] /mol.dm^{-3}	I/I_0	$\frac{[SB]}{[Ga^{3+}]}$
0.5	0.10	0.855	0.2
0.5	0.25	0.670	0.5
0.5	0.40	0.480	0.8
0.5	0.50	0.300	1.0
0.5	0.75	0.040	1.5
0.5	0.90	—	1.8

Table 58

^{71}Ga n.m.r. spectra of Ga^{3+}-PLP-L-threonine complex

$[Ga^{3+}]$ /mol.dm^{-3}	[PLP] and [threon] /mol.dm^{-3}	I/I_0	$\frac{[SB]}{[Ga^{3+}]}$
1.0	0.4	0.7	0.4
1.0	0.7	0.5	0.7
1.0	0.8	0.34	0.8
1.0	1.0	0.21	1.0
1.0	1.4	0.10	1.4
1.0	2.0	—	2.0

Table 58

^{71}Ga n.m.r. spectra of Ga^{3+}-L-threonine

$[Ga^{3+}]$ /mol.dm^{-3}	[L-threonine] /mol.dm^{-3}	I/I_0	$\frac{[L\text{-threonine}]}{[Ga^{3+}]}$
1.0	-	1.000	0.0
1.0	0.1	0.943	0.1
1.0	0.5	0.743	0.5
1.0	0.9	0.607	0.9
1.0	1.3	0.5714	1.3
1.0	1.8	0.250	1.8
1.0	2.0	—	2.0

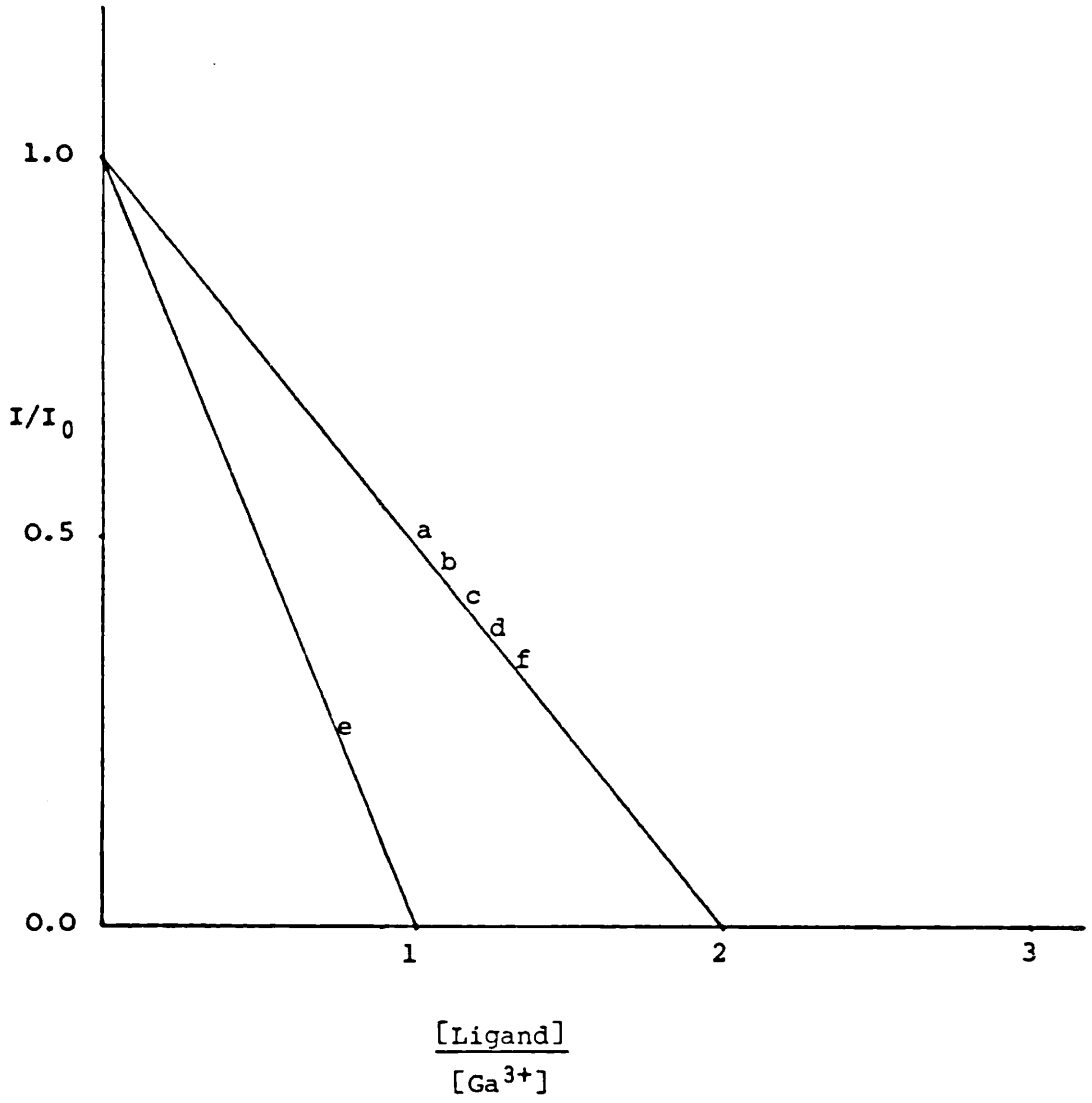

Fig.35: Relative intensities of ^{71}Ga n.m.r. signals (I_0 = Ga^{3+} aqueous; I = Ga^{3+} in the presence of ligand) as ligand to Ga^{3+} ratio is varied a,b,c,d,e,f from Table 12-14.

Table 59

^{71}Ga n.m.r. spectra of Ga^{3+}-H_3PO_4 mixtures

$[Ga^{3+}]$ /mol.dm^{-3}	$[H_3PO_4]$ /mol.dm^{-3}	Chemical shift from external $GaCl_4^-$/p.p.m.	No. of signals	Spectral width /Hz
0.4	—	-246.95	1	850
0.4	0.25	-246.95	1	190
0.4	0.40	-246.95	2	160*
		-279.149		
0.4	5.00	-246.95	2	240
		-280.61		920

*The intensity of the signal decreases, while a second signal appears broader with intensity proportional to the concentration of $[H_3PO_4]$.

Fig. 36 : ^{71}Ga n.m.r. spectra of 0.4 mol.dm^{-3} Ga^{3+} in a series of concentrations of H_3PO_4. (a) 0.25 mol.cm^{-3}; (b) 0.35 mol.dm^{-3}; (c) 0.41 mol.dm^{-3}; (d) 0.80 mol.dm^{-3}; (e) 2.0 mol.dm^{-3}; and (f) 4.9 mol.dm^{-3} H_3PO_4.

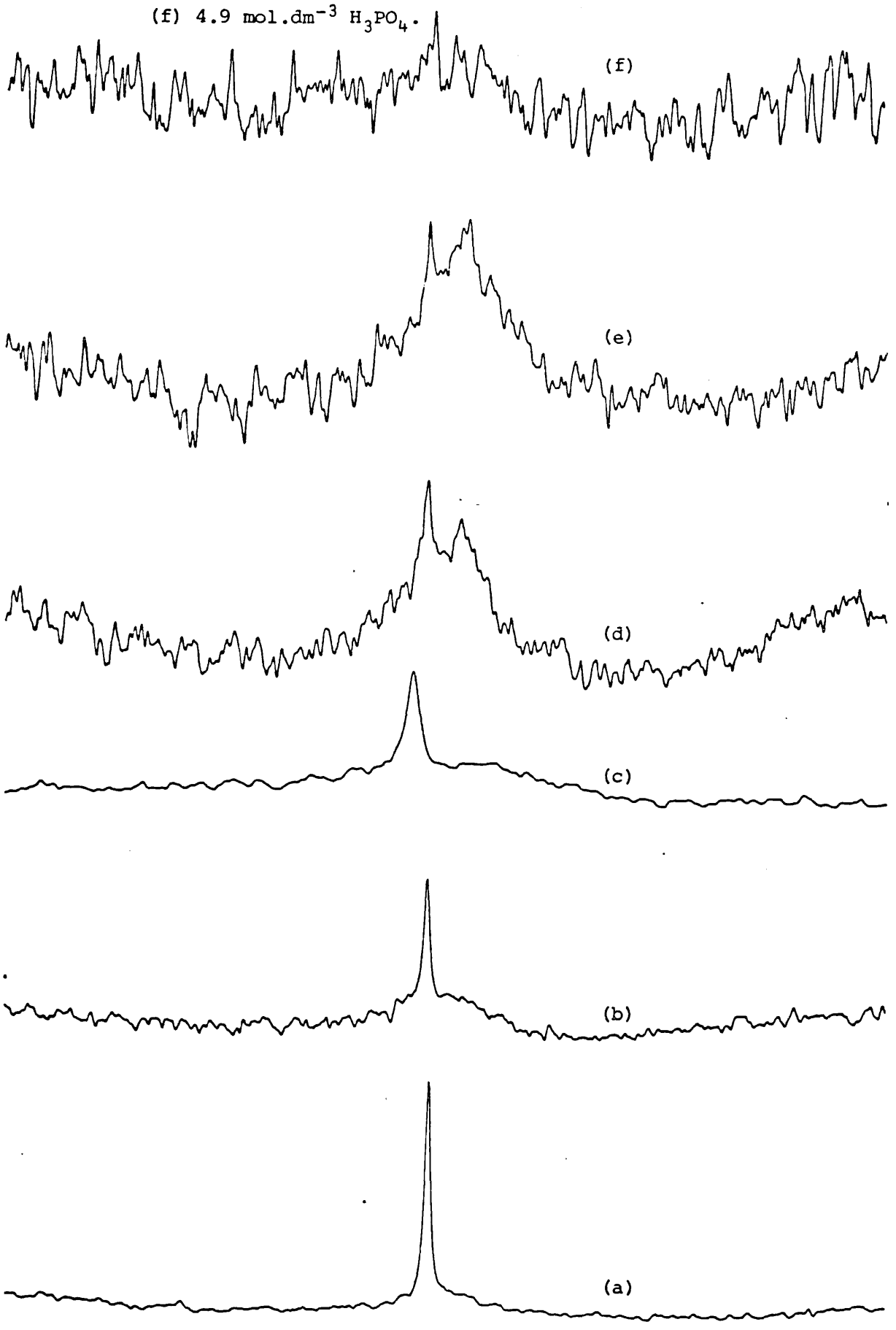

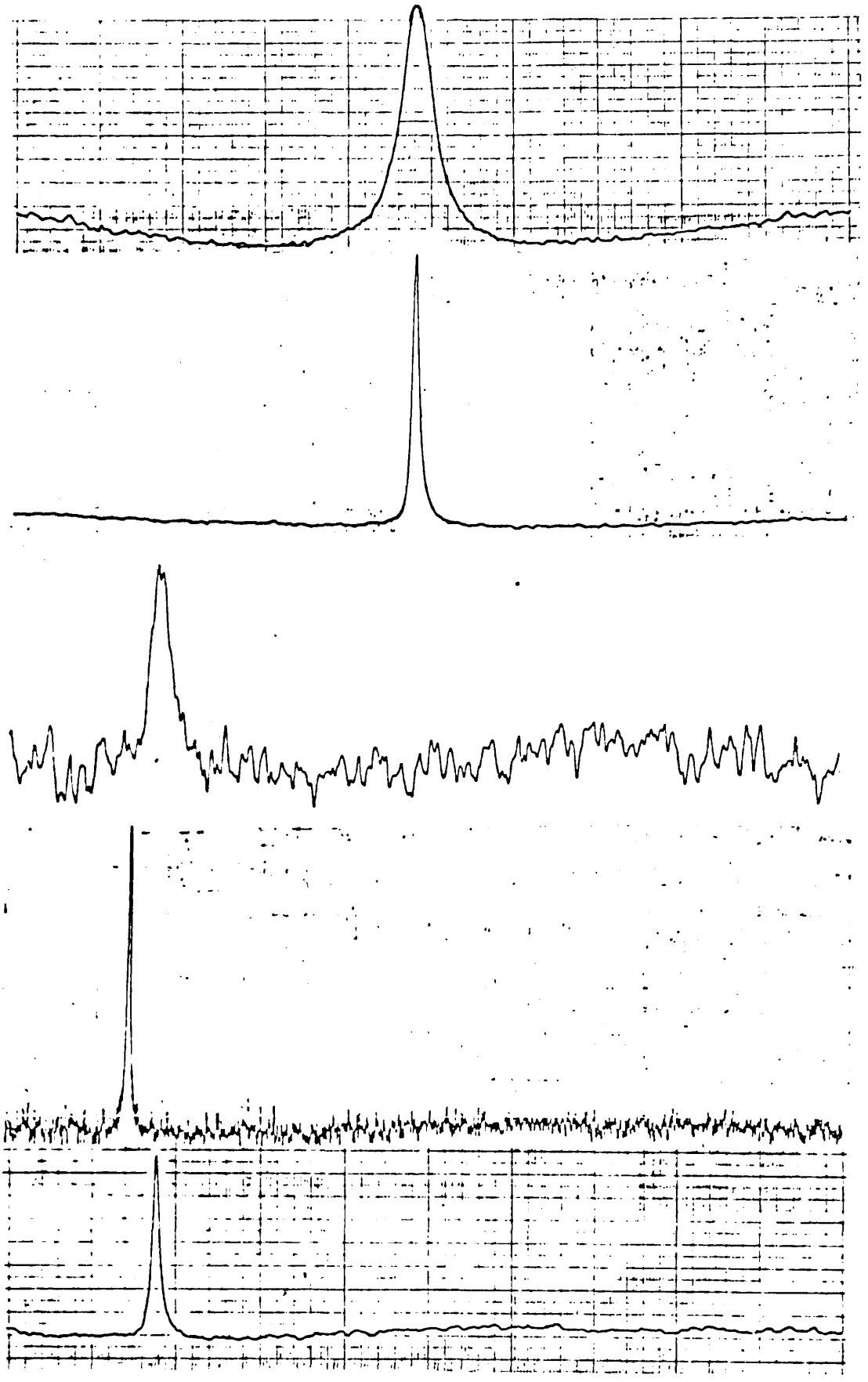

Fig.37 : ^{71}Ga n.m.r. spectra: (a) $Ga(OH_2)_6^{3+}$; (b) Ga-PLP (1:2) complex at pH=2.5; (c) Ga-PLP-Glu (1:2:2) complex at pH=9.0; (d) 0.1M Ga-PLP-Glu in the presence of 5M HCl (e) 0.1M Ga-PLP-Glu in the presence of 5M NaOH.

moment and $\frac{d^2n}{dz^2}$ is the maximum electric field gradient at the nucleus.

C. ^{115}In n.m.r.

^{115}In is a radioactive nucleus (β^- decay) of a very long half-life (5×10^{14}yr), it has a high natural abundance (95.12%), a large magnetic moment and a quite large quadrupole moment, which causes large line widths which are strongly sensitive in the environmental symmetry of the indium nucleus[26,27]. The chemical shifts also vary according to the anion participating in the complex formation and they are only very little affected by the solvent and the concentration.[26,28,29] The shifts cover a range of about 1100 ppm.[26] $In(H_2O)_6^{3+}$ has been used as an arbitrary reference as the size of the nuclear magnetic shielding is unknown.[30]

^{115}In n.m.r. showed a very similar behaviour to that of ^{71}Ga, except that the spectral widths were much wider than those of Ga^{3+}-complexes. Table 60 indicates the character of ^{115}In resonances of the In^{3+}-PLP, In^{3+}-amino-acids and In^{3+}-Schiff-base complexes.

The resonance frequencies of these complexes[26] are coincident with that of $In(H_2O)_6^{3+}$ (19634398 Hz), and if there is any difference, this can not be accurately estimated due to the magnitude of the spectral widths. However, the magnitude of the spectral widths have been used to estimate an idea about the environment of those complexes.

The relatively narrow spectral width[19] (1200 Hz) of In^{3+}-PLP indicates a symmetrical environment in this system. This width remains the same as the concentration of PLP added to In^{3+} increases, even when the PLP to In^{3+} ratio is greater than 3.00. For the other complexes, as the relative concentrations of metal to ligand were increased from 1:0 to 1:3 the intensity of the ^{115}In decreases while the spectral width increases, and finally when all the metal ion is involved in the

Table 60

^{115}In n.m.r. spectra of In^{3+}-complexes in solution at pH = 9.0

Complex	[ligand] /mol.dm^{-3}	[In^{3+}] /mol.dm^{-3}	Spectral width /Hz
$In(H_2O)_6^{3+}$	—	0.1	1130
In^{3+}-PLP	0.1	0.1	2980
	0.2	0.1	1200
	0.3	0.1	1200
In^{3+}-PLP-Glu	0.3	0.3	4680
	0.5	0.3	6960
	0.6	0.3	—
In^{3+}-PLP-Asp	0.5	0.3	4525
	0.5	0.3	4999
	0.6	0.3	—
In^{3+}-PLP-Thr	0.15	0.3	8160
	0.3	0.3	—

Table 61

^{115}In n.m.r. spectra of In^{3+}-glutamate-PLP at pH = 9.0

$[In^{3+}]$ /mol.dm^{-3}	[L-Glutamate] /mol.dm^{-3}	[PLP] /mol.dm^{-3}	Relative intensities (I/I_0) of ^{115}In resonance	$\frac{[SB]}{[In^{3+}]}$
0.3	-	-	1.000	0.000
0.3	0.05	0.05	0.950	0.167
0.3	0.10	0.10	0.830	0.333
0.3	0.15	0.15	0.725	0.500
0.3	0.30	0.30	0.400	1.000
0.3	0.60	0.60	0.030	2.000
0.3	0.90	0.90	-	3.000
0.3	1.20	1.20	-	4.000

Table 62

^{115}In n.m.r. spectra of In^{3+}-PLP-Asp at pH = 9.0

$[In^{3+}]$ /mol.dm^{-3}	[SB] /mol.dm^{-3}	Relative intensities (I/I_0) of ^{115}In resonance	$\frac{[SB]^*}{[In^{3+}]}$
0.3	0.05	0.860	0.1667
0.3	0.20	0.610	0.6667
0.3	0.30	0.525	1.000
0.3	0.36	0.250	1.200
0.3	0.60	-	2.000
0.3	0.70	-	2.333

* Assuming SB is fully formed

Table 63

^{115}In n.m.r. spectra of In^{3+}-threonine-PLP complex at pH = 9.0

$[In^{3+}]$ /mol.dm^{-3}	[L-threonine] /mol.dm^{-3}	[PLP] /mol.dm^{-3}	Relative intensities of ^{115}In resonance I/I_0	$\frac{[SB]^*}{[In^{3+}]}$
0.3	0.05	0.05	0.775	0.167
0.3	0.10	0.10	0.700	0.333
0.3	0.15	0.15	0.500	0.500
0.3	0.20	0.20	0.400	0.667
0.3	0.23	0.23	0.062	0.770
0.3	0.30	0.30	0.020	1.00
0.3	0.50	0.50	—	1.666

* Assuming SB is fully formed

Fig. 38: Plot of the relative intensities of ^{115}In resonance signals (I = intensity of In^{3+} complex, I_0 = intensity of the free metal ion) against the ratio of their concentrations respectively.

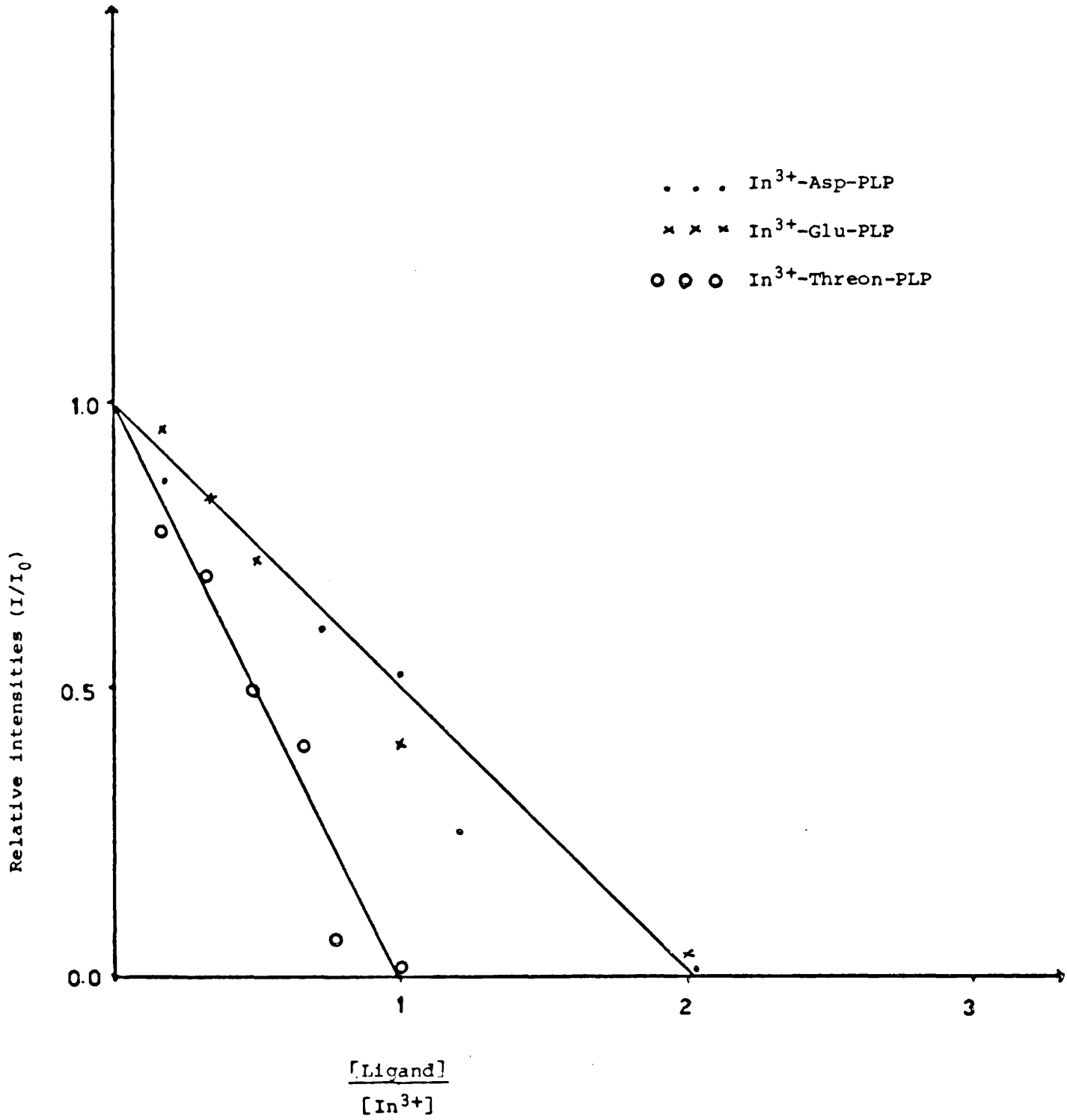

complexation the resonance signals can not be observed since the relaxation times for those asymmetrical systems are very small, giving a very high spectral width coincident with the base line. In the case of In^{3+}-PLP-Glu and In^{3+}-PLP-Asp no resonance could be observed when M:L was 1:2, but in the case of In^{3+}-PLP-Threonine, there was no resonance even when the relative concentrations of M:L was 1:1.

D. ^{31}P n.m.r.

Changes in the electronic environment of a phosphorus atom are accompanied by large variations in the shielding of the phosphorus nucleus. Hence, ^{31}P n.m.r. spectra were recorded to detect any Metal-(III)-Oxygen-Phosphorus bonding of the phosphate group of the PLP compound.

(i) ^{31}P n.m.r. spectra of H_3PO_4 in the presence of Al^{3+}, Ga^{3+} and In^{3+} ions

In order to identify this type of bonding, a series of solutions of M^{3+}-Phosphoric acid combinations was analysed using the molarities tables 65-67 indicate. Figures 40, 41 and 42 show how the resonance signals change as the concentration of Phosphoric acid decreases for Al^{3+}, Ga^{3+} and In^{3+} respectively. The resonance signals are characterized by their different spectral widths and their quite distinct chemical shifts, with respect to the resonance frequency of 8M H_3PO_4, used as an external reference. ^{31}P n.m.r. spectra of 0.2M H_3PO_4 in a series of pH's were recorded for comparison (Table 64), (Fig.39).

The solution of 0.1M Al^{3+} and 0.08M H_3PO_4 gave four overlapping ^{31}P resonances at 1.67, -6.27, -10.84 and -12.34 p.p.m. from the external standard (i.e. 8M H_3PO_4). Increasing the concentration of H_3PO_4 solution while the concentration of Al^{3+} remained the same, the four resonances coalesced and finally a broad single resonance appeared 1.6 p.p.m. downfield from the standard (Fig. 40). The three ^{31}P

Table 64

^{31}P n.m.r. spectra of H_3PO_4. Chemical shifts from the external reference 8M H_3PO_4.

pD	$[H_3PO_4]$ /mol.dm^{-3}	Resonance frequency /Hz	Chemical Shift	
			/Hz	/p.p.m.
>1	8.00	36272336	0.0	0.0
	4.00	36272368	31.93	0.88
	2.00	36272384	48.00	1.323
	1.00	36272396	60.01	1.654
	0.50	36272400	64.04	1.765
	0.25	36272404	68.00	1.8747
	0.125	36272404	68.00	1.8747
1	0.200	36272400	40.02	1.103
2	0.200	36272405	45.03	1.241
6.8	0.200	36272463	103.05	2.840
12.0	0.20	36272543	183.05	5.045

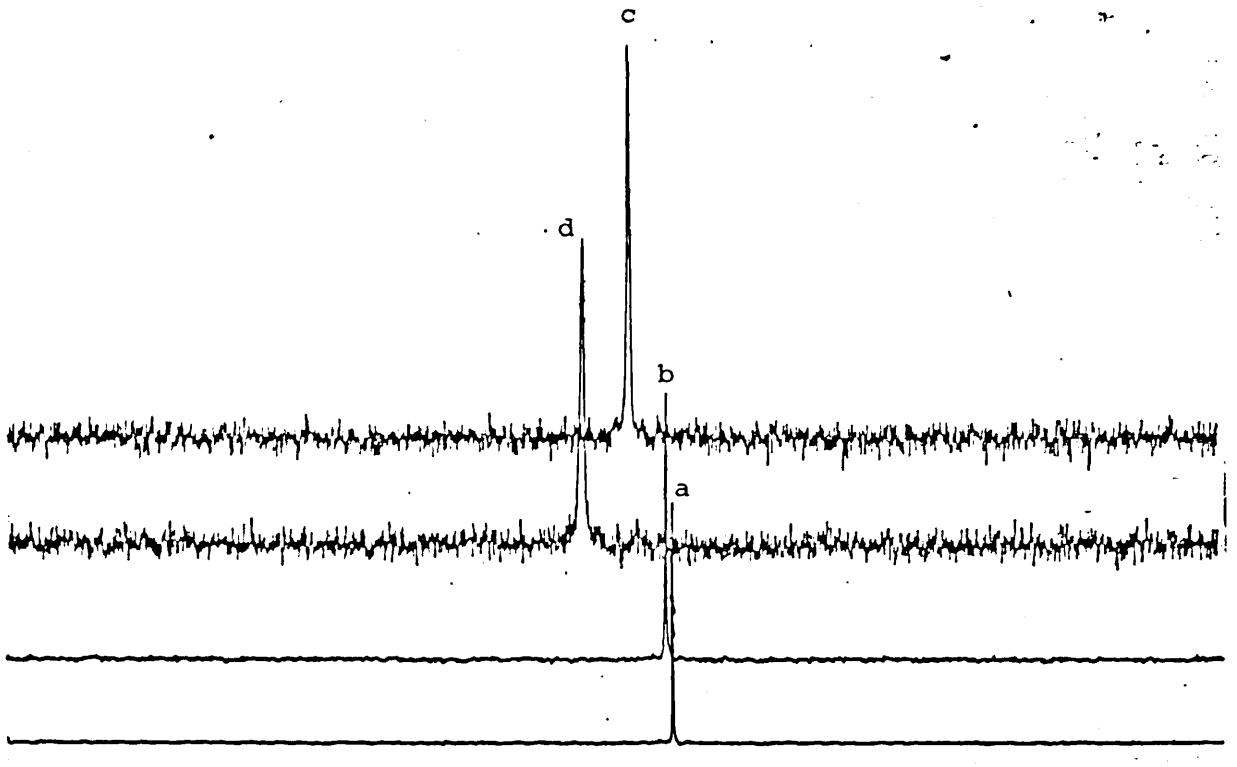

Fig. 39: ^{31}P n.m.r. spectra of 0.5M H_3PO_4

(a) pH = 1, (b) pH = 2.5, (c) 6.8,

(d) pH = 12

Table 65

^{31}P n.m.r. spectra of Al^{3+}-H_3PO_4 in a series of concentrations at 20°C.

Chemical shifts from the external reference 8M H_3PO_4 /p.p.m.

$[Al^{3+}]$ /mol.dm^{-3}	$[H_3PO_4]$ /mol.dm^{-3}	Resonance frequency /Hz	Chemical Shift		Spectral width /Hz
			/Hz	/p.p.m.	
0.1	0.04	36271890	-447.754	-12.344	49
0.1	0.08	36272398	60.547	1.670	11
		36272110	-227.539	-6.273	58
		36271945	-393.066	-10.837	82
		36271890	-447.754	-12.344	41
0.1	0.16	36272398	60.55	1.67	11
		36272110	-227.5	-6.27	25
		36272086	-251.5	-6.94	28
		36271945	-398.07	-10.84	82
		36271890	-447.75	-12.34	41
0.1	0.28	36272398	60.55	1.67	11
		36272110	-227.5	-6.27	45
		36271945	-398.07	-10.84	82
0.1	0.40	36272398	60.55	1.67	11
		36272110	-227.5	-6.27	48
0.1	1.20	36272398	60.55	1.67	13

Fig. 40 : ^{31}P n.m.r. spectra of 0.1 mol.dm^{-3} Al^{3+} in the presence of H_3PO_4

(a) 0.08 mol.dm^{-3} H_3PO_4

(b) 0.16 mol.dm^{-3} H_3PO_4

(c) 0.40 mol.dm^{-3} H_3PO_4

(d) 1.20 mol.dm^{-3} H_3PO_4

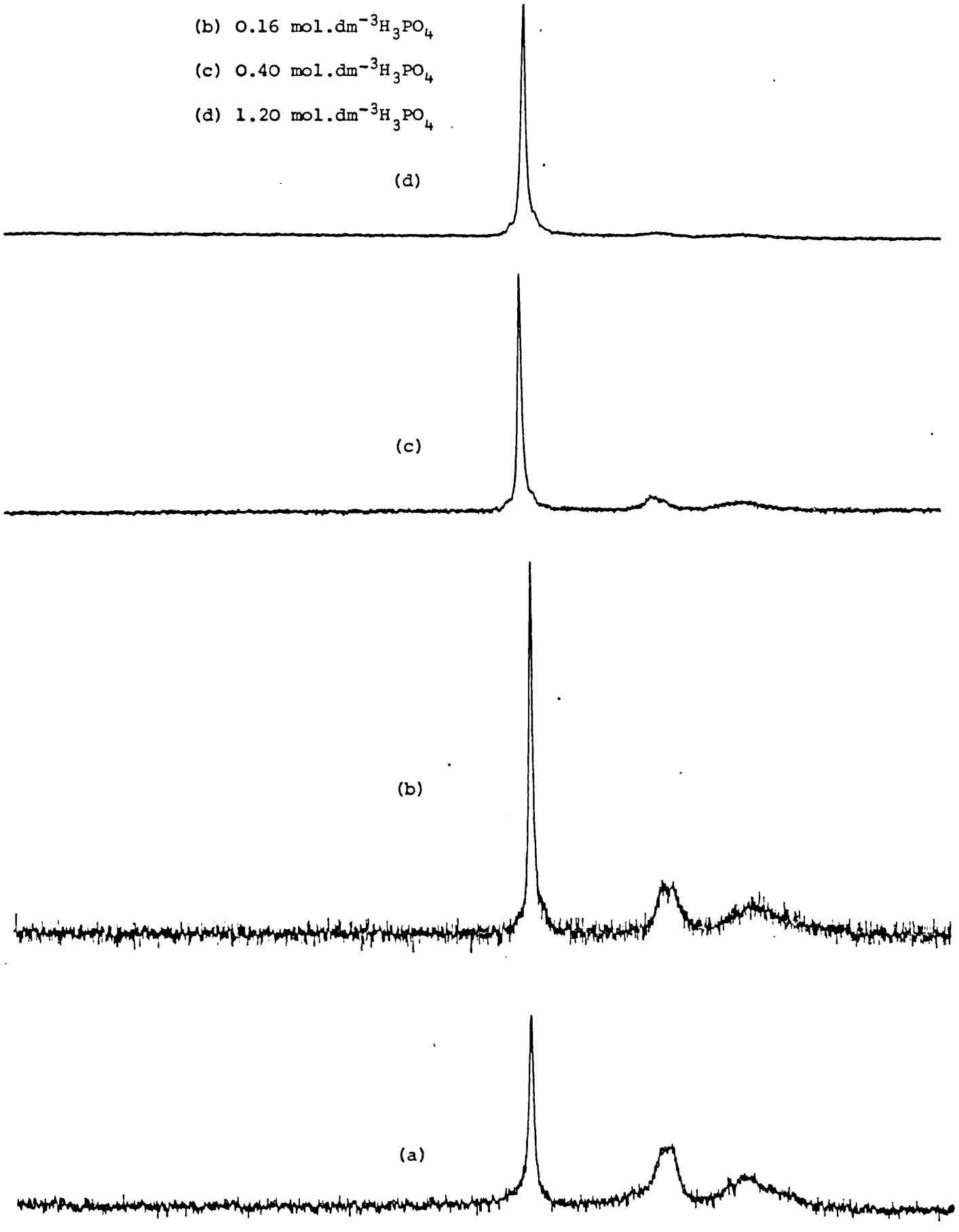

resonances (Fig. 40, sol. a) which appeared upfield of the uncomplexed acid, could be due to the complexes of Al^{3+} with the following ligands: $[HPO_4]^{2-}$, PO_4^{3-}, $[H_2PO_4]^-$, un-ionised H_3PO_4 or polymeric phosphate species. $[HPO_4]^{2-}$ and PO_4^{3-} should be present only in low acid concentrations, as at high concentrations $[HPO_4]^{2-}$ is small and PO_4^{3-} even smaller![12,31,32] To identify the signals, further work is required probably using Raman spectroscopy. The peaks indicated products of constant composition as they do not shift with acid concentration, but only change in intensity.

A solution of 0.1M Ga^{3+} and 0.08M H_3PO_4 gave a ^{31}P n.m.r. spectrum (sol. α , fig. 41), consisting of four broad overlapping peaks as Fig. 41 and table 66 describe. Increasing the molarity of H_3PO_4 added to 0.1M Ga^{3+}, these resonances coalesced and finally a broad single resonance appeared (Fig. 41, sol. d).

0.1M of $In(NO_3)_3$ and 0.04M of H_3PO_4 formed a complex which gave rise to two resonance signals. Increasing the concentration of H_3PO_4 a single broad resonance appeared as Fig. 42 , solution d , indicates. Table 61 shows how the spectral width varies as the different complexes are formed.

(ii) ^{31}P n.m.r. spectra of M^{3+}-PLP and M^{3+}-SB complexes

^{31}P n.m.r. spectra were recorded for the free ligand, PLP, at different pH values, so any shifts from the free ligand or changes in the spectral widths, could certainly indicate that a M-PLP complex or a M-SB complex was formed under the same conditions. Fig. 43 shows few characteristic spectra of M-PLP complexes.

Table 68 contains the chemical shifts and the spectral widths of PLP and M^{3+}-PLP complexes at a series of pH's.

^{31}P n.m.r. showed that in a mixture containing amino-acid, PLP and Metal, in the acidic pH range, the metal is initially bonded to the phosphate group (fig. 43). A rearrangement then takes place (Fig. 44)

Table 66

^{31}P n.m.r. spectra of Ga^{3+}-phosphoric acid mixtures at 20°C.

pH	Ga^{3+} /mol.dm^{-3}	H_3PO_4 /mol.dm^{-3}	Chemical shift from external H_3PO_4		Spectral width /Hz
			/Hz	/p.p.m.	
1.8	0.4	0.5	39.17	1.08	10
2.5	0.4	0.5	24.01	0.662	72
4.0	0.4	0.5	40.01	1.103	64
8.5	0.4	0.5	138.01	3.805	2
	0.1	0.08	52.74	1.454	64
			-116.7	-3.217	14
			-113.28	-3.123	39
			-233.4	-6.435	58
	0.1	0.28	44.43	1.225	57*
			-113.28	-3.123	39
	0.1	0.44	43.46	1.198	46*
			-112.79	-3.11	52**
	0.1	0.84	43.5	1.198	35

* The intensity of the resonance signal increases as the concentration of the acid increases.

** The intensity of the signal decreases as the concentration of the acid increases.

Table 67

^{31}P n.m.r. spectra of In^{3+}-H_3PO_4 at a series of concentrations at 20°C chemical shifts from external 8M H_3PO_4/p.p.m.

In^{3+} /mol.dm^{-3}	H_3PO_4 /mol.dm^{-3}	Resonance frequency /Hz	Chemical Shift		Spectral width /Hz
			/Hz	/p.p.m.	
0.1	0.08	36272281	-56.64	-1.562	71
0.1	0.04	36272378	40.04	1.104	33
		36272214	-123.54	-3.41	37
0.1	1.20	36272377	39.56	1.09	17
		36272212	-125.98	-3.47	38
0.1	3.0	36272377	39.6	1.09	11

Fig. 41 : ^{31}P n.m.r. spectra of 0.1 mol.dm^{-3} Ga^{3+} in the presence of H_3PO_4.

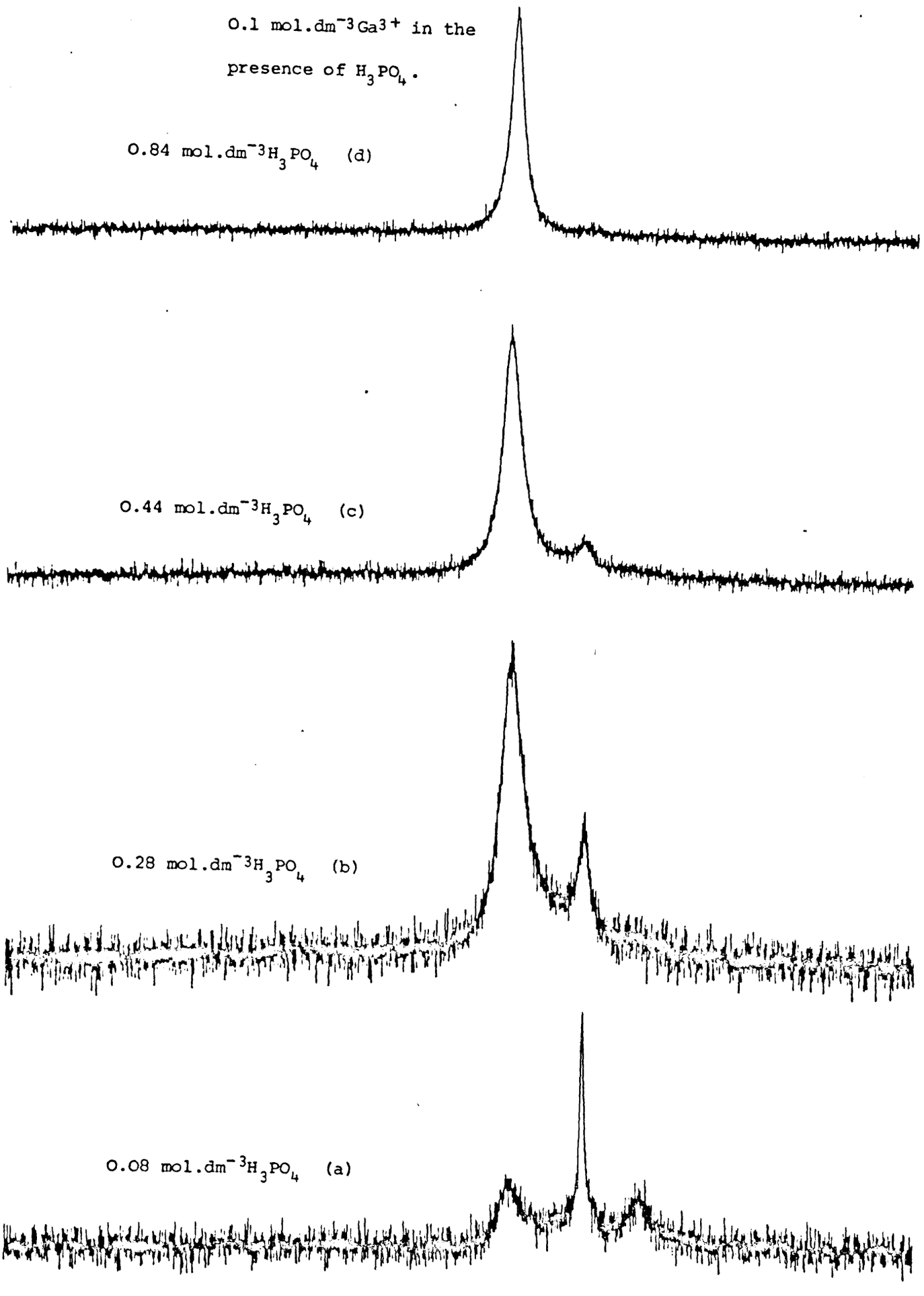

Fig.42: ^{31}P n.m.r. spectra of 0.1 mol.dm^{-3} In^{3+} in the presence of H_3PO_4.

(a) 0.08 mol.dm^{-3} H_3PO_4

(b) 0.04 mol.dm^{-3} H_3PO_4

(c) 1.20 mol.dm^{-3} H_3PO_4

(d) 3.0 mol.dm^{-3} H_3PO_4

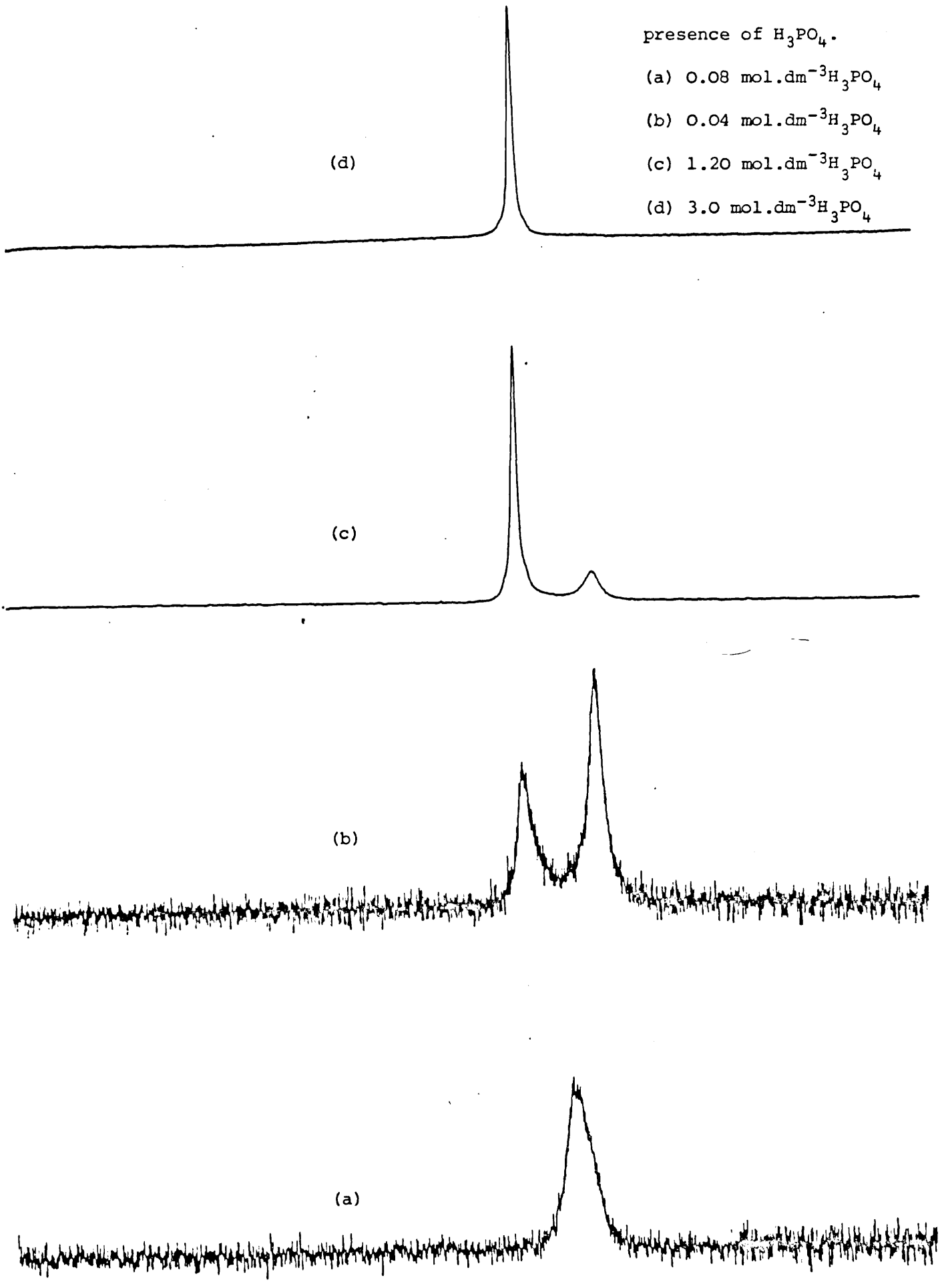

Table 68

^{31}P n.m.r. spectra: Chemical shifts/p.p.m. from external 8M H_3PO_4.

pH	PLP		AL-PLP		Ga-PLP		In-PLP	
	Chemical shift /p.p.m.	Spectral width /Hz	Chemical shift /p.p.m.	Spectral width /Hz	Chemical shift /p.p.m.	Spectral width /Hz	Chemical shift /p.p.m.	Spectral width /Hz
1								
1.0	1.048	7			1.24			
1.5	1.268							
2.0								
2.5	1.186	8	1.875	8	1.213	8	1.4	12
			-3.694	58	-2.316	30		
			-10.256	63	-3.860	60		
					-7.389	65		
3.5	1.35				-2.04			
6.5	-4.742				1.296		-4.0802	22
					1.075			
7.0	-4.963	6	-5.79	6				
8.0					5.51	12		
					5.38	25		
					5.90	27		
9.0	-5.238	8	6.6939					
			6.5589					
			6.8549					
			7.0569					
11.0	-5.597	7			-5.707	16	-6.85	18
					-5.541	17		
					-5.542	19		
					-6.0652	18		
					-7.168	16		
12.0	-5.6452	9						

Fig. 43: ^{31}P n.m.r. spectra of Ga-PLP (1:2) complex, (6 hours after mixing).

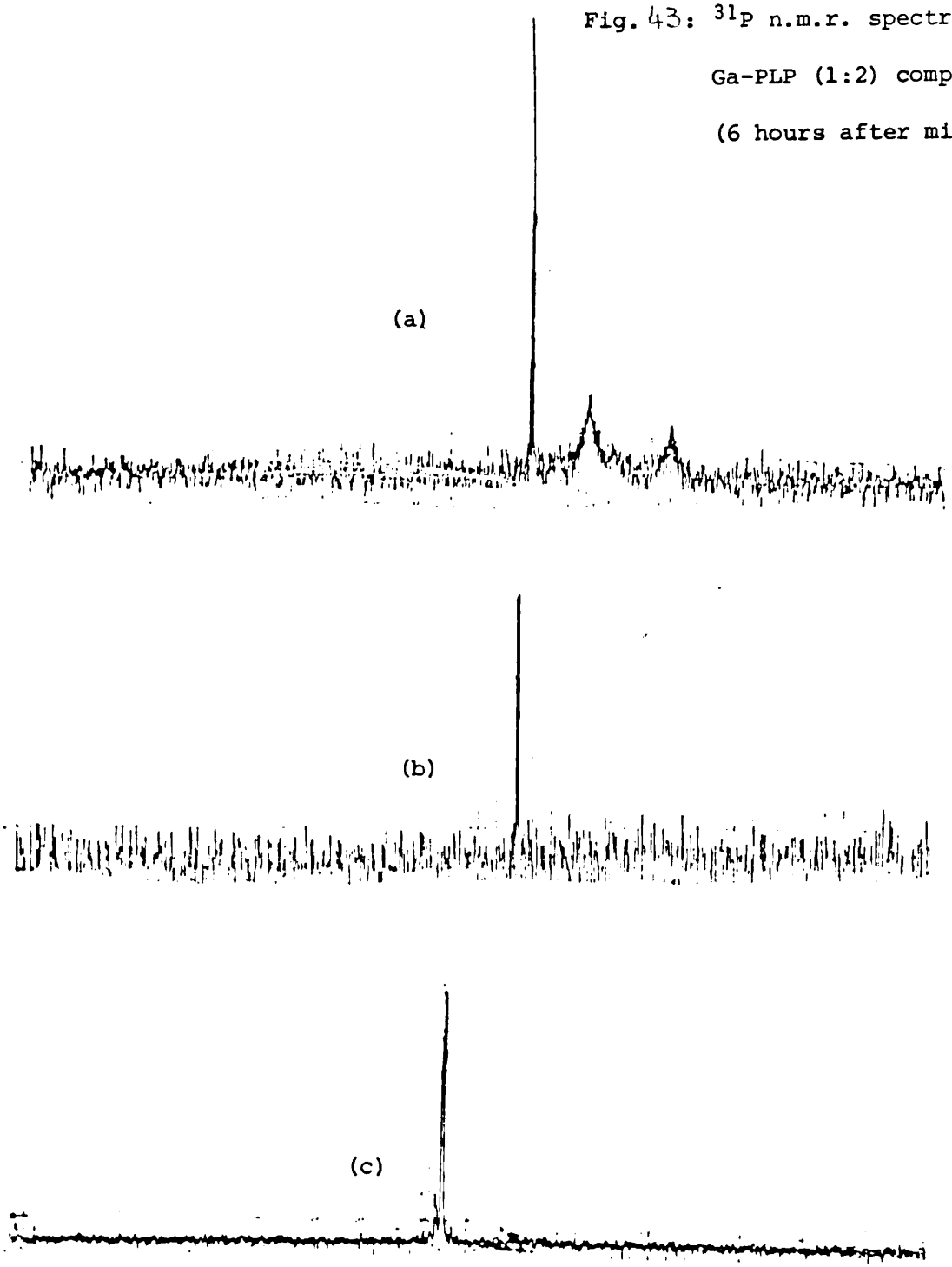

Table 69

^{31}P n.m.r. spectra of SB complexes: Chemical Shifts in p.p.m. from 8M H_3PO_4

pH	PLP-Glu	PLP-Asp	PLP-Threonine
2.5	1.21	1.17	1.1
7.0	-5.12	-5.977	-4.9
		-5.722	
9.0	-5.33	-5.49	-5.71
11.0	-5.41	-5.55	-5.34

Table 70

^{31}P n.m.r. spectra* of M^{3+} -SB in a series of pH's: Chemical Shifts/p.p.m. from external 8M H_3PO_4 solution.

pH	Al-PLP-Glu	Ga-PLP-Glu	In-PLP-Glu	Al-PLP-Asp	Ga-PLP-Asp	In-PLP-Asp	Al-PLP-Threon	Ga-PLP-Threon	In-PLP-Threon
1.0		0.9098							
2.5		-1.351	-1.42		-1.47			-1.31	
3.5		-2.00	-1.96	-2.73	-2.42	-2.89	-1.92	-2.09	
7.0	-3.92	-4.14	-4.93	-5.0176		-7.52		0.993	-4.9
	-4.33	-5.404	-4.86	-4.25		-7.2			-7.82
	-4.75	-5.073	-4.699	-3.78		-6.99			
	-5.40		-4.62		-6.01	-6.8			
	-5.71		-4.5		-4.69	-6.77			
						-6.6			
						-5.76			
						-5.62			
						-5.55			
9.0		-5.183	-5.937	-6.9359		-1.544		-6.096	-6.258
		-5.72		-7.0439				-5.68	-5.845
		-5.601							
11.00	-6.61	-6.045	-6.045						
	-6.7899	-6.045	-5.776						
		-7.003							

*All spectra were recorded 40 min. after mixing. The spectral widths were between 8-15 Hz indicating M^{3+}-O-P bonds were not present.

Fig. 44: ^{31}P n.m.r. spectra of Al^{3+}-PLP-Glu (1:2:2) complex

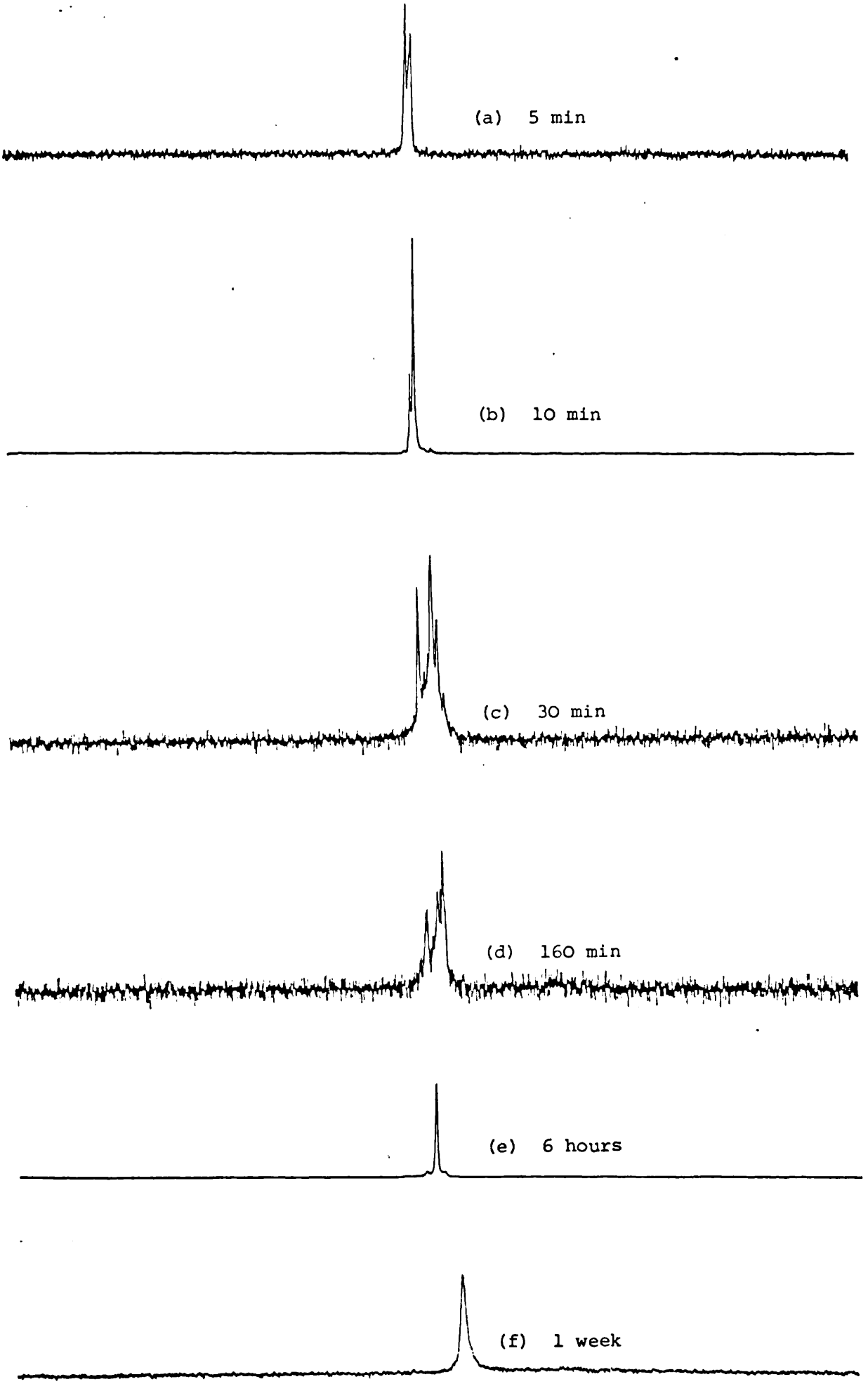

Fig. 45 : Proposed structures for the reaction of Al^{3+} + PLP + L-Glu at pH=3.8.

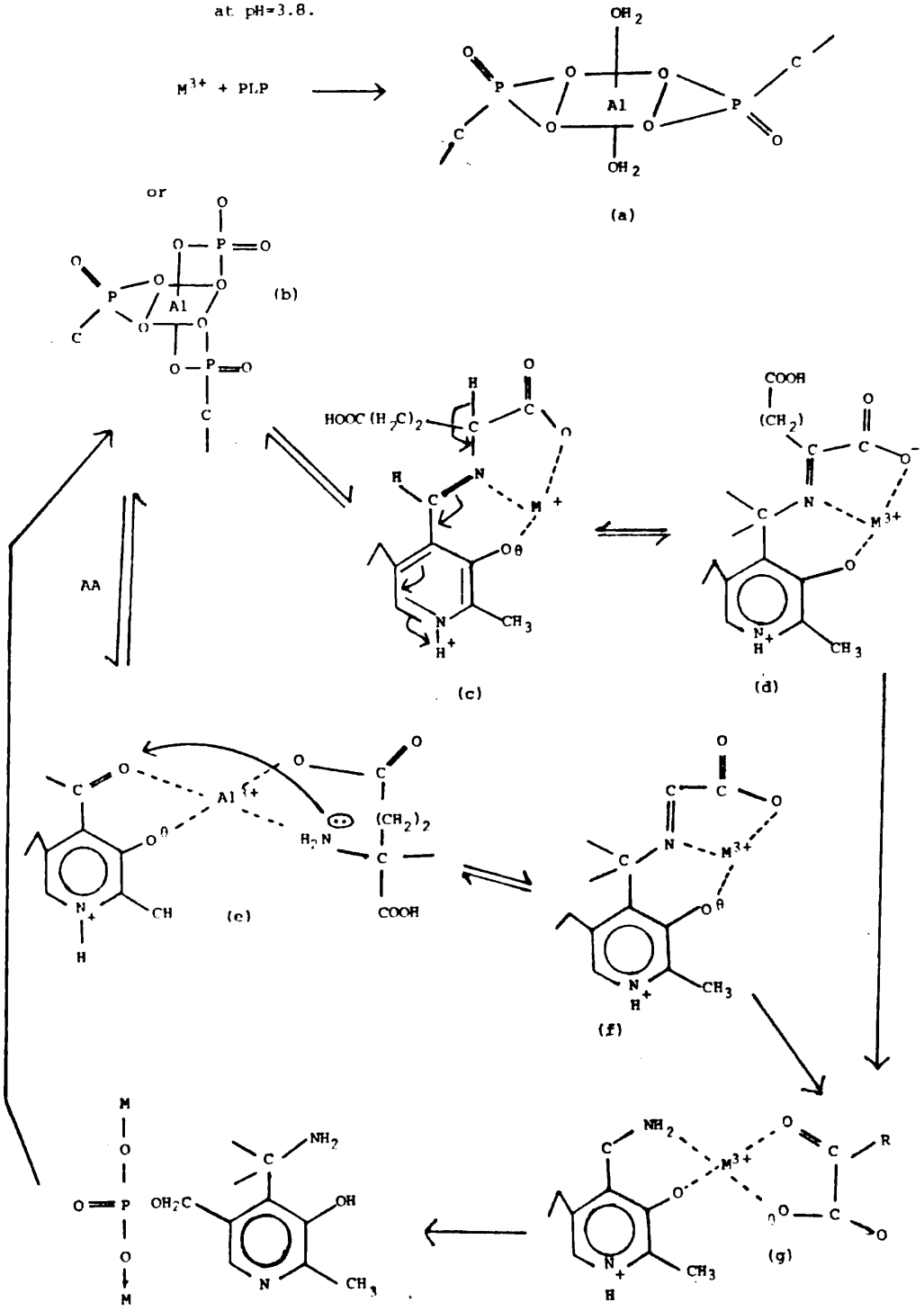

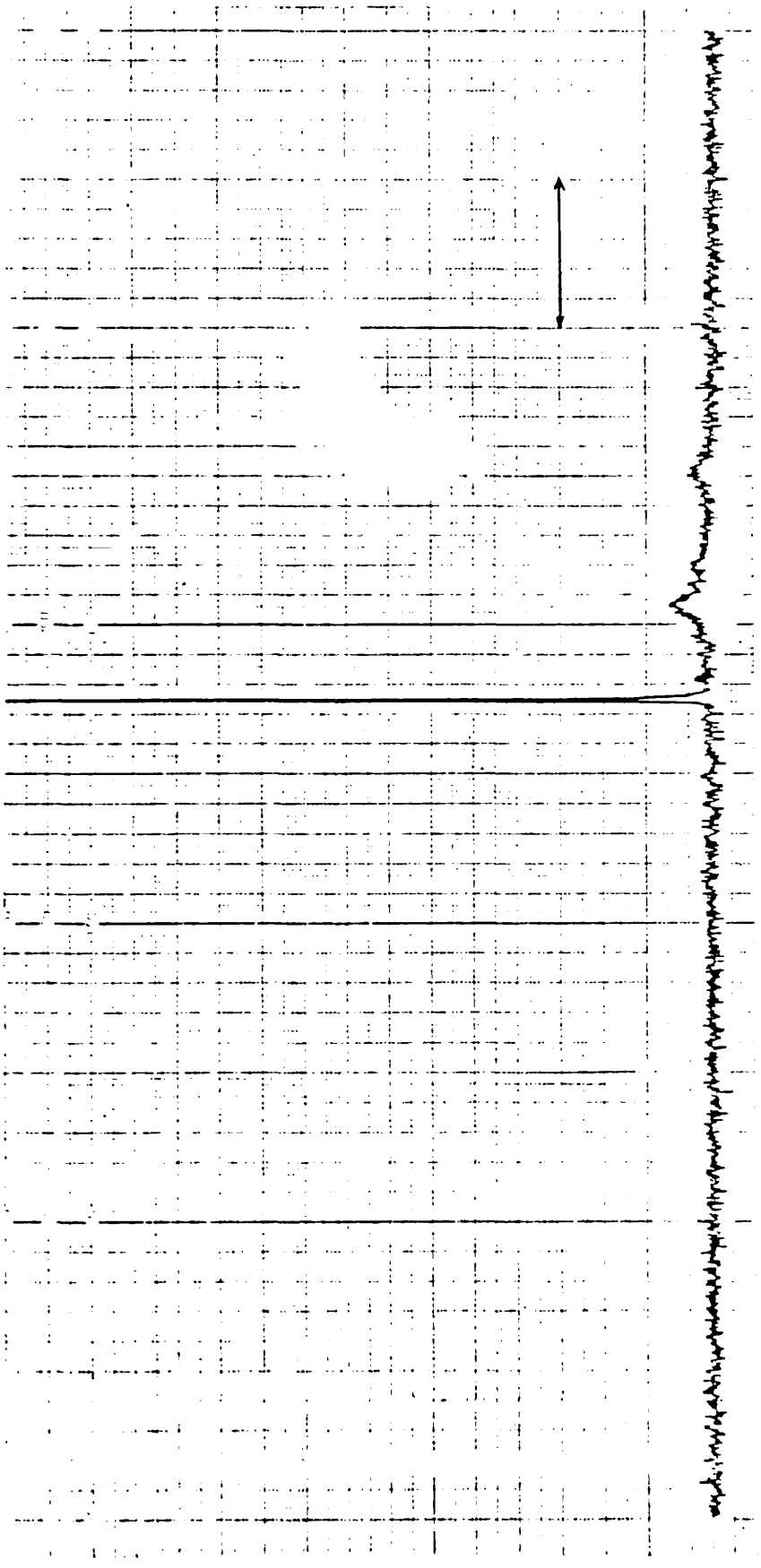

Fig.46: ^{31}P n.m.r. spectrum of Ga-PLP-Glu (1:2:2) complex at pH=2.5.

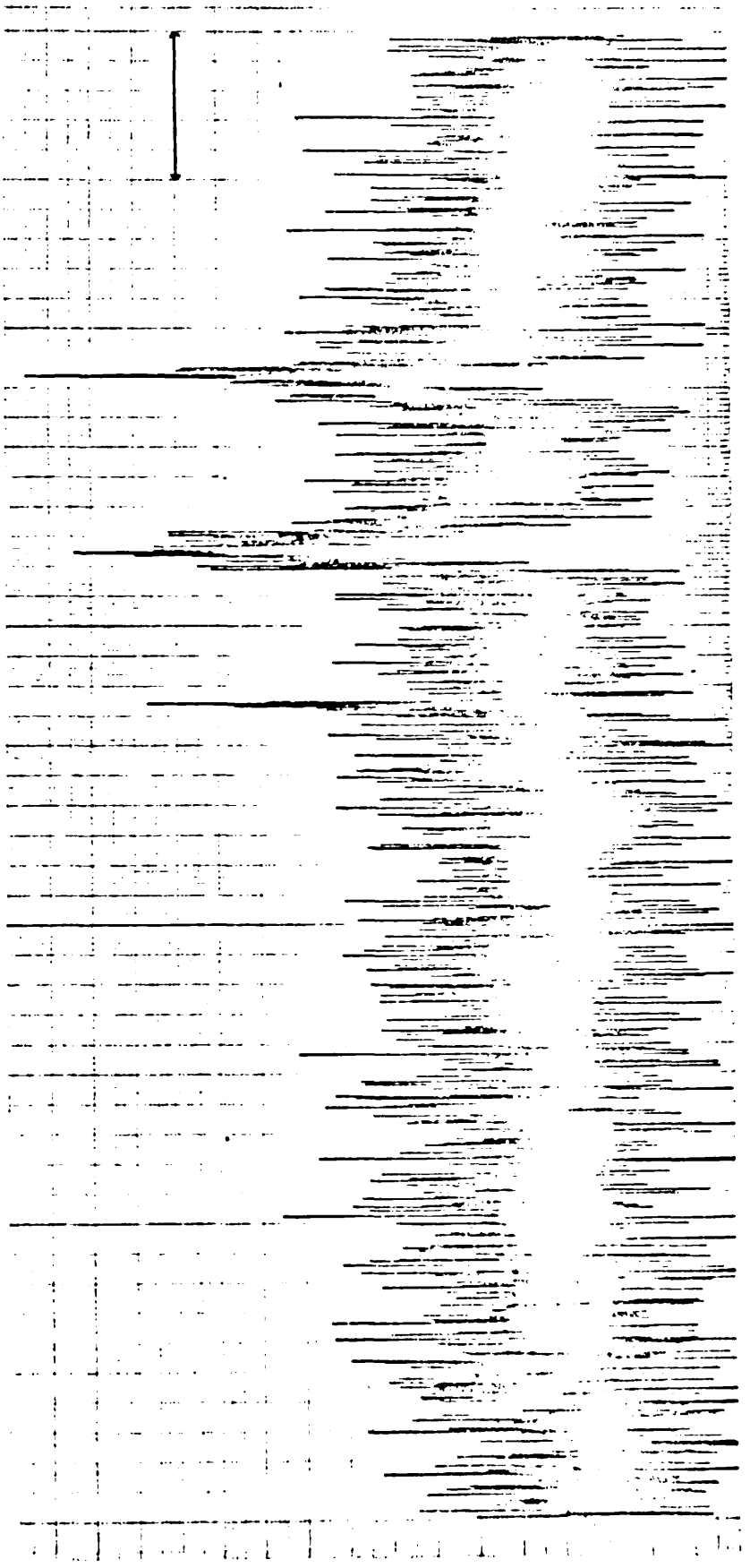

Fig. 47: ^{31}P n.m.r. spectrum of Al^{3+}-PLP (1:2) complex at pH = 2.5.

to either aldimine SB complex or to species in which both PLP and Amino acids are bonded as shown in Fig. 45 . A further rearrangement gives either the ketimine complex (Fig. 45c) or a Metal-Schiff-base intermediate (Fig. 45d) and finally (Fig. 44f) a complex of PAMP-M^{3+} with metal coordinated to phosphate is obtained, (e.g. its ^{31}P resonance is identical to the one the PAMP with Al^{3+} gives under the same experimental conditions). This can suggest the following mechanism for the reaction (Fig. 45).

In the basic pH range, the coordination of metal ion does not appear to involve the phosphate group in any stage (Table 68 , Fig.43).

E. ^{13}C n.m.r. (complete decoupling)

The resonances were assigned on the following basis: All complexes gave a singlet resonance in the region of 15-21 p.p.m. which is due to 2'-methyl carbon atom. The resonance of the 4' carbon atom appeared upfield as electronegativity arguments suggest, while the downfield resonance belongs to the 5'-carbon atom [33,34]. The 5-C resonance is assigned by the observation of three-bond carbon-phosphorus couplings[35] in proton-decoupled spectra. The large (27 Hz) coupling of 4-C to the aldehyde proton means that this resonance, is easy to identify. 2-C appears as a doublet at 152-154 p.p.m. of quartets via its two-bond coupling to 6-H (J = 7 Hz)[33].

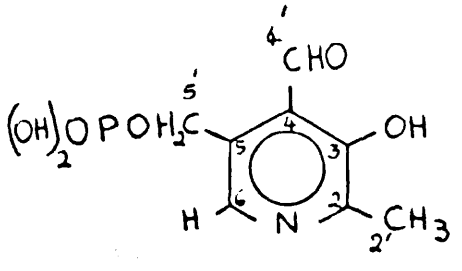

PLP

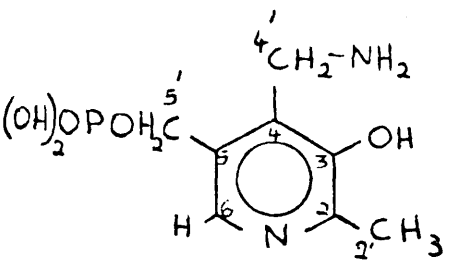

PAMP

The aromatic carbons shift as the pH increases, due to deprotonation of the various groups. Deprotonations at the phosphate group should cause much smaller shifts than the ammonium ($4'-CH_2-NH_3^+$) deprotonation causes, as in the later case there are large electronic changes in the aromatic system due to the inductive effect.

Before the Metal-Schiff-base system was studied, the spectra of the free ligands and Schiff-base complexes were recorded under the same conditions (pH and temperature), as the Metal-SB mixtures. (Tables 71, 72 and 73)

Schiff-base complexes were formed only near neutral and alkaline pH values, in very small amounts (Table 75). As the concentration of the metal ion increases, the formation of Schiff-base increases as well, up to a ratio of Schiff-base to Metal equal to 2:1. This is easily detected from the intensity of the signals of the free ligands, which decrease as more Schiff-base complex is formed.

Concentrations such as to give both 1:2 and 1:1 complexes were used in each pH studied, but the 1:1 complexes appear only in the acidic pH range. Near neutral and alkaline (up to pH 10.5) range, the 1:1 complex undergoes deprotonation and becomes dinegative. This neutral complex is relatively insoluble and thermodynamically unstably to disproportionation, in agreement with Martell's result.[40]

The 1:2 complexes appear near neutral and alkaline pH regions, as the free ligands are completely complexed. (See ^1H n.m.r. p.189, ^{31}P p.176, ^{27}Al p.137). ^{13}C n.m.r. spectra were quite complicated (Fig. 48) because of the large number of species detectable which due to the Schift-base-metal complexes and to the products of the transamination reaction (tables 75, 76) which necessarily takes place during the time required to run the spectrum (i.e. 6 hours).

As tables 71-75 show, in the acidic pH range, the shifts from the free ligands are noticeably small. This indicates that the metal is

Table 71

^{13}C n.m.r. spectra of PLP as a function of pD

pD	C_{-4}	C_{-3}	C_{-2}	C_{-5}	C_{-4}	C_{-6}	$C_{-5'}$	$C_{-2'}$
2.5	196.7	163.51	152.35	135.61	126.78	125.76	61.986	16.40
7.0	196.82	164.86	152.26	137.027	126.66	125.736	62.69	17.068
9.0	197.2	167.42	155.84	134.38	126.83	124.89	63.17	19.02
11.0	197.3	167.98	157.29	133.72	129.1	124.935	63.175	19.73

Chemical shifts are in parts per million relative to tetramethylsilane (Me_4Si).

Table 72

^{13}C n.m.r. spectra of PAMP as a function of pD.

pD	$C_{-4'}$	C_{-3}	C_{-2}	C_{-5}	C_{-4}	C_{-6}	$C_{-5'}$	$C_{-2'}$
2.5	40.584	159.34	148.98	141.99	140.75	137.39	67.564	20.81
7.0	37.62	163.66	145.68	135.67	133.66	124.74	63.01	16.63
11.0	37.4	161.1	150.8	131.6	138.1	134.2	63.9	20.6

Table 73

^{13}C n.m.r. spectra of the acid-ligands as a function of pD. (Chemical shifts in p.p.m. from TMS)

	L-Na-Glutamate			L-Aspartic acid		L-Threonine	α-Keto-Glutaric acid	
	$^{5}NaOOC-{}^{4}CH_2-{}^{3}CH_2-{}^{2}C(H)(NH_2)-{}^{1}COOH$			$^{4}NaOOC-{}^{3}CH_2-{}^{2}C(H)(NH_2)-{}^{1}COOH$		$^{4}CH_3-{}^{3}C(OH)(H)-{}^{2}C(NH_2)-{}^{1}COOH$	$^{5}NaOOC-{}^{4}CH_2-{}^{3}CH_2-{}^{2}C(=O)-{}^{1}COOH$ and $HOOC-{}^{3'}CH=C(OH)-{}^{2'}COOH$	
	pD=7.0	pD=9.0	pD=11.0	pD=7.0	pD=9.0	pD=7.0	pD=2.5	pD=7.0
c_1	175.27	175.6	175.82	174.961	174.961	175.87	160.82	170.8
c_2	55.51	55.51	55.95	52.963	53.159	61.613	151.83	135.81
c_3	27.78	28.17	31.87	37.291	37.4	66.88	33.76	37.1
c_4	34.40	34.20	36.71	178.993	178.34	20.384	33.11	36.4
c_5	181.89	181.8	183.03				182.68	182.3
$c_{6'}$							99.31	
$c_{7'}$							38.80	

Table 74

^{13}C n.m.r. spectra of M^{3+}-PLP and M^{3+}-PAMP complexes

(Chemcial shifts/p.p.m. from T.M.S.)

pD	Complex	$C_{-4'}$	C_{-3}	C_{-2}	C_{-5}	C_{-4}	C_{-6}	$C_{-5'}$	$C_{-2'}$
2.5	Al^{3+}-PLP	196.7	163.6	152.7	135.93	126.7	125.9	63.57	16.3
	Ga^{3+}-PLP	196.8	163.7	152.4	135.67	126.8	125.8	63.60	16.3
	In^{3+}-PLP	196.7	163.4	152.0	135.5	126.7	125.4	63.7	16.4
7.0	Al^{3+}-PLP	196.94	164.56	152.27	136.98	126.77	125.47	62.46	16.74
	Ga^{3+}-PLP	196.39	164.24	151.99	136.63	126.29	124.47	62.78	16.27
	In^{3+}-PLP	197.27	164.36	153.50	135.68	128.59	125.28	62.20	17.59
9.0	Al^{3+}-PLP	197.09	165.75	153.72	140.36	126.29	116.88	61.19	17.92
	Ga^{3+}-PLP	197.302	167.451	156.129	135.51	128.18	125.36	63.28	19.18
	In^{3+}-PLP	183.30	166.80	155.50	134.55	127.93	125.36	62.96	18.89
11.0	Al^{3+}-PLP	198.89	165.73	154.8	130.81	122.74	121.96	61.027	20.32
	Ga^{3+}-PLP	197.37	168.062	157.23	133.28	129.11	124.89	63.34	19.57
	In^{3+}-PLP	197.202		156.95	133.66	128.6	124.6	63.43	19.604
7.0	Al^{3+}-PAMP	36.12	169.52	146.29	135.81	134.99	124.27	65.12	17.02
	Ga^{3+}-PAMP	37.39	167.88	144.37	136.21	134.54	124.54	63.53	17.13
	In^{3+}-PAMP	38.13	172.38	145.27	136.96	134.11	124.82	63.41	17.67
2.5	Al^{3+}-PAMP	40.51	159.0	148.5	141.67	140.8	137.41	67.55	20.75
	Ga^{3+}-PAMP	40.60	159.21	148.7	141.92	140.7	137.39	67.56	20.8
	In^{3+}-PAMP	40.62	159.34	148.9	141.95	140.9	137.6	67.57	20.9

Table 75: ^{13}C n.m.r. spectra of M^{3+}-Schiff-base complexes as a function of pD. (Chemical shifts in p.p.m. from TMS)

pD	Complex	$C_{PLP-4'}$	C_{PLP-3}	C_{PLP-2}	C_{PLP-5}	C_{PLP-4}	C_{PLP-5}	$C_{PLP-5'}$	$C_{PLP-2'}$	C_{a-1}	C_{a-2}	C_{a-3}	C_{a-4}	C_{a-5}
3.5	Al-PAMP- -Kg	37.23	161.78	133.73	133.60	132.56	124.95	62.59	15.25	170.28	144.98	34.17	30.07	178.93
7.0	Al-PAMP- -Kg	35.49	170.87	145.63	135.82	134.14	124.55	62.53	15.99	182.14	147.35	34.14	31.38	206.41
7.0	Ga-PAMP- -Kg	194.67	168.44	150.5	140.21	134.0	129.54	63.24	20.86	175.32	138.38	41.94	36.25	186.92
			175.32	168.44		138.48				186.9	150.50			194.67
7.0	In-PLP-Glu**	196.99	177.41	168.59	140.8	137.1	128.72	63.11	18.41	187.1	150.4	41.72	36.29	199.99
7.0	PLP-Glu		163.65	145.6	135.49	130.74	124.49	61.16	15.96	175.42	55.5	31.38	34.37	182.12
7.0	Al-PLP-Glu**	216.19	166.74	158.57	136.28	131.98	128.79	62.03	19.02	176.65	59.21	26.17	31.31	182.7
									18.11					
									18.27					
7.0	Ga-PLP-Glu**	196.99	164.91	155.80	134.96	130.05	125.20	62.53	17.94	168.54	34.30	27.75	31.48	182.24
		37.00	163.8	145.5	135.5	133.9	124.2		15.90	170.8	135.8	36.38	37.38	
9.0	PLP-Glu	196.8		148.57	133.35			62.12	18.49	159.98		30.16	36.91	180.2
9.0	Al-PLP-Glu**	196.8		156.46	135.71	132.08	128.94	62.25	18.15	148.8	37.01	31.16	34.71	180.95
									16.84					
									16.23					
9.0	Ga-PLP-Glu**	181.64	167.79	155.27	133.3		122.25	62.78	18.40	174.9	55.51	27.9	31.27	181.2
9.0	In-PLP-Glu**	196.9	164.2		132.41	128.7	127.85	62.96	18.62	165.0	55.91	31.01	33.49	183.1
11.0	Ga-PLP-Glu	197.32	165.14		133.99	132.36	129.11	61.88	19.19		31.4	32.5	34.96	183.72

Continued...

pD	Complex	$C_{PLP-4'}$	C_{PLP-3}	C_{PLP-2}	C_{PLP-5}	C_{PLP-4}	C_{PLP-5}	$C_{PLP-5'}$	$C_{PLP-2'}$	C_{a-1}	C_{a-2}	C_{a-3}	C_{a-4}	C_{a-5}
7.0	PLP-Asp	197.86	165.86	156.10	133.08	128.98	117.28	62.59	19.54		42.62	41.91	177.11	
7.0	Al-PLP-Asp	195.511	166.57	156.04	139.58	125.81	116.69	62.2	20.12	176.52	53.03	37.36	178.47	
									18.95					
									18.43					
									16.70					
7.0	Ga-PLP-Asp		161.23	155.9	146.30	135.37	121.44	62.65	18.173	174.44	43.34	37.23	177.95	
									16.03					
									14.40					
7.0	In-PLP-Asp		166.51	156.95	132.8	131.39	120.92	62.33	16.61	174.77	41,97	37.29	178.28	
									17.52					
									18.43					
									18.89					
9.0	PLP-Asp	181.07	166.44	155.91	132.46	132.11	116.63	62.2	18.95	174.76	53.16	42.04	178.2	
9.0	Al-PLP-Asp		165.21	156.04	135.23	132.49	132.30	61.94	18.11	178.34	53.22	37.81	178.67	
9.0	Ga-PLP-Asp	197.20	165.14	155.52	133.21	128.72		62.07		178.7	43.93	42.04	180.75	
9.0	Al-PLP-Thr	197.41	167.41	154.1	132.92	130.74	125.15	61.95	19.40	168.8	62.59	65.01	20.05	
9.0	Ga-PLP-Thr	197.55	166.95	153.9	131.75	129.11	124.70	61.8	19.68	167.9	62.43	64.74	18.73	
9.0	In-PLP-Thr	201.56	166.51	153.24	131.37	128.46	124.56	62.07	19.54	168.5	62.26	63.37	19.93	
		197.07												
9.0	Al-PAMP- -Kg	199.80				132.56		62.00	19.22	180.16	50.51	31.44	30.72	205.79
		34.82						63.3			48.86			
											46.98			
7.0	Al-PAMP- -Kg	35.49		145.63	135.82	134.14	124.55	62.53	15.99	170.9		34.18	31.38	206.41
										182.14				

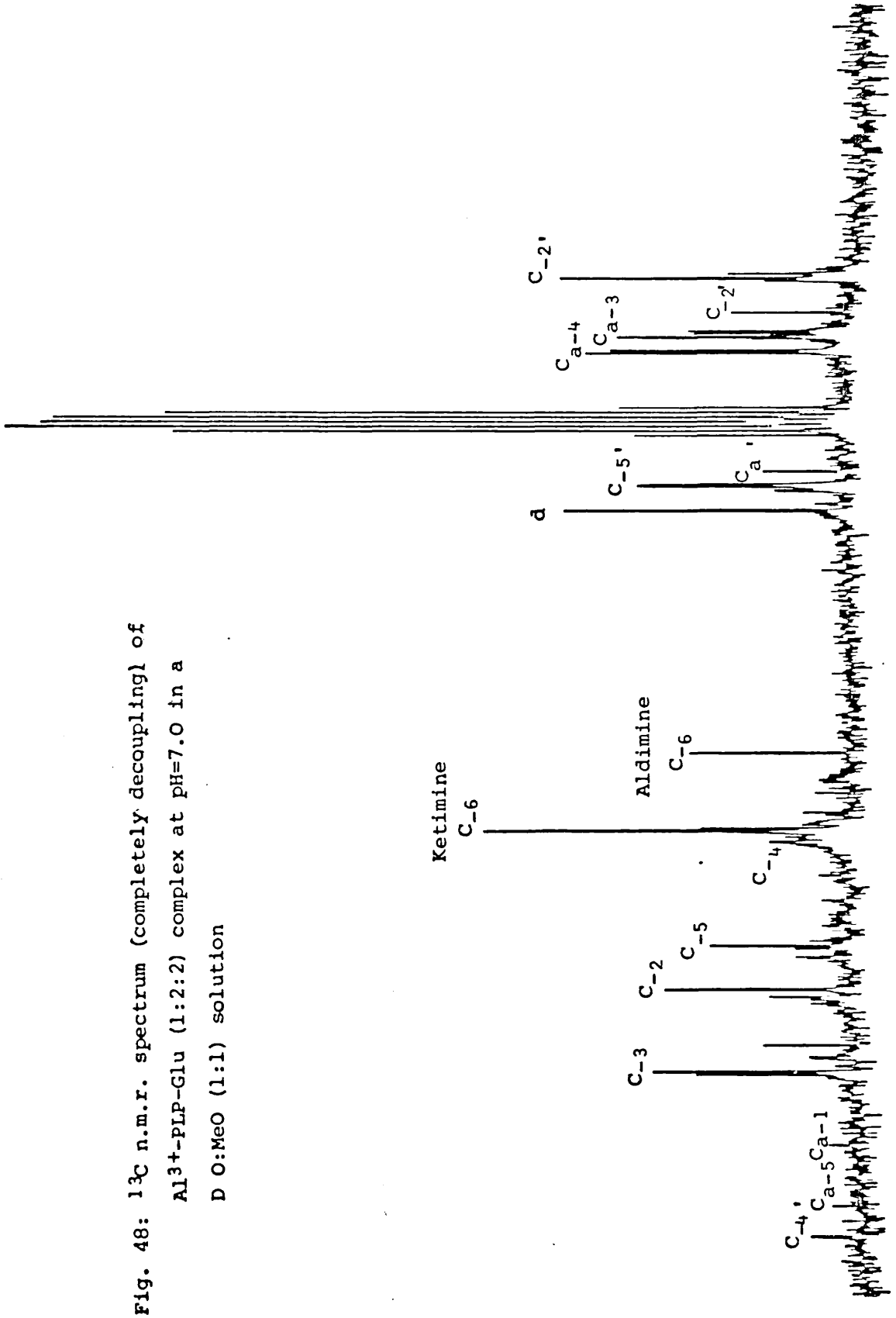

Fig. 48: ^{13}C n.m.r. spectrum (completely decoupling) of Al^{3+}-PLP-Glu (1:2:2) complex at pH=7.0 in a D O:MeO (1:1) solution

Table 76

^{13}C resonances due to the second stage of the reactions indicating transamination reactions (chemical shifts in ppm from TMS)

pD	Complex	$C_{PAMP-4'}$	C_{PAMP-3}	C_{PAMP-2}	C_{PAMP-5}	C_{PAMP-4}	C_{PAMP-6}	$C_{PAMP-5'}$	$C_{PAMP-2'}$	C_{a-1}	C_{a-2}	C_{a-3}	C_{a-4}	C_{a-5}
7.0	Al-PLP-Glu	35.21	170.9	145.75	135.495	133.82	124.61	62.91	16.082	182.1	146.3	34.9	31.42	194.1
	Ga-PLP-Glu	35.74	168.9	145.67	136.10	134.12	124.5	63.08	19.99	175.2	140.6	41.6	36.3	186.5
	In-PLP-Glu	36.02	176.8	145.87	136.00	133.96	124.72	63.12	17.10	183.4	148.32	41.7	36.9	184.3
9.0	Al-PLP-Glu	34.03	162.3	144.62	135.71	132.11	129.1	63.35	19.24	180.2	134.5	31.5	30.75	199.9
	Ga-PLP-Glu	34.95	167.4	145.02	136.42	132.43	128.6	63.00	19.73	181.4	133.71	32.96	31.63	201.4
	In-PLP-Glu	35.42	166.9	146.35	136.9	133.12	128.3	63.03	19.92	191.62	133.9	34.71	33.33	205.8
9.0	Al-PAMP-α-Kg	196.8	168.4	148.57	133.7	127.3	128.9	62.91	18.34	173.1	50.81	27.9	34.6	180.4
				140.27					16.928					
									16.2					
	Ga-PAMP-α-Kg	196.9	167.3	155.3	133.6	128.1	125.2	62.83	18.01	174.3	48.18	27.3	33.9	181.2
									18.94					
	In-PAMP-α-Kg	196.9	167.5	155.8	133.68	128.59	127.1	62.51	18.8	175.1	46.98	31.0	33.2	182.9

not affecting the electronic environment of the ring carbons. This result is in agreement with the ^{31}P n.m.r. results in this system, thus the metal is initially coordinated to PLP through its phosphate group (no noticeable shifts), and then rearranges to form the Shiff-base complex through the phenolic oxygen, amino group and carboxylic group of the amino-acid in order for the Al-SB complex to take part in the transamination (the functional groups shift on coordination, (Table 75).

Around neutral and alkaline pH values (Tables 74,75,76), the chemical shifts are such that coordination must be through the phenolic oxygen and aldehyde group of PLP, as these carbons were shifted the most. The ^{31}P n.m.r. support this, as the spectra do not contain any resonances (tables 68 and 70), assigned to M-O-P groups.

At pH 9.0 some of the Schiff-base-Metal complexes gave two 2-CH_3 resonances as Table 31 shows. Hence a possible configuration should be the one of two approximately planar PLP-AA ligands (one bound to two polar and one of the equatorial sites and the other bound to the remaining three equatorial sites), so that the 2-CH_3 group of one ligand is directly above the π cloud of the azomethine nitrogen of the other ligand and is shielded by it, as Martell suggested[41] (chapter 1, Fig. 1)

Transamination reaction should take place during the time some of the spectra were recorded. Table 76 indicates that PAMP and α-Keto-glutaric acid were the products of the reaction.

F. ^{1}H n.m.r.

The resonance signals of the ligands were directly deduced from previous studies[38].

The chemical shifts of the ligands in the ^{1}H n.m.r. spectra, are strongly pH dependent as the result of the deprotonation of the various functional groups.

At acidic pH's the aldehyde group of PLP is hydrated[39] as the ^{1}H

n.m.r. spectra show (the free aldehyde's proton is absent indicating the existance of the hydrated form, in which the proton exchanges for deuterium) (Fig. 49a) and therefore the metal should be coordinated to this ligand through the phosphate group. This is strongly supported by the ^{31}P n.m.r. spectra (Fig. 49 and 50) which show M-O-P bonding and by the ^{13}C n.m.r. (tables 67 and 68) in which the resonance signals of the ligands do not shift when the Metal complex is formed.

Near neutral pH values the aldehyde is partially hydrated (Fig. 49) and therefore coordination with the metal is possible and exists, as ^{1}H, ^{13}C (strong shifts) and ^{31}P n.m.r. (there is no M-O-P bonding) indicate.

At basic pH values the aldehyde group is fully available (Fig. 49) for coordination and the phosphate group is much less prefered. Strong ^{13}C and ^{1}H shifts and the absence of M-O-P resonances in ^{31}P n.m.r. (Fig. 43, Tables 74, 75, 70, 68 support this case.)

The formation of SB and M-SB is proved by the appearance of new 2-CH_3, 4-CH_2 (Ketimine), 5-CH_2, 6-H and the aldemine (4-CH) signals (Tables 77-79). The intensity of the aldimine signal increases as the pH increases up to 9.5 and then decreases and in strongly basic solutions it disappears completely (Fig. 50).

At constant pH values, the concentration of aldimine formed, increases, as the concentration of the metal added increases, up to a concentration at which the 1:2 Metal-Ligand complex is formed (Fig. 50). Any further increase of the concentration of the metal does not affect the amount of aldimine formed (the integration in ^{1}H n.m.r. spectrum remains the same). The amount of aldimine formed was estimated from the relative intensities of the signals.

Below pD 6, the complexes formed should have 1:1 stoichiometry (^{1}H n.m.r. shows free and coordinated ligands of the same intensity, while a 1:2 M:L complex was thought to be formed). This was also shown

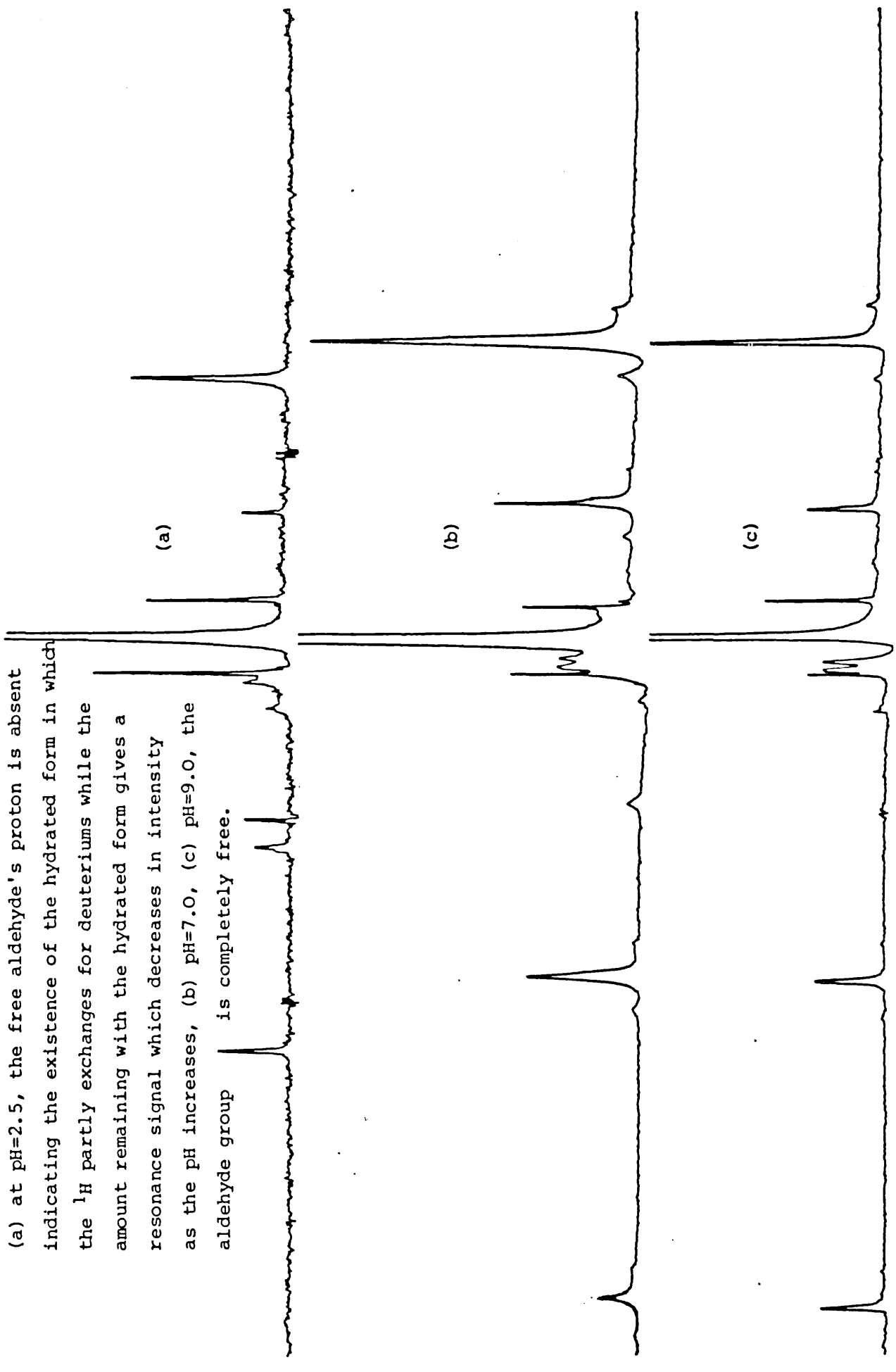

Fig. 49: ^{1}H n.m.r. spectra of PLP

(a) at pH=2.5, the free aldehyde's proton is absent indicating the existence of the hydrated form in which the ^{1}H partly exchanges for deuteriums while the amount remaining with the hydrated form gives a resonance signal which decreases in intensity as the pH increases, (b) pH=7.0, (c) pH=9.0, the aldehyde group is completely free.

Table 77

The effect of pD on 2-CH_3 resonance chemical shift in Hz from TMS.

Complex	pD			
	2.5	7.0	9.0	11.0
PLP	233.32	210.94	207.52	204.32
Al^{3+}-PLP				195.5
Ga^{3+}-PLP	229.1	232.32	211.18	195.40
In^{3+}-PLP			207.4	
Al^{3+}-PLP-Glu				
Ga^{3+}-PLP-Glu	228.4	233.47	204.32	207.32
				201.14
In^{3+}-PLP-Glu				206.58
				191.7
PLP-Glu	228.8			
Al^{3+}-PLP-Asp	229.5			
Ga^{3+}-PLP-Asp	229.6			
In^{3+}-PLP-Asp	230.3		214.37	
			208.5	
PLP-Asp	229.9	218.74	211.43	
Al^{3+}-PLP-Threon	229.1			
Ga^{3+}-PLP-Threon	229.			
In^{3+}-PLP-Threon	230.7	227.95	210.94	
			205.08	
PLP-Threon				

Table 78

The effect of pD on the aldehyde, aldimine 4-CH and Ketimine4-CH_2 resonances. (Chemical shift in Hz from TMS)

Complex	pD			
	2.5	7.0	9.0	11.0
PLP	732.0 hydrated aldehyde 4-CH	925.05 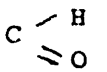	924.71 	923.3 
Al^{3+}-PLP				913.5 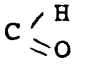
Ga^{3+}-PLP	731.4 4-CH	732.32 4-CH	928.46 	910.25 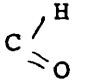
In^{3+}-PLP			922.37 	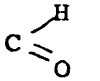
Ga^{3+}-PLP-Glu		730.32 4-CH aldimine	930.3  806.3 (aldimine 4-CH) 460.4 (Ketimine 376.2 4-CH_2)	920.45 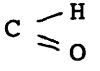 776.2 (aldimine 4-CH) 463.1 (Ketimine 4-CH_2)

Continued...

Complex	pD			
	2.5	7.0	9.0	11.0
Al^{3+}-PLP-Thr				925.11 784.2 4-CH aldimine 366.0 4-CH_2 Ketimine
Ga^{3+}-PLP-Thr			927.1  800.9 4-CH 378.2 4-CH_2	921.8  774.5 4-CH aldimine 363.0 4-CH_2 Ketimine
In^{3+}-PLP-Thr			925.04  799.55 (4-CH aldimine) 492.42 (4-CH_2 Ketimine) 379.14 (4-CH_2)	911.2  374.0 4-CH_2

Complex	pD			
	2.5	7.0	9.0	11.0
In^{3+}-PLP-Glu		927.4 4-CH_2 794.2 388.3	931.5 C(=O)H 815.2 4-CH	923.86 C(=O)H 812.2 aldimine 4-CH 471.0 Ketimine 4-CH_2
PLP-Glu	697.12(s) 4-CH aldimine		924.55 C(=O)H	
Al^{3+}-PLP-Asp			103.85 (aldimine 4-CH) 465.32 (Ketimine 4-CH_2) 378.6 (4-CH_2)	
Ga^{3+}-PLP-Asp			927.3 C(=O)H 789.7 4-CH 376.9 4-CH_2	922.7 C(H)=O 771.4 4-CH aldimine 302.5 4-CH_2 Ketimine
PLP-Asp		927.97 C(H)=O 797.36 (4-CH aldimine) 448.31 (Ketimine 4-CH_2)	796.87 4-CH aldimine	

Continued...

Table 79

The effect of pH on C_6-H resonance chemical shift in Hz from TMS.

Complex	pH			
	2.5	7.0	9.0	11.0
PLP	578.32	684.62	681.50	678.32
Al-PLP				671.72
Ga-PLP	576.4	580.32	688.72	667.3
In-PLP			682.32	
Al-PLP-Glu				
Ga-PLP-Glu	566.3	581.39	691.1	687.3
				685.4
In-PLP-Glu			684.32	694.85
PLP-Glu	697.12		681.63	
Al-PLP-Asp	563.2			
Ga-PLP-Asp				
In-PLP-Asp				
PLP-Asp		679.19	678.7	
Al-PLP-Threon				
Ga-PLP-Threon				
In-PLP-Threon			680.41	
PLP-Thr				
In-PLP-Leucine			686.52	

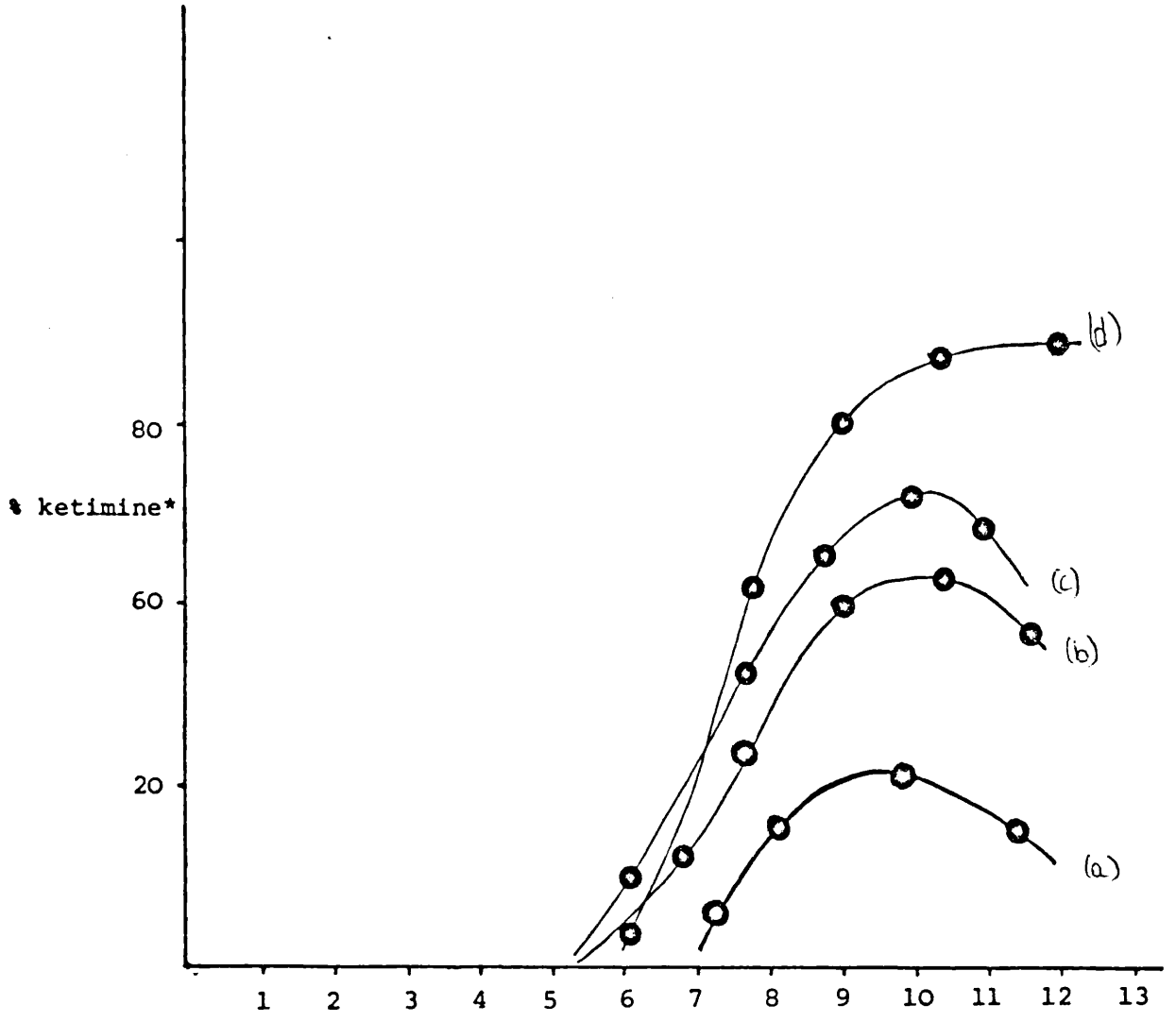

Fig. 50: Amount of ketimine formed as a function of pH and $[Al^{3+}]$ when the concentration of PLP-Glu is 0.08M

a = 0.0 $mol.dm^{-3}Al^{3+}$; b = 0.02 $mol.dm^{-3}Al^{3+}$; c = 0.035 $mol.dm^{-3}Al^{3+}$; d = 0.06 $mol.dm^{-3}Al^{3+}$.

* The amount of ketimine formed was related to ketimine 6-H resonance.

by ^{71}Ga n.m.r. when the L:M ratio was plotted against relative intensity (Fig. 35, Tables 56-58), and ^{27}Al n.m.r. where the free coordinated Al^{3+} was present in the 1:1 ratio at the basic pH range (Fig. 29).

Tables 78-80 show the effect of pH on 2-CH_3, 4-CH_2, 5-CH_2 and 6-H resonances respectively, when the Schiff-base complexes were formed. The spectra of the free ligands and expected products were again recorded for comparison.

About pH 8.0 the resonances of the various 2-CH_3 groups are almost invariant with pH, but below this point, they shift to lower field as the pD decreases. (Table 77).

REFERENCES

1. High Resolution n.m.r. Emsley, Feeney and Sutcliff vol. 2 and K. Tatsumoto and A.E. Martell, J.A.C.S. 1978, 100, 5549.
2. Y. Matsushima and A.E. Martell, J.A.C.S. 89, 1322 (1967).
3. Y. Matsushima and A.E. Martell, ibid., 89, 1331 (1967).
4. A.K. Covington, M. Paabo, R.A. Robinson and R.G. Bates, Anal. Chem. 40, 700 (1968).
5. J.W. Akitt, Ann. Reports NMR Spectry. 5A, 465 (1972).
6. J.W. Akitt, N.N. Greenwood and G.D. Lester, J.C.S. (A), 2450 (1971).
7. C.P. Poole, Jr. H.E. Swift and J.F. Itzel, Jr., J. Chem. Phys. 42, 2576 (1965).
8. R.G. Kidd and D.R. Truax, J.A.C.S. 90, 6867 (1968).
9. J.J. Delpuech, M.R. Khaddar, A. Peguy and P. Rubini, J.A.C.S. 97, 3373 (1975).
10. D.E. O'Reilly, J. Chem. Phys. 32, 1007 (1960).
11. H.E. Swift, C.P. Poole and J.F. Itzel, J. Phys. Chem. 68, 2509 (1964).
12. F.A. Cotton and G. Wilkinson 'Advanced Inorganic Chemistry, third edition, Interscience Publishers, John Wiley (1972).
13. W. Gordy, Discuss, Faraday Soc. 19, 14 (1955).
14. C. Deverell, Prog. nucl. magn. reson. Spectrosc. 4, 299 (1969).
15. A. Abragam, "The Principles of Nuclear Magnetism" (Oxford University Press) (1961).
16. L.D. Supran and N. Sheppard, J.C.S., Chem. Comm., 832 (1967).
17. H. Ihtaki, Bull. Chem. Soc. Japan, 43, 2463 (1970).
18. R.K. Harris and B.E. Mann, Eds., "NMR and the Periodic Table", Academic Press, London/New York 1978.
19. R.A. Ogg and J.D. Ray, J. Chem. Phys., 26, 1339 (1957).
20. J.W. Akitt, N.N. Greenwood and A. Storr, J. Chem. Soc. 814, 4410 (1965).

21. J. Swiff, D.G. Fritz and T.A. Stephenson, J. Chem. Phys., 46, 406 (1967).

22. J.A. Jackson, J.F. Lemons and H. Taube, J. Chem. Phys., 32, 553 (1960).

23. R.E. Connick and D.N. Fiat, J. Chem. Phys., 39, 1349 (1963).

24. D. Fiat and R.E. Connick, J.A.C.S. 88, 4754 (1966).

25. V.P. Tarasov and YU.A. Buslaev, Molecular Physics, Vol.24; No.3, 665-668 (1972).

26. W.G. Procter and F.C. Yu, Phys. Rev. 81, 20 (1951).

27. Y. Ting and D. Williams, Phys. Rev. 89, 595 (1953).

28. H. Haraguchi, K. Fuwa and S. Fujiwaro, J. Phys. Chem. 17, 1497, (1973).

29. M. Rice and R.V. Pound, Phys. Rev. 106, 953 (1957).

30. J. Kodweiss et al, Journal of magnetic resonance, 43, 495-498 (1981).

31. R.F. Jameson and J.E. Salmon, J.C.S. 4013 (1954).

32. J.E. Salmon and J.G.L. Wall, J.C.S., 1128 (1958).

33. T.H. Witherup and E.H. Abbott, J. Org. Chem., Vol.40, No.15, 2229 (1975).

34. Francoise Nepveu-Juras, C.R. Acad. Sc. Paris, t.284, série C-29 (1977).

35. J.B. Stothers "Carbon-13 NMR Spectroscopy", Academic Press, New York, N.Y. 378 (1972) and B. Bordsall and J. Feeney, J.C.S., Perkin Trans. 2, 1643 (1972).

36. N. Muller, J. Chem. Phys. 36, 359 (1962) and H. Dreeskamp and E. Sackmann, Z. Phys. Chem., 34, 273 (1962).

37. K. Aoki and H. Yamazaki, J.C.S. Chem. Comm., 363 (1980).

38. A. Korytnyk and R.P. Singh, J.A.C.S., 81, 2813 (1963).

39. K. Nakamoto and A.E. Martell, J.A.C.S., 81, 5857 (1959).

40. E.H. Abbott and A.E. Martell, J.A.C.S., 95, 5014 (1973).

41. E.H. Abbott and A.E. Martell, J.A.C.S., 92, 20, 5845 (1970).

42. M.D. Tsai, S.R. Byrn, C.-J. Chang, H.G. Floss, and J.R. Weintraub, Biochemistry, 17, 3183 (1978).

43. K. Blake and A. Siegel, J.A.C.S. 85, 294 (1963).

CONCLUSION

The present work has investigated both reactions of bivalent and of trivalent metals with Pyridoxal phosphate and amino acids.

Reactions of PLP with amino acids and bivalent metals have been studied previously[1-4] Matthews[5] and Farago and Matthews[6] have shown that Cu^{2+} traps the Schiff-base of PLP and Glu in acid solution. This work has confirmed this conclusion.

The polarimetric studies have shown that with Cu^{2+} and Zn^{2+} the mutarotation and the formation of the aldimine complex proceed at the same rate.

$$\text{PLP} + \text{Glu} \xrightarrow{\text{slow}} \underset{\text{SB}}{\text{aldimine}} \xrightarrow[\text{fast}]{M^{2+}} M^{2+}\ \text{aldimine-complex}$$

In the case of Cu^{2+} a second stage of the reaction occurs in which the optical activity of the complex is lost.

The racemization process takes place in the Cu^{2+}-aldimine chelate much faster than the subsequent transamination reaction (Fig. 5). Thus with the Cu^{2+} aldimine chelate the proton is removed from the α-carbon and its replacement involves racemization but not the isomerization to the Ketimine SB complex. It was not possible to show if there was exchange of this α-proton in the Zn^{2+} aldimine complex with complete retention of configuration because the ^1H n.m.r. signals could not be resolved. However further work is required to elucidate this point.

It was shown (p.62) that Zn^{2+} ions are replaced by Cu^{2+} ions in the aldimine chelate in a very fast exchange reaction.

$$\underset{\substack{\text{(optically}\\ \text{stable)}}}{Zn^{2+}\text{-SB}} \xrightarrow{Cu^{2+}} \underset{\text{(racemizes)}}{Cu^{2+}\text{-SB}}$$

This exchange reaction reflects the high thermodynamic stability of the Cu^{2+}-SB complex. Matthews[5] reported $\log K_c$ at 25°C and pH 3.94 to be 14.28 for the complex of Cu^{2+} with the aldimine SB of PLP and glutamate.

The reaction of PLP with glutamate and Cu^{2+} ions was exceptional since it was the only one investigated which showed the racemization behaviour. An explanation for this phenomenon has been attempted in terms of the steric effects of the β substituents of the amino acids and the d^9 configuration of the Cu^{2+} ion (see p. 67 and 68).

In the absence of the metal ion the Schiff-base is largely dissociated in acid solution as the following table shows.

Equilibrium constants for the formation of Schiff-base from PLP and Glu 25°C (data from ref.5)

pH	3.95	4.57	5.04	5.86	6.37
log K	0.81	0.87	0.86	1.05	1.21

Matthews[5] has also shown that the stability constants of bivalent metals with PLP are low where those for PAMP are much higher[5,7]. The reactions of the trivalent metals are different. They have high affinity for oxygen donors and form less labile complexes. In the presence of M^{3+} the electronic spectra show the formation of PLP-M^{3+} complexes (Fig. 16, 17). Complex formation is also shown by the n.m.r. studies as discussed below. The reactions involved are shown in equations 1-4 below.

$$M^{n+} + PLP \underset{}{\overset{K_{eq}}{\rightleftharpoons}} M^{n+} - PLP \qquad (1)$$

$$PLP + AA \longrightarrow SB \qquad (2)$$

$$M^{n+}\text{-}PLP + AA \longrightarrow M^{n+} - SB \qquad (3)$$

$$SB + M^{n+} \longrightarrow M^{n+} - SB \qquad (4)$$

For bivalent metal ions reactions (2) and (4) are involved with (2)

being rate determining step. With trivalent metals reactions (1) and (3) dominate. The rate of the reaction is given by

$$\text{rate} = k.K_{eq}[M^{3+}][PLP][AA]$$

If K_{eq} is large then the reaction becomes second order and independent of the concentration of metal. This type of behaviour was observed in this work.

The situation is however complicated by the fact that the M^{3+} metal ions form complexes with amino acids. This may be a contributing factor to the induction period observed in these reactions. Further work in the thermodynamic stability constants of the M^{3+} complexes involved in these systems is required. Similarly a kinetic study of the first few seconds of the reaction by stopped flow techniques should be carried out.

u.v. (Fig. 16, 17) and n.m.r. (Fig. 27, 32) measurements have proved that Ga-PLP, In-PLP and Al-PLP complexes exist in solutions and their structures are affected by the pH of the solution. In the acidic pH range, the M^{3+} ion prefers bonding with the phosphate group of the PLP as ^{31}P n.m.r. indicated (Fig. 43). This perhaps comes about as a result of the hydration of the aldehyde group shown by ^{1}H n.m.r. (Fig.49a). Near netural pH the aldehyde is less hydrated and at the basic pH range is completely free (Fig.49c) for bonding with the metal ion. This agrees with the ^{31}P n.m.r. results (Fig.43c) where the M-O-P bonding is absent in the higher pH range. In the acidic pH range M^{3+}-PLP complexes appear to be rather symmetrical species. This last point was shown by ^{71}Ga n.m.r. (Fig. 32) where the spectral width of Ga-PLP signal is very narrow. This is the result of a longer relaxation time which arises from symmetrically arranged ligands. ^{115}In n.m.r. (Table 60) and ^{27}Al n.m.r. (Fig. 27) for the same ligand, behaved similarly indicating symmetrical species

coordinated through the phosphate group (Table 47) in acidic media. In the basic pH range, however, the complex appeared to be less symmetrical (Fig. 43, 33,49c, tables 47-48). Coordination could occur through the phenolic oxygen of the aldehyde group. The suggested structure in the acidic pH range for Al^{+} PLP is shown in Fig. 45 and a possible structure near neutral and in alkaline media might be of the type:

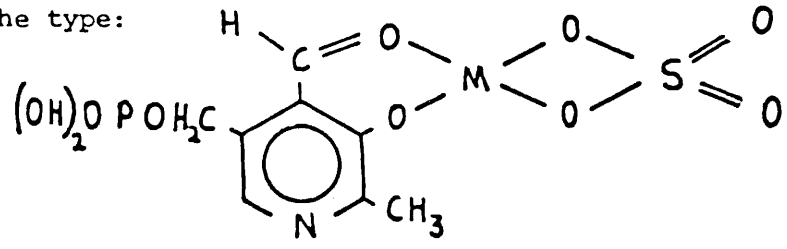

Al^{3+}, Ga^{3+} and In^{3+} as ^{27}Al n.m.r. (Fig. 3), ^{71}Ga n.m.r. (Fig. 32) and ^{115}In n.m.r. (Table 61) reveal complexes with amino acids of 1:2 metal to ligand ratio. Hence the rate constant varies with the order of the addition. As tables 20a and 20b show the rate constant for the reaction of Ga^{3+} in the presence of PLP and L-aspartic acid is slightly different when the order of the reactants added alters.

In the Schiff base complexes coordination to M^{3+} in acidic media was via the phenolic oxygen group and not through the phosphate group. Thus a rearrangement must take place so that the phosphate group which is bound to M^{3+} in the M^{3+} PLP complexes becomes free in the M^{3+} SB complexes. This point was shown by the ^{31}P n.m.r. studies, and a possible mechanism has been suggested on p. 181, Fig. 45. This mechanism is in good agreement with the results of chromatography (tables 43, 44) which show the products of transamination reaction (PAMP appears as an orange spot of Rf=6 with ninhydrin; PLP, blue colour disappears under u.v. L-Glu purple, Rf=24, with ninhydrin disappears, PL Rf=59 blue under u.v. showed a small amount of dephosphorylated PLP).

^{13}C n.m.r. confirmed the presence of the products of the

transamination reaction i.e. PAMP and α-Kg (table 44) (after one week) as well as the M^{3+}-SB complexes (Table 43) after 4-6 hours.

In the reactions of Al^{3+} and Ga^{3+} with PLP and threonine, carbon-carbon bond fission occurs producing acetaldehyde and the M^{3+}-SB complex of glycine-PLP. This result confirms that of Martell[8] (scheme 3 p.18). The ^{13}C n.m.r. work also confirmed in H n.m.r. of Martell in which he suggested the structures shown in Fig. 1.

The relative intensities of the ^{71}Ga n.m.r. signals of the Ga^{3+} in the presence of ligands and free Ga^{3+} ion versus the concentration ratio of the Ga^{3+}-ligand and Ga^{3+} showed the number of ligands coordinated to the metal ion and it was found that all complexes were of 1:2 metal to ligand ratio except in the case of L-threonine the M^{3+}-SB formed was of 1:1 ratio.

The reactions of M^{3+} with PLP and AA proceed much faster in alkaline media (table 41) and appear to be of a second order. There is no induction period (unlike acid media) and the increase of the concentration of the metal has very little effect on the rate constant.

This work has confirmed the trapping of the SB by Cu^{2+} and Zn^{2+}, and has shown that with M^{3+} ions coordination to the separate ligands is important.

It has also been shown that the phosphate group cannot be ignored in the reaction sequences. However, these systems are still not yet fully understood and much work remains to be done.

REFERENCES

1. R.D. Gillard, P.O'Brien, P.R. Norman and D.A. Phipps, J.C.S. Dalton 1988 (1979).

2. T. Ichikawa, T. Okamoto, S. Maeda, S. Ohdan, Y. Araki and Y. Ishido, Tetrahedron Letters 1, 79 (1971).

3. L.G. Stadthevv and R.J. Angelici, Inorg. Chem., 1975, 74, 925.

4. Y. Matsushima and A.E. Martell, J.A.C.S. 1331, 89 (1967).

5. T. Matthews, thesis, Bedford College Chemistry Department (1971).

6. M.E. Farago and T. Matthews; J.C.S. 609 (1969).

7. Pyridoxal catalysis: enzymes and model systems, E.E. Snell, A.E. Braunstein, E.S. Severin and Yu.M. Torchinsky, Interscience N.Y. (1968).

8. E.H. Abbott and A.E. Martell, J.A.C.S., 95, 5014 (1973).

9. E.H. Abbott and A.E. Martell, J.A.C.S., 92, 20, 5845 (1970).

Appendix I

Abbreviations

PLP = pyridoxal-5'-phosphate

PAMP = pyridoxamine-5'-phosphate

PL = pyridoxal

u.v. = ultra-violet

Glu = glutamate

Asp = aspartic acid

Threon = thrionine

α-Kg = α-Keto-glutaric acid (α-oxo-glutaric acid)

PW_1 = pulse width

PM = Pyridoxamine

PD = pulse delay

PI = pulse interval

OBFRQ = observation frequency

Appendix II

Buffer solutions

In 50 cm^3 of 1 $mol.dm^{-3}$ sodium acetate solution, x cm^3 of 1 $mol.dm^{-3}$ HCl were added and the solution was made up to 250 cm^3. The pH of those solutions was measured with a Pye Dynacap pH meter at 30°C.

volume of 1 $mol.dm^{-3}$ HCl /cm^3	pH
56.0	1.68
52.5	1.86
40.0	3.88
15.1	4.90
0.25	6.65

Appendix III

An attempt was made to measure the spin-lattice relaxation times of the M^{3+}-PLP and M^{3+}-SB complexes, where M is Al and Ga and the SB is PLP-Glu, in order to gain more information about the symmetry of the complexes.

Experimental

All solutions were digassed by passing N_2 through the samples before measurements. The following solutions were prepared:

(a) Al $NH_4(SO_4)_2$ at pH 9 (NaOH)

(b) Al-PLP (1:2) at pH 9

(c) Al-PLP-Glu (1:2:2) at pH 9

(d) $Ga(NO_3)_3$ at pH 4 (NaOH)

(e) Ga-PLP at pH 4

Initially the 90^0 pulse was accurately determined for all the solutions.

Results and Discussion

Fig. 51 shows the results for solution (a). An inversion occurs and T_1 was calculated to be 70.71 ms. Fig. 52 shows the results for solution (b). Although there was no inversion of the signal an approximate value of T_1 was calculated to be 60.08 ms. Further work is required on this system to obtain accurate values. For solutions (c), (d) and (e) no inversions were found and further work would be required on these systems. For example more accurate values of PW_1 and complete removal of oxygen from the solutions are needed.

The value of T_1 found here for the aquo aluminate ion in basic medium (70.71ms) is of the same order as that found by O'Reilly[1] for the aquo aluminate at pH.

The low value of T_1 for Al-PLP indicates that the complex is asymmetrical. However further work is necessary.

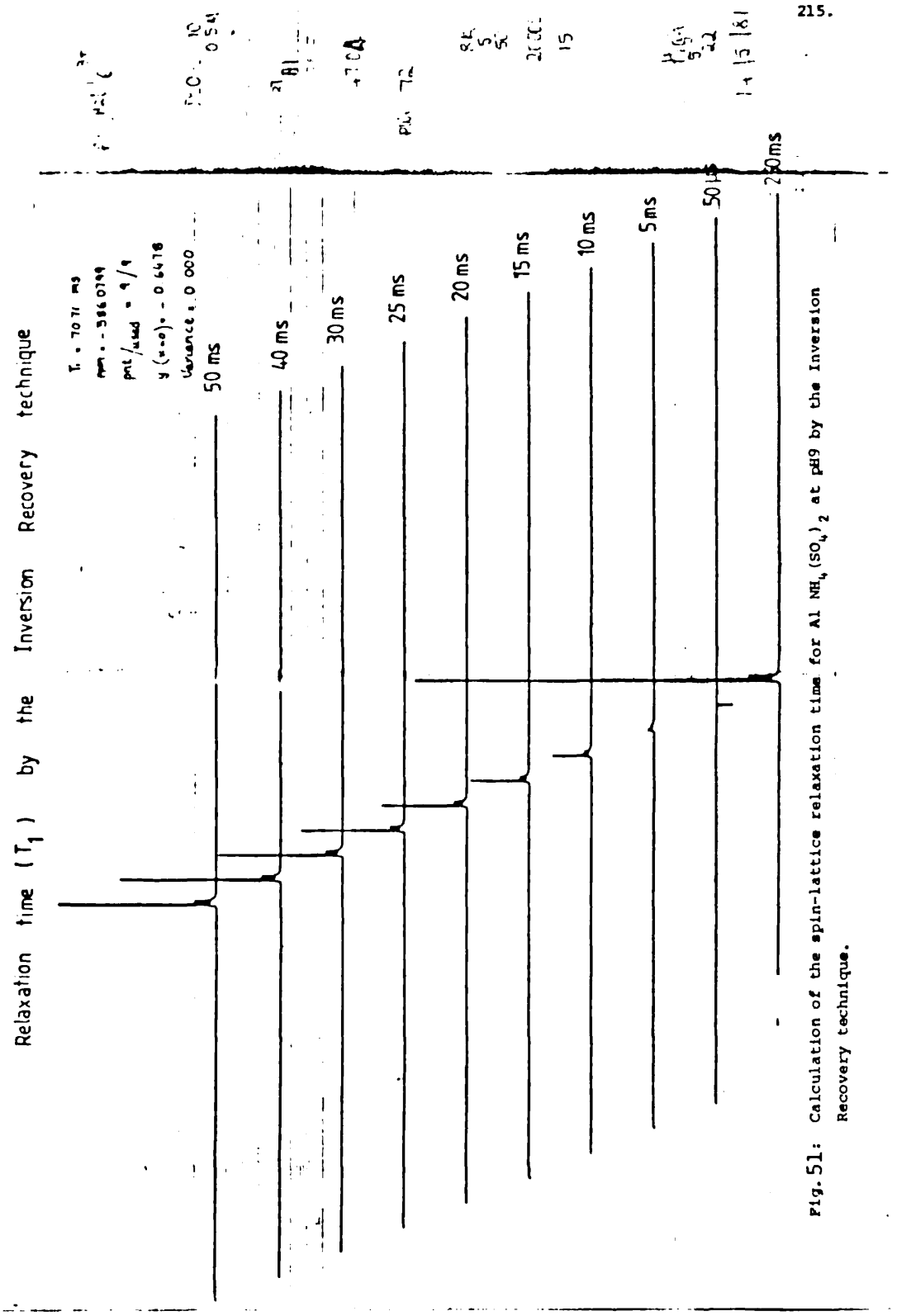

Fig.51: Calculation of the spin-lattice relaxation time for Al $NH_4(SO_4)_2$ at pH9 by the Inversion Recovery technique.

Reference

1. D.E. O'Reilly, J. Chem. Phys. 32, 1007, (1960).

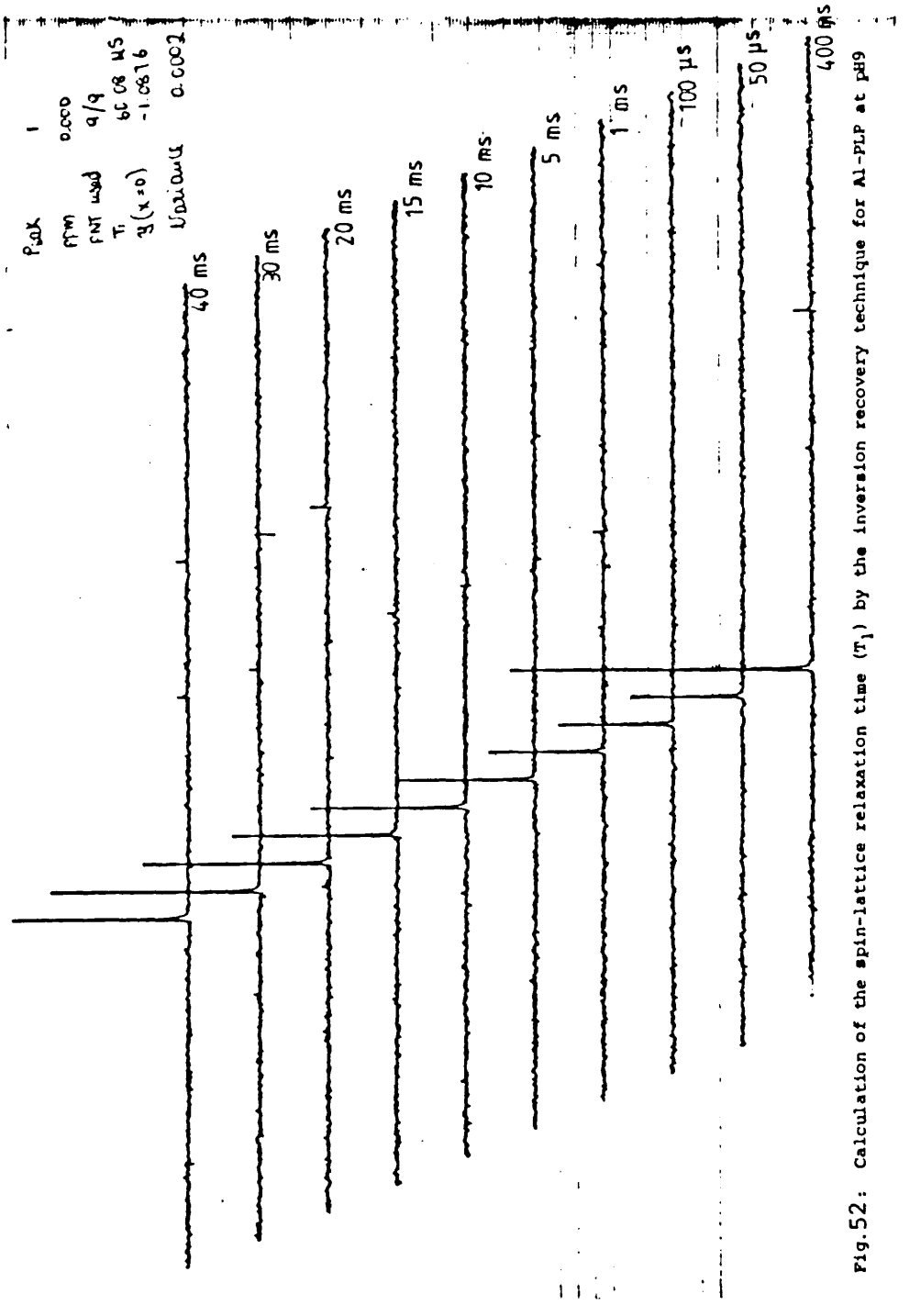

Fig.52: Calculation of the spin-lattice relaxation time (T_1) by the inversion recovery technique for Al-PLP at pH9